UNIVERSAL
LIBRARY

OU_160621

UNIVERSAL
LIBRARY

G.11665
531.1
H66K
Hinkle, Rotland T.
Kinematics of machines
1958.

OSMANIA UNIVERSITY LIBRARY

Call No. 531.11 H66K Accession No. G.11665

Author Hinkle, Rolland T.

Title Kinematics of machines. 19

This book should be returned on or before the date last marked below.

Kinematics of Machines

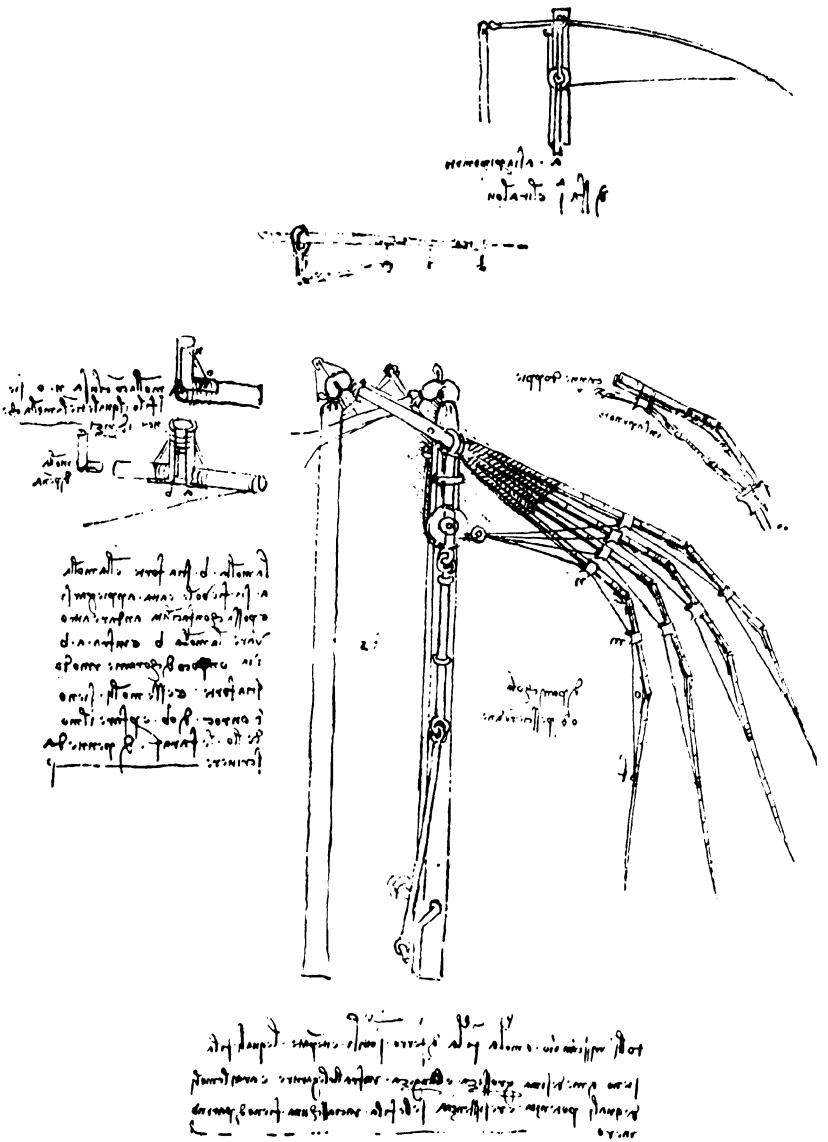

Study of Mechanism of Wing of Flying Machine. Drawing by Leonardo da Vinci. (Courtesy of Bettmann Archive.)

Kinematics of Machines

by

ROLLAND T. HINKLE

Professor of Mechanical Engineering
Michigan State College

Englewood Cliffs, N. J.

PRENTICE-HALL, INC.

Copyright, 1953, by Prentice-Hall, Inc., Englewood Cliffs, N. J. All rights reserved. No part of this book may be reproduced in any form, by mimeograph or any other means, without permission in writing from the publishers.

Library of Congress
Catalog Card Number:

53-12080

First Printing.....*October, 1953*
Second Printing.....*January, 1955*
Third Printing.....*March, 1956*
Fourth Printing.....*May, 1957*
Fifth Printing.....*September, 1958*

PRINTED IN THE UNITED STATES OF AMERICA

51534

Preface

Kinematics of machines is usually defined as the study of the relative motions of machine parts. The emphasis has been placed here rather than on the descriptions of mechanisms. However, a wide variety of mechanisms are used in the development of the theory and in the examples.

The basic concepts have been reduced to a minimum number. Their inclusion in the first two chapters makes it possible to omit sections in the remaining ten chapters without loss of continuity. Because of their basic importance, relative motion, inversion, and the angular velocity theorem are extensively treated. Some special constructions have been included in Chapter 6, not for their own sake, but to point out that basic theory can be used in many ways and that short cuts can often be developed.

The book presupposes a knowledge of engineering mechanics. However, calculus is sufficient if the reader spends additional time on the first two chapters.

The amount of material on cycloidal gears and flat belts has been reduced. New material has been included on velocity and acceleration polygons, equivalent linkages, special constructions, chains, rolling bodies, gears, and miscellaneous mechanisms. The derivation of Coriolis' acceleration is a special case, but it should make it possible for the reader to visualize the vector in magnitude and direction.

Problems of varying difficulty are included at the end of each chapter.

Material taken directly from other sources is acknowledged in the book. The author wishes to express appreciation to Professors L. C. Price and Ching-U Ip of Michigan State College for their help and encouragement during the writing of this volume.

ROLLAND T. HINKLE

Contents

1. Terminology and Basic Concepts *1*
2. Equations of Motion, Relative Motion, and Transmission of Motion *11*
3. Velocities in Mechanisms, Instant Centers and Resolution *30*
4. Velocity Polygons *46*
5. Acceleration *66*
6. Velocity and Acceleration Graphs, Special Constructions, Analytical Methods *84*
7. Cams *99*
8. Rolling Contact *123*
9. Gearing *134*
10. Flexible Connectors *179*
11. Gear Trains, Translation Screws *194*
12. Miscellaneous Mechanisms *210*

Index *227*

CHAPTER 1

Terminology and Basic Concepts

1.1. Introductory. Certain phases of kinematics are as old as recorded history. One of the simplest devices, the wheel, has been used for five thousand years. The frontispiece in this book shows Leonardo da Vinci's (1452–1519) "Study of Mechanism of Wing of Flying Machine." A slider-crank mechanism is clearly shown. This slider crank is the basic mechanism of modern aircraft engines. Da Vinci would have been unable to calculate the acceleration of the slider. This is now considered a simple problem. In modern high-speed engines the inertia forces are often greater than the gas forces. An acceleration analysis is necessary for satisfactory design.

The Linotype shown in Fig. 1.1 is an example of a machine that contains many mechanisms. Its operation is almost as simple as that of the typewriter; an operator can write about 150 letters a minute. The rest is automatic. Cast slugs of the proper length, similar to that of Fig. 1.2, emerge from the machine. Most of the mechanisms are hidden from view. One series is shown in Fig. 1.3. When the key is pressed, a sequence of motions is started that in the end forms one letter in the slug. The cams in Fig. 7.1 actuate and control most of the mechanical actions of the Linotype.

A book filled with descriptions of mechanisms would be interesting and useful to the graduate engineer, but would be of little value to the person who is not well grounded in the theory of kinematics of machines. This book was written to present this groundwork. Terminology and the fundamentals of motion are presented first. This is followed with additional theory, and applications to specific mechanisms. The last chapter contains brief discussions of mechanisms not considered in earlier chapters.

1.2. Kinematics of machines treats of the relative motion of machine parts. The kinematic scheme of a machine can be investigated without regard to forces. This makes it possible to treat kinematics of machines as a separate subject.

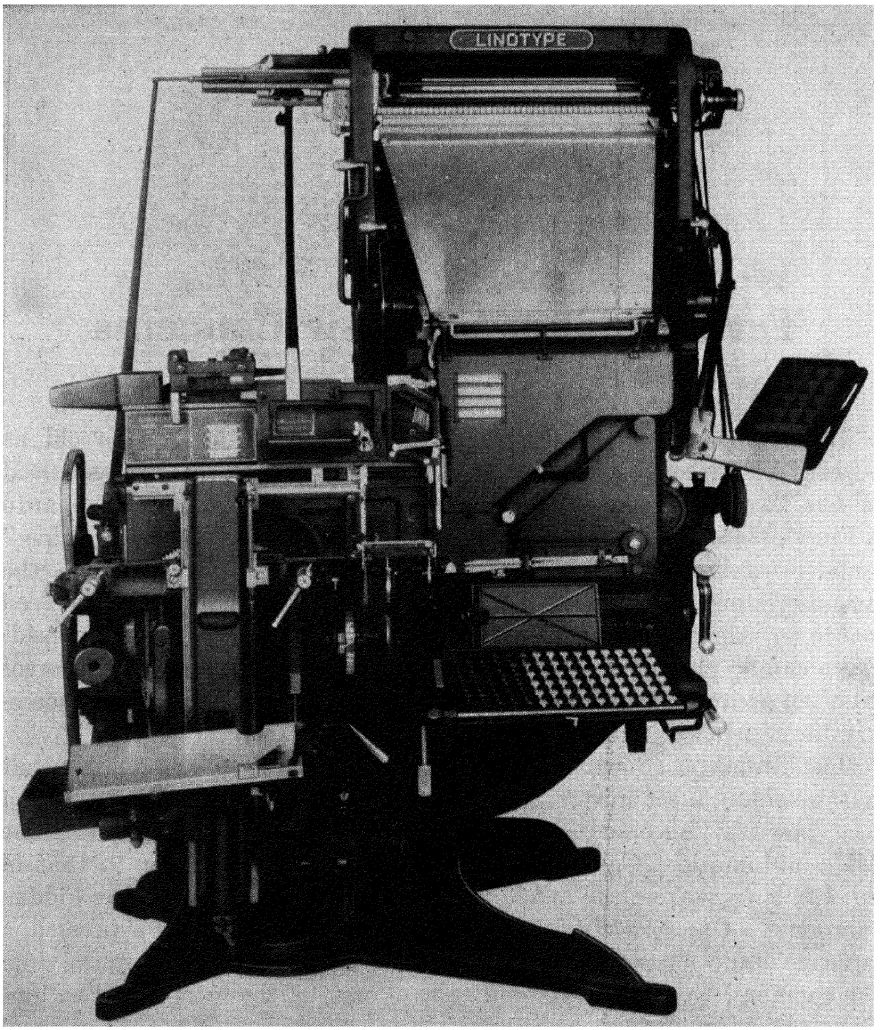

Fig. 1.1. Linotype machine. (Courtesy of Mergenthaler Linotype Co.)

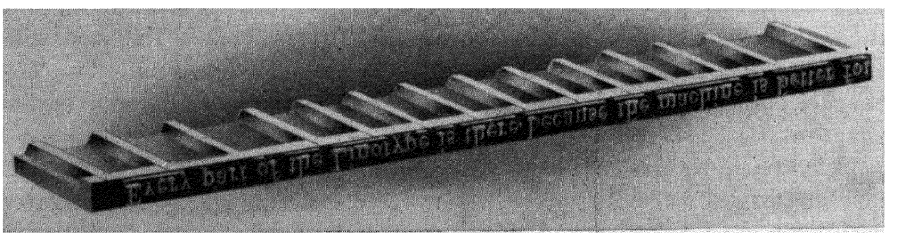

Fig. 1.2. (Courtesy of Mergenthaler Linotype Co.)

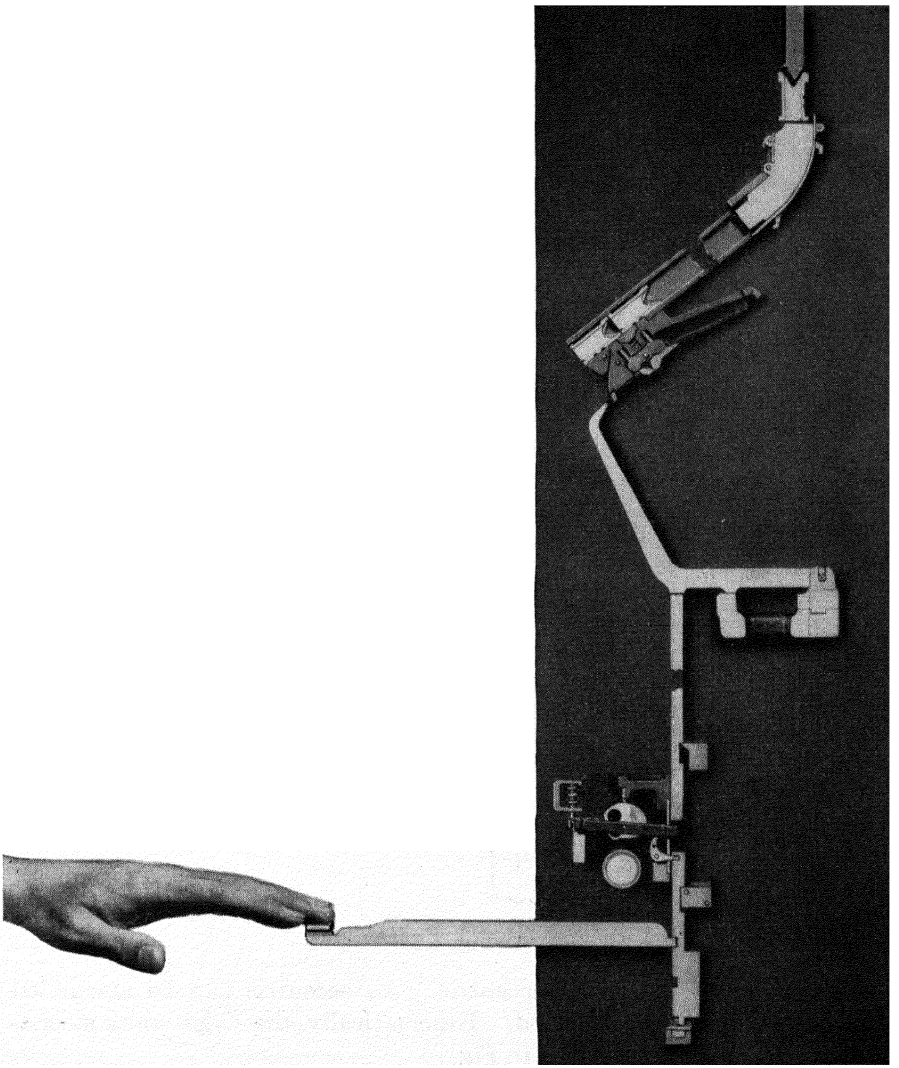

Fig. 1.3. (Courtesy of Mergenthaler Linotype Co.)

The design of a machine may be divided into three steps:

1. Determination of the kinematic scheme
2. Determination of the forces
3. Proportioning of the parts

These three steps may not always be independent. When inertia forces are considered, the mass of the parts will contribute to the forces, and it might be necessary to alter the kinematic scheme to reduce accelerations. It is usually convenient, however, to consider the first two

steps separately and then apply them in machine design, where the third step is considered. Forces will be considered briefly in several sections of this book.

1.3. Pairs. A pair is a joint that permits relative motion. As implied by the name, a pair has two elements. A slider-crank mechanism that is commonly used in gasoline engines is shown in Fig. 1.4, where A is a turning pair. The surface of the crankshaft that turns in the bearing is an element, and the surface of the bearing is the other element. Here B and C are similar turning pairs, and D is a pair. The surface of the piston and the surface of the cylinder form a sliding pair.

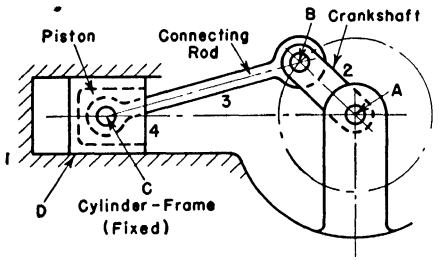

Fig. 1.4

In Fig. 1.5, the diameter of the journal with center at B has been increased in size so that it includes the shaft with center at A. This

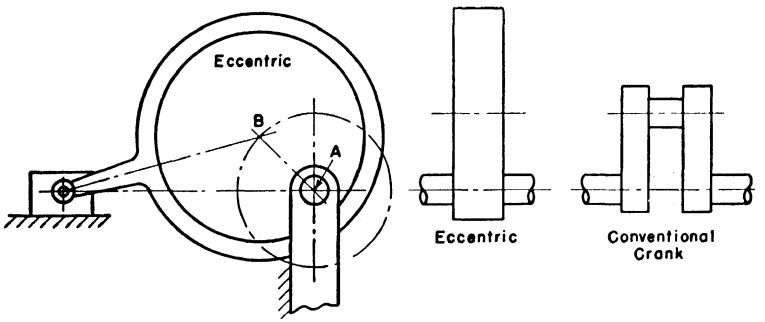

Fig. 1.5

type of crank is called an eccentric. An eccentric can be assembled with a one-piece connecting rod. Kinematically, the slider-crank mechanism in Fig. 1.5 is equivalent to Fig. 1.4.

A wheel and the surface on which it rolls form a rolling pair at the point of contact. A nut and screw form a helical pair (Fig. 1.7). A ball-and-socket joint forms a spherical pair (Fig. 1.8).

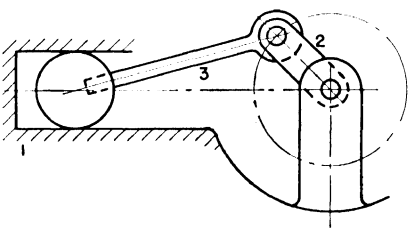

Fig. 1.6

1.4. Higher and lower pairs. If a pair has surface contact, it is a lower pair. If a pair has theoretical point or line contact, it is a higher pair. Thus A, B, C, and D in Fig. 1.4 are lower pairs. In Fig. 1.6, a

mechanism is shown that is equivalent to Fig. 1.4. The piston has been replaced by a sphere, rigidly fastened to the connecting rod. The cylinder and sphere have line contact, and form a higher pair. This would result in excessive wear, and is therefore not good design. Kinematically, it makes no difference whether a pair is higher or lower.

1.5. Closed and unclosed pairs. Elements of pairs that are held together mechanically are closed pairs. The pairs of Figs. 1.4, 1.5, 1.6,

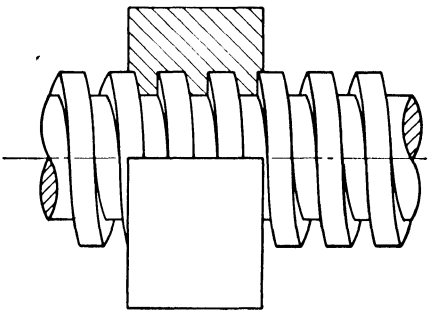

Fig. 1.7

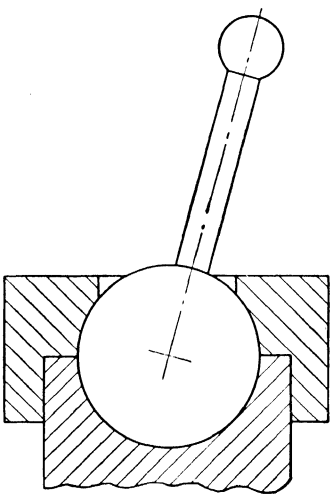

Fig. 1.8

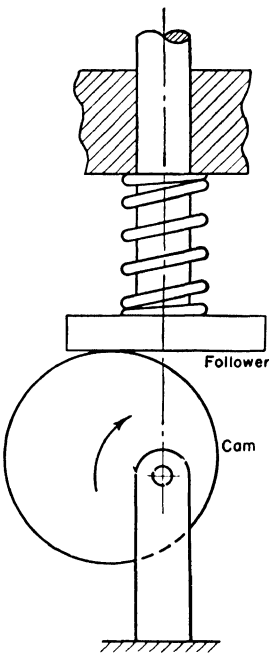

Fig. 1.9

1.7, and 1.8 are closed. Pairs that are not held together mechanically are unclosed pairs. The cam and follower shown in Fig. 1.9 form an unclosed pair. The cam and follower are held in contact by the forces

of gravity and the spring. At excessive speeds the cam and follower would not remain in contact at all times.

1.6. Kinematic link. A kinematic link is a rigid body with two or more elements of pairs. In Fig. 1.4, the crank and connecting rod have two elements of turning pairs each. The piston and frame have a turning element and a sliding element each. The master connecting rod of a nine-cylinder radial aircraft engine, shown in Fig. 1.10, has ten elements of turning pairs.

All materials have some elasticity, but in most cases the deformations are so small that they can be neglected in a kinematic analysis. Flexible connectors, such as belts and chains, act only in tension, and fluid in a tube acts in compression. While so acting, these can be treated as equivalent rigid links with elements of pairs.

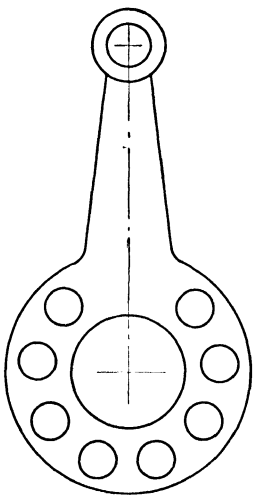

Fig. 1.10

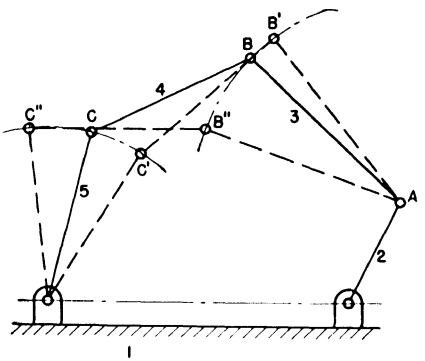

Fig. 1.11

1.7. Kinematic chain. When several links are joined in such a way that with one link fixed the others move according to a definite law, the chain of links is a kinematic chain. This type of motion is called constrained motion. When the frame in Fig. 1.4 is fixed, the piston has a definite location for each position of the crank. This chain of links has constrained motion, and is a kinematic chain. The chain of links shown in Fig. 1.11 does not have constrained motion. For an assumed position of link 2, there is an infinite number of positions for links 3, 4, and 5. Two sets of positions are shown with broken lines. This chain of links is not a kinematic chain. The chain in Fig. 1.12 is a structure. When one link is fixed,

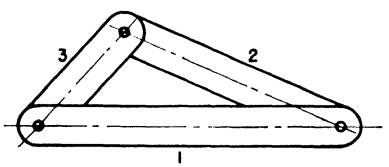

Fig. 1.12

the others cannot be moved. Only kinematic chains will be considered in this book.

1.8. Mechanism. When one link of a kinematic chain is fixed, the chain becomes a mechanism. This will be discussed further in Art. 2.8.

1.9. Machine. A machine is a mechanism or a group of mechanisms used to perform useful work. Gasoline engines, lathes, and hoists are examples of machines. A watch is a mechanism. The stored energy in the spring is used to overcome friction and move the hands. No external work is done.

1.10. Plane motion. If a body moves in such a way that all points in it remain at constant distances from a reference plane, the body has plane motion. This reference plane is called the plane of motion. The three types of plane motion are described in the following three articles.

1.11. Plane rotation. If a body has plane motion and moves in such a way that each point in it remains a constant distance from a fixed axis perpendicular to the plane of motion, the body has plane rotation. The crankshaft of the engine mechanism shown in Fig. 1.4 has plane rotation when the frame is fixed.

1.12. Plane translation. If a body has plane motion and moves in such a way that a line joining any two points in it (except lines normal to the plane of motion) remains parallel to all previous positions, the body has plane translation. If, in addition to this, the body moves in a straight line, it has rectilinear translation. The piston in Fig. 1.4 has rectilinear translation. It is sometimes convenient to consider rectilinear translation as a special case of rotation, with an axis of rotation at infinity. The motion of a body moving with translation in a curved path is called curvilinear translation. The cars of a ferris wheel have this type of motion.

1.13. Combined translation and rotation. If a body has plane motion that is neither pure rotation nor pure translation, it is a combina-

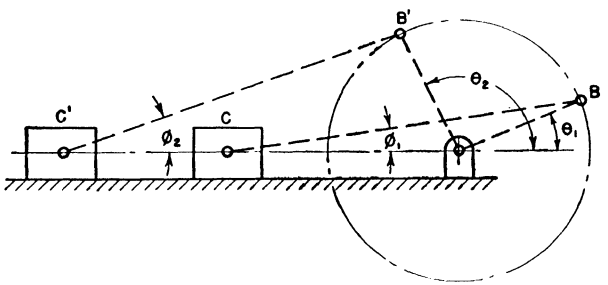

Fig. 1.13

tion of the two. The motion of the connecting rod shown in Fig. 1.4 is of this type. This mechanism is shown again in Fig. 1.13. Consider the motion of the connecting rod as it moves from position CB to $C'B'$.

In Fig. 1.14, it is shown that this is equivalent to translation from CB to $C'B''$, and then rotation from $C'B''$ to $C'B'$. The same displacement could be accomplished as shown in Fig. 1.15. The connecting rod is

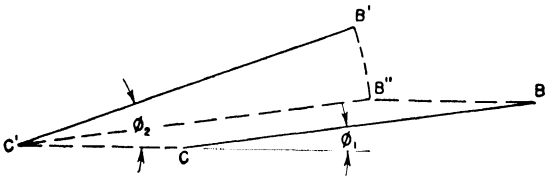

Fig. 1.14

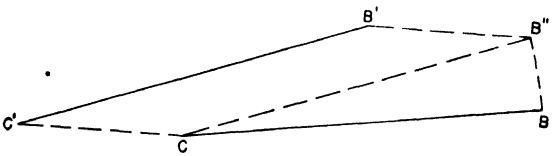

Fig. 1.15

rotated from CB to CB'' and then translated from CB'' to CB'. At any instant the motion of the connecting rod can be considered to be a combination of rotation about some point, and translation.

1.14. Helical motion. A body having rotation combined with translation along the axis of rotation has helical motion. A nut that is turned on a screw has helical motion (Fig. 1.7). This is three-dimensional motion.

1.15. Spherical motion. If each point in a body moving in space remains a constant distance from a fixed point, the body has spherical motion. The ball, and any part that is rigidly attached to the ball of the ball-and-socket joint shown in Fig. 1.8 have spherical motion. This is three-dimensional motion.

1.16. Phase, cycle, and period of motion. The simultaneous relative positions of the links of a mechanism or machine at any instant constitute a phase. The two phases of the mechanism shown in Fig. 1.13 can be indicated by specifying the position of the crank as θ_1 and θ_2. A machine completes a motion cycle when it starts from some phase, passes through all possible positions, and returns to the original phase. The slider-crank mechanism completes a motion cycle each time the crank turns one revolution. The valve mechanism of a 4-cycle gasoline engine requires two revolutions of the crank to complete one motion cycle. The period is the time required to complete one motion cycle.

1.17. Vectors. Quantities that have only magnitude, such as time, distance, and volume, are scalar quantities. Quantities that have both

magnitude and direction, such as displacement, velocity, and acceleration, are vector quantities. A vector quantity can be represented by a straight line with an arrowhead. The length of the line represents the magnitude; the angular orientation represents the line of action. The arrowhead is called the *terminus*, and the other end is called the *tail*, or *origin* of the vector. If the origin of the vector is placed at the origin of the quantity that it represents, it is called a localized vector. If the vector is drawn anywhere else in the plane, it is called a free vector. The localized vector and a free vector representing the velocity of crankpin A are shown in Fig. 1.16.

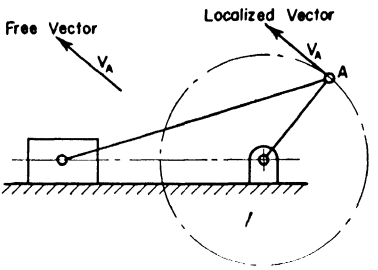

Fig. 1.16

1.18. Addition and subtraction of vectors. The symbols $+\triangleright$ and $-\triangleright$ are commonly used to denote vector addition and subtraction. In Fig. 1.17, let A and B represent successive displacements of a body. These two displacements are equivalent to the single displacement $A +\triangleright B$. All vector quantities can be added in this manner. The order in which the vectors are added does not matter. Vector B can be subtracted from A by changing the sign of B and adding, as shown in Fig. 1.18. Vector A can be subtracted from B, as shown in Fig. 1.19.

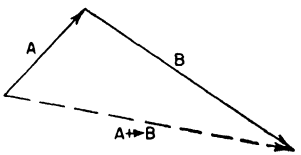

Fig. 1.17

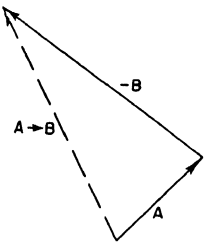

Fig. 1.18

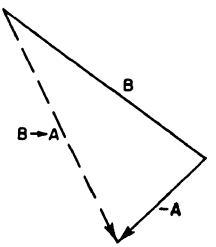

Fig. 1.19

An examination of Figs. 1.18 and 1.19 shows that $A -\triangleright B$ is equal and opposite to $B -\triangleright A$, or $(A +\triangleright -B) = -(B -\triangleright A) = -(-A +\triangleright B)$.

1.19. Composition and resolution of vectors. The adding or combining of vectors is called composition of vectors. The breaking up or resolving of a vector into equivalent components is called resolution of vectors. A vector can be resolved into an infinite number of combinations of components. It is often convenient to resolve a vector into two components; for example, the components parallel to the x and y axes.

Two component vectors represent two magnitudes and two directions. If any two of these four quantities are known, the other two can be deter-

mined. In Fig. 1.20, vector A is to be resolved into two components; the magnitude and direction of one component, b, is known. This known vector is laid off from the origin of vector A. The closing line determines the other component, C. A second solution, B' and C', is shown. This is equivalent to the solution B and C.

In Fig. 1.21, vector A is to be resolved into two components of magnitude b and c. Arcs of radii b and c are drawn from centers at the origin and terminus of vector A. The intersections of the arcs determine two distinct solutions, BC and $B'C'$. If the magnitudes b and c are equal, there is one solution. If the sum of the magnitudes b and c is less than the magnitude of A, there is no solution.

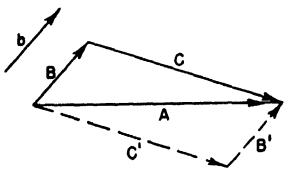

Fig. 1.20

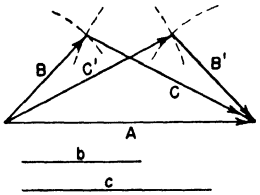

Fig. 1.21

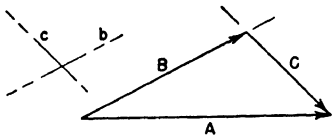

Fig. 1.22

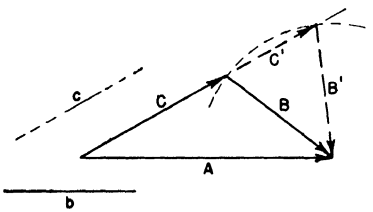

Fig. 1.23

In Fig. 1.22, vector A is to be resolved into two components having directions b and c. Lines parallel to b and c are drawn through the origin and terminus of vector A. The intersection of these lines determines the single solution, B and C.

In Fig. 1.23, vector A is to be resolved into two components; one is to be of magnitude b and the other is to be in the direction c. A line parallel to c is drawn through the origin of vector A. An arc of radius b is drawn from a center at the terminus of vector A. The intersection of the arc with the line of direction c determines two solutions, CB and $C'B'$. If the arc is tangent to the line of direction c, there is one solution. If the arc does not reach the line of direction c, there is no solution.

CHAPTER 2

Equations of Motion, Relative Motion, and Transmission of Motion

2.1. Displacement of a point. Displacement is the change of position of a moving point. In Fig. 2.1, point P moves from position D to E along the path C. The displacement of P is Δs. This displacement can be expressed by a single vector equation in terms of components parallel to the x and y axes.

$$\Delta s = \Delta x +\triangleright \Delta y \tag{2.1}$$

Two algebraic equations are required to express this displacement. A vector symbol enclosed in bars represents the magnitude of the vector. The magnitude is

$$|\Delta s| = \sqrt{|\Delta x|^2 + |\Delta y|^2} \tag{2.2}$$

and the direction is

$$\beta = \tan^{-1} \frac{|\Delta y|}{|\Delta x|} \tag{2.3}$$

In the limit, E approaches D and the chord Δs approaches the tangent at D. The direction of motion of a point as it moves along a path is therefore tangent to the path.

The angular displacement of point P can be expressed as the change in the angle made by its radius vector with respect to some reference point and line, in this case the origin and the x axis.

$$\Delta\theta = \theta_1 - \theta_2 \tag{2.4}$$

In order to obtain a relationship between linear and angular displacement, the displacement Δs (see Fig. 2.2) is written

$$\Delta s = R_1 \Delta\theta +\triangleright \Delta R$$

In the limit,

$$ds = R_1\, d\theta +\triangleright dR$$

For the important case of a circular path (see Fig. 2.3) dR is equal to zero, and

$$ds = R\, d\theta \tag{2.5}$$

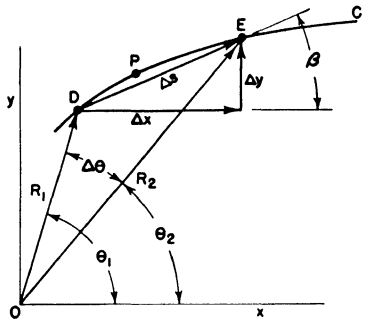

Fig. 2.1

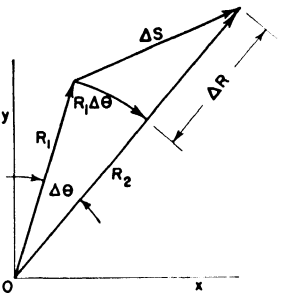

Fig. 2.2

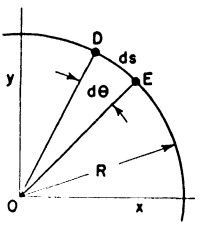

Fig. 2.3

2.2. Linear and angular velocity. Linear velocity is the time rate of change of linear displacement. In Fig. 2.1, point P moves from D to E in time Δt. The average velocity is

$$V = \frac{\Delta s}{\Delta t}$$

The instantaneous velocity of point P at position D is obtained by taking the limit

$$V = \underset{t=0}{\text{Limit}} \frac{\Delta s}{\Delta t} = \frac{ds}{dt} \tag{2.6}$$

The direction of the velocity is tangent to the path.

Angular velocity is the time rate of change of angular displacement. When the radius vector (Fig. 2.1) moves through an angle $\Delta\theta$ in time Δt, the average angular velocity is

$$\omega = \frac{\Delta\theta}{\Delta t}$$

where ω is radians per unit time. In the limit, the instantaneous angular velocity is

$$\omega = \frac{d\theta}{dt} \tag{2.7}$$

A relationship between linear and angular velocities for the case of circular motion can be obtained by substituting Eqs. (2.6) and (2.7) in Eq. (2.5), giving

$$V = R\omega \tag{2.8}$$

2.3. Linear and angular acceleration. The acceleration of a point having rectilinear motion will be considered first. Since the motion of the particle does not change in direction, the acceleration is due only to the change in magnitude of the velocity. Linear acceleration is the time rate of change of the magnitude of velocity. For a time interval Δt, the average acceleration is

$$A = \frac{V - V_0}{\Delta t} = \frac{\Delta V}{\Delta t} \tag{2.9}$$

where V_0 is the initial velocity and V is the final velocity for the time interval. In the limit, the instantaneous acceleration is

$$A = \frac{dV}{dt} = \frac{d^2s}{dt^2} \tag{2.10}$$

If the motion of the point is that of constant or uniform acceleration, the average acceleration for any time interval is equal to all the instantaneous values. For this special case the time interval can be of any value, and Eq. (2.9) can be written

$$A = \frac{V - V_0}{t} \qquad \text{or} \qquad V = V_0 + At \tag{2.11}$$

If a point has uniform velocity, the displacement s in time t is

$$s = Vt \tag{2.12}$$

If a point has variable velocity, the displacement is the product of the average velocity and the time. For uniform acceleration, the displacement is

$$s = \frac{1}{2}(V_0 + V)t \tag{2.13}$$

Substituting the value of V from Eq. (2.11) in Eq. (2.13) gives

$$s = V_0t + \frac{1}{2}At^2 \tag{2.14}$$

Substituting the value of t from Eq. (2.11) in Eq. (2.13) gives

$$V^2 = V_0^2 + 2As \tag{2.15}$$

Angular acceleration α is the time rate of change of angular velocity. This is expressed as

$$\alpha = \frac{d\omega}{dt} = \frac{d^2\theta}{dt^2} \tag{2.16}$$

If a point moves in a circular path with uniform angular acceleration, and angular symbols θ, ω, and α are used in place of linear symbols s, V, and A, Eqs. (2.13), (2.14), and (2.15) will be derived in the form of (2.17), (2.18), and (2.19), respectively.

$$\theta = \frac{1}{2}(\omega_0 + \omega)t \tag{2.17}$$

$$\theta = \omega_0t + \frac{1}{2}\alpha t^2 \tag{2.18}$$

$$\omega^2 = \omega_0^2 + 2\alpha\theta \tag{2.19}$$

2.4. Normal and tangential acceleration. When a point moves in a circular path, the velocity changes in direction, and may or may not change in magnitude. In Fig. 2.4, a point moves from position B to C in time dt. The initial velocity is V and the final velocity is $V + dV$. In Fig. 2.5, the change in velocity dV is resolved into two components dV^n and dV^t. Component dV^n is normal to the path; it results from the change in direction of the velocity. Component dV^t is tangent to the path; it results from the change in magnitude of the velocity.

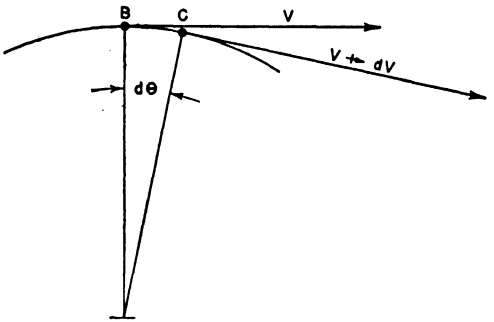

Fig. 2.4

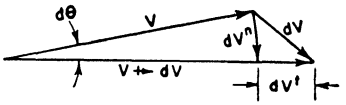

Fig. 2.5

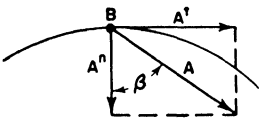

Fig. 2.6

The acceleration in the normal direction (A^n, normal acceleration) is the time rate of change of velocity in this direction.

$$A^n = \frac{dV^n}{dt} \tag{2.20}$$

From Fig. 2.5,

$$dV^n = V\,d\theta$$

Hence

$$A^n = V\frac{d\theta}{dt} \tag{2.21}$$

Substituting Eqs. (2.7) and (2.8) in (2.21) gives

$$A^n = V\omega = R\omega^2 = \frac{V^2}{R} \tag{2.22}$$

The acceleration in the tangential direction (A^t, tangential acceleration) is the time rate of change of the magnitude of the velocity. Equation (2.10) applies.

$$A^t = \frac{dV^t}{dt} \tag{2.23}$$

Substituting the derivative of Eq. (2.8) in (2.23) gives

$$A^t = R\frac{d\omega}{dt} = R\alpha \tag{2.24}$$

From Fig. 2.6, the magnitude of the total acceleration is

$$|A| = \sqrt{|A^n|^2 + |A^t|^2} \tag{2.25}$$

and the direction is

$$\beta = \tan^{-1}\left|\frac{A^t}{A^n}\right| \tag{2.26}$$

A point moving in a curved path always has normal acceleration. It has tangential acceleration if the magnitude of the velocity is changing. If a point has rectilinear motion, the normal acceleration is always

$$A^n = \frac{V^2}{R = \infty} = 0$$

Angular displacement, velocity, and acceleration are vector quantities. There are only two possible directions, clockwise (CW) and counterclockwise (CCW). The signs + and − will be used in place of $+\triangleright$ and $-\triangleright$. In this book, the counterclockwise direction will be considered positive.

2.5. Simple harmonic motion. *When the acceleration of a particle having rectilinear motion is always proportional to the distance of the particle from a fixed point on the path and is directed toward the fixed point, the particle is said to have simple harmonic motion.* The relationship can be expressed by the equation

$$A = \frac{d^2x}{dt^2} = -Kx \tag{2.27}$$

in which A is the acceleration of the particle moving along the x axis, x is the position coordinate, and K is a constant. The negative sign indicates that the acceleration is to the left when the particle is to the right of the origin, and vice versa.

It is often convenient to consider simple harmonic motion as the motion of the projection, on a diameter, of a point moving in a circle with constant angular velocity. In Fig. 2.7, point Q moves in a circular path with constant angular velocity ω, and P is the projection of this point on a diameter. The displacement of P from the center O is

$$x = OP = r\cos\omega t \tag{2.28}$$

The velocity of point P is

$$V_P = \frac{dx}{dt} = -r\omega\sin\omega t \tag{2.29}$$

and the acceleration is

$$A_P = \frac{d^2x}{dt^2} = -r\omega^2\cos\omega t = -\omega^2 x \tag{2.30}$$

Here ω is a constant, and Eq. (2.30) is therefore the same as Eq. (2.27), which is the definition of simple harmonic motion.

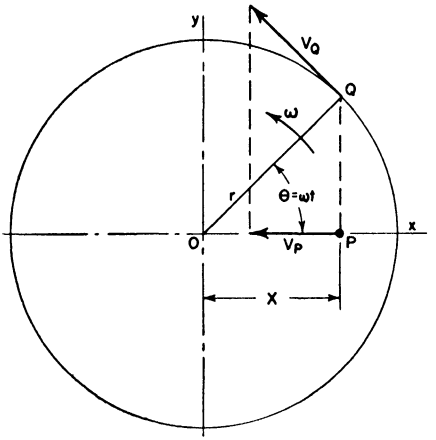

Fig. 2.7

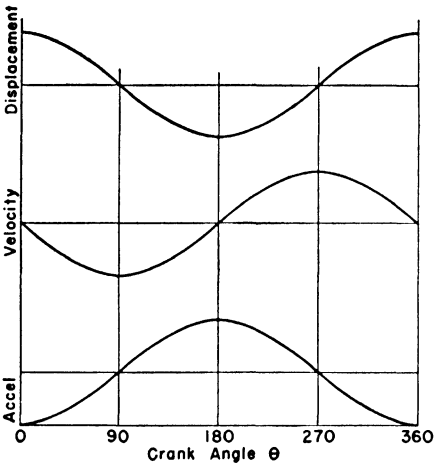

Fig. 2.8

2.6. Scotch yoke. A Scotch-yoke mechanism is shown in Fig. 2.9. A comparison of Figs. 2.9 and 2.7 shows that the horizontal slide performs simple harmonic motion when crank OQ rotates with constant angular

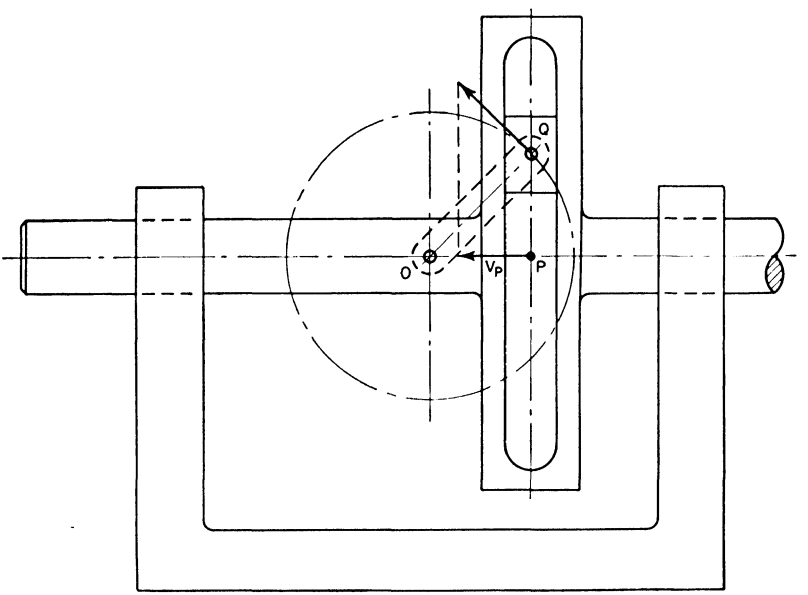

Fig. 2.9

velocity. Equations (2.28), (2.29), and (2.30) are plotted in Fig. 2.8. The nature of simple harmonic motion can be visualized by studying

Figs. 2.7 and 2.8. When Q is at the extreme right, the velocity of P is zero and its acceleration is a maximum to the left. As Q moves through the first quadrant, the velocity of P increases. The acceleration continues to the left, but at a diminishing rate. When Q has moved through 90°, the velocity of P is a maximum and the acceleration is zero. As Q moves through the second quadrant, the velocity of P decreases and the acceleration is to the right.

2.7. Relative motion. The motions previously considered were absolute motions. The motions were defined with respect to axes or a body considered to be at absolute rest. There is no point in the universe that is known to be at absolute rest. For most purposes the earth can be considered to be at absolute rest, and in many cases the frame of a machine can be considered to be at absolute rest even though it is moving with respect to the earth. An investigation of crankshaft failures in certain military trucks revealed that the gyroscopic effect of the flywheel resulting from the frame movement while operating over rough terrain was a contributing factor. This theory is covered in dynamics, and not in kinematics. In this book, unless otherwise stated, the frame will be at absolute rest.

The relative motion of a point or body is the motion with respect to some other point or body. The two following examples will help to clarify the concept of relative motion.

Example 1. Consider two automobiles, A and B, having respective velocities of 50 and 65 mph relative to the earth, as shown in Fig. 2.10. The velocity of

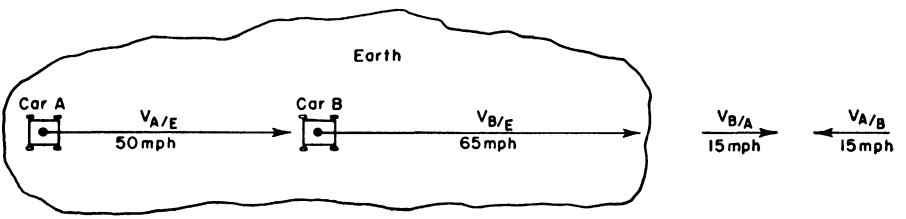

Fig. 2.10

car B relative to car A (written $V_{B/A}$) is the velocity of car B that would be apparent to an observer in car A if he thought of himself as being fixed; $V_{B/A}$ would be 15 mph to the right. The velocity of A relative to B, $V_{A/B}$, would be the velocity of car A that would be apparent to an observer in car B if he considered himself fixed. To such an observer, car A would appear to be backing at the rate of 15 mph. Note that $V_{A/B} = -V_{B/A}$.

It can be seen that

$$V_{A/B} = V_{A/E} \longrightarrow V_{B/E}$$

and

$$V_{B/A} = V_{B/E} \longrightarrow V_{A/E}$$

In everyday life, most motions are observed as absolute motions. Train passengers are often confused by relative motion. A passenger

seated in a train that is in a station may observe that the train on the adjacent track is backing. A glance at the platform reveals that the adjacent train is stationary and that his train is moving forward.

Example 2. Consider two ships, A and B, that have absolute velocities represented by the vectors $V_{A/E}$ and $V_{B/E}$, shown in Fig. 2.11. An observer on ship B thinks of himself as being fixed. Like the train passenger, he can do this by considering that the sea is moving backwards with a velocity of $-V_{B/E}$ (see Fig. 2.12).

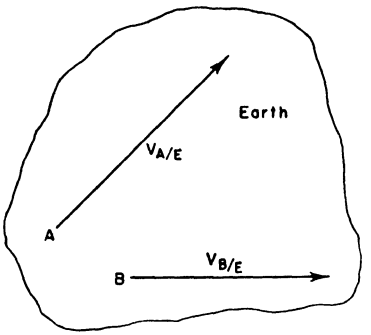

Fig. 2.11

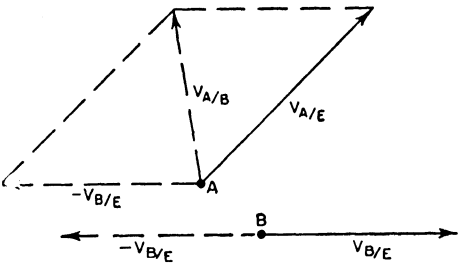

Fig. 2.12

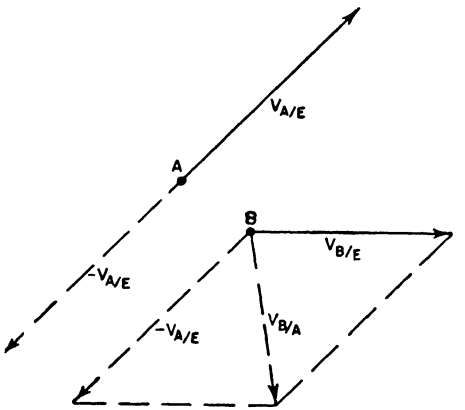

Fig. 2.13

From the observer's point of view, this assumed motion of the sea, $-V_{B/E}$, also carries ship A backwards, with the result that the observed velocity of A relative to B is $V_{A/B}$, as shown. In this example, as in the one above, use was made of the important principle, *the addition of equal velocities to two bodies does not change the relative velocities of the two bodies.*

In a similar manner, the velocity of B relative to A is determined in Fig. 2.13. Note again that

$$V_{A/B} = V_{A/E} \multimap V_{B/E}$$

$$V_{B/A} = V_{B/E} \multimap V_{A/E}$$

and

$$V_{A/B} = -V_{B/A}$$

In vector equations, the terms can be transposed and the subscripts reversed if the signs are changed. For example,

$$V_{A/B} = -V_{E/A} - \triangleright V_{B/E}$$
$$V_{A/E} = V_{A/B} + \triangleright V_{B/E}$$
$$-V_{E/B} = V_{A/E} + \triangleright V_{B/A}$$

etc. These equations can be verified by drawing vector diagrams.

The motion of one body relative to a second body can be defined as the motion of the first body minus the motion of the second body, or, simply stated, *relative motion is the vector difference.* If the motion of the second body is zero, the motion of the first body relative to the second body is the same as the absolute motion of the first body. Absolute motion is a special case of relative motion. When a vector symbol has only one subscript, for example V_A, it is understood that this represents the absolute velocity of A.

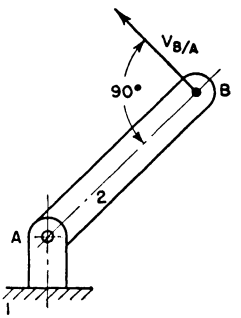

Fig. 2.14

In Fig. 2.14, the rigid link AB is pinned to the frame at point A. Point B cannot move towards or away from A, as this would cause failure of the link. An observer attached to link 2 at A would not observe any motion of point B as link 2 rotates. Point A is a double point; it is common to both 1 and 2. If an observer is attached to link 1 at A, he would observe the motion of B as link 2 rotates. This is understood when it is stated that *a point in a rigid body moves relative to another point in the same body, but in a direction at right angles to the line joining the two points.*

Leonardo da Vinci understood the concept of relative motion; he wrote, "But when the bird finds itself within the wind, it can sustain itself above it without beating its wings, because the function which the wing performs against the air when the air is motionless is the same as that of the air moved against the wings when they are without motion."* In wind tunnels, the airplane or model is stationary, and the air is caused to move.

In Art. 1.2, it was stated that kinematics of machines treats of the relative motion of machine parts. It is essential that the concept of relative motion be understood.

2.8. Inversion is the making of different mechanisms by fixing different links in a kinematic chain. As many mechanisms as there are links can be made from a given chain. The slider-crank chain has four links, and the four mechanisms made from this chain are shown in Figs. 2.15 to 2.18.

* *The Notebooks of Leonardo da Vinci,* MacCurdy, ed., London: Jonathan Cape, Ltd.

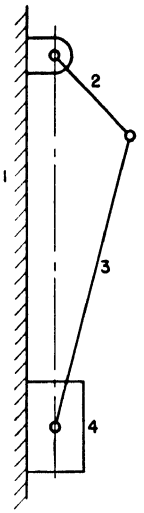

Fig. 2.15

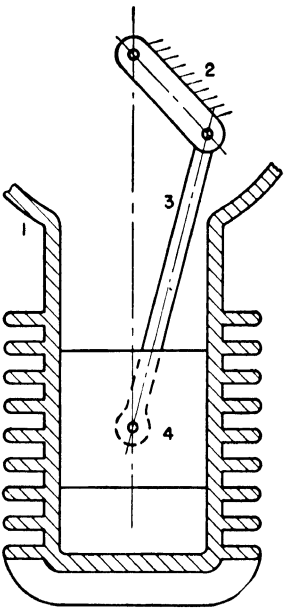

Fig. 2.16

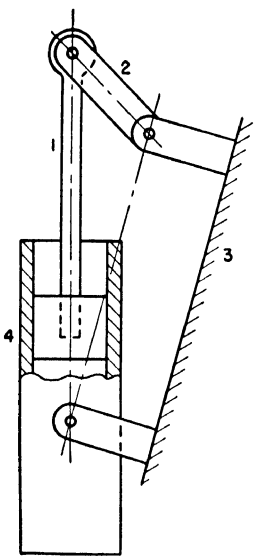

Fig. 2.17

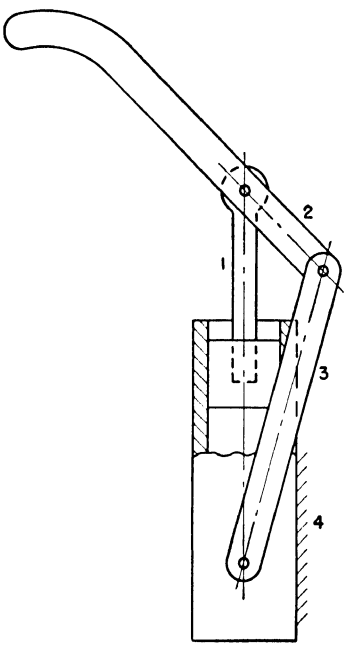

Fig. 2.18

The mechanism shown in Fig. 2.16 was used in the Gnome aircraft engine during World War I. The crankshaft was held stationary and the crankcase and cylinders rotated. The propeller was attached to the crankcase. This inversion is also used for a quick-return mechanism.

The mechanism shown in Fig. 2.17 is used in toy steam engines, and in the past has been used in marine engines. The piston of Fig. 2.15 has now become an oscillating cylinder. As crank 2 rotates, the piston slides in the cylinder and causes it to oscillate. This oscillatory motion of the cylinder is used to open and close steam ports, thus making a separate valve mechanism unnecessary.

The fourth inversion, shown in Fig. 2.18, is used for a pump.

2.9. Inversion and relative motion. A slider-crank chain is shown in Fig. 1.13. When the crank is moved from position θ_1 to θ_2, measured from the center line through the crank bearing and the wrist pin, the slider moves along this center line from position C to C'. This will always be true, regardless of which link is fixed. The motion of a point or link in a kinematic chain relative to some other point or link in the same chain is a property of the chain, and not of the mechanism. It does not matter which link is fixed. *Inversion has no effect upon relative motion.* This law will be used throughout the book.

2.10. Methods of transmitting motion. The four methods of transmitting motions are: (1) direct contact, Fig. 2.19; (2) intermediate rigid link, Fig. 2.20; (3) flexible connector, Fig. 2.21; (4) nonmaterial connectors, such as magnetic forces. The latter will not be considered in this book.

The driver is the link that receives motion from an external source. The driver imparts motion to the follower. In Fig. 2.19, the driver, link 2, rotates in a counterclockwise direction and imparts clockwise rotation to the follower, link 4. Link 4 could be the driver in a counterclockwise direction.

In Fig. 2.20, either link 2 or 4 can be the driver in either direction. The driver imparts motion to the follower through the intermediate rigid link 3. Link 3 can act in either tension or compression. The link connecting the driver and follower of a four-bar linkage is called the *coupler*.

Either pulley in Fig. 2.21 can be the driver in either direction. The driver imparts motion to the follower through the flexible belt 3. One side of the belt is always in tension.

2.11. Line of transmission. The driver imparts motion to the follower along the line of transmission. In Fig. 2.20, the line of transmission lies along link 3. Link 3 is pin-connected at P_2 and P_4. It can transmit motion and force only in tension and compression.

In Fig. 2.21, the line of transmission lies along the tension side of the belt. The belt is flexible, and can therefore transmit motion or force only along the centerline of the tension side.

In Fig. 2.19, the driver imparts motion to the follower along the common normal to the surfaces at the point of contact. The common normal and the line of transmission are the same line. The point of contact is a double point; it is designated P_2, a point in link 2, and P_4, a point in link 4. The center of rotation of 2 relative to 1 is designated O_{21}, a point common to 2 and 1. The center of rotation of 4 relative to 1 is designated O_{41}. Let the vector P_2R_2, perpendicular to $O_{21}P_2$, represent the velocity of point P_2. Then P_2R_2 is resolved into two components, P_2Q along the common normal, and P_2S_2 along the common tangent;

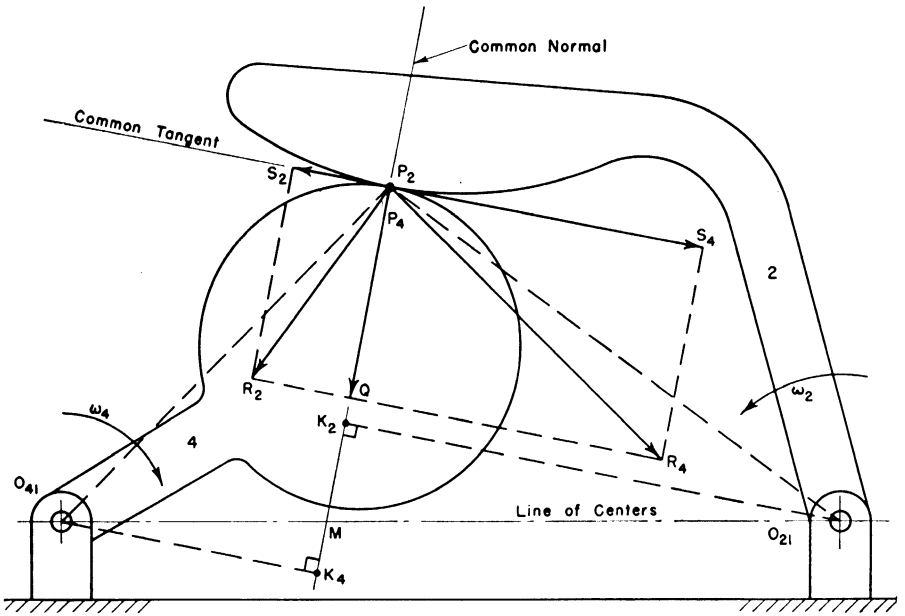

Fig. 2.19

P_2Q along the common normal is the driving component and P_2S_2 is the sliding component. The velocity of P_4 must be perpendicular to the line $O_{41}P_4$. It is represented by P_4R_4. The component of P_4R_4 along the common normal must equal P_2Q. If the component is greater, link 4 will leave contact with link 2. If the component is less, one of the links must bend or break. The driving component P_2Q then determines the length of vector P_4R_4. The sliding component P_4S_4 is then obtained. The vector difference of P_2S_2 and P_4S_4 represents the velocity of sliding of P_2 and P_4 due to the motion of both links.

2.12. Angular velocity ratio theorem. *The angular velocities of driver and follower are inversely as the segments on the line of centers cut by the line of transmission or inversely as the perpendiculars from the centers to the line of transmission.*

Referring to Fig. 2.19, the theorem is expressed by the equation

$$\frac{\omega_2}{\omega_4} = \frac{O_{41}M}{O_{21}M} = \frac{O_{41}k_4}{O_{21}k_2} \tag{2.31}$$

The proof that follows is from Fig. 2.19.

$$\omega_2 = \frac{V}{R} = \frac{P_2R_2}{P_2O_{21}} \qquad \text{and} \qquad \omega_4 = \frac{P_4R_4}{P_4O_{41}}$$

$$\frac{\omega_2}{\omega_4} = \frac{P_2R_2}{P_2O_{21}} \times \frac{P_4O_{41}}{P_4R_4} \tag{2.32}$$

Triangles QR_2P_2 and $k_2P_2O_{21}$ are similar since their sides are mutually perpendicular. From these triangles

$$\frac{P_2R_2}{P_2O_{21}} = \frac{P_2Q}{O_{21}k_2} \tag{2.33}$$

From similar triangles QR_4P_4 and $k_4P_4O_{41}$

$$\frac{P_4R_4}{P_4O_{41}} = \frac{P_4Q}{O_{41}k_4} \tag{2.34}$$

Dividing Eq. (2.33) by (2.34) gives

$$\frac{R_2P_2}{P_2O_{21}} \times \frac{P_4O_{41}}{P_4R_4} = \frac{P_2Q}{O_{21}k_2} \times \frac{O_{41}k_4}{P_4Q} = \frac{O_{41}k_4}{O_{21}k_2} \tag{2.35}$$

Substituting Eq. (2.35) in (2.32) gives

$$\frac{\omega_2}{\omega_4} = \frac{O_{41}k_4}{O_{21}k_2}$$

From similar triangles $O_{41}k_4M$ and $O_{21}k_2M$,

$$\frac{O_{41}k_4}{O_{21}k_2} = \frac{O_{41}M}{O_{21}M}$$

Hence

$$\frac{\omega_2}{\omega_4} = \frac{O_{41}M}{O_{21}M}$$

It is convenient to determine the angular-velocity ratio by drawing the common normal. When the intersection of the common normal and the line of centers lies off the paper, the perpendiculars can be used.

The notation in Fig. 2.20 is similar to that in Fig. 2.19. The same proof applies in this case.

The proof of the angular-velocity ratio theorem for Fig. 2.21 is simpler than that for the two previous cases, but is not so general. Let pulley 2 be the driver and V be the velocity of the belt.

$$P_2Q'' = V = r\omega_2 \qquad \text{and} \qquad P_4Q' = V = R\omega_4$$

Eliminating V from these two equations gives

$$\frac{\omega_2}{\omega_4} = \frac{R}{r}$$

where R and r are perpendiculars from the centers of rotation to the line of transmission. Triangles $MO_{41}P_4$ and $MO_{21}P_2$ are similar; hence

$$\frac{R}{r} = \frac{O_{41}M}{O_{21}M}$$

Therefore

$$\frac{\omega_2}{\omega_4} = \frac{O_{41}M}{O_{21}M}$$

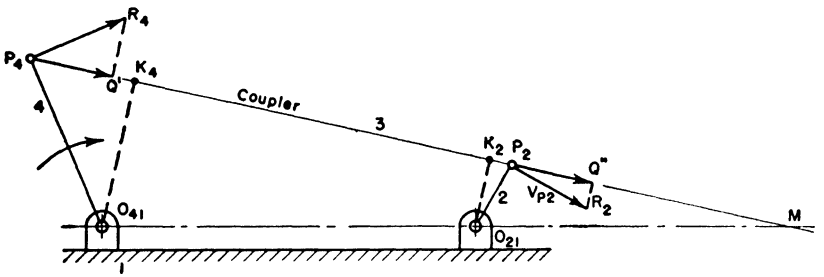

Fig. 2.20

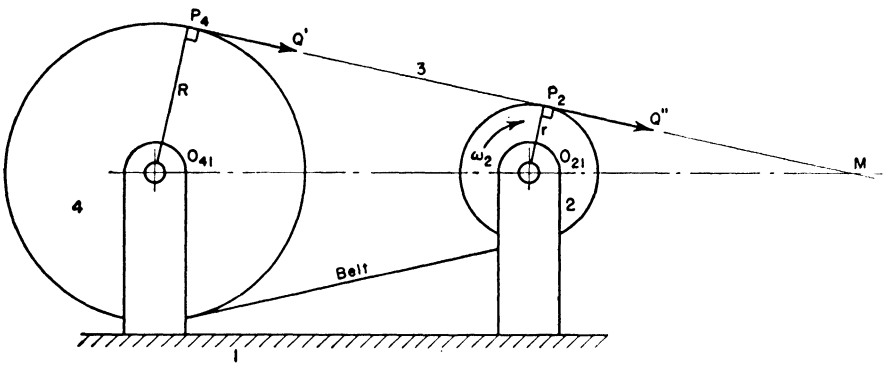

Fig. 2.21

2.13. Constant angular-velocity ratio. The center distance $O_{41}O_{21}$ is fixed. It follows that, *for constant angular-velocity ratio of driver and follower, the line of transmission must cut the line of centers at a fixed point.*

2.14. Directional relationship of driver and follower. In Fig. 2.19, the line of transmission cuts the line of centers between the centers, and links 2 and 4 rotate in opposite directions. In Fig. 2.20, the line of transmission cuts the line of centers outside of the centers, and links 2 and 4 rotate in the same direction. This is always true. It can be stated that *when the line of transmission cuts the line of centers between the centers the driver and follower rotate in opposite directions; when the line of transmission cuts the line of centers outside of the centers the driver and follower rotate in the same direction.*

2.15. Dead-center phase. In Fig. 2.22, link 2 is the driver. The line of transmission passes through the center of rotation of the follower. It can be seen that link 2 cannot drive 4. Link 2 merely subjects link 4 to compression. For dead-center phases, the angular-velocity ratio of follower to driver from Eq. (2.31) is infinity. In Fig. 2.23, a slider-crank mechanism is shown in top dead-center or head-end dead-center phase. A force applied to the piston will not cause rotation of the follower, link 2, because the line of transmission lies along link 3, which is collinear with the follower and passes through center O_{21}. A flywheel is necessary in engines to carry the links through the dead phases. The two slider-crank mechanisms of a steam locomotive are arranged with the cranks at 90° to each other so that both cannot be in dead phases at the same time. Sometimes failure occurs and the locomotive must operate with one cylinder. When this

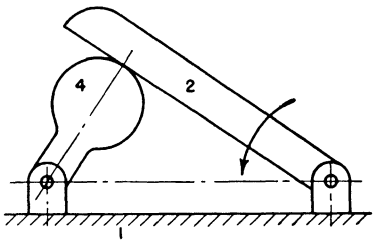

Fig. 2.22

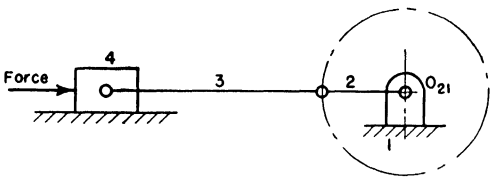

Fig. 2.23

happens the engineer must not stop the locomotive with the working cylinder on a dead phase, otherwise he would not be able to start again.

When the slider-crank mechanism is used for a compressor or pump, the crank is the driver, and there are no dead phases.

In Fig. 2.19, it can be seen that 2, when rotating clockwise, will not drive 4. For positive driving, the component of motion of the driver along the common normal must be directed toward the follower.

It can be stated that *for positive driving the line of transmission must not pass through the center of rotation of the follower, and the motion of the driver along the common normal must be directed toward the follower.*

2.16. Rolling contact. The direct-contact mechanism shown in Fig. 2.24 has contact on the line of centers for the phase shown. Let link 2 be the driver, and let the velocity of point P_2 be represented by the vector P_2R_2. The driving component along the common normal is P_2Q, and the sliding component is P_2S_2. The velocity of P_4 is P_4R_4. It will be equal to P_2R_2 since they coincide, and their components along the common normal must be equal. The sliding components P_2S_2 and P_4S_4

are equal. The velocity of sliding is the vector difference of P_2S_2 and P_4S_4. Since these vectors are equal, the sliding is zero.

When the point of contact is not on the line of centers, as shown in Fig. 2.19, vectors P_2R_2 and P_4R_4 do not coincide and the vector difference of P_2S_2 and P_4S_4 is not zero. Sliding exists. It can be stated that, *in direct-contact mechanisms, pure rolling exists when the point of contact lies on the line of centers.*

In Fig. 2.24, the line of transmission cuts the line of centers at the point of contact. The contact radii are equal to the segments into which

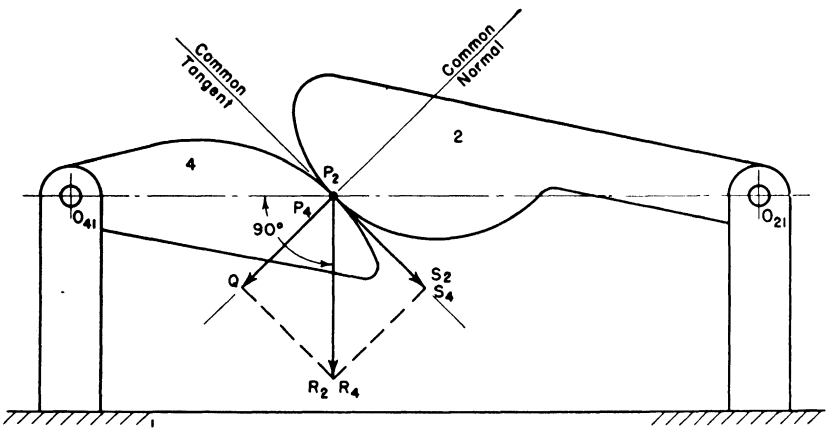

Fig. 2.24

the line of transmission cuts the line of centers. It can be stated that *the angular velocity ratio of driver and follower of mechanisms having rolling contact is inversely proportional to the contact radii.*

2.17. Huckert's theorem.* The nature of motion transfer can be summarized in a theorem: *The transfer of motion from one rigid body to another in a mechanism fulfills the necessary and sufficient conditions for turning when the relative displacement of the coincident particles is continuously zero; for rolling when the relative displacement is not zero and normal to the profiles at the point of contact; and for sliding when the relative displacement is not zero and along the tangent to the profiles at the point of contact.*

Any motion transfer that is not defined by one of these conditions is then a combination.

Turning and sliding are evident. Rolling will be illustrated with the cycloid. In Fig. 2.25, cylinder 2 is placed between flat surfaces 1 and 3. When 3 is moved horizontally, 2 rolls between 1 and 3. A point P'_2, on 2, will trace a cycloid on member 1, and P'_2 will contact 1 at the coincident point P_1P_2. This is a cusp in the cycloid. The two branches have

* Professor Jesse Huckert, The Ohio State University.

a common vertical tangent. The relative velocity of P_2 to P_1 is actually zero at the point of contact; the relative displacement changes from approach to recess. Points P_2 and P_1 come together and then move apart with relative motion along the common normal. All points on the roller make contact in this manner. Bridge rollers, rockers, and other devices having slow rolling contact and large loads are subject to fretting corrosion. A fine iron oxide powder appears. The theory is that contacting particles weld together and are pulled out of their parent members. The nature of rolling contact is consistent with this theory.

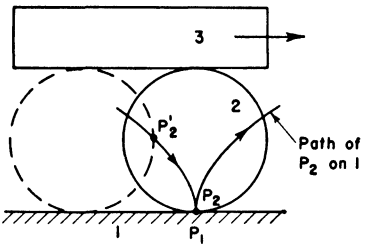

Fig. 2.25

PROBLEMS

2.1. A drag link mechanism is shown in Fig. P 2.1. The links are proportioned so that b can rotate continuously and pull d continuously but with a variable angular velocity. In order that there be no dead-center phase it is necessary that $b + c > a + d$ and $c + d > b + a$. Show that this leads to the additional relationship $c > a$.

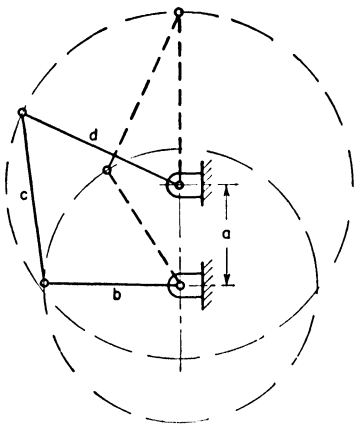

Fig. P 2.1

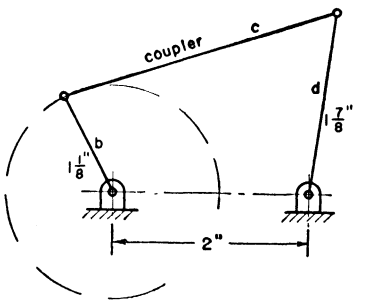

Fig. P 2.2

2.2. In Fig. P 2.2, link b is to rotate continuously, and d is to oscillate. Determine the theoretical maximum and minimum lengths for coupler c. Why, in practice, should the length be greater than the minimum and less than the maximum?

2.3. The Scott-Russell straight-line mechanism is shown in Fig. P 2.3. Here $OC = CB = DC$, and DCB is a rigid link. Show that D moves in a straight line that passes through O and is perpendicular to OB.

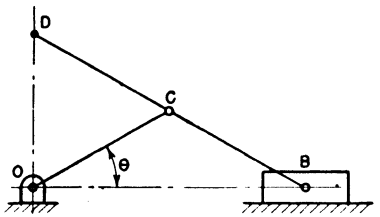

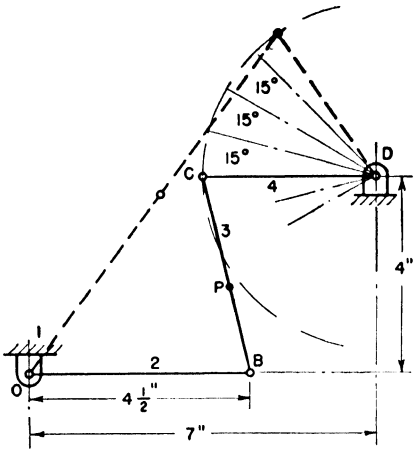

Fig. P 2.3 (above)
Fig. P 2.4 (right)

2.4. The Watt straight-line mechanism is shown in Fig. P 2.4. When the proportions are $CP/BP = OB/CD$ a portion of the path of P is very nearly straight. Plot the path of P using 15° intervals and the limiting positions for link CD. One limiting position is shown dotted. $CD = 3\frac{1}{2}$ in.

2.5. A steel cylinder 10 in. in diameter is to be machined in a lathe. The cutting speed is to be 95 fpm. Determine the required speed of rotation in rpm.

2.6. An automobile wheel 28 in. in diameter is rotating at 550 rpm. Determine the speed of the automobile in (a) mph, (b) fps, and (c) the angular speed of the wheel in radians per sec.

2.7. The relative velocity of two points lying on a radial line of a revolving disk is 40 fps. The points are 4 in. apart. Determine the rpm of the disk.

2.8. An automobile starts from rest and accelerates at the rate of 5 fps^2 until a speed of 60 mph is attained. Determine the time in seconds and the distance traveled in feet.

2.9. A body starts from rest and accelerates uniformly for a distance of 4 ft and then decelerates uniformly for a distance of 2 ft and comes to rest. The total time is 4 sec. Determine the maximum (a) acceleration, (b) deceleration, (c) velocity.

2.10. Same as Prob. 2.9 except there is an additional travel of 2 ft at uniform velocity between the acceleration and deceleration periods.

2.11. A gasoline engine is started from rest and attains a speed of 3000 rpm in 5 sec. Assuming that the angular acceleration is constant determine (a) the angular acceleration of the crankshaft in radians per second squared (b) the number of revolutions made in coming up to speed.

2.12. A wheel 32 in. in diameter is turning with a speed of 420 rpm and is accelerating at the rate of 20 rps^2. Determine in feet and seconds: (a) the tangential acceleration of a point on the rim, (b) the normal acceleration, (c) the total acceleration.

2.13. A Scotch-yoke mechanism is shown in Fig. P 2.13. Let $\theta = 60°$, $R = 11$ in., and the speed of the crank be 175 rpm. Determine the velocity and acceleration of slider 3.

2.14. Referring to Fig. P 2.13, let the stroke of the slider 3 be 18 in. and the time for one stroke be 0.06 sec. Determine (a) the rpm of the crank, (b) the maximum velocity of the slider, (c) the maximum acceleration.

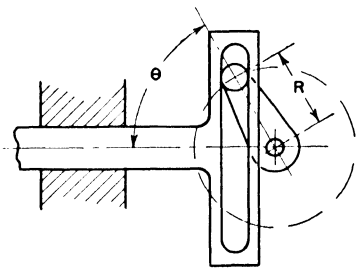

Fig. P 2.13

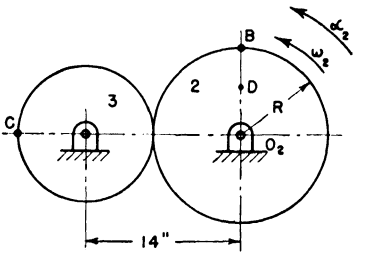

Fig. P 2.16

2.15. Measurements taken with a vibration meter show that a body is vibrating with harmonic motion at a frequency of 370 cycles per minute with a maximum acceleration of 260 in. per sec^2. Determine (a) amplitude of vibration, (b) maximum velocity.

2.16. Two wheels that roll together are shown in Fig. P 2.16. Let $R = 9$ in., $\omega_2 = 250$ rpm, $\alpha_2 = 75$ radians per sec^2. Determine A_B^n, A_B^t, A_B, A_C^n, A_C^t, A_C, $A_{C/B}$.

2.17. Same as Prob. 2.16 except $\omega_2 = 340$ rpm, $\alpha_2 = 125$ radians per sec^2, $R = 10$ in., and D, located midway between B and O_2, is used instead of B.

2.18. In Fig. P 2.18, frame 2 moves to the left with a velocity of 40 mph. Wheels 4 and 3 are 72 in. and 42 in. in diameter, respectively. Determine the velocities V_{O_4}, V_{B/O_4}, V_B, $V_{B/C}$, ω_4, ω_3, $\omega_{4/3}$, $\omega_{3/4}$.

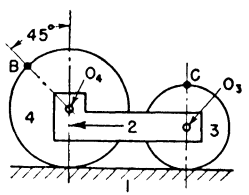

Fig. P 2.18

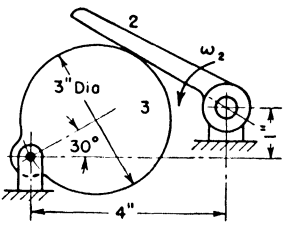

Fig. P 2.19

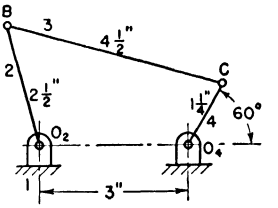

Fig. P 2.20

2.19. In Fig. P 2.19, $\omega_2 = 175$ rpm. Determine the angular velocity of member 3 in rpm and the velocity of sliding at the point of contact in fps.

2.20. In Fig. P 2.20, $\omega_2 = 150$ rpm CCW. Determine the angular velocity of member 4 in rpm.

2.21. Same as Prob. 2.20 except determine the angular velocity of link 3. (*Hint:* Use inversion, fix 2, and give proper ω to member 1; determine $\omega_{3/2}$, then absolute value of ω_3.)

CHAPTER 3

Velocities in Mechanisms

Instant Centers and Resolution

3.1. Introductory. There are two reasons why it is often necessary to make a velocity analysis: (1) The velocity analysis is used to determine cutting speeds in machine tools, to determine kinetic energy of parts that are designed to do work by virtue of their kinetic energy, to determine flow rates of fluids in machines such as engines and pumps, to determine load-carrying capacities of parts having film lubrication, etc. (2) The velocity analysis is a necessary step in making an acceleration analysis.

The illustrative examples that follow were chosen to represent the types of problems that are encountered in practice. The mechanisms are drawn in the simplest manner so that attention can be focused on the application of basic concepts to achieve the desired analysis.

3.2. Instant centers. An axis of rotation is an axis about which one body rotates relative to another body. In Fig. 3.1, member 2 rotates relative to member 1 about the axis O_{21}. This notation was first used in Art. 2.11. It can be written O_{21} or O_{12}. In plane motion, the motions of all points in a line perpendicular to the plane of motion are equal. It is not necessary to consider the thickness of the body; a study of the motion can be confined to one plane. The axis of rotation is often called the center of rotation.

An instant center of velocity is the point about which one body rotates relative to another for the particular phase being considered. It is a double point. The bodies have no linear velocity relative to each other at this point. At this point the two bodies have the same linear velocity relative to any other body.

Instant centers are of three types: fixed, permanent, and of a nature that is neither fixed nor permanent. These three types of centers occur in Fig. 3.5. Center O_{41} is a fixed instant center. It remains in the same place for all phases. Center O_{34} is the center about which link 3 rotates relative to 4 for the phase shown. This center moves when the mecha-

nism moves, but the joint is of a permanent nature; O_{34} is a permanent instant center. It will be shown later that O_{31} is the point about which 3 rotates relative to 1 for the phase shown. Links 3 and 1 have no material connection at this point, and the location of the point varies for each phase. Center O_{31} is an instant center that is neither fixed nor permanent.

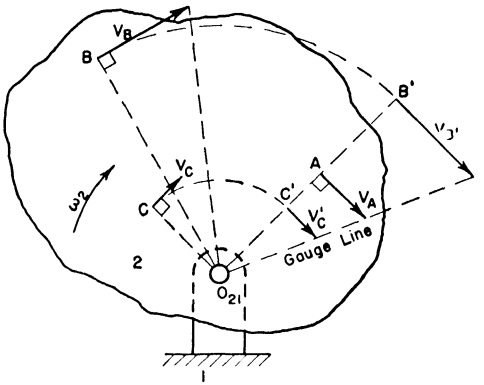

Fig. 3.1

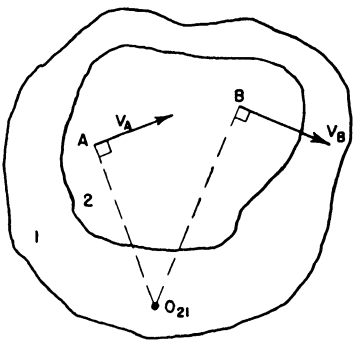

Fig. 3.2

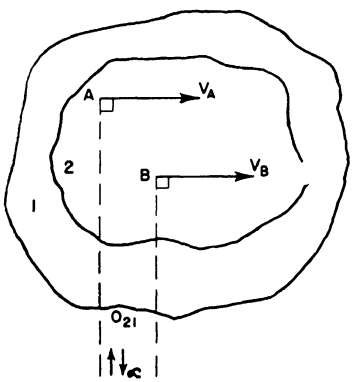

Fig. 3.3

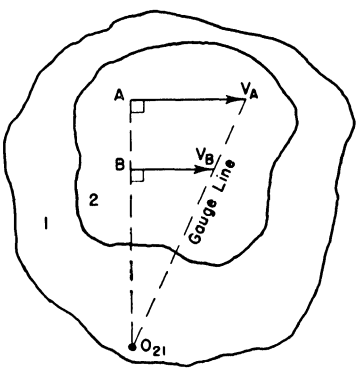

Fig. 3.4

In Fig. 3.1, let V_A be the velocity of point A. From Art. 2.7 and Eq. (2.8) it is known that the direction of the velocity of any point in 2 relative to O_{21} is perpendicular to the line joining the point and O_{21}. The magnitude is $V = R\omega_2$. The value of ω_2 is the same for all points in the body; the velocity of any point in 2 is therefore proportional to R, the radius of the circular path described by the point. The velocity of point B can be determined graphically as follows. A gage line is drawn through the center of rotation O_{21} and the terminus of the known velocity vector V_A. An arc of radius $O_{21}B$ is drawn locating B'. The velocity of point B' is $V_{B'}$. When this vector is rotated back to B it becomes V_B; V_C is determined in the same manner.

If the directions of the velocities of two points in a body relative to a second body are known, the center of rotation can be determined. In Fig. 3.2, V_A and V_B are the known velocities of points A and B, respectively, relative to a fixed body 1. Perpendiculars erected to the vectors at A and B intersect at the instant center of rotation O_{21}.

In Fig. 3.3, perpendiculars erected to the known velocity directions at A and B are parallel. The center of rotation of 1 and 2 is at infinity. Member 2 must therefore have translation relative to member 1. If 2 is a rigid body, V_A and V_B must be equal.

In Fig. 3.4, perpendiculars erected to the known velocity directions at A and B are collinear. The location of the center cannot be determined unless the magnitudes of the velocities are known. If they are known, a gage line, as shown, can be drawn, locating center O_{21}.

3.3. Instant centers in mechanisms. A four-bar linkage is shown in Fig. 3.5. Points O_{41} and O_{21} are fixed centers, and points O_{34} and O_{23}

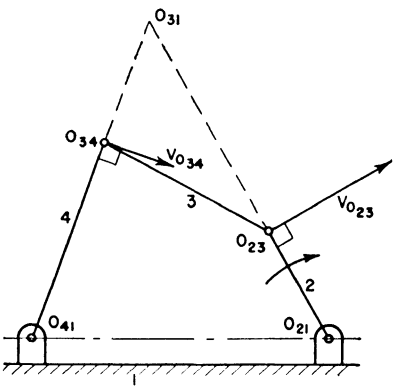

Fig. 3.5

are permanent centers. The direction of motion of O_{23} relative to 1, considered as a point in 2, is perpendicular to $O_{23}O_{21}$. Point O_{23} is also a point in 3; hence $V_{o_{23}}$ is also the velocity of point O_{23} relative to 1, considered as a point in 3. In a similar manner, $V_{o_{34}}$ is the velocity relative to 1 of point O_{34}, considered as a point in 3. The directions of motion of two points in 3 relative to 1 are known. The instant center O_{31} is located at the intersection of perpendiculars to these known velocities. Links 1 and 3 do not extend to include this point. If they did, it could be observed that links 1 and 3 have only relative rotation at this point.

Inversion does not affect relative motion (Art. 2.9). Only relative motions are being considered. Link 1 can be released and link 4 fixed, as shown in Fig. 3.6. The direction of $V_{o_{21}}$ is the direction of motion of point O_{21}, considered as a point in both 1 and 2, relative to 4. The

direction of $V_{O_{23}}$ is the direction of motion of point O_{23}, considered as a point in both 2 and 3, relative to 4. The directions of motion of two points in 2 relative to 4 are known. The instant center of rotation O_{24} is located by drawing perpendiculars to these directions.

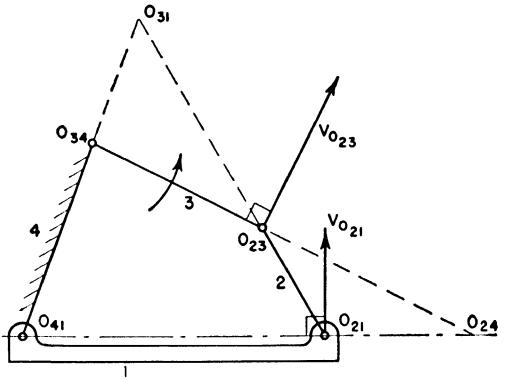

Fig. 3.6

The number of instant centers* in a mechanism is

$$\frac{n(n-1)}{2} \tag{3.1}$$

where n is the number of links. Locating the instant centers of a complex mechanism by the above method is tedious. A shorter method will be developed in the following articles.

3.4. Kennedy's theorem. *If three bodies have plane motion their instant centers lie on a straight line.* This theorem will be proved by showing that the third center cannot lie off the line passing through the other two, and then showing that it can lie on this line. In Fig. 3.7, center O_{21} is the instant center of 2 and 1, and O_{31} is the instant center of 3 and 1. Center O_{23} is assumed to lie off the line passing through O_{31} and O_{21}, as shown. The velocity of point O_{23} as a point in 3 is perpendicular to $O_{31}O_{23}$. The velocity of point O_{23} as a point in 2 is perpendicular to $O_{23}O_{21}$. These two velocities do not coincide. At this point, member 2 has linear velocity relative to member 3. This is contrary to

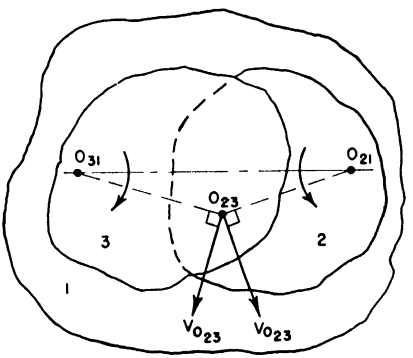

Fig. 3.7

* The number of pairs of links (or the number of instant centers) is the number of combinations of n links taken two at a time, which is

$${}_nC_2 = \frac{n!}{2!(n-2)!} = \frac{n(n-1)}{2}$$

the definition of an instant center. In Fig. 3.8, center O_{23} is assumed to lie on the line $O_{31}O_{23}$. In this case the velocity of O_{23} as a point in 3 coincides with the velocity of O_{23} as a point in 2. There is no relative linear velocity between the parts of this double point. The exact location of O_{23} on the line depends on the directions and magnitudes of the angular velocities of 2 and 3 relative to 1.

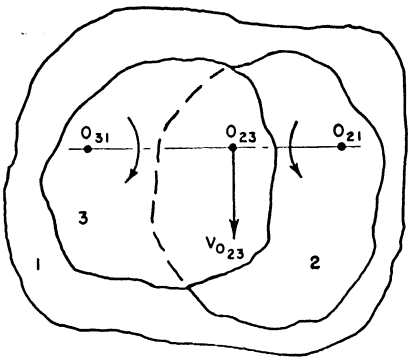

Fig. 3.8

In Fig. 3.6, note that the instant centers of 1, 3, and 4 (O_{41}, O_{34}, O_{31}) lie on a line, the instant centers of 3, 2, and 4 (O_{34}, O_{23}, O_{24}) lie on a line, etc.

3.5. Direct-contact mechanisms. In Fig. 3.9, the point of contact of 2 and 4 is the double point P_2P_4. The velocity of P_2 relative to the frame is the velocity vector P_2R_2, and the velocity of P_4 relative to the frame is P_4R_4 (see Fig. 2.19). The only velocity that P_4 can have relative to P_2 is sliding along the common tangent. The velocity of sliding of P_4 on P_2 is V_{P_4/P_2}. The center of rotation of 2 and 4 lies on the

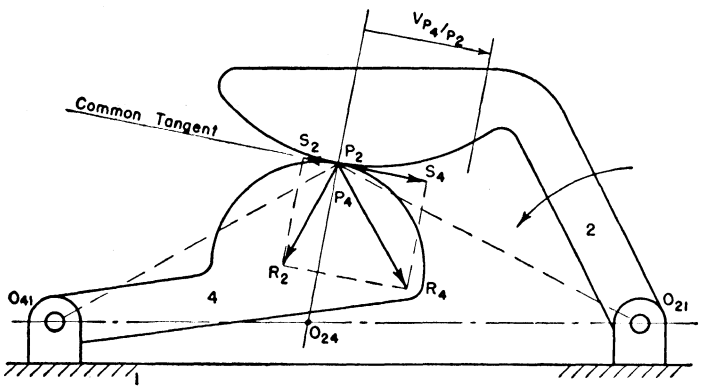

Fig. 3.9

perpendicular (the common normal) through the origin of this vector. The velocity of sliding V_{P_2/P_4} is equal and opposite to V_{P_4/P_2}. This is not an independent vector, but just another way of stating what is already known. Additional information can be obtained from Kennedy's theorem. It is known that center O_{24} lies on a line through O_{41} and O_{21}. The intersection of this line with the common normal locates center O_{24}.

3.6. Linear velocities. If the linear velocity of any point in a mechanism relative to the fixed member is known, the velocity of any

other point in the mechanism relative to the fixed member can be determined by the use of instant centers. In Fig. 3.10, $V_{O_{23}}$ is the known velocity of O_{23} considered as a point in 2. The velocity of O_{34} as a point in 4 can be determined as follows. Using O_{21} as a center, rotate vector $V_{O_{23}}$ to the position B on the line of centers. This vector is indicated as $V'_{O_{23}}$. It should be remembered that if link 2 is extended to include B, then $V'_{O_{23}}$ would be the velocity of this point in link 2. A gage line through the center O_{21} and the terminus of vector $V'_{O_{23}}$ is used to determine the velocity of point O_{24} considered as a point in 2. Point O_{24} is also a point in 4. A gage line through center O_{41} and the terminus of $V_{O_{24}}$ can be used to determine the velocity of any other point in member 4. Using O_{41} as a center, an arc from O_{34} is drawn to C on the line of centers.

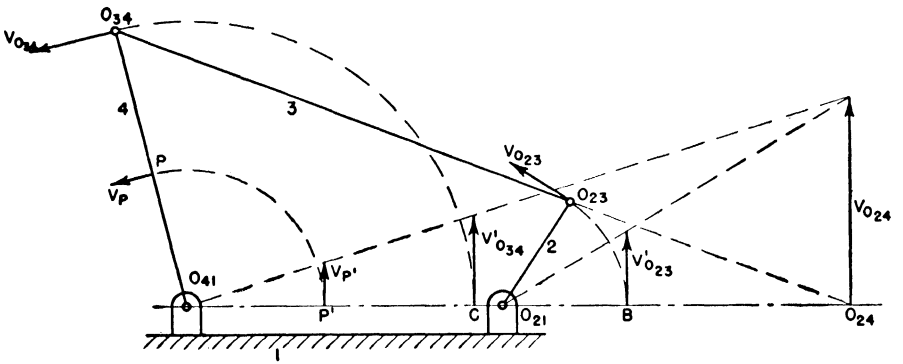

Fig. 3.10

Velocity $V'_{O_{34}}$ is the velocity of point C as a point in 4; $V'_{O_{34}}$ is rotated to position $V_{O_{34}}$, giving the desired vector.

In the above example, O_{24} was used as a transfer point. It was used to transfer from the known member 2 to the unknown, 4. This method is general. From Kennedy's theorem, the centers of rotation of known and unknown members and their common center or transfer point lie on a line.

The above example could have been solved in another manner, as shown in Fig. 3.11. Points O_{23} and O_{34} are both in member 3. The velocity of O_{23} as a point in 3 relative to 1 is known. A gage line through O_{31} and the terminus of $V_{O_{23}}$ can be used to determine the velocity of any other point in member 3. $V_{O_{34}}$ is determined as shown.

If $V_{O_{23}}$ is given, and it is desired to determine the velocity V_P, then $V_{O_{34}}$ must be determined first; then a gage line through O_{41} and the terminus of $V_{O_{34}}$ is used to determine V_P. By the method used in Fig. 3.10, V_P can be found without first determining $V_{O_{34}}$.

If the velocity of one point in a mechanism relative to some other point in the mechanism is desired, the absolute velocities are determined

first. These are used to determine the relative velocity, as explained in Art. 2.7.

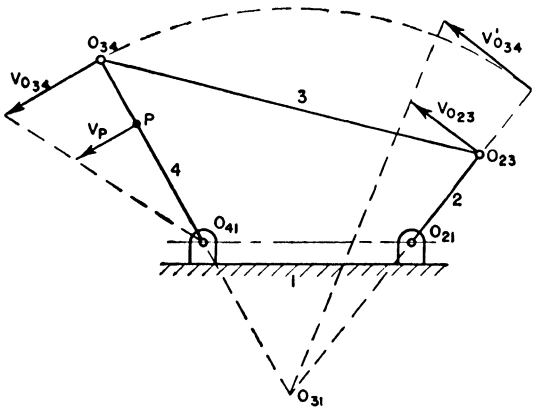

Fig. 3.11

3.7. Parallel line construction. A four-bar linkage is shown in Fig. 3.12. The velocities of D and C are to be determined from the

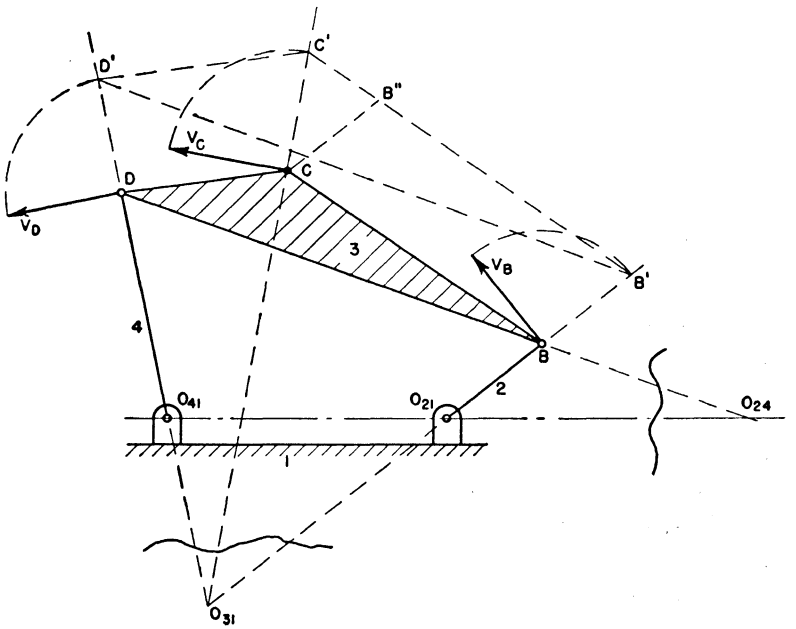

Fig. 3.12

known velocity of B. Assume that O_{24} and O_{31} lie off the paper and are not available for making constructions. The desired velocities can be determined as follows. Lay off BB' equal to V_B along the line $O_{21}B$ which passes through the center O_{31}. Construct $B'C'D'$ by drawing

lines parallel to the sides of link BCD. Then CC' is equal to $|V_C|$; the direction of V_C is perpendicular to CC'. This construction can be proved as follows. Draw CB'' parallel to BB'. Triangles $O_{31}BC$ and $CB''C'$ are similar. The velocities of points in a rotating body are proportional to their distances from the center of rotation; hence

$$\frac{V_B}{V_C} = \frac{O_{31}B}{O_{31}C} = \frac{CB''}{CC'} = \frac{BB'}{CC'}$$

Since BB' was made equal to $|V_B|$, CC' is equal to $|V_C|$; and V_D is determined in a similar way.

The parallel line construction is used for determining the velocities of points in a link from the known velocity of a point in the same link.

3.8. Angular velocities. Angular velocities can be determined from linear velocities, and vice versa. If, in Fig. 3.10, ω_2 is known, $V_{O_{23}}$ can be determined from the equation

$$V_{O_{23}} = R\omega = (O_{21}O_{23})\omega_2$$

and $V_{O_{34}}$ is determined by one of the methods of the previous articles. Then ω_4 is

$$\omega_4 = \frac{V}{R} = \frac{V_{O_{34}}}{O_{41}O_{34}}$$

A more direct method of obtaining ω_4 from ω_2 is to use O_{24} as a transfer point. The term $V_{O_{24}}$ is a velocity of points in 2 and 4.

$$\omega_2 = \frac{V}{R} = \frac{V_{O_{24}}}{O_{21}O_{24}}, \qquad \omega_4 = \frac{V_{O_{24}}}{O_{41}O_{24}}$$

Dividing the second equation by the first gives

$$\frac{\omega_4}{\omega_2} = \frac{V_{O_{24}}}{O_{41}O_{24}} \times \frac{O_{21}O_{24}}{V_{O_{24}}} = \frac{O_{21}O_{24}}{O_{41}O_{24}} \tag{3.2}$$

or

$$\omega_4 = \omega_2 \frac{O_{21}O_{24}}{O_{41}O_{24}}$$

In the same manner, ω_3 can be determined from ω_2 (see Fig. 3.11). Here $V_{O_{23}}$ is the velocity of points in 2 and 3; ω_2 and the centers of rotation O_{21} and O_{31} are known; hence

$$\omega_3 = \omega_2 \frac{O_{21}O_{23}}{O_{31}O_{23}}$$

Equation (3.2) can be stated as a theorem: *The angular velocities of two members are inversely proportional to the distances from the centers of rotation of the two members to their instant center (the third center located by Kennedy's theorem).*

Compare Fig. 3.9 with Fig. 2.19. Note that point M in Fig. 2.19 corresponds to O_{24} in Fig. 3.9. Make the same comparison with Fig. 3.10 and Fig. 2.20. It is always true that the intersection of the line of centers and the common normal of driver and follower is the instant center of

driver and follower. The above theorem is equivalent to the angular velocity theorem of Art. 2.12.

3.9. Obvious centers. In order to locate instant centers, using Kennedy's theorem, it is first necessary to locate all the obvious centers. If these are not located, some of the others cannot be found. In direct-contact mechanisms such as Fig. 3.9, the intersection of the common normal with the line of centers of driver and follower should be recognized as an instant center. The mechanism shown in Fig. 3.13 is of no practical value, but is shown because it includes all other types of obvious centers. Wheel 4 rolls on track 1; it pushes the slider 2 on the

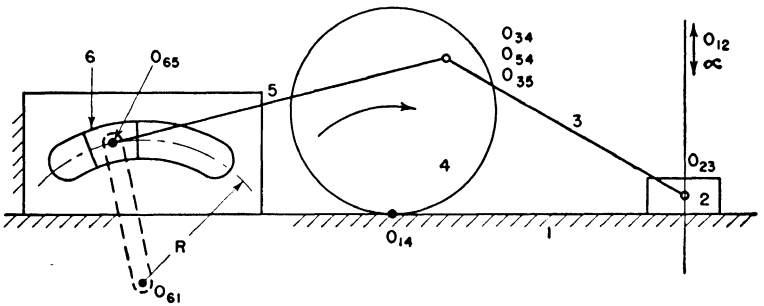

Fig. 3.13

horizontal surface of 1, and pulls slider 6 in the curved slot in 1. All centers shown are obvious and must be indicated before Kennedy's theorem can be applied for locating the other centers. The pin connections in the sliders are O_{23} and O_{65}. Members 3, 4, and 5 are pinned at one point. Centers O_{34}, O_{54}, and O_{35} are located here. Wheel 4 rolls on the track without sliding. At the point of contact the wheel and track have no relative linear motion. This point is therefore the instant center O_{14}. If block 6 is extended, as shown by broken lines, and pinned to 1 at the center of curvature of the slot, block 6 will have the same motion that it has when moving in the guide. Point O_{61} is the instant center of 6 and 1. Block 2 has rectilinear motion relative to 1. The center of curvature of the path of 2 relative to 1 is at infinity. Point O_{12} is therefore at infinity (see Fig. 3.3).

Example 1. Locate all the instant centers for the mechanism shown in Fig. 3.14. The number of instant centers is

$$\frac{n(n-1)}{2} = \frac{4(4-1)}{2} = 6$$

The obvious centers O_{34}, O_{23}, O_{21}, and O_{41} are located first. From Kennedy's theorem it is known that O_{31} lies on a line through O_{21} and O_{32}. It also lies on a line through O_{41} and O_{34}. It therefore lies at the intersection of these two lines. Center O_{24} will be located at the intersection of lines $O_{34}O_{23}$ and $O_{41}O_{21}$. Line $O_{41}O_{21}$ is at infinity. Point O_{24} therefore lies on line $O_{34}O_{23}$ at infinity.

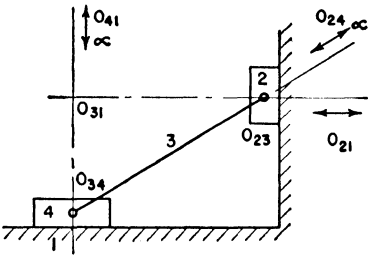

Fig. 3.14

Example 2. A steam-locomotive mechanism is shown in Fig. 3.15. The motion of the frame relative to the track will be considered. The number of instant centers is

$$\frac{6(6-1)}{2} = 15$$

When a mechanism has a large number of instant centers, some simple method of recording them is desirable. One method is shown in Fig. 3.16. Points with numbers corresponding to the links are located in a circular arrangement. When

Fig. 3.16

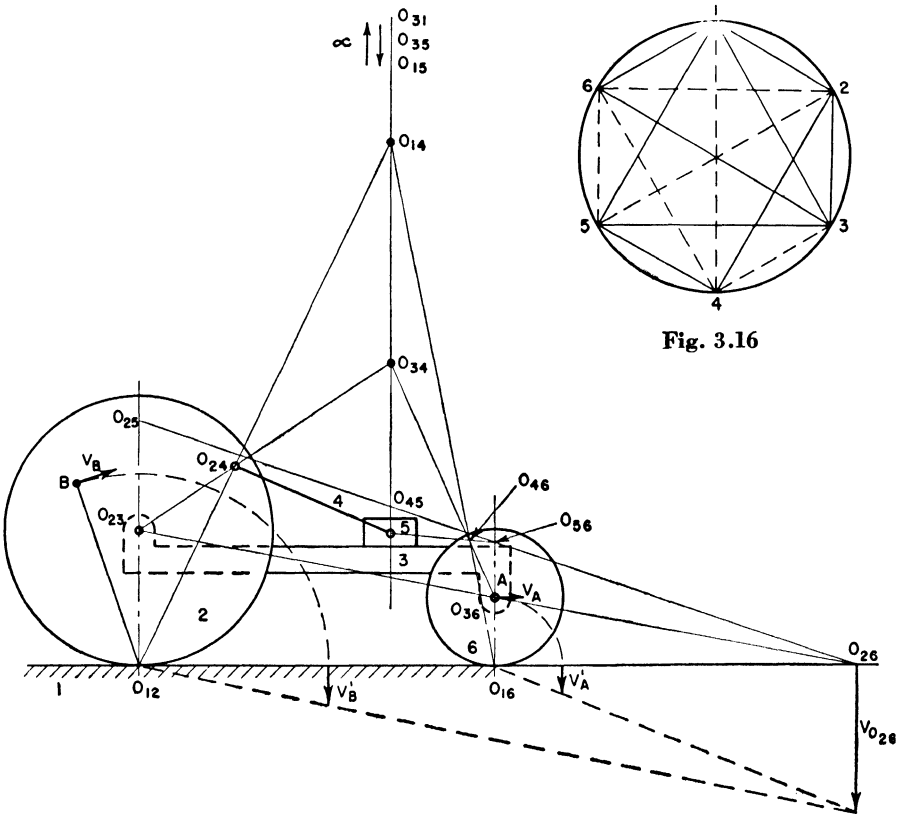

Fig. 3.15

a center is located on the mechanism, a line is drawn joining the corresponding points in Fig. 3.16. Point O_{23} is an obvious center. It is indicated on the mechanism, and then a line is drawn from 2 to 3 in Fig. 3.16. The other obvious centers are located and recorded with solid lines.

The broken lines in Fig. 3.16 represent the centers that are located with the use of Kennedy's theorem. There is no definite order for locating these points. Point O_{34} can be located next. In Fig. 3.16, solid lines exist from 2 to 3 and 2 to 4. A line through these available centers O_{23} and O_{24} contains O_{34}. A solid line connects 1 and 3 but not 1 and 4. Center O_{41} is not yet known. This condition exists at point 6. From point 5, solid lines extend to 3 and 4. These centers are available, and a line through O_{35} and O_{45} can be drawn and O_{34} located. A solid line is now drawn from 3 to 4, indicating that O_{34} is available for use in determining other centers. The remaining centers are located in a similar manner.

Assume that the velocity of the locomotive is known. It is desired to determine the velocity of point B in wheel 2 relative to the track. The velocity of frame 3 is that of the locomotive. This known velocity is laid off as V_A at point A on the frame. This is also a point in 6. Point O_{26} is used as a transfer point to obtain the velocity of B in 2. The velocity V_A could have been laid off at O_{23}, thus obtaining the velocity of a point in 2 directly.

3.10. Linear velocities by resolution. In Art. 1.13, it was shown that the displacement of a body having plane motion can be considered separate rotational and translational displacements. It was stated that the motion at any instant can be considered a combination of rotation and translation relative to some point. This will now be shown. In Fig. 3.17, body 2 has rotation ω_2 about instant center O_{21}. This completely defines the motion of 2 relative to 1 for the instant shown. The velocity of B is V_B.

If a point in 1 other than O_{21} is chosen for the reference point, the motion must be specified as a rotation with angular velocity ω_2 about the new point, plus a translation. A translation component can be assumed and the new reference point determined, or a reference point can be chosen and the translation determined. The first case will be considered first.

If an arbitrary translational velocity is added to body 2, the linear velocity of every point in the body relative to 1 will be changed, but ω_2, the relative angular velocity of the bodies, will not be changed since no angular velocity is added. A translational velocity $V_B(t)$ is added to the body. The velocity of B relative to 1 is now $V_B(r)$, the vector sum of $V_B(t)$ and V_B. The new instant center will lie on a perpendicular at the origin of vector $V_B(r)$. Since ω_2 is unchanged, the location of this center can be calculated from the equation

$$BD = \frac{V_B(r)}{\omega_2}$$

or can be obtained graphically by making θ' equal to θ. The double point

D_1D_2 is the instant center. If body 2 is now given translation V_{D_2/D_1}, equal but opposite to $V_B(t)$, the instantaneous motion will be restored to its original state. The original motion can therefore be specified as a rotation ω_2 about D_1 and a translation V_{D_2/D_1}.

The second case will now be considered. In Fig. 3.18, the motion of body 2 is ω_2 about O_{21}. The point D_1D_2 is arbitrarily chosen as a reference point. The velocity V_{D_2/D_1} is determined from the gage line as shown. The instantaneous velocity of 2 relative to 1 can be specified as rotation ω_2 about D_1 and translation V_{D_2/D_1}.

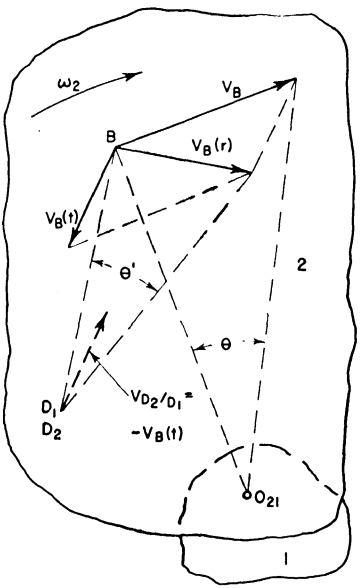

Fig. 3.17

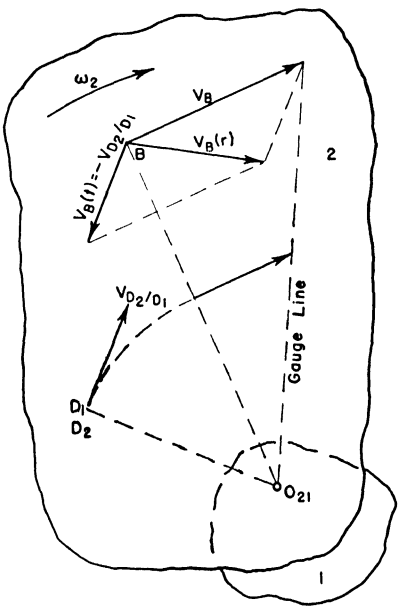

Fig. 3.18

In the resolution method for determining linear velocities, it is convenient to use a particular reference point. Link BC is shown in Fig. 3.19. The velocity of B is known and the direction of V_C is known. The instant center of the link O_{21} can be located as shown. The reference point D_1 that is used in the resolution method can be determined by drawing a perpendicular from the center O_{21} to the line joining the points of known velocity and known velocity direction. The translation component V_{D_2/D_1} can be determined from gage line [1] as shown, and V_{D_2/D_1} lies along line BC. This is why D_1 was so chosen. All points in link 2 have this translation component. In the resolution method, all the instant centers are not available. The reference point is obtained in a different manner. The translation component $V_B(t)$ is obtained by drawing EF perpendicular to BC. Then $V_C(t)$, the translation component of V_C, is equal to $V_B(t)$. The perpendicular at the terminus of

$V_C(t)$ determines the magnitude of V_C. The rotational components $V_B(r)$ and $V_C(r)$ are determined by completing the rectangles as shown. Gage line [2] through the termini of $V_B(r)$ and $V_C(r)$ locates the reference point D_1D_2.

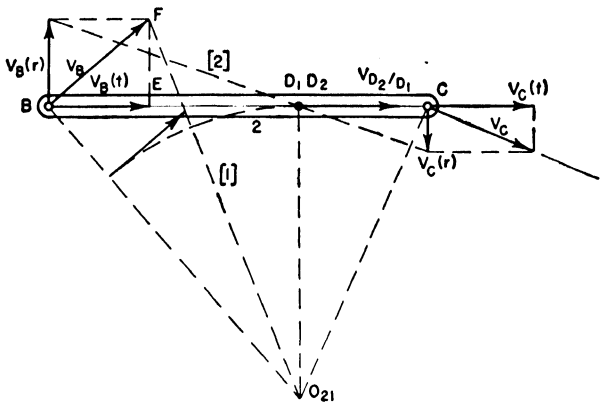

Fig. 3.19

Example 3. A four-bar linkage is shown in Fig. 3.20. The velocity of B is known, and it is desired to determine the velocities of C and E. The translational component $V_B(t)$ along line BC is determined by drawing a perpendicular from the terminus of V_B to line BC. Velocity $V_C(t)$ is equal to $V_B(t)$. The direction of V_C is perpendicular to CO_{21}. A perpendicular to BC at the terminus of $V_C(t)$

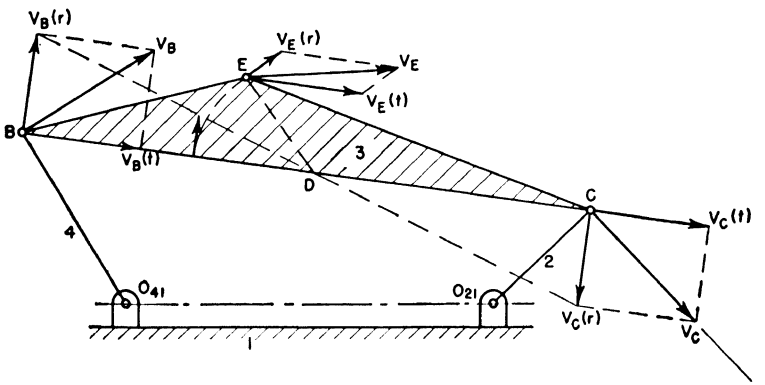

Fig. 3.20

determines the magnitude of V_C. The center of rotation D is determined from the gage line through the termini of $V_B(r)$ and $V_C(r)$. Then $V_E(r)$, the rotational component of E, is determined from this gage line. The translational component $V_E(t)$ is equal to $V_B(t)$, and V_E is the vector sum of $V_E(r)$ and $V_E(t)$.

Example 4. In Fig. 3.21, the velocity V_{B_2} is known, and the velocities of D and E are desired. The component of V_{B_2} that lies along the common normal of 2 and 4 (see Fig. 2.19) is V_{B_4}. The translational component along B_4C, obtained

by drawing a perpendicular from the terminus of V_{B_4} to B_4C, is zero. This results from the fact that the instant center O_{41} and the reference point D_1 coincide (see Fig. 3.19). The value of V_C is determined from the gage line as shown. The translational component of V_C along link 5 is $V_C(t)5$. The translational com-

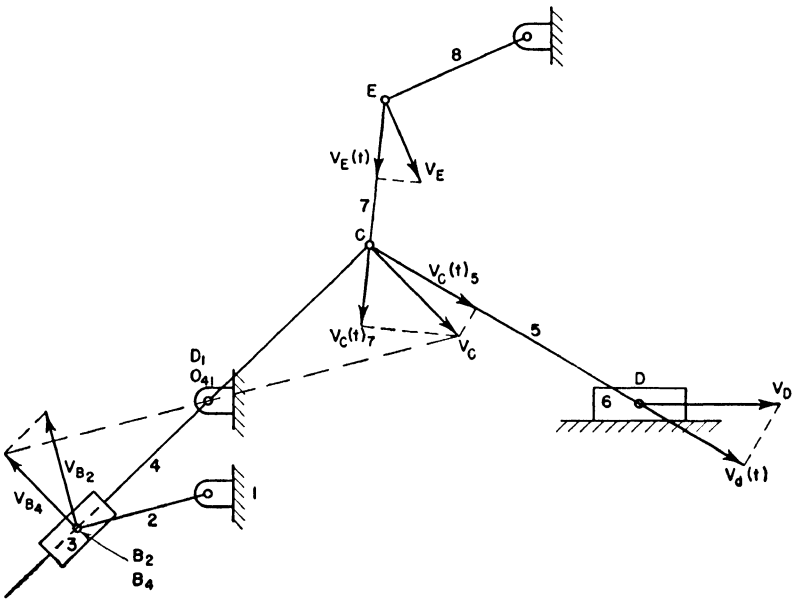

Fig. 3.21

ponent of D, velocity $V_D(t)$, is equal to $V_C(t)5$. The resultant velocity of D is horizontal. It is determined from the known component $Vd(t)$. Velocity $V_C(t)7$ is the translational component of V_C along link CE, and V_E is determined from the component $V_E(t)$.

PROBLEMS

3.1. Locate all the instant centers for the mechanism shown in Fig. P 3.1.

3.2. Locate all the instant centers for the mechanism shown in Fig. P 3.2.

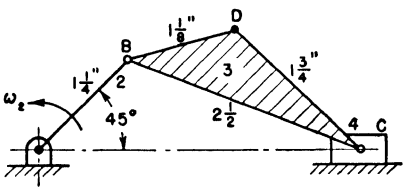

Fig. P 3.1

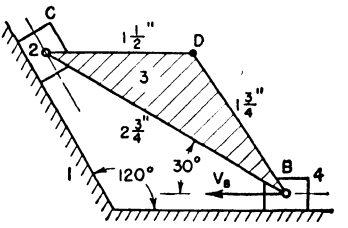

Fig. P 3.2

3.3. Locate all the instant centers for the mechanism shown in Fig. P 3.3.

3.4. Locate all the instant centers for the mechanism shown in Fig. P 3.4.

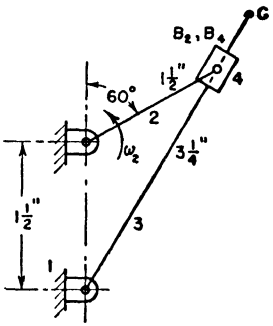

Fig. P 3.3

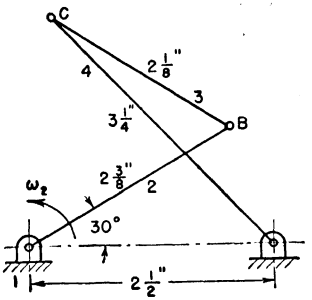

Fig. P 3.4

3.5. Locate all the instant centers for the mechanism shown in Fig. P 3.5.

3.6. Locate all the instant centers for the mechanism shown in Fig. P 3.6.

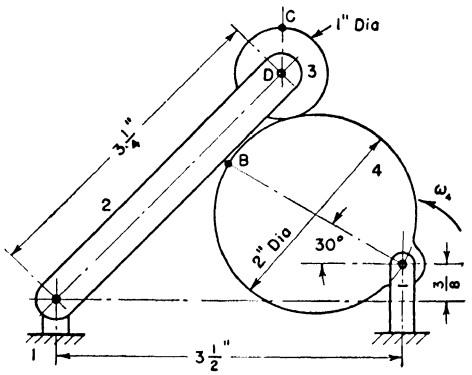

Fig. P 3.5

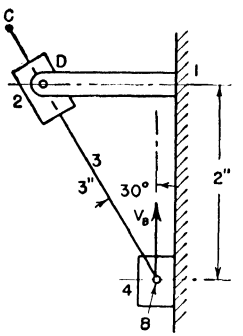

Fig. P 3.6

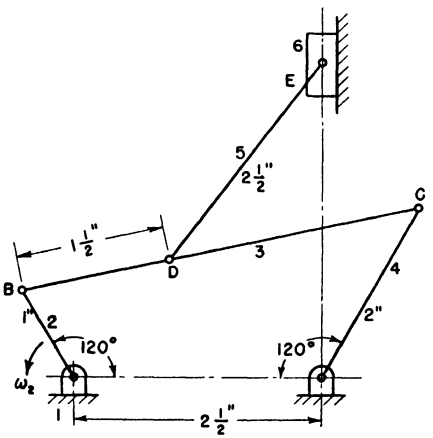

Fig. P 3.7

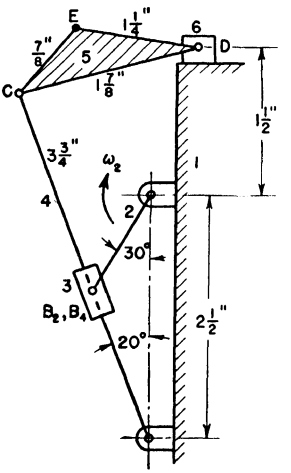

Fig. P 3.8

3.7. Locate all the instant centers for the mechanism shown in Fig. P 3.7.

3.8. Locate all the instant centers for the mechanism shown in Fig. P 3.8.

3.9. In Fig. P 3.1, let V_B be represented by a vector 1 in. long. Determine the vectors V_D and V_C.

3.10. In Fig. P 3.2, let V_B be represented by a vector 1 in. long. Determine the vectors V_D and V_C.

3.11. In Fig. P 3.3, let V_{B_2} be represented by a vector 1 in. long. Determine the vector V_C.

3.12. In Fig. P 3.4, let V_B be represented by a vector 1 in. long. Determine the vector V_C.

3.13. In Fig. P 3.5, let V_B be represented by a vector 1 in. long. Determine the vector V_C.

3.14. In Fig. P 3.6, let V_B be represented by a vector 1 in. long. Determine the vector V_C.

3.15. In Fig. P 3.7, let V_B be represented by a vector 1 in. long. Determine the vector V_E.

3.16. In Fig. P 3.8, let V_{B_2} be represented by a vector 1 in. long. Determine the vectors V_C, V_E, and V_D.

3.17. In Fig. P 3.1, let $\omega_2 = 150$ rpm. Determine ω_3.

3.18. In Fig. P 3.2, let $V_B = 20$ fps. Determine ω_3.

3.19. In Fig. P 3.3, let $\omega_2 = 250$ rpm. Determine ω_3.

3.20. In Fig. P 3.4, let $\omega_2 = 75$ rpm. Determine ω_3 and ω_4.

3.21. In Fig. P 3.5, let $\omega_4 = 100$ rpm. Determine ω_2 and ω_3.

3.22. In Fig. P 3.6, let $V_B = 30$ fps. Determine ω_3.

3.23. In Fig. P 3.7, let $\omega_2 = 80$ rpm. Determine ω_3, ω_4, ω_5, and ω_6.

3.24. In Fig. P 3.8, let $\omega_2 = 90$ rpm. Determine ω_3, ω_4, ω_5, and ω_6.

3.25. Using Fig. 2.19, show that the velocity of sliding at the point of contact is $(\omega_2 + \omega_4)PM$. When M lies outside the centers, show that the velocity of sliding is $(\omega_2 - \omega_4)PM$. (*Hint:* M is an instant center.)

3.26. In Fig. P 3.1, let V_B be represented by a vector 1 in. long. Determine V_C and V_D. Use the resolution method.

3.27. In Fig. P 3.6, let V_B be represented by a vector 1 in. long. Determine the vector V_C. Use the resolution method.

3.28. In Fig. P 3.7, let V_B be represented by a vector 1 in. long. Determine V_C, V_D, and V_E. Use the resolution method.

3.29. In Fig. P 3.8, let V_B be represented by a vector 1 in. long. Determine V_C, V_D, and V_E. Use the resolution method.

CHAPTER 4

Velocity Polygons

4.1. Velocity polygons. The velocity polygon or relative velocity method is a very useful and rapid way of determining linear and angular velocities in mechanisms. This method has the additional advantage over the instant center and resolution methods that it can be extended to make acceleration analyses. This will be considered in the next chapter. The key to the construction is, *the velocity of any point in a link relative to any other point in the same link is perpendicular to the line joining the two points.*

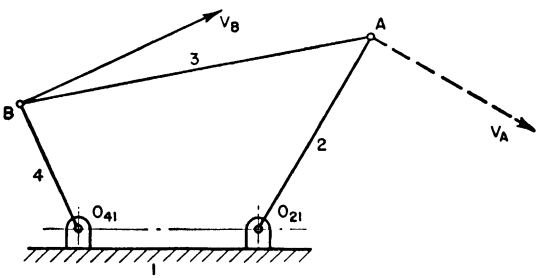

Fig. 4.1

Linear velocities are obtained by the use of the key and equations of relative velocity. In Fig. 4.1 the velocity of B is known, and the velocity of A is desired. A vector equation involving A and B is

$$V_{A/B} = V_A -\triangleright V_B$$

This equation can be written in the form

$$V_A = V_B +\triangleright V_{A/B} \tag{4.1}$$

The direction of V_A is known, V_B is known in magnitude and direction, and the direction of $V_{A/B}$ is known. This information is sufficient for solving the equation. In Fig. 4.2, V_B is laid off and a line in the direction of $V_{A/B}$ (perpendicular to BA) is drawn through the terminus of V_B. The origin of V_A will lie at the origin of V_B and the terminus of V_A will lie on the line containing $V_{A/B}$. A line is drawn through the origin of V_B in the direction of V_A. The intersection determines the magnitudes of V_A and

$V_{A/B}$. The notation that will be used in this book is shown in Fig. 4.3, where *ob* represents V_B, *oa* represents V_A, *ba* represents $V_{A/B}$, and *ab* represents $V_{B/A}$. The pole *o* is the point of zero velocity.

The mechanism in Fig. 4.4 is similar to that of Fig. 4.1. It is desired to determine the velocities of all lettered points. The velocity of B is known and V_A is determined as in the example above. The velocity of C

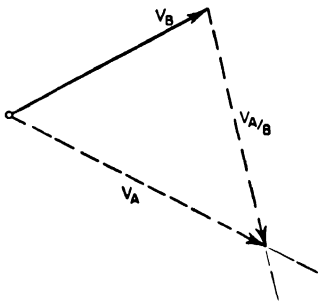

Fig. 4.2

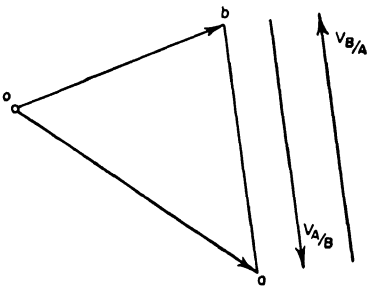

Fig. 4.3

can now be determined from the known velocities of B and A. An equation involving C and B is

$$V_C = V_B + \triangleright\ V_{C/B} \tag{4.2}$$

The magnitude and direction of V_B and the direction of $V_{C/B}$ are known. This information is not sufficient to solve the equation. An equation involving C and A is

$$V_C = V_A + \triangleright\ V_{C/A} \tag{4.3}$$

There is not sufficient information to solve this equation. Equations (4.2) and (4.3) can be solved simultaneously as shown in Fig. 4.5. From Eq. (4.2), V_B is laid off as *ob*. A line through *b* in the direction $V_{C/B}$ (perpendicular to *BC*) will contain the terminus of V_C. From Eq. (4.3), V_A is laid off as *oa*. A line through *a* in the direction $V_{C/A}$ (perpendicular to *CA*) will contain the terminus of V_C. Then *oc* is the vector V_C. In working problems separate diagrams are not drawn for determination of the velocity of each point. All work is done on one diagram or velocity polygon. Figures 4.3 and 4.5 are combined in Fig. 4.6. Point *a* on the diagram was determined by drawing lines of known direction through known points *o* and *b*, and *c* was determined by drawing lines of known direction through known points *a* and *b*. The directions of the velocities of $V_{D/B}$, $V_{D/C}$, and $V_{D/A}$ are known. Point *d* can be located by drawing lines of known direction containing the terminus of V_D through *b* and *c* or through *c* and *a*.

Point *d* can also be located by proportion. Each link in Fig. 4.4 has an image in Fig. 4.6 that is similar. Line *ob* is perpendicular to

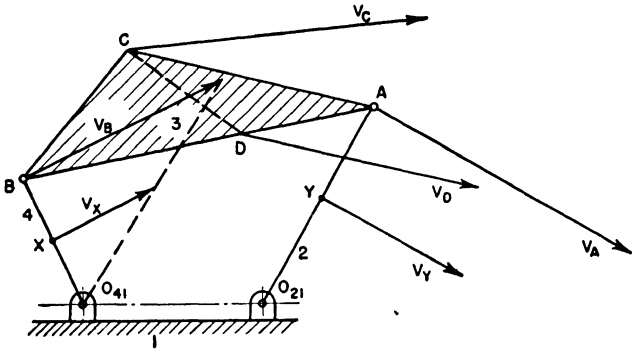

Fig. 4.4

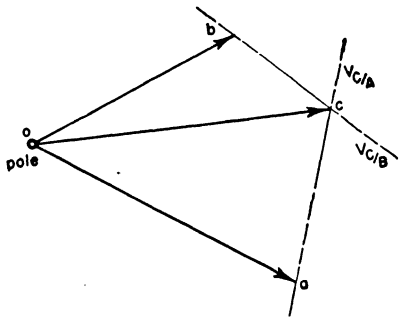

Fig. 4.5

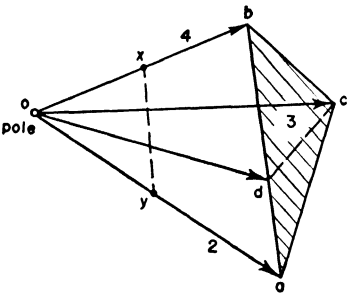

Fig. 4.6

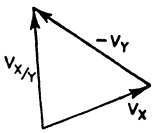

Fig. 4.7

$O_{41}B$, ba is perpendicular to BA, cd is perpendicular to CD, etc. These velocity images are rotated 90° relative to the links in the original mechanism. The frame has zero velocity. Its image is a point at the pole o. Then d can be located from the ratio

$$\frac{bd}{ba} = \frac{BD}{BA}$$

Now V_X can be determined from a gage line as shown in Fig. 4.4. It can also be obtained by properly locating x on ob, the velocity image of link 4. From similar triangles

$$\frac{V_X}{V_B} = \frac{O_{41}X}{O_{41}B}$$

Then ob represents V_B, ox will represent V_X if it is obtained from the ratio

$$\frac{ox}{ob} = \frac{O_{41}X}{O_{41}B}$$

and oy representing V_Y can be obtained in a similar manner.

The velocity of X relative to Y is

$$V_{X/Y} = V_X - \triangleright V_Y$$

This construction is shown in Fig. 4.7. The vector $V_{X/Y}$ is equal to the line from y to x in Fig. 4.6, and $V_{Y/X}$ is the line from x to y. Lines from the pole to points on the velocity polygon represent absolute velocities of the corresponding points on the mechanism. A line joining any two points on the velocity polygon represents the vector difference of the absolute velocities. From this it can be stated that *the velocity of any point on a mechanism relative to any other point on the mechanism is represented by the line joining the corresponding points on the velocity polygon.*

4.2. Angular velocities. The angular velocity of a link can be determined by dividing the velocity of a point in the link relative to any other point in the link by the distance between them. The angular velocity of link 3 in Fig. 4.4 is

$$\omega_{3/1} = \frac{V}{R} = \frac{V_{A/B} = ba}{AB}$$

or

$$\omega_{3/1} = \frac{V_{B/A} = ab}{AB}$$

or

$$\omega_{3/1} = \frac{V_{C/D} = dc}{CD}$$

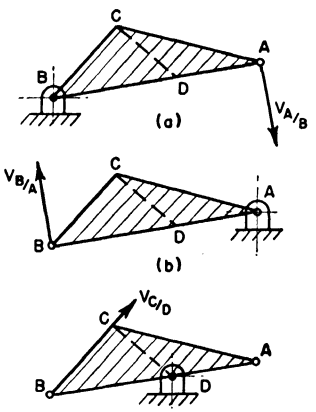

Fig. 4.8

etc. In the first case the velocity of A relative to B is taken. This means that B is thought of as being fixed. It is shown fixed in Fig. 4.8(a), and the vector $V_{A/B}$ is placed at A. It can be seen that link 3 has clockwise rotation. When considering a point fixed as is done above, the translation component that is associated with this reference point is eliminated. This does not affect the angular velocity.

Example 1. In Fig. 4.9 the angular velocity of link 2 is 443 rpm CCW. The velocity of C and the angular velocity of link 5 are desired. The velocity polygon

is shown in Fig. 4.10. All data apply to the original drawing. The velocity of A is

$$V_A = AO_{21}\omega_2 = \frac{1.125}{12} \times \frac{2\pi 443}{60} = 4.36 \quad \text{fps}$$

This is laid off as oa to an assumed velocity scale of 1 in. $= k_v = 2$ fps. The velocity of B relative to A is perpendicular to BA. A line through a in this direction contains b. The velocity of B relative to O_{41} is perpendicular to BO_{41}. A line through pole o in this direction contains b. Thus b is located at the intersection of these two lines. The motion of C relative to the frame is horizontal. A horizontal line through o contains c. The velocity of C relative to B is perpendicular to CB. A line through b in this direction contains c. Thus c is

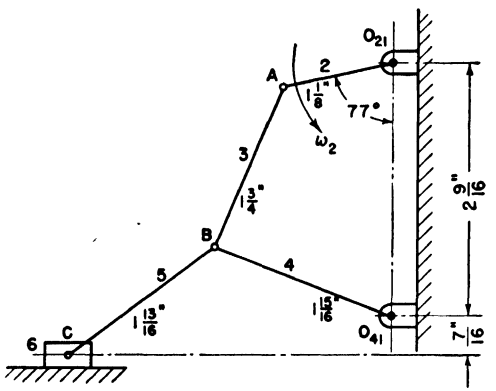

Fig. 4.9

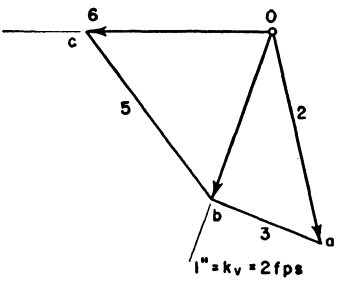

Fig. 4.10

located at the intersection of these two lines. On the drawing oc scales 1.9 in. The velocity of C is

$$V_C = ock_v = 1.9 \times 2 = 3.8 \quad \text{fps}$$

Block 6 has rectilinear translation relative to the frame. All points in it have the same velocity. The velocity image of 6 is a point at c.

The value of $V_{B/C}$ is obtained from the velocity polygon and is used to determine the angular velocity of link 5.

$$\omega_5 = \frac{V_{B/C}}{BC} = \frac{4.26}{1.8125/12} = 28.2 \quad \text{radians per sec CW}$$

Example 2. A direct-contact mechanism is shown in Fig. 4.11. Here ω_2 is known and the velocity of B is desired. Velocity V_{D_2} is the product of the radius D_2O_{21} and ω_2. This vector is laid off as od_2 in Fig. 4.12. The only motion that D_4 can have relative to D_2 is sliding along the common tangent at the point of contact. A line through d_2 in this direction contains d_4. The motion of D_4 relative to the frame is perpendicular to D_4O_{41}. A line through o in this direction contains d_4, and d_4 is located at the intersection of these two lines. To aid in visualizing the problem, BD_4O_{41} is indicated as a triangular member. For the

phase shown this triangular link has the same angular velocity as the circular link. Point b is determined from the known points o and d_4.

Example 3. A quick-return mechanism is shown in Fig. 4.13. Velocity V_{B_2} is known and the velocity of D is desired. Velocity V_{B_2} is laid off as ob_2 in Fig. 4.14. The direction of motion of B_4 is perpendicular to link CO_{41}. A line through o in this direction contains b_4. The motion of B_4 relative to B_2 is sliding along the link CO_{41}. A line through b_2 in this direction contains b_4, and b_4 is located at the intersection of these two lines. Then c is located by proportion. It is

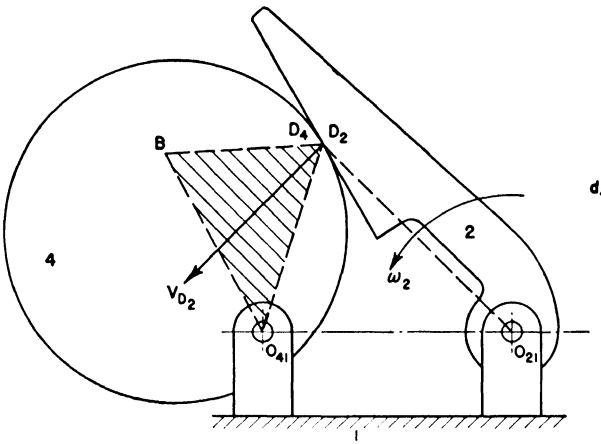

Fig. 4.11

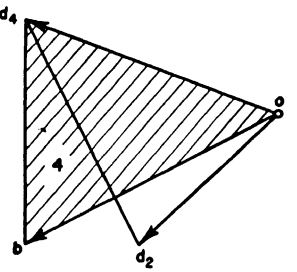

Fig. 4.12

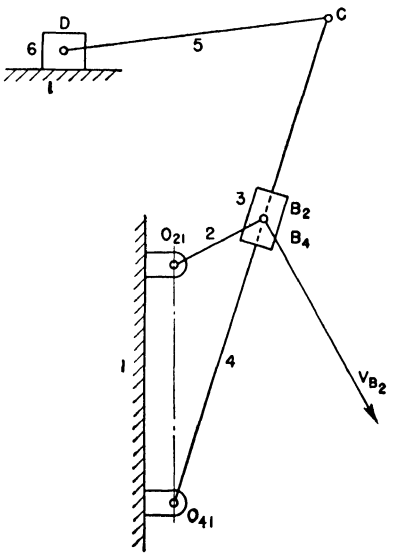

Fig. 4.13

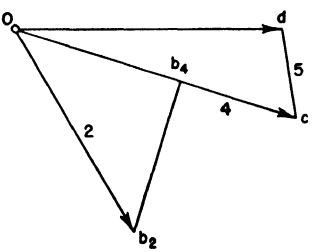

Fig. 4.14

known that link $O_{41}B_4C$ has a velocity image similar to it. Then b_4c is determined from the proportion

$$\frac{b_4c}{ob_4} = \frac{B_4C}{O_{41}B_4}$$

Point d is determined from the known points c and o.

Example 4. An oscillating cylinder mechanism is shown in Fig. 4.15. Here V_A is known and the velocity of point B is desired. Velocity V_A is laid off as oa in Fig. 4.16. The direction of motion of B is not known. It is necessary to select some point in 3 of known velocity direction. Member 3 is extended to include

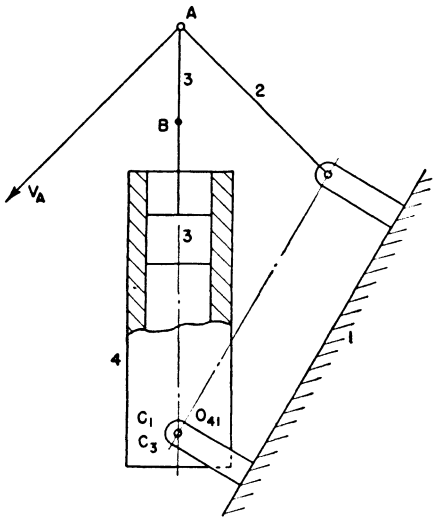

Fig. 4.15

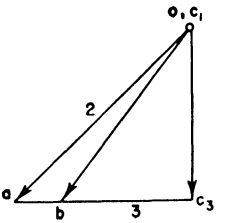

Fig. 4.16

point O_{41}. This does not alter the motions of the links. Point O_{41} is also indicated at C_1C_3, a double point in 1 and 3. The direction of motion of C_3 relative to C_1 is along the line AC_1. A line through o in this direction contains C_3. The direction of motion of C_3 relative to A is perpendicular to C_3A. A line through a in this direction contains c_3, and c_3 is located at the intersection of these lines. Then ac_3 is the velocity image of AC_3, and b is located by proportion.

Example 5. Trial solution. A quick return mechanism is shown in Fig. 4.17. Here V_{B_2} is known and the velocity of point D is desired. Velocity V_{B_2} is laid off as ob_2 in Fig. 4.18. A horizontal line through o contains d, a vertical line through o contains c, and a line through b_2 parallel to link 4 contains b_4. This information is not sufficient to locate a point in link 4. It is necessary to use a trial solution. It is known that link 4 will have a velocity image that is similar and perpendicular to DC. It is also known that one end of the image will lie on the line containing d, and the other end on the line containing c. A trial solution $(c)(d)$ is drawn and (b_4) is located by proportion. All conditions are satisfied except one: (b_4) does not lie on the line containing b_4. This solution is not correct. A second trial solution $((c))$ $((d))$ is made and $((b_4))$ is located by proportion. This solution is not correct. A line through (b_4) and $((b_4))$ will be the locus of b_4 for all trial solutions

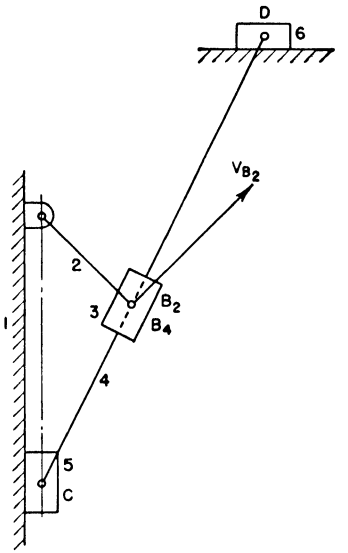

Fig. 4.17

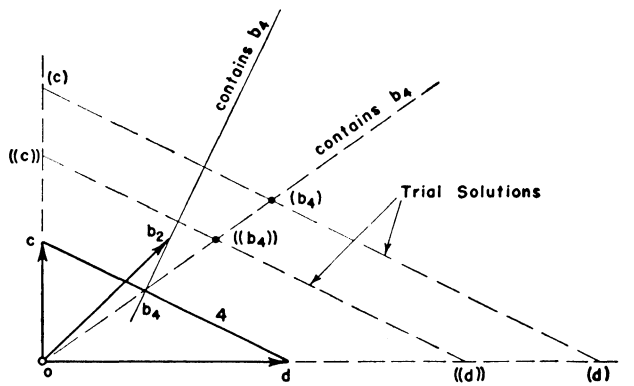

Fig. 4.18

and will therefore contain the correct b_4. The intersection of this line with the line through b_2 parallel to DC is the correct b_4. The correct image cb_4d is drawn. It can be seen that the line through (b_4) and $((b_4))$ passes through the intersection of the lines containing c and d. If this intersection is used only one trial solution is necessary.

Example 6. In Fig. 4.19 the velocity of B is known and the velocity of D is desired. Velocity V_{A_2} is determined from V_B as shown in Fig. 4.19. Wheels 2 and 3 have rolling contact; therefore $V_{A_2} = V_{A_3}$. Velocity V_F is determined from V_{A_3} as shown. Now V_B and V_F are laid off as ob and of, respectively, in Fig. 4.20. A line through f perpendicular to EF contains e, a line through b perpendicular to CB contains c, a vertical line through o contains d. A trial solution is necessary. Line $(e)(c)$ is drawn perpendicular to EC with one end on the line

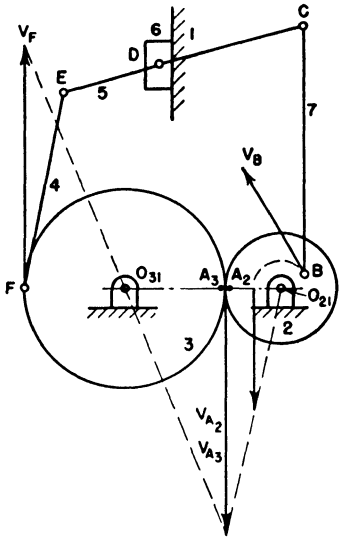

Fig. 4.19

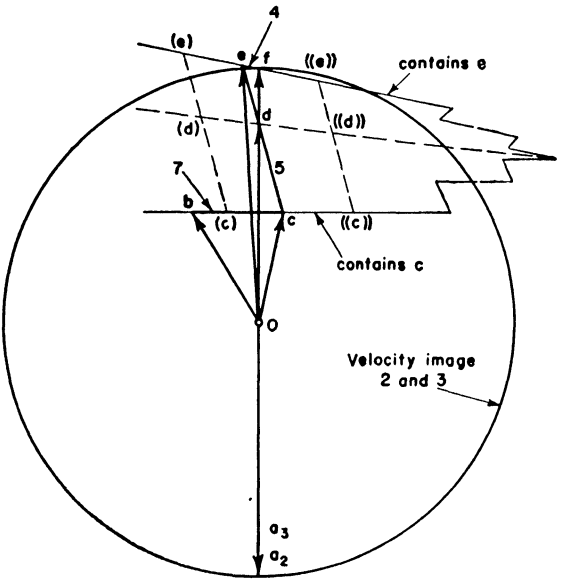

Fig. 4.20

containing e and the other end on the line containing c; (d) is located by proportion. The intersection of the lines containing e and c lies off the paper and is not available for use. A second trial solution $((e))((d))((c))$ is necessary. The intersection of the line through $(d)((d))$ and the vertical line containing d locates d.

The velocity images of 2 and 3 are shown. Both wheels have zero velocity at their centers and the same peripheral speed. One circle with its center at o

represents both wheels. The position of oa_2 relative to $O_{21}A_2$ shows that the image of 2 is rotated 90° CCW relative to member 2 in Fig. 4.19. The relative positions of oa_3 and $O_{31}A_3$ show that image 3 is rotated 90° CW relative to member 3.

Example 7. In Fig. 4.21 the velocity of A is known and the velocity of D is desired. An attempt to solve this problem will lead to trial solutions for links

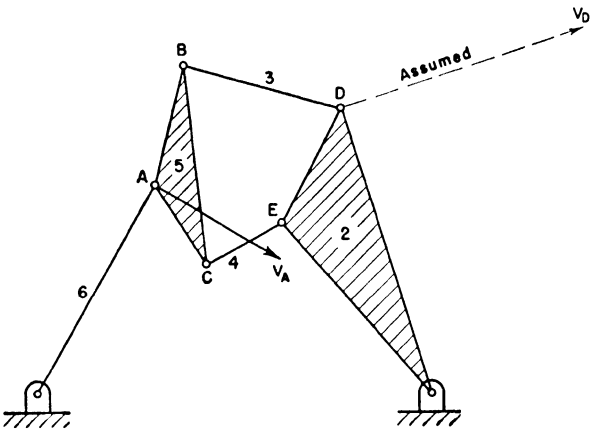

Fig. 4.21

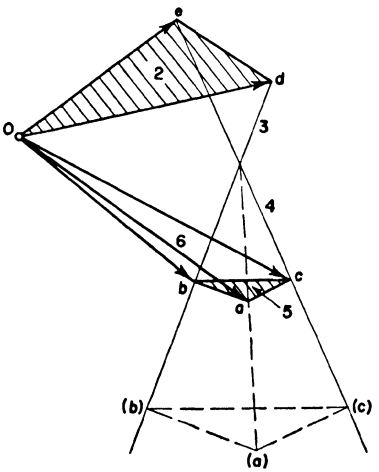

Fig. 4.22

3, 4, and 5. Information is not available to make this solution. A solution can be obtained as shown in Fig. 4.22 by neglecting V_A and assuming a velocity vector V_D. When this is done a trial solution is necessary only for link 5. The length of oa is measured on the drawing, and the velocity scale is calculated, using this length and the known value of V_A. All other velocities can be determined from Fig. 4.22 and this scale.

4.3. Simultaneous trial solutions for two links. A Walschaert valve gear that is used on steam locomotives is shown in Fig. 4.23. The construction of the velocity polygon for this mechanism requires trial solutions for links 6 and 8. The reversing lever is stationary most of the time, and H will be assumed fixed. The piston and crosshead 4,

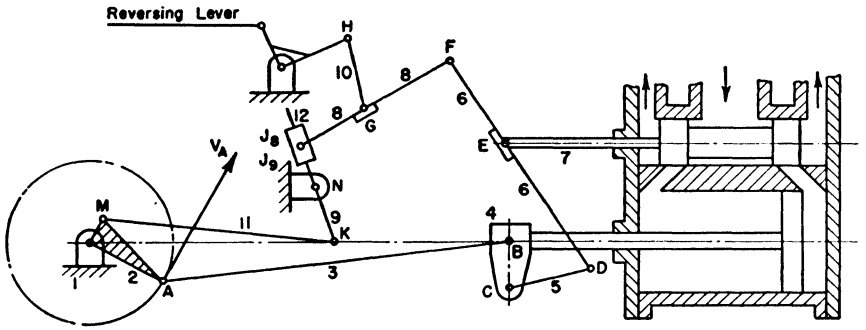

Fig. 4.23

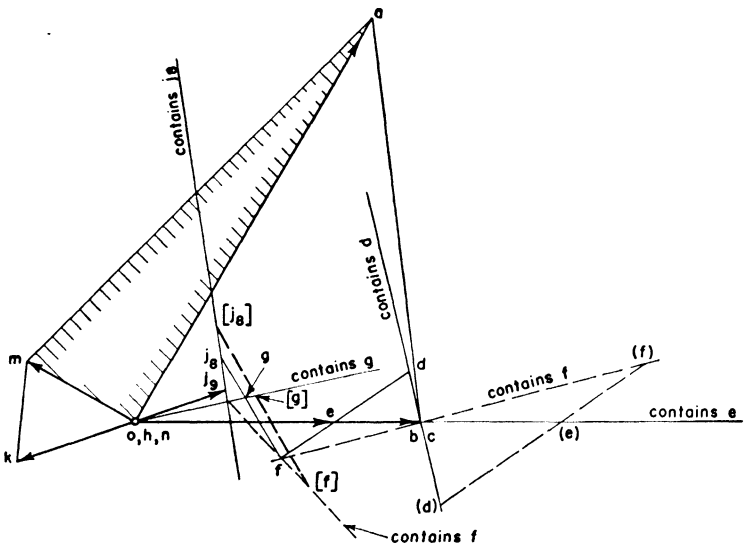

Fig. 4.24

connecting rod 3, crank 2, and frame 1 form a simple slider crank mechanism. The valve 7 receives motion from the crosshead at C and the crank at M. The velocity of crank pin A is known. The velocity polygon for the entire mechanism is shown in Fig. 4.24. Points a, m, b, k, and j_9 are determined in the usual manner. The velocity of C is equal to that of B; therefore c coincides with b in Fig. 4.24. A trial solution for link 6 will be made first. A line through c perpendicular to CD contains d. A line through o in the direction of sliding of valve 7 will contain e.

Line $(d)(e)$ is laid off perpendicular to DE; (f) is located by proportion. A line through (f) and the intersection of lines containing e and d will contain the correct location for point f. No more can be done here. A trial solution for link 8 is required next. A line through j_9 parallel to the direction of sliding of block 12 on 9 contains j_8. A line through h perpendicular to GH contains g. Line $[j_8][g]$ is drawn perpendicular to J_8G, and $[f]$ is located by proportion. A line through $[f]$ and the intersection of lines containing j_8 and g contains f. The intersection of this line with the previously determined line containing f locates f. The correct images fed and fgj_8 are drawn.

4.4. Determination of mechanical advantage from the velocity polygon. In Art. 1.1 it was stated that kinematic schemes can be investigated without regard to forces. This is usually true except in cases where a mechanical advantage is specified. The linkage must be proportioned to give this mechanical advantage. The theory and one example will be given to show that the velocity polygon can be used to determine the mechanical advantage of a mechanism.

A simple lever supported at O is shown in Fig. 4.25. The mechanical advantage is CO/BO. If a force P is applied at C a balancing force Q is required at B. The ratio of the forces is

$$\frac{CO}{BO} = \frac{\text{force } Q}{\text{force } P}$$

The mechanical advantage can also be determined using the principle of virtual (infinitesimal) displacements, virtual velocities, or virtual work.

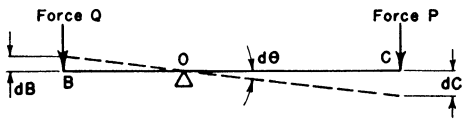

Fig. 4.25

Let the bar rotate through an angle $d\theta$. The displacement of C is $dC = OC\,d\theta$, and the displacement of B is $dB = OB\,d\theta$; then

$$\frac{dC}{dB} = \frac{OC\,d\theta}{OB\,d\theta} = \frac{OC}{OB} = \frac{\text{force } Q}{\text{force } P}$$

When the bar rotates through the angle $d\theta$ it has an angular velocity. The magnitude of this angular velocity does not matter. The linear velocity of point C is $V_C = OC\omega$ and the linear velocity of B is $V_B = OB\omega$; then

$$\frac{V_C}{V_B} = \frac{OC\omega}{OB\omega} = \frac{OC}{OB} = \frac{\text{force } Q}{\text{force } P}$$

This shows that instantaneous velocities can be considered to represent virtual displacements drawn to a large scale. Since a ratio is to be taken, the scale does not enter into the calculations and need not be considered.

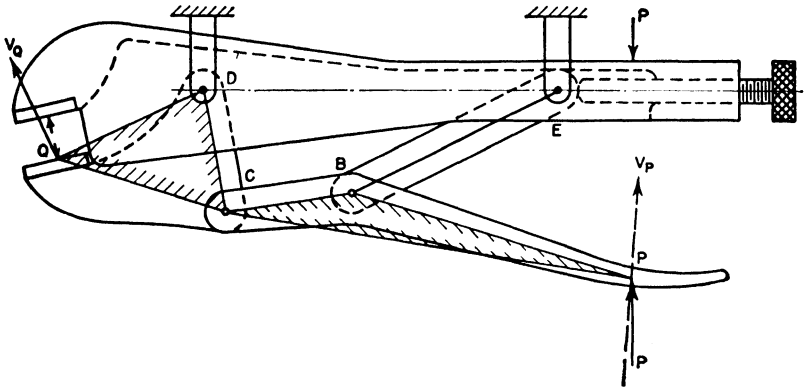

Fig. 4.26

Toggle pliers and the equivalent linkage are shown in Fig. 4.26. A force P is applied as shown. A velocity polygon can be drawn by assuming a velocity for some point in the linkage. The direction of the velocity of P is shown. This cannot be used as a starting point, since the direction is determined from the polygon. One of the points Q, C, or B can be chosen, since the links containing these points are pinned to the fixed member and the directions of motions are known. In this example V_Q is assumed and is laid off as oq in Fig. 4.27. The velocity polygon is completed in the usual manner. These velocities can be considered to represent virtual displacements on a large scale.

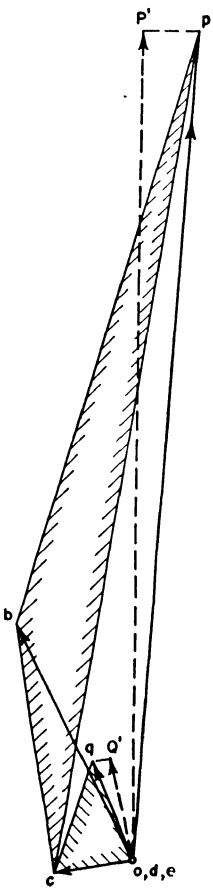

Fig. 4.27

Work is the product of force and displacement. It is only the component of force that acts in the direction of the displacement that does work, or work is the product of the force and the component of displacement that is in the direction of the force. Force P is applied in a vertical direction; hence it does work along oP', the vertical component of the virtual displacement op. The component of displacement $P'p$ is perpendicular to the force. No work is done along this displacement. At Q work is done along the component oQ' that is perpendicular to the jaw. The work at P must equal that at Q.

$$\text{force } P \times oP' = \text{force } Q \times oQ'$$

$$\frac{oP'}{oQ'} = \frac{\text{force } Q}{\text{force } P} = \text{mechanical advantage}$$

If the mechanical advantage is not the desired value a study of Figs. 4.26 and 4.27 will indicate

what links to alter to obtain this mechanical advantage. If the shape of the handle is altered so that force P is applied in the direction of the displacement op, the mechanical advantage will be greater. In this case op and oP' are nearly equal and there is little to be gained. The theory of virtual displacements is based on infinitesimal displacements. In practice the forces are large, and because of the elasticity of the materials, the displacements are small but measurable. If the piece being clamped in the jaws is round, the displacement component qQ' will cause a slight rolling of the piece. If the piece is flat the displacement component qQ' represents sliding or shear distortion of the piece. In this case work is done along the component qQ' and the mechanical advantage is not so great as that indicated above. In some types of clamping devices this action might be undesirable.

It is often necessary to determine the mechanical advantage of mechanisms in motion. This method can of course be used in these cases. The pliers were chosen to show that a problem in statics can be solved using a velocity polygon. The method is not only rapid but it reveals conditions that are not usually apparent from the conventional force analysis.

PROBLEMS

The following problems are to be solved by the velocity polygon method. Label the velocity images. The directions as well as magnitudes of angular velocities should be determined. Let the scale of the velocity polygons be 1 in. = k_v = 10 fps except where otherwise stated.

4.1. (a) Construct the velocity polygon for Fig. P 4.1. Let the length of V_B = 2 in. Place vectors V_E, V_C, and V_F on the configuration (space) diagram.

(b) Determine ω_2, ω_3, and ω_4.

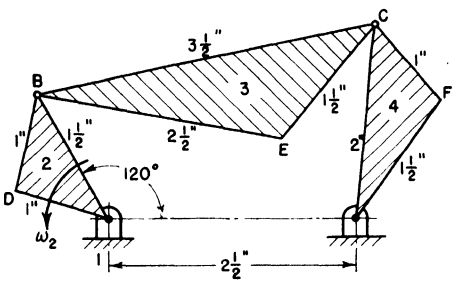

Fig. P 4.1

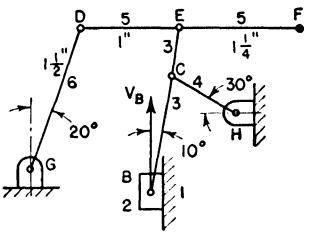

Fig. P 4.2

4.2. (a) Construct the velocity polygon for Fig. P 4.2. Let the length of $V_B = 1\frac{1}{4}$ in., $BC = 1\frac{1}{4}$ in., $CE = \frac{1}{2}$ in., $CH = \frac{3}{4}$ in.

(b) Determine ω_3, ω_4, and ω_5.

4.3. (a) Construct the velocity polygon for Fig. P 4.3. Let the length of V_B = 2 in. Wheels 2 and 4 roll on 1.

(b) Determine ω_2, ω_4, and ω_3.

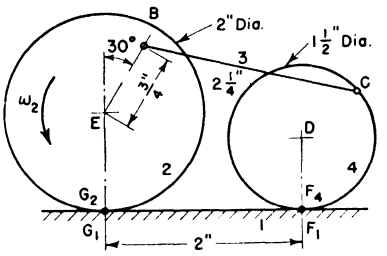

Fig. P 4.3

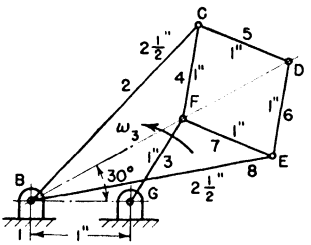

Fig. P 4.4

4.4. (a) Construct the velocity polygon for Peaucellier's straight-line mechanism shown in Fig. P 4.4. Let the length of V_F = 1½ in.

(b) Determine ω_2, ω_3, and ω_5.

4.5. (a) Construct the velocity polygon for Fig. P 3.1. Let the length of V_B = 2 in.

(b) Determine ω_2, ω_3, and ω_4.

4.6. (a) Construct the velocity polygon for Fig. P 3.2. Let the length of V_B = 2 in.

(b) Determine ω_3.

4.7. (a) Construct the velocity polygon for Fig. P 3.3. Let the length of V_{B_2} = 2 in.

(b) Determine ω_3.

4.8. (a) Construct the velocity polygon for Fig. P 3.4. Let the length of V_B = ½ in.

(b) Determine ω_3 and ω_4.

4.9. (a) Construct the velocity polygon for Fig. P 3.5. Let the length of V_B = 2 in.

(b) Determine ω_2 and ω_3.

4.10. (a) Construct the velocity polygon for Fig. P 3.6. Let the length of V_B = 2 in.

(b) Determine ω_3.

4.11. (a) Construct the velocity polygon for Fig. P 3.7. Let the length of V_B = 2 in.

(b) Determine ω_3, ω_4, and ω_5.

4.12. (a) Construct the velocity polygon for Fig. P 3.8. Let the length of V_{B_2} = 2 in.

(b) Determine ω_3, ω_4, and ω_5.

4.13. (a) Construct the velocity polygon for Fig. P 4.13. Let the length of V_{B_2} = 2 in.

(b) Determine ω_3 and ω_4.

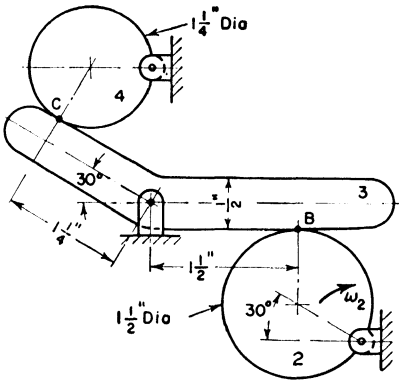

Fig. P 4.13

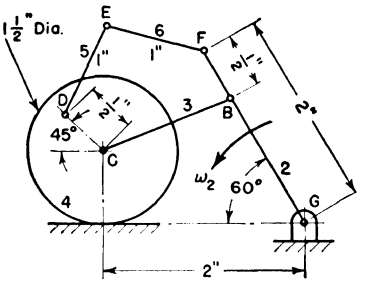

Fig. P 4.14

4.14. (a) Construct the velocity polygon for Fig. P 4.14. Let the length of $V_F = 2$ in.

(b) Determine ω_3, ω_4, ω_5, and ω_6.

4.15. (a) Construct the velocity polygon for Fig. P 4.15. Let the length of $V_{B_2} = 2$ in. $GC = 2$ in., $FD = 6$ in., $ED = 2$ in.

(b) Determine ω_4 and ω_7.

4.16. (a) Construct the velocity polygon for Fig. P 4.16. Let the length of $V_B = 1\frac{1}{2}$ in.

(b) Determine ω_3, ω_4, and ω_5.

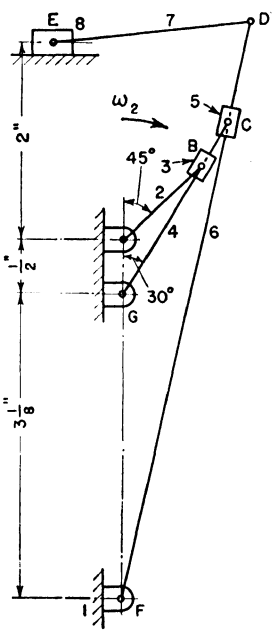

Fig. P 4.15

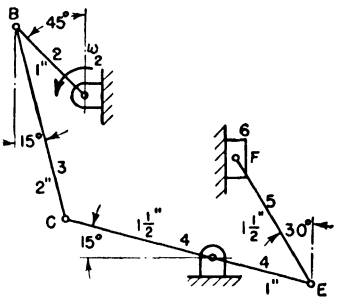

Fig. P 4.16

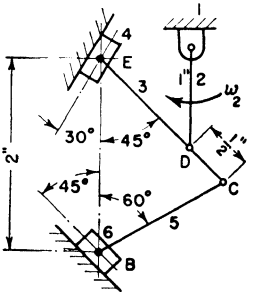

Fig. P 4.17

4.17. (a) Construct the velocity polygon for Fig. P 4.17. Let the length of $V_D = \frac{1}{2}$ in.

(b) Determine ω_3 and ω_5.

4.18. (a) Construct the velocity polygon for Fig. P 4.18. Let the length of $V_B = 1$ in. Wheels 2 and 7 have rolling contact.

(b) Determine ω_3, ω_4, and ω_6.

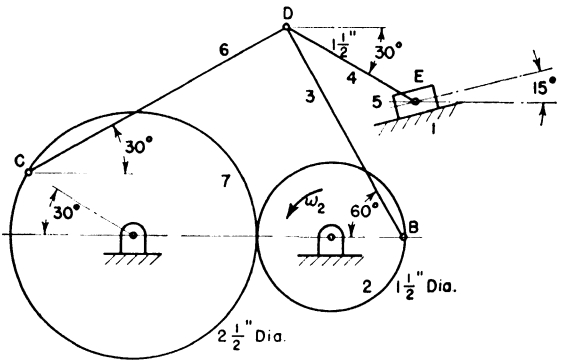

Fig. P 4.18

4.19. Construct a velocity polygon for Fig. P 4.19. Assume a vector 2 in. long to represent the velocity of a point that leads to a simple solution.

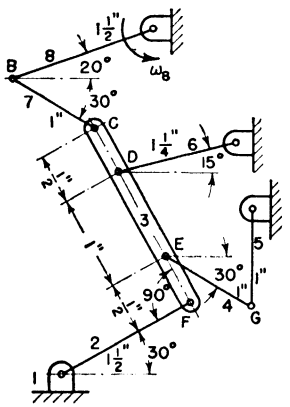

Fig. P 4.19

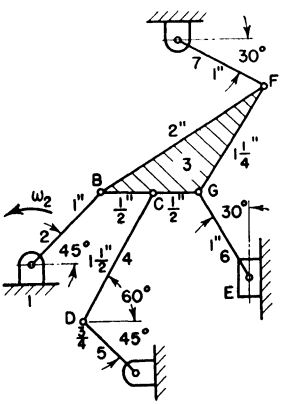

Fig. P 4.20

4.20. Construct a velocity polygon for Fig. P 4.20. Assume a vector to represent the velocity of a point that leads to a simple solution.

4.21. (a) Construct the velocity polygon for Fig. P 4.21. Let the length of $V_B = \frac{1}{2}$ in.

(b) Explain how this problem could be solved without using a trial solution.

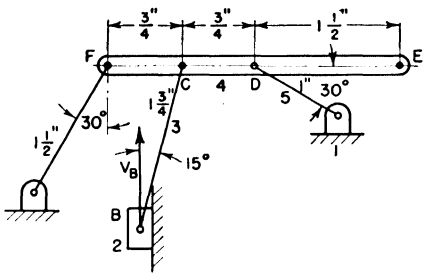

Fig. P 4.21

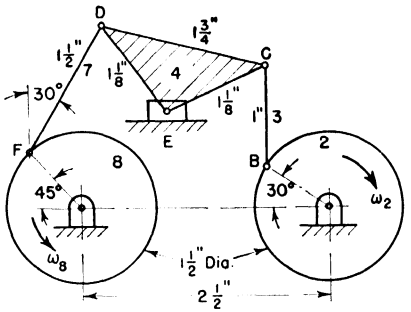

Fig. P 4.22

4.22. Construct the velocity polygon for Fig. P 4.22. Let $\omega_2 = 400$ rpm and $\omega_8 = 800$ rpm. Let the velocity scale be 1 in. = $K_v = 2.5$ fps.

4.23. Construct the velocity polygon for Fig. P 4.23. Let the length of the $V_G = 1\frac{1}{2}$ in.

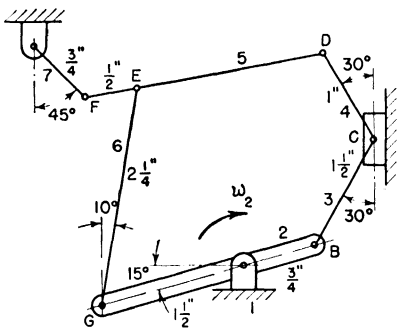

Fig. P 4.23

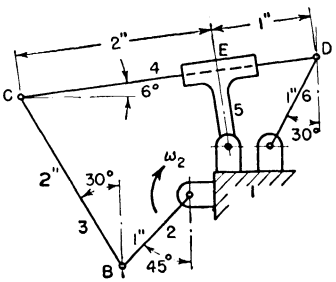

Fig. P 4.24

4.24. Construct the velocity polygon for Fig. P 4.24. Let the length of $V_B = 1\frac{1}{2}$ in.

4.25. A modified computor linkage is shown in Fig. P 4.25(a). Let the input velocities be represented by vectors $V_G = 1\frac{1}{2}$ in. and $V_F = 3$ in. Construct the velocity polygon.

Note: In complex mechanisms it is sometimes difficult to tell if the motion is constrained. A criterion for constraint is

$$B + \tfrac{1}{2}C = \tfrac{3}{2}D - 2 \qquad (1)$$

where B = number of binary joints. A ternary joint (a joint connecting three links, for example, K) is equivalent to two binary joints, and a quaternary joint is equivalent to three binary joints. C = number of unclosed pairs (all are closed in Fig. P 4.25). D = number of links. If the right side of the equation is less than the left, the chain is locked. If equal the chain is constrained. If the right side is greater than the left the chain is unconstrained.

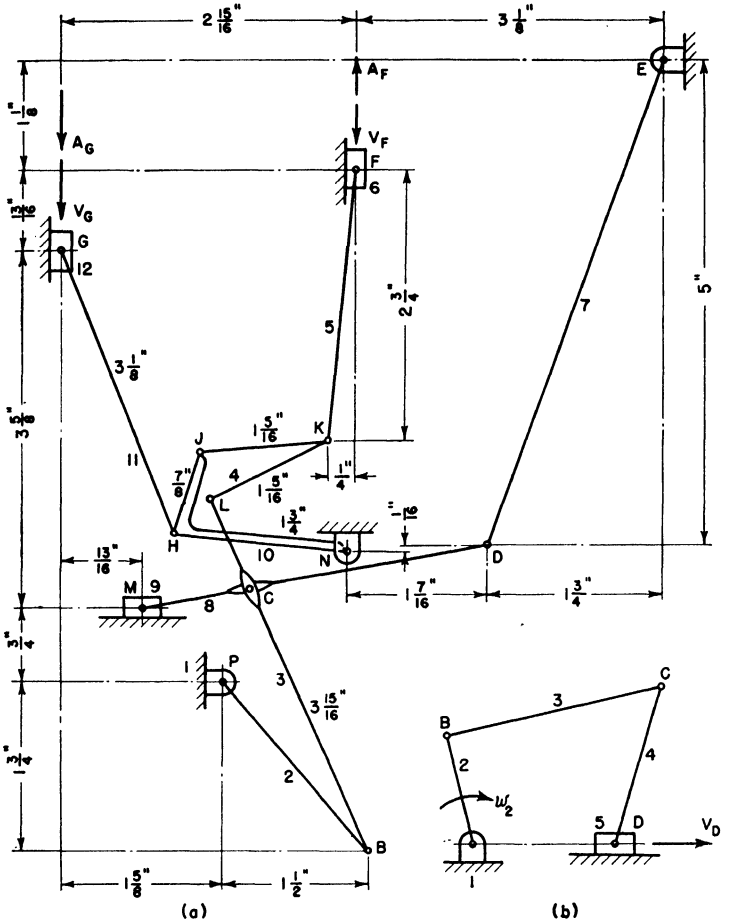

Fig. P 4.25

In Fig. P 4.25(a) when all joints including sliding joints and all members including sliders are considered, the equation gives

$$17 + 0 = \tfrac{3}{2}(13) - 2 = 17\tfrac{1}{2} \tag{2}$$

This indicates that the mechanism does not have constrained motion, which is not the case. Consider the linkage at (b). If ω_2 and V_D are controlled in a definite manner, C will have constrained motion. Substitution in the equation gives

$$5 + 0 = \tfrac{3}{2} \times 5 - 2 = 5\tfrac{1}{2} \tag{3}$$

Again the equation indicates that the linkage does not have constrained motion. If V_D is taken as zero and 5 is considered a part of 1, the equation gives

$$4 + 0 = \tfrac{3}{2} \times 4 - 2 = 4 \tag{4}$$

The linkage is constrained. It can be seen that if ω_2 is definite and V_D is not

definitely controlled, C will not have constrained motion. For this case Eq. (3) gives the correct answer. The equation is not set up to handle both conditions.

If, in Fig. P 4.25(a), $V_G = 0$ and 12 is fixed to 1, the equation is

$$16 + 0 = \tfrac{3}{2} \times 12 - 2 = 16 \tag{5}$$

Hence to apply the criterion to a mechanism with more than one input motion it is necessary to fix all input links but one. If the linkage has constraint for this condition, it will have constraint when one or more additional links are given a definite input motion.

Computor mechanisms commonly have more than one input motion.

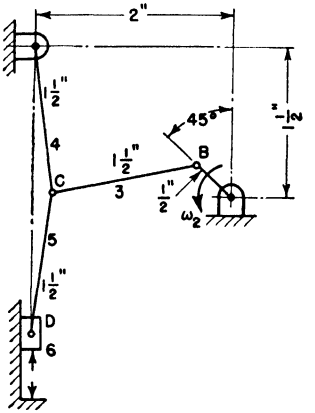

Fig. P 4.26

4.26. A toggle mechanism is shown in Fig. P 4.26. Here 2 is the input member and 6 the output member. Assume a force at B and determine the mechanical advantage.

CHAPTER 5

Acceleration

5.1. Introductory. The development of engineering materials, manufacturing processes, and other phases of engineering makes it possible to build machines that operate at higher speeds than were considered possible a few years ago. Since the normal acceleration is proportional to the square of the speed, the doubling of a machine speed will increase four times the stresses due to centrifugal forces. When a high-speed machine is designed, the acceleration analysis is one of the most important steps. The development of machinery is continually increasing the complexity of mechanisms. Some of these present a challenge to the engineer when an acceleration analysis is required. Methods of dealing with these mechanisms are treated in this chapter. As in the chapters on velocity, the mechanisms are drawn in the simplest manner so that attention can be focused on the application of basic concepts.

5.2. Acceleration polygons. One advantage of the use of velocity polygons is that the method can be extended to make acceleration analyses. The notation used in the acceleration polygon is similar to that used in the velocity polygon except the letters are primed. The pole o' of the acceleration polygon represents the point of zero acceleration. Lines from the pole to points in the acceleration polygon represent absolute accelerations. A line joining two points in the acceleration polygon represents the relative acceleration of the corresponding points on the mechanism. It will be shown later that acceleration images are similar to the corresponding links in the mechanism. The key to the construction of acceleration polygons is, *the normal and tangential accelerations of a point are perpendicular to each other.* In addition to the concepts used for velocity polygons and the key above, the following equations will be used.

$$A^n = \frac{V^2}{R} = R\omega^2 = V\omega \tag{5.1}$$

$$A^t = R\alpha \tag{5.2}$$

$$A = A^n +\triangleright A^t \tag{5.3}$$

$$\text{Coriolis' acceleration} = 2V\omega \tag{5.4}$$

Coriolis' acceleration will be considered in a later article.

5.3. Linear acceleration. An example will be used to illustrate the method for determining linear accelerations. In Fig. 5.1 the crank rotates with uniform angular velocity as shown. The acceleration of C is desired. The velocity polygon is shown in Fig. 5.2 and the acceleration polygon in Fig. 5.3. The acceleration of C can be determined from the equation

$$A_C = A_B +\triangleright A_{C/B} = A_B^n +\triangleright A_B^t +\triangleright A_{C/B}^n +\triangleright A_{C/B}^t$$

The acceleration polygon is the graphical solution of this equation. Point C moves in a horizontal path. A horizontal line through pole o'

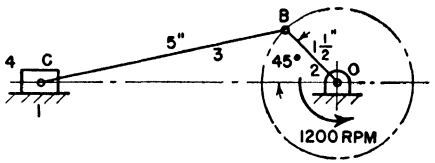

Fig. 5.1

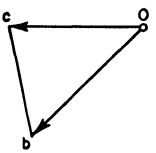

Fig. 5.2

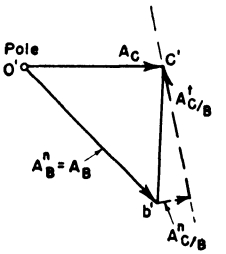

Fig. 5.3

contains c', the terminus of A_C. The normal acceleration* of B is

$$A_B^n = BO\omega_2^2 = \frac{1.5}{12}\left(\frac{1200 \times 2\pi}{60}\right)^2 = 1975 \quad \text{fps}^2$$

Since A_B^t is zero, $A_B^n = A_B$. This is laid off as $o'b'$ in the direction of B to O. Then $A_{C/B}^n$ is calculated by using the value of $V_{C/B}$ from the velocity polygon.

$$A_{C/B}^n = \frac{V_{C/B}^2}{CB} = \frac{(11.5)^2}{\frac{5}{12}} = 318 \quad \text{fps}^2$$

This is laid off from b' in the direction C to B. The direction of $A_{C/B}^t$ is perpendicular to $A_{C/B}^n$. A line through the terminus of $A_{C/B}^n$ in this direction contains c', the terminus of $A_{C/B}^t$. The intersection of this line with the horizontal line through o' containing c' locates c', and $o'c'$ represents A_C. It scales 1410 fps^2.

5.4. Acceleration images. In Fig. 5.4 the angular velocity and acceleration of link 2 are given. The velocity and acceleration polygons are shown in Figs. 5.5 and 5.6. Here A_D can be determined from the equation

$$A_D = A_C +\triangleright A_{D/C}$$

This can be written

$$A_D^n +\triangleright A_D^t = A_C^n +\triangleright A_C^t +\triangleright A_{D/C}^n +\triangleright A_{D/C}^t$$

* The unit of acceleration, feet per second per second, is abbreviated as fps^2 throughout this text.

The value of A_D^n is obtained from Eq. (5.1), using the value of V_D from the velocity polygon. This vector is laid off from o'. A perpendicular at the terminus of A_D^n contains d', the terminus of A_D^t. The vectors on the right side of the equation are laid off starting from o'. The values

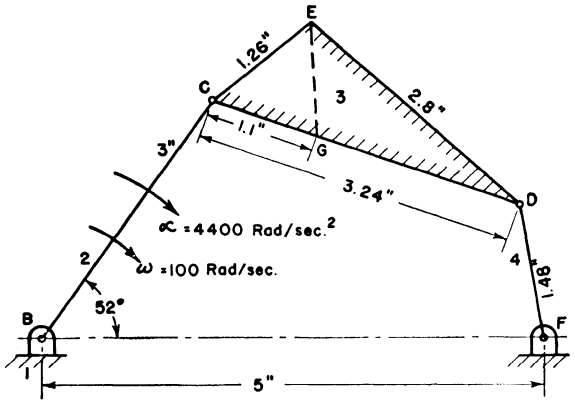

Fig. 5.4

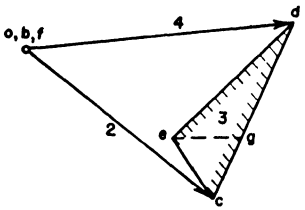

Fig. 5.5

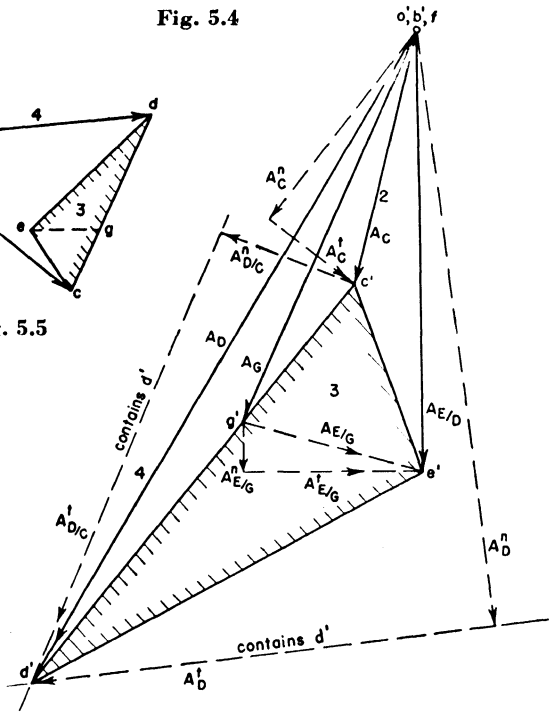

Fig. 5.6

of A_C^n and A_C^t are calculated from the known motion of link 2 and laid off as shown. The vector sum of A_C^n and A_C^t is A_C. This is represented by $o'c'$, and $A_{D/C}^n$ is calculated using the value of $V_{D/C}$ from the velocity polygon and is laid off from c'. A perpendicular at the terminus of $A_{D/C}^n$ contains d', the terminus of $A_{D/C}^t$. The intersection of this line

with the previously determined line containing d' locates d'. Then $o'd'$ represents the vector A_D.

The point e' can be located in a similar manner by laying off $A^n_{E/C}$ from c' and $A^n_{E/D}$ from d' and obtaining the intersection of the perpendiculars to these vectors. A more rapid way is to construct the acceleration image $c'd'e'$ similar to CDE. The similarity of the link and image can be proved as follows.

$$A_{C/D} = A^n_{C/D} + \triangleright\, A^t_{C/D} = \omega_3^2 CD + \triangleright\, \alpha_3 CD$$

Since $A^n_{C/D}$ and $A^t_{C/D}$ are perpendicular to each other,

$$|A_{C/D}| = \sqrt{\omega_3^4 CD^2 + \alpha_3^2 CD^2} = CD\sqrt{\omega_3^4 + \alpha_3^2}$$

In like manner

$$|A_{E/C}| = EC\sqrt{\omega_3^4 + \alpha_3^2}$$
$$|A_{D/E}| = DE\sqrt{\omega_3^4 + \alpha_3^2}$$

etc. The magnitudes of relative accelerations of points on a link are equal to the distances between the points on the original link times a constant. Since distances between points on the acceleration image represent relative accelerations, these distances must be proportional to the corresponding distances on the link. Points d' and c' are located on the acceleration image. The acceleration image of link 3 can be completed from the proportions

$$\frac{c'd'}{CD} = \frac{c'e'}{CE} = \frac{e'd'}{ED} = \frac{c'g'}{CG}$$

The cyclic order must be maintained. If $CEDG$ is clockwise, $c'e'd'g'$ must be clockwise.

5.5. Angular acceleration. The angular acceleration of a link can be obtained from Eq. (5.2). The angular acceleration of a link is equal to the tangential acceleration of any point in the link relative to any other point in the link divided by the distance between the points. The value of $A^t_{D/C}$ can be taken from Fig. 5.6, and $A^t_{E/G}$ is obtained by resolving $A_{E/G}$ (Fig. 5.6) into its normal component parallel to EG, and tangential component perpendicular to EG. The angular acceleration of link 3 is

$$\alpha_3 = \frac{A^t_{D/C}}{DC} \text{ clockwise} \qquad \text{(a)}$$

$$\alpha_3 = \frac{A^t_{C/D}}{CD} \text{ clockwise} \qquad \text{(b)}$$

$$\alpha_3 = \frac{A^t_{E/G}}{EG} \text{ clockwise} \qquad \text{(c)}$$

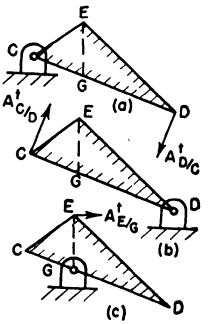

Fig. 5.7

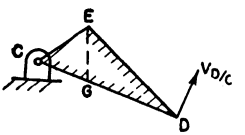

Fig. 5.8

etc. The angular velocity of link 3 from Fig. 5.8 is counterclockwise. The angular velocity of link 3 is therefore decreasing.

5.6. Graphical determination of normal accelerations. The units used in making calculations and drawing polygons can be any of the standard units; however, it is customary to use feet and seconds. On the drawings of the mechanism, let the scale be 1 in. $= k_s$ ft. In drawing velocities, let the scale be 1 in. $= k_v$ fps. In drawing accelerations, let the scale be 1 in. $= k_a$ fps^2.

A rotating link BC is shown in Fig. 5.9. The velocity V_C is indicated as CV. These two values, the lengths BC and V_C, are drawn to the scales indicated above. A right triangle BVN is constructed as shown. Triangles BCV and CVN have perpendicular sides and are therefore similar. Then

$$\frac{CN}{CV} = \frac{CV}{BC} \qquad \text{or} \qquad CN = \frac{(CV)^2}{BC} \tag{5.5}$$

Let

$$\frac{CNk_a}{CVk_v} = \frac{CVk_v}{BCk_s} \qquad \text{or} \qquad CNk_a = \frac{(CVk_v)^2}{BCk_s} \tag{5.6}$$

Equation (5.6) holds if the scales have a certain relationship. This relationship can be obtained by dividing Eq. (5.6) by (5.5), giving

$$\frac{k_a}{k_v} = \frac{k_v}{k_s} \qquad \text{or} \qquad k_a = \frac{k_v^2}{k_s} \tag{5.7}$$

A dimensional check shows that the units chosen are correct.

$$\text{fps}^2 = \frac{(\text{fps})(\text{fps})}{\text{ft}} = \text{fps}^2 \tag{5.8}$$

By construction CVk_v is equal to V_C on the mechanism, and BCk_s is equal to the actual length of BC on the mechanism. Therefore CNk_a

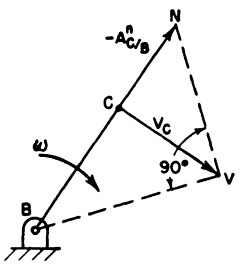

Fig. 5.9

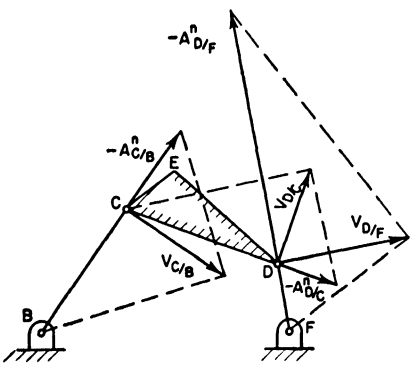

Fig. 5.10

from Eq. (5.7) must represent the normal acceleration of C relative to B on the mechanism on the scale indicated above. In Fig. 5.9 it can be

seen that the sense of this vector is reversed. When it is used in the acceleration polygon it must be drawn in the correct direction.

The mechanism of Fig. 5.4 is shown in Fig. 5.10, and the constructions for the determination of the normal accelerations are shown. This graphical construction reduces the time required to make an acceleration analysis. The velocities can be transferred from the polygon to the drawing of the mechanism with dividers. The normal accelerations can then be transferred to the acceleration polygon. None of the vectors need be scaled until the acceleration polygon is completed, and then only those desired need be scaled. Any two scales can be assumed and the third calculated using Eq. (5.7). Usually k_s and k_v are assumed.

5.7. Equivalent linkages. A direct-contact mechanism consisting of two circular members with centers at C and B is shown in Fig. 5.11. The equivalent links 2′, 3′, and 4′ can replace links 2 and 4 for making an acceleration analysis. The accelerations of 2′ and 4′ will be the same as those of 2 and 4. It can be seen that link 3′ lies along the common normal at the point of contact of 2 and 4; hence the angular velocity ratio of 2′ and 4′ will be the same as that of 2 and 4. This will be true for any phase of the mechanism. If the equivalent linkage gives the correct velocities for any series of displacements it can be used for an acceleration analysis.

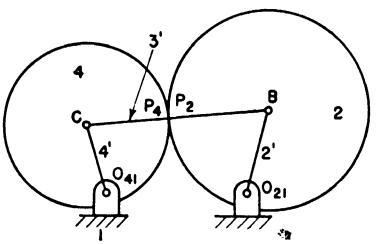

Fig. 5.11

In Fig. 5.12 the active profile of member 2 consists of two circular arcs, GE of radius R_1 and EF of radius R_2. For the phase shown with solid lines the equivalent linkage is O_{41}-C-B-O_{21}. A different equivalent linkage, O_{41}-C'-D'-O_{21}, is required for the phase shown dotted. For the

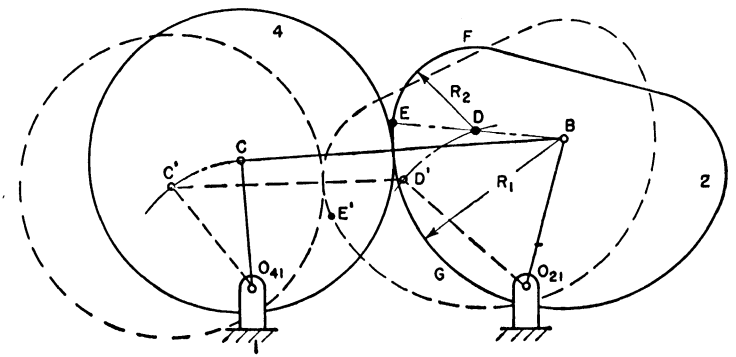

Fig. 5.12

phase in which point E of member 2 contacts member 4, both linkages result. Both are correct and should be analyzed. This represents a

discontinuity in the acceleration due to the finite change in radius from R_1 to R_2.

If the radius of curvature of the profile of one or both members changes continuously, the equivalent linkage changes continuously and must be determined for each phase. Accelerations are obtained from the equations $A^t = R\alpha$ and $A^n = R\omega^2$, where R, ω, and α are instantaneous

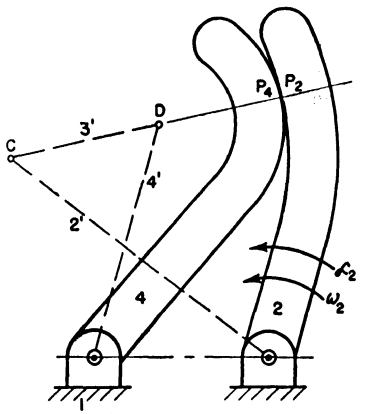

Fig. 5.13

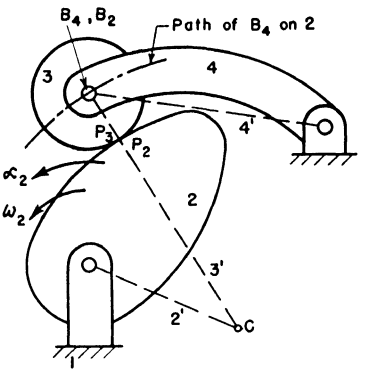

Fig. 5.14

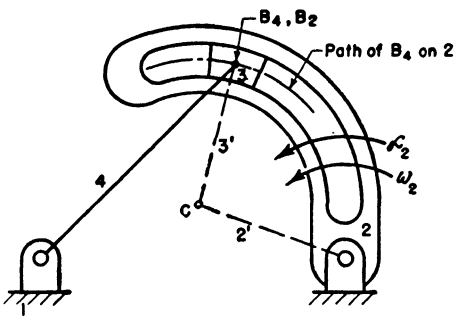

Fig. 5.15

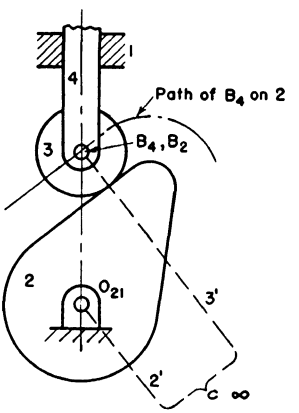

Fig. 5.16

values. Their rate of change does not affect the instantaneous values of acceleration.

Three mechanisms and their equivalent linkages are shown in Figs. 5.13, 5.14, and 5.15. In Fig. 5.16 the roller is in contact with a flat surface of the cam. The normal acceleration of C is

$$A_c^n = O_{21}C\omega_2^2 = \infty$$

The solution of this problem with the equivalent linkage will not be considered in this book. Another type of solution will be considered in the next article.

5.8. Coriolis' law. *If a point moves along a path that has rotation, the absolute acceleration of the point is the vector sum of the acceleration of the point relative to the coincident point in the path, the absolute acceleration of the coincident point in the path, and a third component. The third component is called Coriolis' component.*

In Fig. 5.17, rod DE moves with constant angular velocity from DE to DE' in time dt. During this time a slider moves outward along the

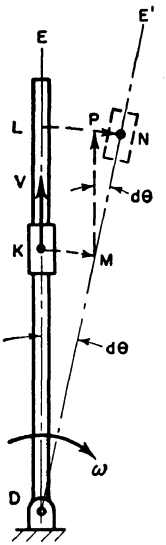

Fig. 5.17

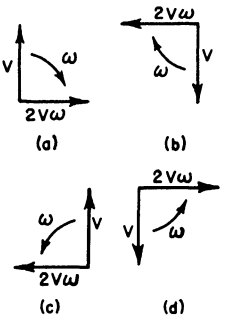

Fig. 5.18

rod with velocity V from position K to position N. Consider the displacement of the slider from K to N in the following stages: K to M due to the rotation of the rod, M to P due to the outward velocity V, and P to N due to an acceleration perpendicular to the rod. This is Coriolis' acceleration. An expression for it can be obtained as follows.

$$\text{arc } PN = \text{arc } LN - \text{arc } KM$$

$$PN = LD\,d\theta - KD\,d\theta = PM\,d\theta = V\,dt\,\omega\,dt = V\omega\,dt^2$$

For a constantly accelerated particle

$$PN = \tfrac{1}{2}A\,dt^2$$

Eliminating PN from the above equations gives

$$A = 2V\omega \qquad \text{Coriolis' acceleration} \tag{5.9}$$

The directional relationship of V, ω, and $2V\omega$ for the case of Fig. 5.17 is shown in Fig. 5.18(a). If the velocity of the slider is toward the center D the relationship will be that of Fig. 5.18(b). If ω is reversed, the

relationships for the two velocity directions will be according to Figs. 5.18(b) and (c). Figure 5.18 can be used as a key for determining the direction of Coriolis' acceleration. The key can be stated as follows: *the direction of Coriolis' acceleration is the direction of the relative velocity vector after it has been rotated 90° in the direction of the angular velocity of the path.*

The derivation given above is for the special case shown. In the general case the path is curved and has angular acceleration, and the moving point has acceleration along the path. The proof for the general case is included in most engineering mechanics books.*

In the previous examples it was not necessary to consider relative acceleration of coincident points on paths that had rotation. In Figs. 5.13, 5.14, and 5.15 this was avoided by using equivalent linkages.

The acceleration of B_4, Fig. 5.15, can be determined using Coriolis' acceleration, and A_{B_4} can be calculated. The Coriolis component $2V_{B_4/B_2}\omega_2$ can be calculated. The normal acceleration of B_4 relative to B_2 can be calculated since the radius of curvature of the path of B_4 on 2 is known. This information is sufficient for completing the problem.

The same conditions exist for Fig. 5.14. The path of B_4 on 2 is a curve parallel to the contour of member 2. The center of curvature of the path is at C.

In Fig. 5.13 the radius of curvature of the path of P_4 on 2 is not evident.† However, the equivalent linkage can be used to make the acceleration analysis.

In Fig. 5.16 the equivalent linkage method breaks down because of the infinite length.† This produces a straight path; hence the path of B_4 on 2 is known. The Coriolis method can be used.

Examples will be worked to illustrate the theory.

Example 1. A governor mechanism is shown in Fig. 5.19(a). The links and their angular motions are shown in (b). The acceleration of P_3 is wanted. This problem will be worked without Coriolis' acceleration and then with the acceleration. The velocity polygon is shown in Fig. 5.20. The value of $V_{P_3/C}$ cannot be determined graphically. It is

$$V_{P_3/C} = R\omega_{3/1} = (1.56)(10) = 15.6 \quad \text{fps}$$

It should be remembered that the velocity of any point in a link relative to some other point in the link is the product of the distance between them and the absolute angular velocity of the link.

* Higdon and Stiles, *Engineering Mechanics*, New York: Prentice-Hall, Inc., 1949, p. 307. Hall, A. S., "Teaching Coriolis' Law," *ASEE Journal*, June, 1948.

† In Fig. 5.13 the radius of curvature of the path that P_2 traces on 4 and the radius of curvature of the path that P_4 traces on 2 can be determined analytically or graphically. In Fig. 5.16 the equivalent linkage can be used to make the acceleration analysis if inversion is used. This will not be considered in this book.

The accelerations are

$$A_c^n = CO\omega_{2/1}^2 = (1.4)(12)^2 = 202 \quad \text{fps}^2$$
$$A_c^t = CO\alpha_{2/1} = (1.4)(75) = 105 \quad \text{fps}^2$$
$$A_{P_3/C}^n = PC\omega_{3/1}^2 = (1.56)(10)^2 = 156 \quad \text{fps}^2$$
$$A_{P_3/C}^t = PC\alpha_{3/1} = (1.56)(60) = 93.5 \quad \text{fps}^2$$

These vectors are laid off as solid lines in Fig. 5.21. Then $o'p_3'$ is the desired vector A_{P_3}.

Fig. 5.19

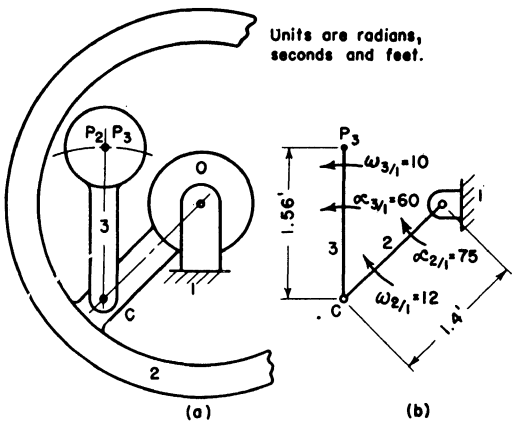

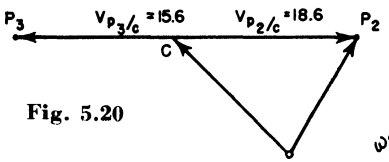

Fig. 5.20

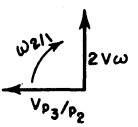

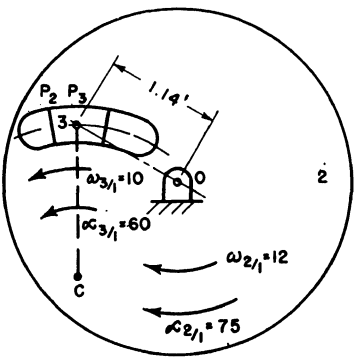

Fig. 5.22

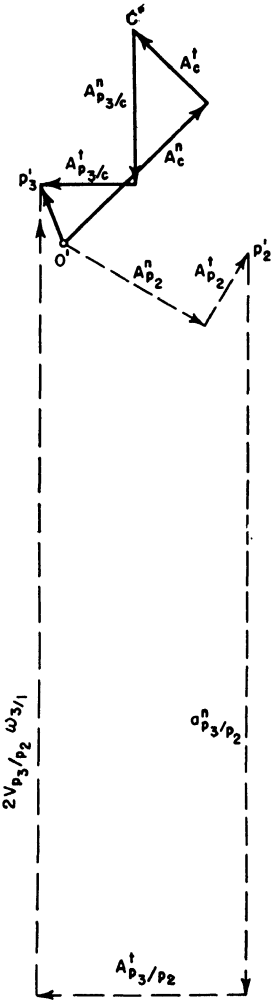

Fig. 5.21

The mechanism shown in Fig. 5.22 is equivalent to that of Fig. 5.19. The acceleration of P_3 is the vector sum of the accelerations of P_2 relative to the frame, the acceleration of P_3 relative to P_2, and Coriolis' acceleration.

$$A_{P_3} = A^n_{P_2} +\triangleright A^t_{P_2} +\triangleright a^n_{P_3/P_2} +\triangleright A^t_{P_3/P_2} +\triangleright 2V_{P_3/P_2}\omega_{2/1}$$

A lower-case letter is used for the normal acceleration of P_3 relative to P_2 to indicate that the Coriolis' acceleration must be used with it. The values are

$$A^n_{P_2} = PO\omega^2_{2/1} = (1.14)(12)^2 = 163.5 \quad \text{fps}^2$$

$$A^t_{P_2} = PO\alpha_{2/1} = (1.14)(75) = 85.5 \quad \text{fps}^2$$

$$a^n_{P_3/P_2} = \frac{(V_{P_3/P_2} = V_{P_3/C} -\triangleright V_{P_2/C})^2}{PC} = \frac{[15.6 - (-18.6)]^2}{1.56} = 750 \quad \text{fps}^2$$

$$A^t_{P_3/P_2} = PC(\alpha_{3/2} = \alpha_{3/1} - \alpha_{2/1}) = (1.56)[60 - (-75)] = 210 \quad \text{fps}^2$$

$$2V_{P_3/P_2}\omega_{2/1} = (2)(34.2)(12) = 820 \quad \text{fps}^2$$

These vectors are laid off with broken lines. From the drawing, A_{P_3} scales 65 fps².

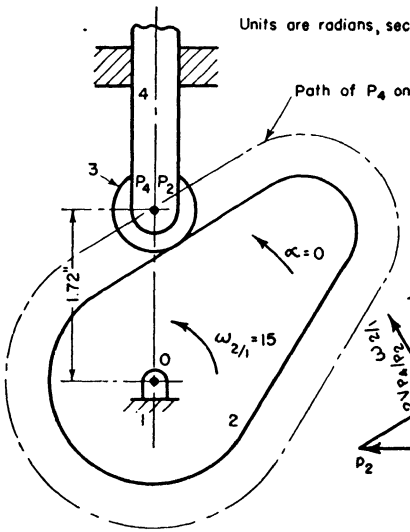

Fig. 5.23

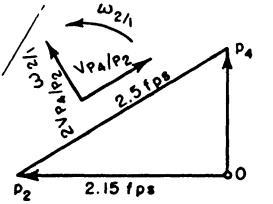

Fig. 5.24

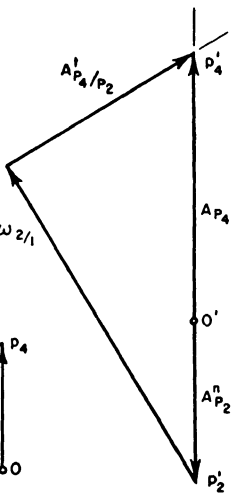

Fig. 5.25

Example 2. A cam mechanism is shown in Fig. 5.23. It is desired to determine the acceleration of the reciprocating follower 4. The path that P_4 traces on 2 is shown. The velocity polygon is shown in Fig. 5.24 and the acceleration polygon in Fig. 5.25. The acceleration of P_4 is

$$A_{P_4} = A^n_{P_2} +\triangleright A^t_{P_2} +\triangleright A^t_{P_4/P_2} +\triangleright a^n_{P_4/P_2} +\triangleright 2V_{P_4/P_2}\omega_{2/1}$$

The components are

$$A^n_{P_2} = OP\omega^2_{2/1} = \frac{1.72}{12}(15)^2 = 32.2 \quad \text{fps}^2$$

The cam has no angular acceleration; therefore

$$A^t_{P_2} = 0$$

$$a^n_{P_4/P_2} = \frac{V^2_{P_4/P_2}}{R} = \frac{V^2_{P_4/P_2}}{\infty} = 0$$

where R is the radius of curvature of the path of P_4 on 2 at the point of contact.

$$2V_{P_4/P_2}\omega_{2/1} = (2)(2.5)(15) = 75 \quad \text{fps}^2$$

These two vectors are laid off starting from o'. The direction of $A^t_{P_4/P_2}$ is tangent to the path that P_4 traces on 2. A line in this direction through the terminus of $2V_{P_4/P_2}\omega_{2/1}$ contains p'_4. The acceleration of P_4 relative to the frame is along the centerline of the follower. A line in this direction through o' contains p'_4, and p'_4 is located at the intersection of these two lines. On the drawing A_{P_4} scales 54.8 fps^2.

Example 3. A quick-return mechanism is shown in Fig. 5.26. Member 2 has constant angular velocity as shown. The angular acceleration of link 3 is desired.

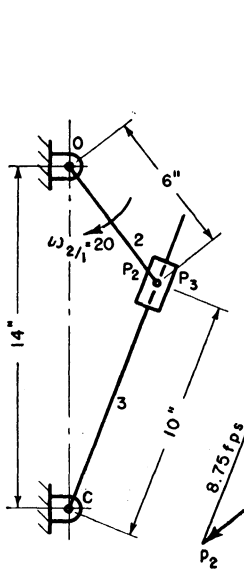

Fig. 5.26

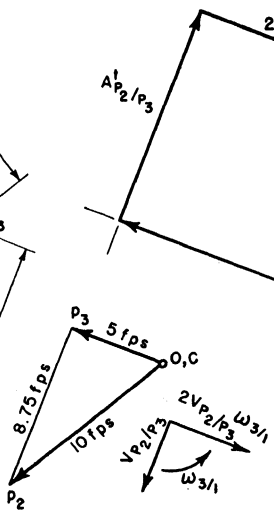

Fig. 5.27

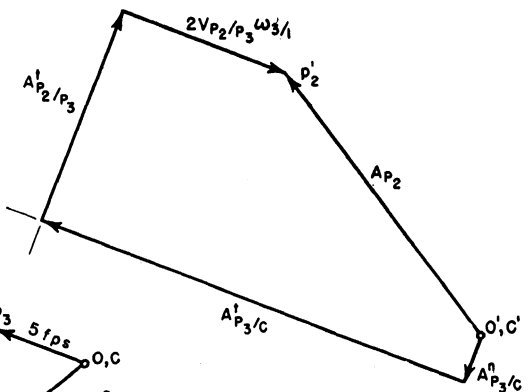

Fig. 5.28

The acceleration of P_3 must be determined first. The equation is

$$A_{P_3} = A^n_{P_2} +\triangleright A^t_{P_2} +\triangleright A^t_{P_3/P_2} +\triangleright a^n_{P_3/P_2} +\triangleright 2V_{P_3/P_2}\omega_{2/1}$$

In order to solve this equation it is necessary to know the radius of curvature of the path that P_3 traces on 2. This is not known. The path that P_2 traces on 3 is a straight line along the link. This path can be used if the equation is written as though solving for the acceleration of P_2.

$$A_{P_2} = A^n_{P_3/C} +\triangleright A^t_{P_3/C} +\triangleright A^t_{P_2/P_3} +\triangleright a^n_{P_2/P_3} +\triangleright 2V_{P_2/P_3}\omega_{3/1}$$

The vectors that can be calculated are

$$A_{P_2} = P_2O\omega_{2/1}^2 = \frac{6}{12}(20)^2 = 200 \quad \text{fps}^2$$

$$A^n_{P_3/C} = \frac{V^2_{P_3/C}}{P_3C} = \frac{(5)^2}{\frac{10}{12}} = 30 \quad \text{fps}^2$$

$$a^n_{P_3/P_2} = 0$$

$$\omega_{3/1} = \frac{V_{P_3/C}}{P_3C} = \frac{5}{\frac{10}{12}} = 6 \quad \text{radians per sec}$$

$$2V_{P_2/P_3}\omega_{3/1} = (2)(8.75)(6) = 105 \quad \text{fps}^2$$

The directions of $A^t_{P_3/P_2}$ and $A^t_{P_3/C}$ are known. This information is sufficient for completing the polygon. One arrangement is shown in Fig. 5.28. The known vectors A_{P_2}, $A^n_{P_3/C}$, and $2V_{P_2/P_3}\omega_{3/1}$ are laid off as shown. Lines in the known directions of the other two vectors complete the polygon. Then $A^t_{P_3/C}$ scales 275 fps^2.

$$\alpha_{3/1} = \frac{A^t_{P_3/C}}{P_3C} = \frac{275}{\frac{10}{12}} = 330 \text{ radians/sec}^2$$

5.9. Complex mechanisms. In Chapter 4 it was found that some mechanisms require trial solutions in the construction of velocity polygons. If a trial solution is required for a link in a velocity polygon, a trial solution for the same link is required in the acceleration polygon. If simultaneous trial solutions are required for two links in a velocity polygon, simultaneous trial solutions are required for the same links in the acceleration polygon. The trial solution method for velocity polygons was made possible by the fact that the velocity image of a link is perpendicular to the link. The angular orientation of an acceleration image relative to the link is determined by the relationship between the normal and tangential accelerations. This relationship is not known until the polygon is completed. The normal accelerations can be calculated using velocities from the velocity polygon. When these are laid off on the acceleration polygon, only the tangential components are left. These are perpendicular to the link, and a trial solution for the tangential components can be made in the same manner as in a velocity polygon. No new basic concepts are required; those that have been used in the earlier part of this chapter are sufficient.

Example 4. In Fig. 5.29 the angular velocity and acceleration of link 2 are known. The velocity polygon is shown in Fig. 5.30. A trial solution was required for link 4. The acceleration polygon is shown in Fig. 5.31. The order in which the lines were drawn is indicated by numbers in brackets. Accelerations $A^n_{B/F}$ [1] and $A^t_{B/F}$ [2] are calculated and laid off, locating b'. Then $A^n_{D/B}$ [3] is calculated and laid off from b'. A line [4] perpendicular to $A^n_{D/B}$ will contain d', the terminus of $A^t_{D/B}$. Acceleration $A^n_{C/H}$ [5] is calculated and laid off from o'. A line [6] perpendicular to $A^n_{C/H}$ contains c', the terminus of $A^t_{C/H}$. Then $A^n_{E/G}$ [7]

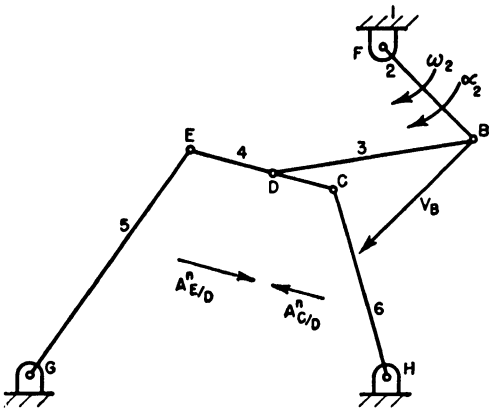

Fig. 5.29

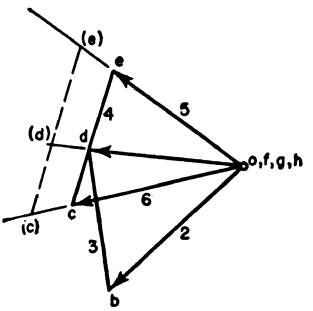

Fig. 5.30

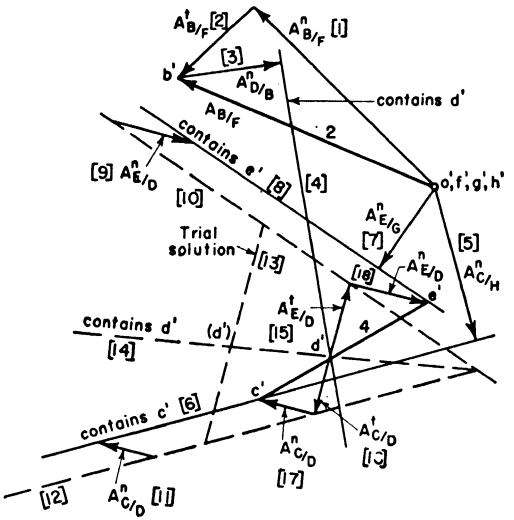

Fig. 5.31

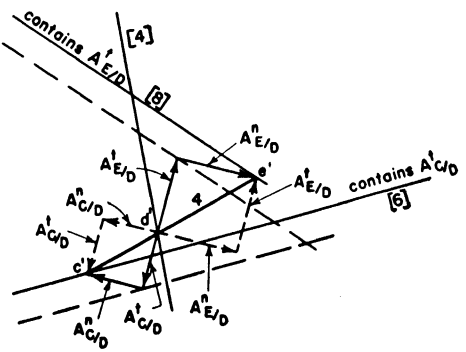

Fig. 5.32

is calculated and laid off from o'. A line [8] perpendicular to $A^n_{E/G}$ contains e', the terminus of $A^t_{E/G}$. A trial solution is now necessary. A portion of Fig. 5.31 is shown in Fig. 5.32. For purposes of explanation it is assumed that the location of d' is known; $A^n_{E/D}$ is calculated and laid off from d' (this vector is shown with a broken line). A perpendicular to $A^n_{E/D}$ (shown broken) contains e', the terminus of $A^t_{E/D}$. The intersection of this line with line [8] containing e' locates e', and c' is located in a similar manner. This is the usual arrangement for laying off normal and tangential components. The acceleration image $c'd'e'$ of link 4 is shown. Accelerations $A^n_{E/D}$, $A^t_{E/D}$, $A^n_{C/D}$, and $A^t_{C/D}$ can be arranged differently, as shown by the solid line vectors. This latter arrangement is necessary in making trial solutions. In Fig. 5.31 $A^n_{E/D}$ [9] is laid off in an arbitrary position such that its terminus touches line [8] containing e'. A line [10] through the origin of $A^n_{E/D}$ and parallel to line [8] will contain the terminus of $A^t_{E/D}$, and $A^n_{C/D}$ [11] is laid off in an arbitrary position such that its terminus touches line [6] containing c'. A line [12] through the origin of $A^n_{C/D}$ and parallel to line [6] contains the terminus of $A^t_{C/D}$. A trial solution [13] for the tangential components $A^t_{E/D}$ and $A^t_{C/D}$ is made by drawing a line between [10] and [12] perpendicular to link EDC (Fig. 5.29). Point (d') is located by proportion from link EDC. A line [14] through (d') and the intersection of lines [10] and [12] contains (d') for all trial solutions. The intersection of lines [4] and [14] locates d'. Vectors [15], [16], [17], and [18] determine the acceleration image of link 4.

Example 5. A portion of a Walschaert valve gear is shown in Fig. 5.33. In order to reduce the number of lines in the acceleration polygon some of the links that require only elementary technique have been omitted. Member 2 has been given arbitrary angular velocity and acceleration, and point G has been given arbitrary linear velocity and acceleration. The velocity polygon, Fig. 5.34, is similar to a portion of Fig. 4.24. Links 3 and 5 require trial solutions. The acceleration polygon is shown in Fig. 5.35. The order in which the lines are drawn is indicated by numbers in brackets. First $A^n_{C/H}$ [1] is calculated and laid off. A perpendicular line [2] through the terminus of $A^n_{C/H}$ contains c', the terminus of $A^t_{C/H}$. The known value of A_G is laid off as $o'g'$ [3]. The slider E has horizontal motion. Line [3] will also contain e'. Acceleration $A^n_{F/G}$ [4] is calculated and laid off from g'. A perpendicular line [5] through the terminus of $A^n_{F/G}$ contains f', the terminus of $A^t_{F/G}$. Acceleration $A^n_{B_2/K}$ [6] is calculated and laid off. Then $A^t_{B_2/K}$ [7] and $2V_{B_3/B_2}\omega_2$ [8] are calculated and laid off as shown. A perpendicular line [9] through the terminus of $2V_{B_3/B_2}\omega_2$ contains b'_3, the terminus of $A^t_{B_3/B_2}$. It is now necessary to make trial solutions. Link 3 will be considered first. Acceleration $A^n_{B_3/C}$ [11] is calculated and laid off in an arbitrary position such that its terminus touches line [9] containing b'_3. The perpendicular line [12] between the origin of $A^n_{B_3/C}$ [11] and line [2] is a trial solution for $A^t_{B_3/C}$. Acceleration $A^t_{D/C}$ [13] is laid off using the proportions of link 3, and $A^n_{D/C}$ [14] is calculated and laid off from the terminus at $A^t_{D/C}$. Lines [11], [12], [13], and [14] form a trial solution for link 3. If $A^n_{B_3/C}$ [14] is laid off again in some position other than [11] it can be seen that a line [15] through the origins of these two vectors is parallel to line [9]. Line [15] contains the termini of $A^t_{B_3/C}$ for all trial solutions. Line [16] through the terminus of $A^t_{D/C}$ [13] and the intersection of lines [2] and [15] contains the termini of $A^t_{D/C}$ for all trial solutions. Line [17] through the terminus of $A^n_{D/C}$ [14] and parallel to line [16] contains the termini of $A^n_{D/C}$ for all trial solu-

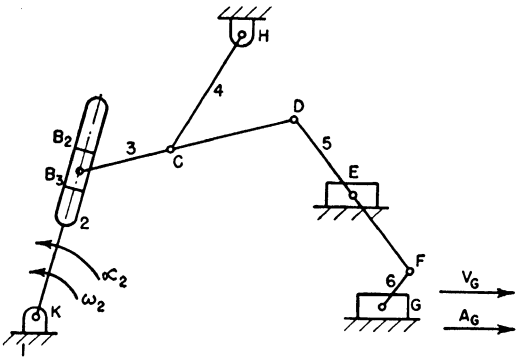

Fig. 5.33

Fig. 5.34.

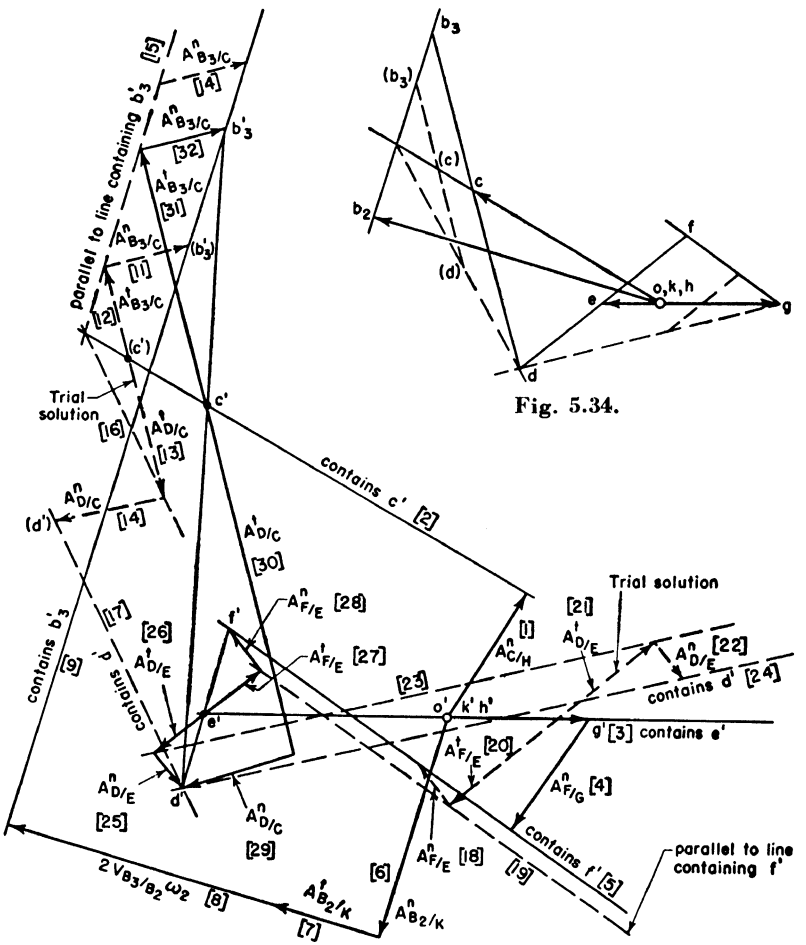

Fig. 5.35

tions. Line [17] therefore contains d'. A trial solution for link 5 is now necessary. It is made in a manner similar to that for link 3. Acceleration $A^n_{F/E}$ [18] is calculated and laid off with its terminus touching line [5] containing f'. Line [19] is drawn parallel to line [5]. The trial value of $A^t_{F/E}$ [20] is laid off as shown. Acceleration $A^t_{D/E}$ [21] is determined by proportions, and $A^n_{D/E}$ [22] is calculated and laid off from the terminus of $A^t_{D/E}$ [21]. Line [23] is drawn through the terminus of $A^t_{D/E}$ [21] and the intersection of lines [3] and [19]. Line [24] is drawn through the terminus of $A^n_{D/E}$ [22] parallel to line [23]. Line [24] contains d', so that d' is located at the intersection of lines [24] and [17]. Starting from d', the correct normal and tangential accelerations for links 3 and 5 can now be drawn.

PROBLEMS

5.1. (a) Construct the acceleration polygon for Fig. P 4.1. Here ω_2 is constant. Use data of Prob. 4.1 and assume a suitable acceleration scale or use the graphical construction of Art. 5.6. Draw vectors A_E, A_C, and A_F on the configuration diagram. Indicate their numerical values in fps^2.

(b) Determine α_3 and α_4. Indicate whether the links are increasing or decreasing in angular speed.

5.2. (a) Construct the acceleration polygon for Fig. P 3.1. Here ω_2 is constant. Use data of Prob. 4.5.

(b) Determine α_3 and α_4. Indicate whether the links are increasing or decreasing in angular speed.

5.3. (a) Construct the acceleration polygon for Fig. P 3.2. Velocity V_B is constant. Use data of Prob. 4.6.

(b) Determine α_3. Indicate whether the link is increasing or decreasing in angular speed.

5.4. (a) Construct the acceleration polygon for Fig. P 3.4. Here ω_2 is constant. Use data of Prob. 4.8.

(b) Determine α_3 and α_4. Indicate whether the links are increasing or decreasing in angular speed.

5.5. (a) Construct the acceleration polygon for Fig. P 4.2. Velocity V_B is constant. Use data of Prob. 4.2.

(b) Determine α_5.

5.6. (a) Construct the acceleration polygon for Fig. P 4.16. Here ω_2 is constant. Use data of Prob. 4.16.

(b) Determine α_3 and α_4.

5.7. Determine the vectors A_C and A_E for Fig. P 4.17. Here ω_2 is constant. Use data of Prob. 4.17.

5.8. Construct the acceleration polygon for Fig. P 4.18. Here ω_2 is constant. Use data of Prob. 4.18.

5.9. Construct the acceleration polygon for Fig. P 4.19. Here ω_6 is constant in a CCW direction. Let the length of V_D be represented by a vector $1\frac{1}{4}$ in. long. Use the graphical construction of Art. 5.6.

5.10. Construct the acceleration polygon for Fig. P 4.14. Here $\omega_2 = 60$ rpm, $\alpha_2 = 0$.

5.11. Determine α_2 for Fig. P 3.5. Here $\omega_4 = 80$ rpm, $\alpha_4 = 0$.

5.12. Determine the acceleration of slider 3 in Fig. P 5.12. The speed of 3 along link 2 is constant.

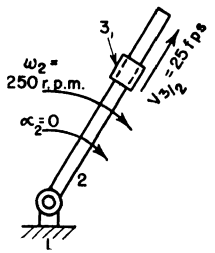

Fig. P 5.12

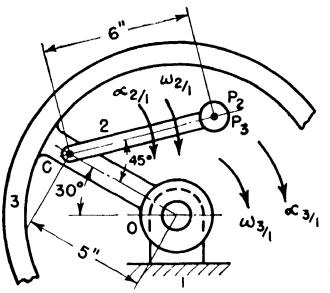

Fig. P 5.13

5.13. In Fig. P 5.13, $\omega_{3/1} = 60$ radians per sec, $\omega_{2/1} = 25$ radians per sec, $\alpha_{3/1} = \alpha_{2/1} = 0$.

(a) Determine A_{P_2} without using Coriolis' law.

(b) Determine A_{P_2} using Coriolis' law.

5.14. Determine A_C for Fig. P 3.3. Here $\omega_2 = 120$ rpm, $\alpha_2 = 0$.

5.15. Construct the acceleration polygon for Fig. P 4.21. Let the magnitude of the velocity $V_B = \frac{1}{2}$ in. and the acceleration $A_B = 1$ in. The velocity and acceleration are both in the direction of V_B in Fig. P 4.21. Use the graphical construction of Art. 5.6.

5.16. Construct the acceleration polygon for Fig. P 4.25. Velocity $V_G = 1\frac{1}{2}$ in., $V_F = 3$ in., $A_G = 2\frac{1}{2}$ in., $A_F = 2\frac{3}{4}$ in. Use the graphical construction of Art. 5.6.

CHAPTER 6

Velocity and Acceleration Graphs, Special Constructions, Analytical Methods

In the preceding chapters, methods were developed for determining velocities and accelerations in mechanisms for a chosen phase. Usually it is necessary to determine the velocities and accelerations of the links for a complete cycle. This can be done by determining the values for a series of phases through the cycle, plotting these values, and drawing curves through the points. In this chapter, graphs and special constructions will be considered.

6.1. Graphical differentiation. A velocity-time graph can be obtained from a displacement-time graph, and an acceleration-time graph can be obtained from a velocity-time graph using graphical differentiation.

A displacement-time graph is shown in Fig. 6.1. The velocity of point P is $V = ds/dt$. A line BD is drawn tangent to the curve at P. A line parallel to the time axis is drawn through B, and a line parallel to the displacement axis is drawn through D forming a right triangle BCD. The velocity is then

$$V = \frac{DCk_s}{BCk_t}$$

The fact that DCk_s and BCk_t are not infinitesimal does not matter since they were constructed in such a manner that their ratio is equal to the ratio of the corresponding infinitesimal quantities. Their ratio gives the correct slope at point P. The velocity can be plotted to any scale desired. However, it is convenient to use a particular scale. The velocity graph derived from the displacement graph is shown below it. The velocity of P is plotted as DC. This can be done with dividers. The velocity scale corresponding to this is

$$1 \text{ in.} = k_v = \frac{\text{velocity of point on machine}}{\text{length of line on drawing that represents velocity}}$$

$$= \frac{DCk_s/BCk_t}{DC} = \frac{k_s}{BCk_t} \tag{6.1}$$

The velocity graph was obtained by constructing tangent triangles, using a constant value for BC, at a series of points along the displacement graph. A constant BC produces a constant k_v scale.

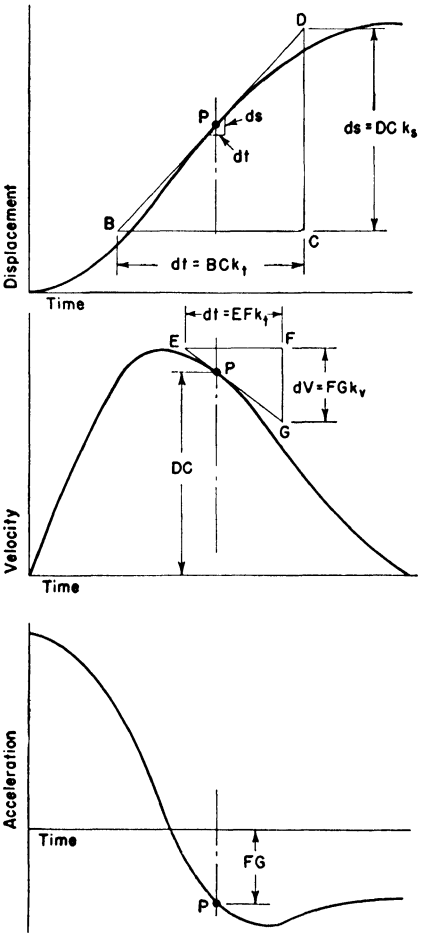

Fig. 6.1

The acceleration graph shown below the velocity graph was obtained in the same manner.

$$A^t = \frac{dV}{dt} = \frac{FGk_v}{EFk_t}$$

When the vertical leg of the triangle is used to represent the acceleration, the scale is

$$1 \text{ in.} = k_a = \frac{FGk_v/EFk_t}{FG} = \frac{k_v}{EFk_t} \tag{6.2}$$

The horizontal leg EF is again an assumed constant. The acceleration is indicated above as the tangential component since it is determined

from the change in magnitude of velocity. If the point moves in a curved path the normal acceleration must be determined in some other manner.

The hypodermic gun shown in Fig. 6.2 is an example where graphical differentiation can be useful. In operation the nozzle is held against the flesh. When the springs are released they drive the piston forward at a high velocity causing the jet from the nozzle to enter the flesh. If certain assumptions are made the velocity of the jet can be calculated. The validity of the assumptions can be determined only by experiment. If a scale is attached to the frame and a pointer to the piston rod, a high-speed motion picture can be taken to obtain data for plotting a displacement-time graph. The velocity graph for the piston can be obtained by

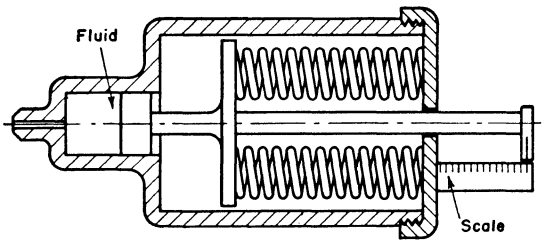

Fig. 6.2

using graphical differentiation. The velocity of the jet at any instant will be

$$\text{vel. of jet} = \text{vel. of piston} \times \frac{\text{area of piston}}{\text{area of nozzle}}$$

The constructions in the previous chapters can be made quite accurately since points are determined from intersecting lines. In graphical differentiation judgment must be used in drawing tangents. Sufficient points must be plotted and a smooth curve carefully drawn. The use of a reflecting bar will increase the accuracy. The cross section of the reflecting bar is rectangular. The bar is laid across the curve and rotated to a position such that the visible curve and the reflection form a smooth curve. The edge of the bar is then normal to the curve.

If the slope of the tangent to a curve is 74° (Fig. 6.3) and an error of 1° is made in drawing the tangent, the resulting relative error is

$$\text{relative error} = \left(\frac{\tan 74° - \tan 75°}{\tan 74°}\right) 100 = 7\%$$

At P_2 the relative error is approximately the same. The relative error curve for 1° error in the tangent is shown in Fig. 6.4. When the slope is small or large the relative error is large. For small slopes the absolute error is small. When the tangent is horizontal any error in drawing the tangent will produce an infinite relative error even though the abso-

lute error is negligible. Steep slopes should be avoided. This can usually be accomplished by choosing a suitable time scale. Errors made in deriving a velocity graph from a displacement graph are not cumulative. If an acceleration curve is derived from this curve and errors are

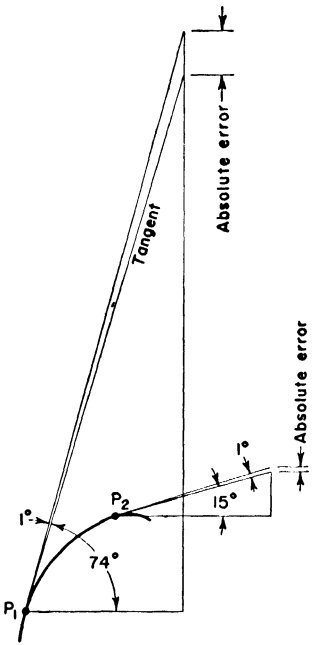

Fig. 6.3

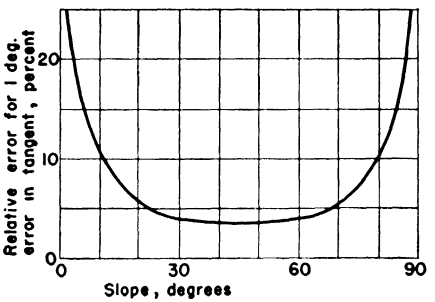

Fig. 6.4

made, the errors in the corresponding points for the two curves may be cumulative.

6.2. Revolved polygon. When it is necessary to determine velocities in a mechanism for many phases, or if in the early stages of design it is necessary to investigate similar mechanisms of different proportions, time can often be saved by using revolved polygons. In the revolved polygon the images are parallel to the links. The use of the revolved polygon will be illustrated with two examples.

Example 1. A slider crank is shown in Fig. 6.5(a). All data apply to the original drawing. The crank has uniform rotation of 200 rpm clockwise. The velocity of the piston C will be determined for 12 equally spaced positions of the crank. The velocity polygon for the number one phase is shown at (b). In (c) the polygon is revolved 90°. The velocity images are parallel to the links. The velocity scale is calculated so that vector ob is equal to O_2B on the drawing.

$$V_B = \frac{2.875}{12} \times \frac{200 \times 2\pi}{60} = 5 \quad \text{fps}$$

Since O_2B on the drawing is 1.4375 in., the velocity scale is

$$1 \text{ in.} = k_v = \frac{5}{1.4375} = 3.48 \quad \text{fps}$$

The revolved polygon is shown superimposed upon the original mechanism so that ob coincides with the crank. Line O_2c represents the magnitude of the velocity of

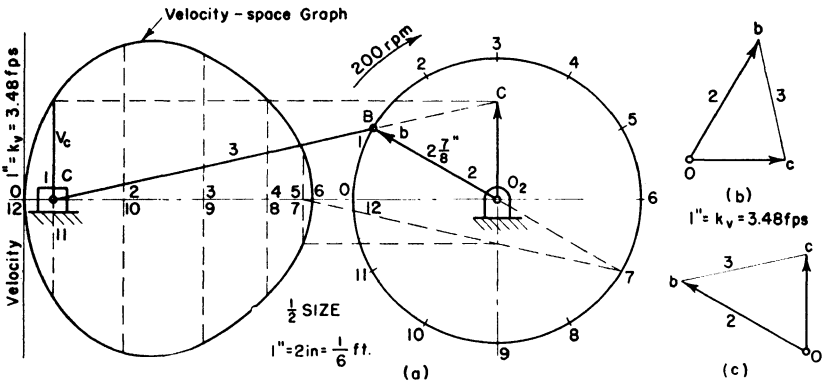

Fig. 6.5

C. For any position of the piston, point c is located on the vertical line through O_2 at the intersection with the connecting rod or the rod extended. The construction is also shown for position 7.

The velocities for the 12 positions are plotted against time in Fig. 6.6. Since the crank rotates uniformly and the positions are equally spaced on the crank

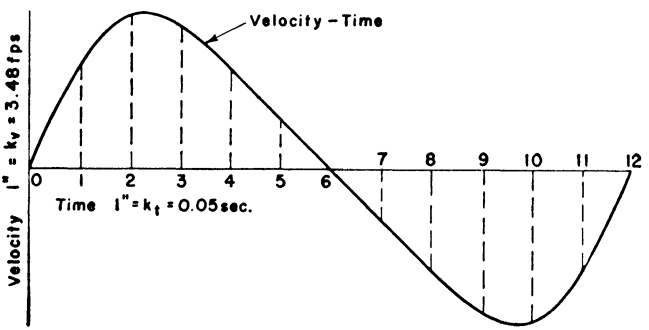

Fig. 6.6

circle, the time intervals are equal. The time for one revolution is $\frac{60}{200} = 0.3$ sec. The time axis is 6 in. long. The time scale is 1 in. $= k_t = 0.3/6 = 0.05$ sec.

Example 2. A quick-return mechanism is shown in Fig. 6.7(a). Crank 2 rotates with constant velocity. The velocity polygon is shown at (b) and the revolved polygon at (c). The velocity scale is chosen so that ob_2 is equal to O_2B_2 on the drawing (d). The revolved polygon is shown superimposed upon the mechanism. The line through O_2 that is parallel to link 4 contains b_4 and c_4. Point b_4 is located by drawing a perpendicular to link 4 through b_2. The inter-

section D is obtained by extending this line. A line through D and C locates c_4. From similar triangles it can be shown that $c_4b_4/b_4O_2 = C_4B_4/B_4O_4$. Point c_5 is located on the perpendicular to link 4 passing through c_4. This construction can be used for all phases except for vertical positions of the crank. For these two

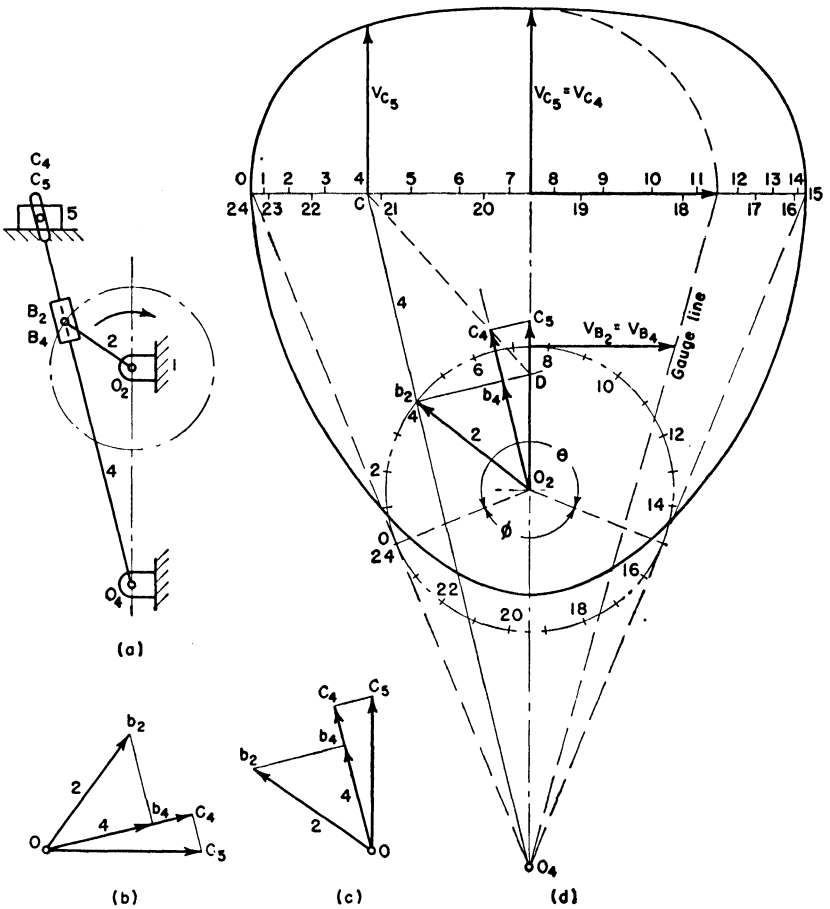

Fig. 6.7

position V_{B_2} can be laid off as shown, and V_{C_5} can be determined from a gage line. For these phases $V_{C_4} = V_{C_5}$.

The time required for the stroke from left to right is the time required for the crank to turn through the angle θ. The time for the return stroke is the time required for the crank to turn through angle ϕ. The ratio of these angles can be altered by altering the proportions of the mechanisms.

There are no general rules for constructing a revolved polygon. A method must be developed for each mechanism.

6.3. Polar velocity graphs. A slider crank is shown in Fig. 6.8. In the previous article it was shown that O_2c represents the velocity of

the piston if the crank is turning uniformly and the velocity scale is chosen so that the velocity of B is represented by the length O_2B on the drawing. These values can be plotted by rotating c about O_2 to the crank. The resulting curves are shown. The velocity of the piston for

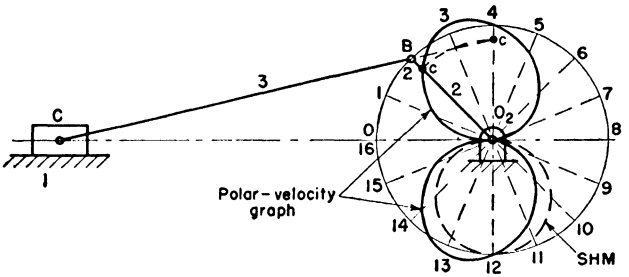

Fig. 6.8

any phase can be determined by drawing the crank in the phase and measuring the distance along the crank from O_2 to the curve.

As the ratio of the length of the connecting rod and crank is increased the motion of the piston approaches simple harmonic motion. The polar velocity graph approaches the circle shown.

A four-bar linkage is shown in Fig. 6.9. The velocity of B is laid off radially outward along crank 2. When 2 rotates uniformly Bb is con-

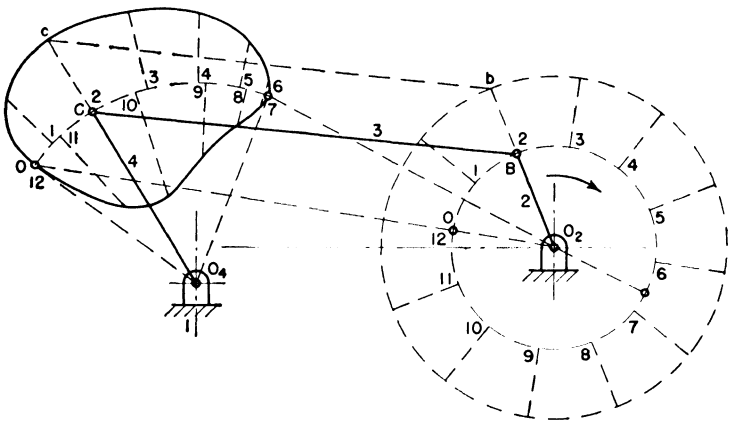

Fig. 6.9

stant and the polar velocity graph for B is a circle with center at O_2. The velocity of C is Cc. Here c is the intersection of a line through b parallel to link 3, and link 4 extended. This is the parallel line construction that was proved in Art. 3.7. Any velocity scale can be assumed.

6.4. Angular velocity graphs. It is sometimes necessary to plot angular velocity graphs. A rapid method that can be used with many

mechanisms will be described. A Geneva stop is shown in Fig. 6.10(a). The driver, member 2, rotates with uniform motion. While 2 is rotating uniformly through one-fourth revolution, 4 is rotating with a variable angular velocity through one-fourth revolution; and 4 is stationary while

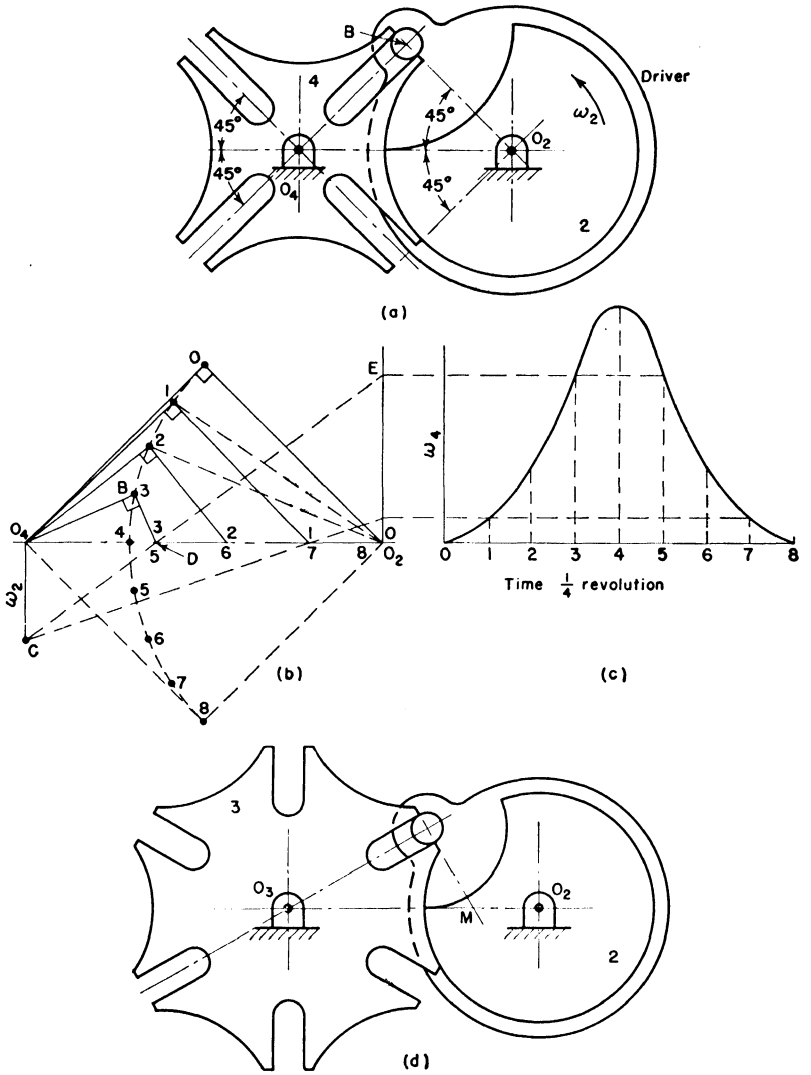

Fig. 6.10

2 is rotating through the remaining three-fourths revolution. The angular velocity time curve will be plotted for member 4. In Art. 2.12 it was shown that the angular velocities of driver and follower are inversely proportional to the segments into which the common normal (line of transmission) cuts the line of centers. The constructions for

determining the intersections of the common normal and the line of centers are shown in (b) for positions 0 to 4. For position 3 the angular velocity ratio is

$$\frac{\omega_4}{\omega_2} = \frac{O_2D}{O_4D}$$

Here ω_2 is laid off vertically from O_4 to a chosen scale. A line through C and D will intersect a vertical line through O_2 at E, forming similar triangles O_4CD and DEO_2. Then

$$\frac{\omega_4}{\omega_2} = \frac{O_2D}{O_4D} = \frac{O_2E}{O_4C}$$

and O_2E will represent ω_4 on the same scale that O_4C represents ω_2. The angular velocity time graph is shown at (c).

The Geneva stop shown at (d) has 6 slots; 3 will make $\frac{1}{6}$ turn for each turn of 2. The line of transmission intersects the line of centers at M for the phase where motion begins. This will cause impact loading. Except for low speeds, member 2 should be designed with center O_2 at M.

6.5. Ritterhaus construction. The slider crank mechanism is of such importance that special constructions have been developed for rapid

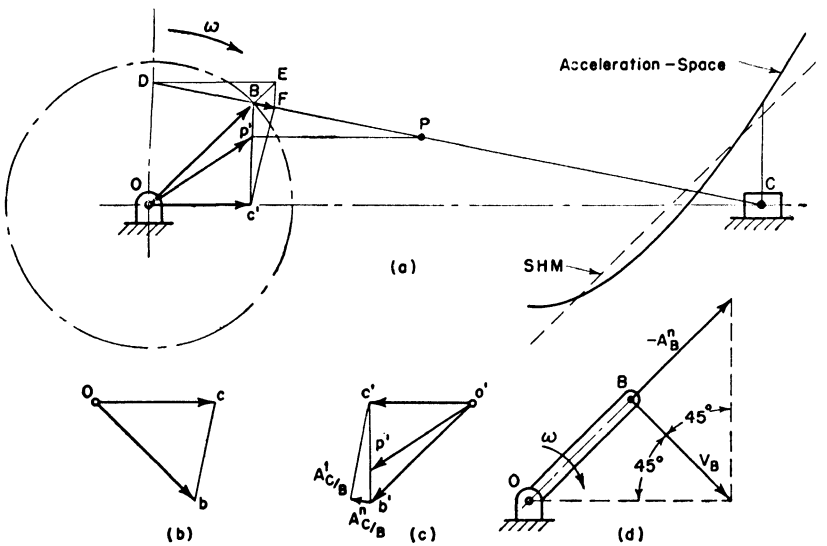

Fig. 6.11

determination of accelerations. One of these, the Ritterhaus construction, is shown in Fig. 6.11(a). The crank rotates with uniform angular velocity. The velocity polygon is shown at (b). The velocity scale was chosen in accordance with Art. 6.2; that is, the vector *ob* is equal to the length of the crank *OB* on the drawing. The acceleration polygon is shown at (c). Since there is no tangential acceleration of B, the image $o'b'$ is parallel to OB. If the acceleration scale is chosen so that the

length of the vector $o'b'$ is equal to the length of the crank on the drawing, the polygon, when rotated 180°, will fit on the mechanism as shown in (a). The directions of all accelerations are reversed. The graphical construction for determining normal accelerations (Art. 5.6) is shown at (d). The length of V_B was made equal to the crank OB. It can be seen that the normal acceleration vector is also equal to the length of the crank. The scale relationship of Eq. (5.7) therefore holds for the Ritterhaus construction.

The construction is made as follows: extend the connecting rod to the vertical center line through O, obtaining intersection D; through D draw a horizontal line; extend the crank to obtain E; a vertical line through E intersects the connecting rod at F; a perpendicular to the connecting rod at F intersects the horizontal centerline at c'. This construction can be proved as follows. Triangles OCB and DBE are similar. Triangles DOB and BEF are similar. Then

$$\frac{DB}{BC} = \frac{BE}{BO} \quad \text{and} \quad \frac{BF}{BD} = \frac{BE}{BO}$$

Eliminating BE/BO from these equations gives

$$\frac{BD}{BC} = \frac{BF}{BD} \quad \text{or} \quad BF = \frac{(BD)^2}{BC}$$

where BD represents $V_{C/B}$ and BC is the corresponding radius. Hence $BF = A^n_{C/B}$.

This construction is indeterminate for the head-end and crank-end dead-center phases. The construction shown in Fig. 6.12 can be used

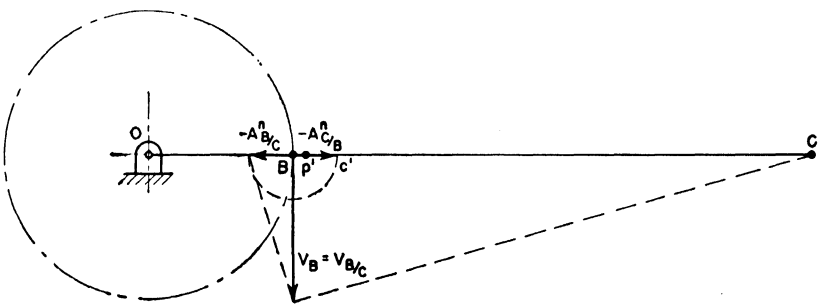

Fig. 6.12

to determine the piston acceleration for these phases. An examination of the revolved polygon in (a) shows that $A^t_{C/B}$ is zero for these phases. Since C has no velocity, $V_{B/C} = V_B$. Velocity V_B is laid off from B and the graphical construction of Art. 5.5 is used to determine $-A^n_{B/C}$. When this vector is rotated through 180° it becomes $-A^n_{C/B}$. Since all the other vectors are reversed, this is consistent.

The acceleration space graph is shown in Fig. 6.11(a). The *SHM* acceleration space graph for an infinite connecting rod is a straight line.

Sometimes it is necessary to determine the acceleration of a point on the rod such as P, the center of percussion. The line Bc' is the acceleration image of the connecting rod. A horizontal line through P locates p'. In Fig. 6.12, p' is located by proportion.

An offset slider crank mechanism is shown in Fig. 6.13. It is a quick-return mechanism. The ratio of the times for the two strokes is θ/ϕ.

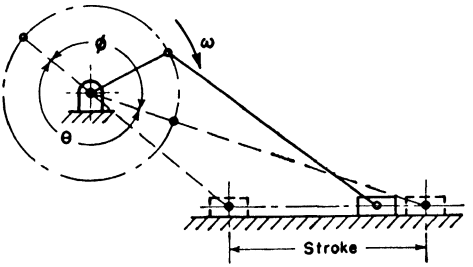

Fig. 6.13

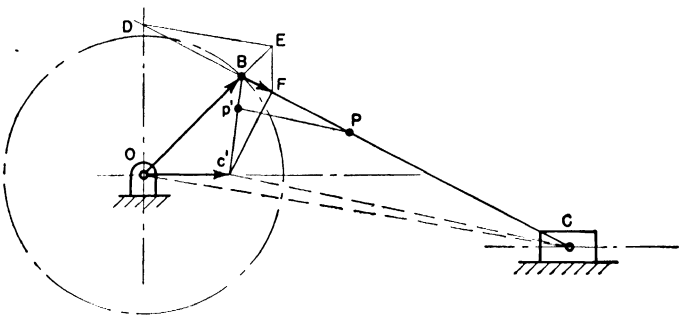

Fig. 6.14

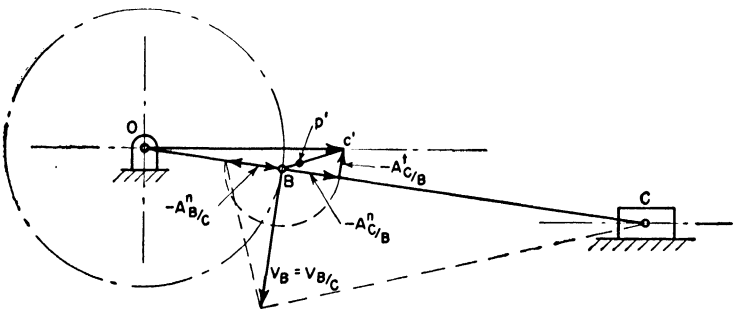

Fig. 6.15

A modified Ritterhaus construction can be used to determine accelerations in this mechanism. In Fig. 6.14 OBD is the revolved velocity polygon. In the construction DE is drawn parallel to OC. The proof given above applies. Point p' is located by drawing a line through

P parallel to Cc'. When the crank and connecting rod are collinear the construction fails. For these two phases the construction can be made as shown in Fig. 6.15. Acceleration $-A^n_{C/B}$ is determined as in Fig. 6.12, and $-A^t_{C/B}$ is perpendicular to the terminus of $-A^n_{C/B}$. Point c' must lie on the horizontal line through o. It is located as shown.

6.6. Analytical analysis. Equations for linear and angular velocities and accelerations can be obtained by differentiating displacement equations. The slider crank, Fig. 6.16, will be used to illustrate the

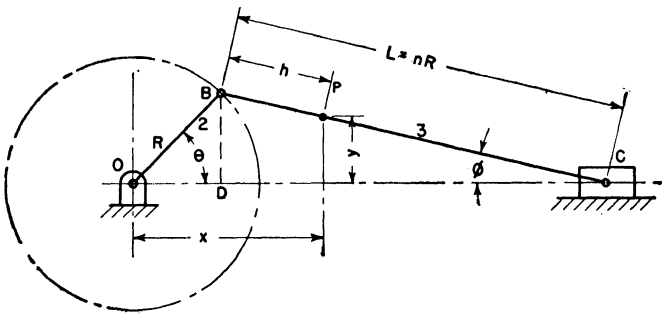

Fig. 6.16

method. Let $n = L/R$ and $m = h/L$. A relationship between θ and ϕ is

$$BD = L \sin \phi = R \sin \theta$$

$$\sin \phi = \frac{\sin \theta}{n} \tag{6.3}$$

One of the fundamental trigonometric identities is

$$\cos \phi = (1 - \sin^2 \phi)^{\frac{1}{2}}$$

Then

$$\cos \phi = \left(1 - \frac{\sin^2 \theta}{n^2}\right)^{\frac{1}{2}}$$

This can be expressed as a binomial series

$$\left(1 - \frac{\sin^2 \theta}{n^2}\right)^{\frac{1}{2}} = 1 - \frac{1}{2}\frac{\sin^2 \theta}{n^2} - \frac{1}{2 \cdot 4}\frac{\sin^4 \theta}{n^4} - \frac{1 \cdot 3}{2 \cdot 4 \cdot 8}\frac{\sin^6 \theta}{n^6} - \frac{1 \cdot 3 \cdot 5}{2 \cdot 4 \cdot 8 \cdot 16}\frac{\sin^8 \theta}{n^8} \cdots$$

When $n = 4$ and all terms are dropped but the first two; the maximum error in the accelerations calculations is about 0.6 per cent. Only the first two terms will be considered here. If greater accuracy is desired an additional term can be included. Then

$$\cos \phi = \frac{1}{n}\left(n - \frac{1}{2n} \sin^2 \theta\right) \quad \text{approximately} \tag{6.4}$$

The displacement of any point P on the connecting rod is

$$x = R\cos\theta + h\cos\phi = R\cos\theta + \frac{h}{n}\left(n - \frac{1}{2n}\sin^2\theta\right) \tag{6.5}$$

$$y = (L - h)\sin\phi = \left(\frac{L - h}{n}\right)\sin\theta \tag{6.6}$$

Differentiating these equations with respect to time gives

$$V_P^x = \frac{dx}{dt} = -R\omega_2\left(\sin\theta + \frac{m}{2n}2\sin\theta\cos\theta\right)$$

$$= -R\omega_2\left(\sin\theta + \frac{m}{2n}\sin 2\theta\right) \tag{6.7}$$

$$V_P^y = \frac{dy}{dt} = R\omega_2(1 - m)\cos\theta \tag{6.8}$$

If the angular velocity of the crank is constant,

$$A_P^x = \frac{dV_P^x}{dt} = -R\omega_2^2\left(\cos\theta + \frac{m}{n}\cos 2\theta\right) \tag{6.9}$$

$$A_P^y = \frac{dV_P^y}{dt} = -R\omega_2^2(1 - m)\sin\theta \tag{6.10}$$

The acceleration of the piston is obtained by substituting $m = 1$ in the above equations.

$$A_c^x = -R\omega_2^2\left(\cos\theta + \frac{1}{n}\cos 2\theta\right) \tag{6.11}$$

$$A_c^y = 0 \tag{6.12}$$

It can be seen that when n is infinite the motion of the piston is simple harmonic.

From Eq. (6.3) the angular displacement of the connecting rod is

$$\phi = \sin^{-1}\left(\frac{\sin\theta}{n}\right)$$

The angular velocity of the connecting rod is

$$\omega_3 = \frac{d\phi}{dt} = \frac{\omega_2^2(1 - n^2)\sin\theta}{(n^2 - \sin^2\theta)^{\frac{3}{2}}} \tag{6.13}$$

and the angular acceleration is

$$\alpha_3 = \frac{d\omega_3}{dt} = \frac{\omega_2^2(1 - n^2)\sin\theta}{(n^2 - \sin^2\theta)^{\frac{3}{2}}} \tag{6.14}$$

For most mechanisms an analytical analysis becomes quite tedious.

PROBLEMS

6.1. (a) Plot the velocity-space graph for the slider of Fig. P 6.1 (see Fig. 6.5). The mechanism is to be drawn one-half size. Use 30° intervals for θ. Calculate the velocity scale.

(b) Plot the velocity-time graph. Let the velocity scale be the same as in part (a) and let the time axis be 6 in. long (see Fig. 6.6). Calculate the time scale.

(c) Determine the acceleration-time graph using graphical differentiation. Let the horizontal leg of the tangent triangle be 1 in. Calculate the acceleration scale.

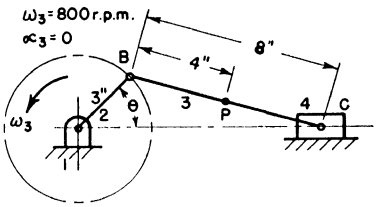

Fig. P 6.1

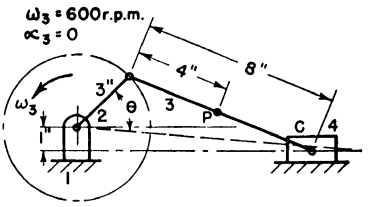

Fig. P 6.2

6.2. Same as Prob. 1, except Fig. P 6.2 is to be used.

6.3. Plot the polar-velocity graph for the slider of Fig. P 6.1 (see Fig. 6.8).

6.4. Same as Prob. 6.3 except Fig. P 6.2 is to be used.

6.5. Plot the polar-velocity graph for point C, Fig. P 6.5. Indicate the velocity scale used.

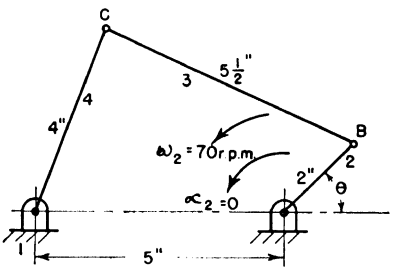

Fig. P 6.5

6.6. The center distance of driver and follower of a Geneva stop mechanism is to be 3 in. The driver is to rotate 5 times for each revolution of the follower. The driving pin is to enter the slot tangentially so that there will be no impact loading.

(a) Draw a Geneva stop mechanism that meets these requirements.

(b) Plot the angular velocity graph for the stop member for one-fifth revolution. The time axis is to be 3 in. long and is to be divided into 6 equal time spaces. Use the method of Art. 6.4. The angular velocity of the driver is to be represented by a line $1\frac{1}{4}$ in. long. The speed of the driver is 140 rpm. Calculate the angular velocity scale.

6.7. Plot the angular velocity graph for member 4 of Fig. P 6.5. Use 30° intervals for θ. Apply the method of Art. 6.4. The angular velocity of member 2 is to be represented by a line 2 in. long, and the time axis is to be 3 in. long. Calculate the angular velocity scale and the time scale.

6.8. Plot the angular velocity graph for member 3, Fig. P 6.5. Indicate the scale used. The time axis is to be 6 in. long and 30° intervals for θ are used. The revolved polygon method can be used to obtain $V_{B/C}$ for each phase and the values plotted; $\omega_{3/1} = V_{B/C}/BC$. Since BC is a constant, the $V_{B/C}$ graph will represent the $\omega_{3/1}$ graph if the scale for it is calculated.

6.9. Determine the velocity and acceleration of slider C, Fig. P 6.1, for 45° intervals of θ. Draw the mechanism one-half size and use the Ritterhaus construction.

6.10. Same as Prob. 9, but applied to Fig. P 6.2.

6.11. Plot the angular acceleration graph for the connecting rod of Fig. P 6.1. Use 45° intervals for θ. Here $A^t_{C/B}$ can be taken from the Ritterhaus construction for each phase and plotted; $\alpha_{3/1} = A^t_{C/B}/CB$. Since CB is a constant, the $A^t_{C/B}$ graph will represent $\alpha_{3/1}$ if the scale for it is calculated.

6.12. Same as Prob. 11, but applied to Fig. P 6.2.

6.13. Using analytical methods, calculate the velocity and acceleration of the slider, Fig. P 6.1, for $\theta = 0, 45°, 90°, 180°$.

CHAPTER 7

Cams

7.1. Introductory. A cam is a direct-contact machine element so formed that its prescribed motion imparts a prescribed motion to a follower. Within reasonable limits the motions of cam and follower can be arbitrarily chosen and the cam profile made to fit these conditions. Usually the cam rotates with uniform angular velocity.

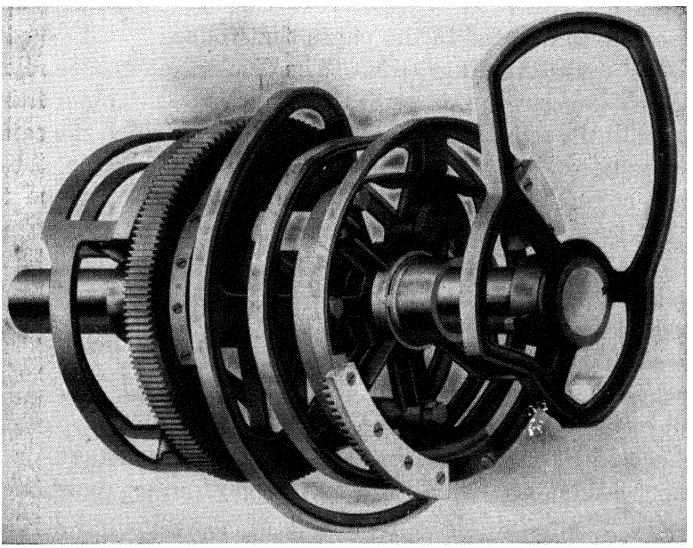

Fig. 7.1. The cams assembled on the shaft actuate and control most of the mechanical action of the Linotype. (Courtesy of Mergenthaler Linotype Co.)

The previous chapters in this book deal largely with determination of motions of assumed linkages. Kinematic synthesis is the reverse of this; that is, the motion is assumed and the mechanism to give this motion is then determined. When pin-connected links are used it is often difficult or impossible to obtain the desired motion. In many cases satisfactory approximations can be obtained. Cam design is an example of a case where kinematic synthesis can be easily applied.

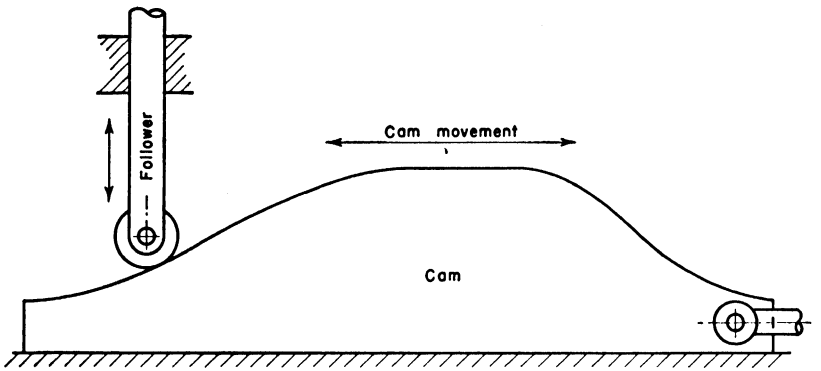

Fig. 7.2. Translation cam with reciprocating roller follower.

7.2. Classification. Most cams fall into one of the three major classifications.

1. Disk cams
2. Translation cams
3. Cylindrical cams

These types are illustrated in the pages that follow.

7.3. Displacement diagrams. The displacement-time relationship of the follower governs the shape of the cam profile. This relationship is chosen to fulfill the requirements of the machine in which the cam mechanism is to be used. In many applications, as for example, the internal combustion engine valve cam, considerable latitude can be taken in choosing the type of motion. Four common types of motion are listed below.

1. Constant acceleration
2. Modified constant velocity
3. Simple harmonic
4. Cycloidal

These will be considered in detail.

7.4. Constant acceleration. A motion of constant or uniform acceleration is sometimes called gravity motion or parabolic motion. The equation of motion is

$$s = \frac{1}{2} At^2 \tag{7.1}$$

This is Eq. (2.14) with an initial velocity of zero. When A is the acceleration of gravity this is the equation of motion of a freely falling body that has started from rest. The graph of this equation is a parabola. For equal time intervals the distances traveled will be in the ratio 1, 3, 5, 7, 9, . . . The total distance traveled after each time interval will be 1, 4, 9, 16, 25, . . . The method of constructing a displacement-time diagram for this motion will be illustrated with an example.

A follower is to move radially outward 1 in. with constant accelera-

tion while the cam turns through 90°. (This can be any type of disk cam with reciprocating follower, as for example that of Fig. 7.9.) During the next 90° of cam rotation the follower is to continue to move outward with constant deceleration and is to have zero velocity at the end of this time. The follower is to return with constant acceleration and deceleration during the next 150° of cam rotation. The follower dwells or rests during the remaining 30° of cam rotation. The graph is shown in Fig.

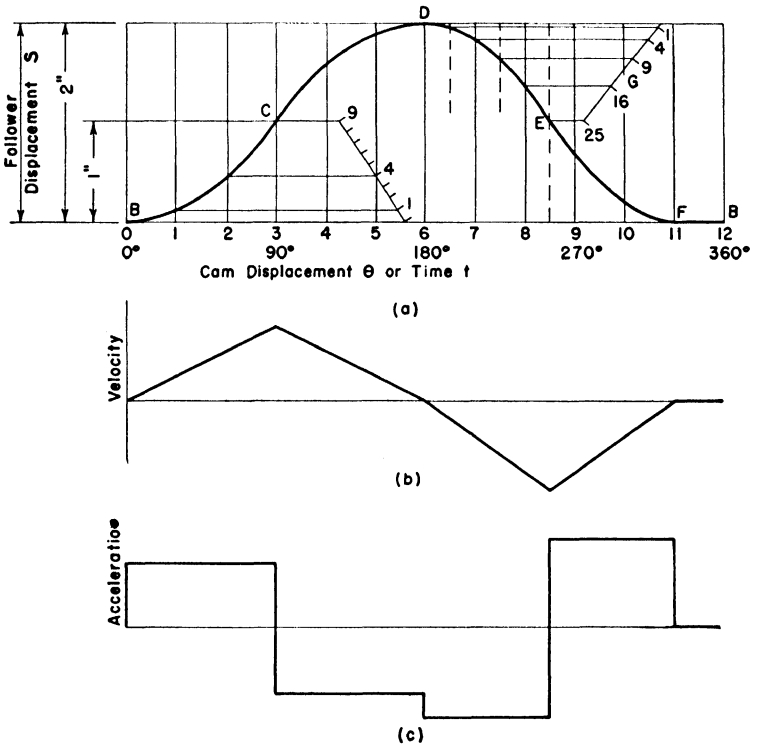

Fig. 7.3

7.3(a). It is assumed that the cam rotates with constant angular velocity. Equal angular displacements can then be represented by equal time intervals. The abscissa represents one revolution of the cam. Each division represents the time required for the cam to turn through 30°. The first portion of the curve is a plot of Eq. (7.1), starting with $t = 0$ and $s = 0$. It starts at B with a horizontal tangent and terminates at C. This curve can be constructed by drawing any line between the time axis and a horizontal line through C that can be conveniently divided into 9 equal lengths. Points 1, 4, and 9 are projected as shown. The curve CD is constructed in the same way. The two curves BC and CD have a common tangent at C. This results from equal distances moved during acceleration and deceleration in equal time intervals.

The follower returns from D to E in $2\frac{1}{2}$ time intervals. For convenience the intervals 6–7 and 7–8 are divided to give a total of 5 equal lengths. Points 1, 4, 9, and 25 are projected as shown. Curve EF is constructed in the same manner. Here FB represents a dwell.

The velocity and acceleration graphs are shown at (b) and (c). The maximum acceleration occurs between D and F. Assuming that the cam is rotating 100 rpm the acceleration can be determined as follows. The distance traveled from D to E is $\frac{1}{12}$ ft. The corresponding time is

$$\frac{2.5}{12} \times \frac{60}{100} = 0.125 \quad \text{sec}$$

$$A = \frac{2S}{t^2} = \frac{2 \times \frac{1}{12}}{(0.125)^2} = 10.3 \text{ fps}^2$$

The maximum velocity occurs midway between points 8 and 9. Its value is

$$V = At = 10.3 \times 0.125 = 1.29 \quad \text{fps}$$

7.5. Modified constant velocity. The displacement, velocity, and acceleration diagrams for a follower having constant outward velocity for one-half revolution of the cam, constant return velocity for 150°, and dwell for 30° are shown in Fig. 7.4. Theoretically the velocity changes instantaneously, causing an infinite acceleration. This is of course impossible; the parts would deform and reduce the acceleration to a finite value. Except at low speeds there would be impact loading and large forces. This type of motion should be avoided if possible. Part

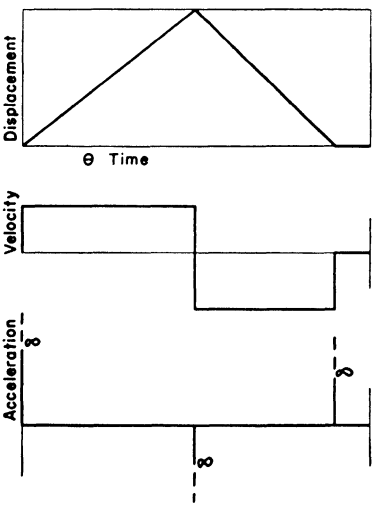

Fig. 7.4

of the follower motion can be constant if the follower is brought up to speed and then brought to a stop over a period of time. This motion is called modified constant velocity. The construction of a displacement-time diagram for this type of motion will be illustrated with an example.

A follower is to move outward 2 in. It is to be constantly accelerated for 60°, then move with uniform velocity for 30°, then decelerate for 90° of the cam rotation. The return motion is to be constant acceleration for 60° and constant deceleration for 90°. The follower is to dwell

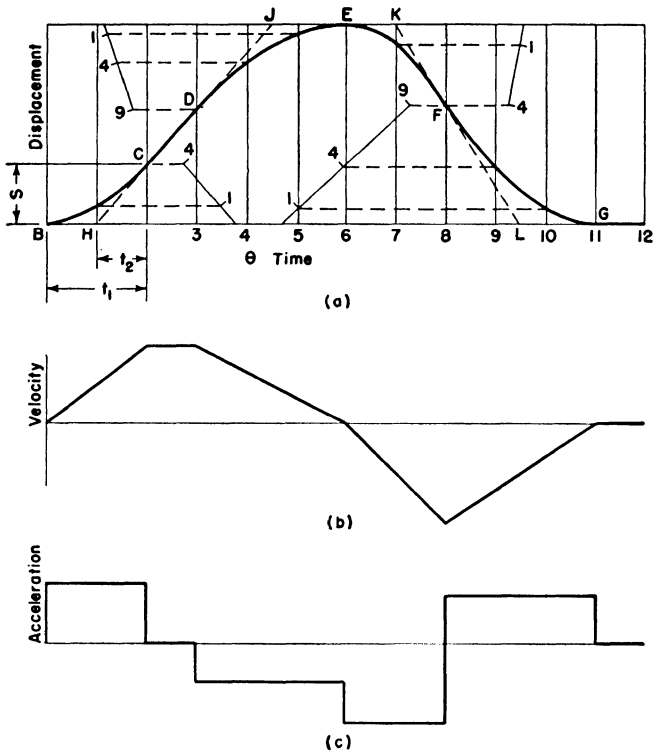

Fig. 7.5

for the remaining 30°. The displacement, velocity, and acceleration graphs are shown in Fig. 7.5. Here BC represents constant acceleration. A terminal velocity V is attained at C, and CD is a continuation of this terminal velocity. Here DE is constant deceleration. Points C and D are located on a straight line through H and J, the mid-points of the acceleration and deceleration periods. This results from the fact that a point moving with constant velocity V through a distance S requires only half as much time as a point starting from rest and accelerating uniformly through the same distance and attaining the same velocity. This can be shown as follows: HC represents uniform velocity; the equation of motion is

$$S = Vt_2$$

and for BC,

$$S = \frac{1}{2} A t_1^2$$

The final velocity is

$$V = At_1$$

These three equations give

$$\tfrac{1}{2}At_1^2 = At_1t_2 \qquad \text{or} \qquad \tfrac{1}{2}t_1 = t_2$$

For the return motion, F is located by drawing a line through K and L, the mid-points of the acceleration and deceleration periods.

7.6. Simple harmonic motion. This motion was discussed in Art. 2.5. The method of constructing a SHM (simple harmonic motion) graph will be illustrated with an example. A follower is to move outward 2 in. with SHM while the cam turns through one-half revolution. The follower is to return with SHM during the next 150° and then dwell for 30°. The displacement, velocity, and acceleration graphs are shown in Fig. 7.6. Use is made of the fact that the projection on the diameter,

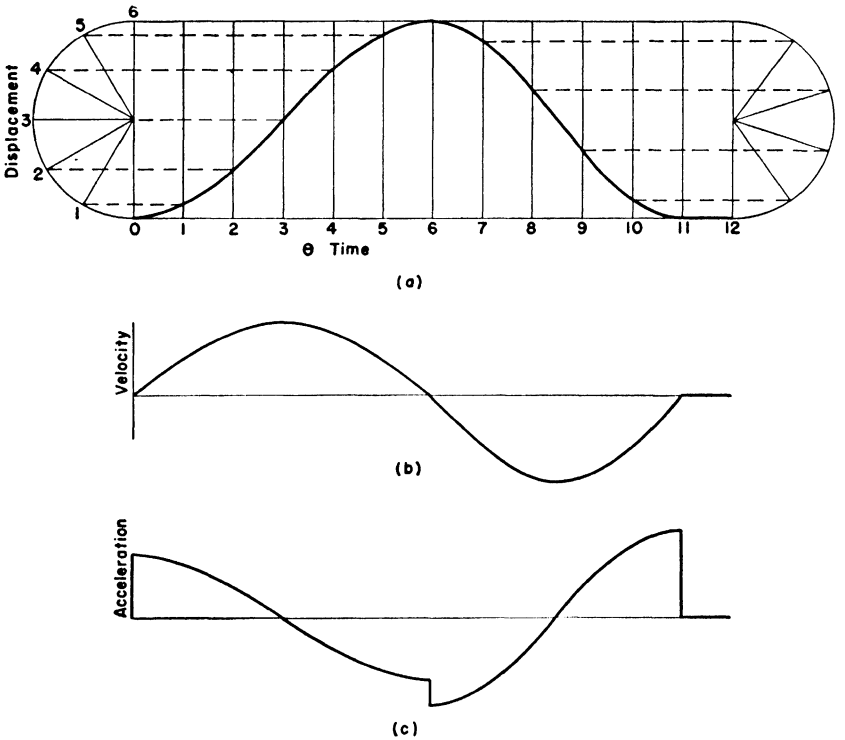

Fig. 7.6

of a point moving with constant speed on a circle, is harmonic motion. A semicircle is drawn on the left end of Fig. 7.6(a). It is divided into 6 equal sectors corresponding to the 6 equal time intervals on the time axis. The points on the semicircle are projected as shown to determine the curve. The follower returns in 5 time intervals. The semicircle on the right is divided into 5 equal sectors corresponding to these time intervals.

The maximum acceleration occurs at the beginning and end of the return stroke. It can be determined as follows. Assume that the speed of the cam is 100 rpm. The time for the return stroke is

$$\tfrac{60}{100} \times \tfrac{5}{12} = 0.25 \quad \text{sec}$$

During this time the imaginary point that is used for projection moves around the semicircle, or π radians. The angular velocity of this point is

$$\omega = \frac{\pi}{0.25} = 4\pi \quad \text{radians per sec}$$

The acceleration is

$$A = r\omega^2 \cos\theta = \tfrac{1}{12}(4\pi)^2 = 13.2 \quad \text{fps}^2$$

7.7. Cycloidal motion.* Cycloidal motion is defined by the equation

$$s = S\frac{\theta}{\theta_0} - \frac{S}{2\pi}\sin\frac{2\pi\theta}{\theta_0} \tag{7.2}$$

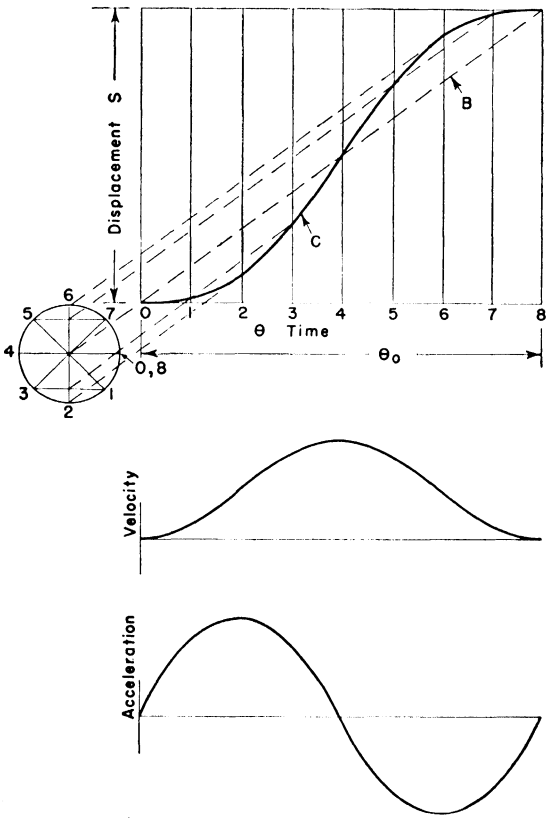

Fig. 7.7

* J. A. Hrones, "An Analysis of the Dynamic Forces in a Cam-Drive System," Paper 47-A-46, *Trans. ASME*, 1948.

where θ_0 is the angle turned through by the cam corresponding to the total displacement S, and θ is any intermediate angle corresponding to a displacement s. Curve C in Fig. 7.7 is the displacement graph that is obtained from this equation. The curve can be obtained graphically. The broken line B represents the first term in Eq. (7.2). The construction for the second term is similar to that for harmonic motion. The displacements are superimposed on line B. The radius of the circle shown at the left is $S/2\pi$. It is divided into sectors corresponding to the intervals on the time axis. The points on the circumference are projected to the vertical centerline of the circle and then parallel to line B, to the corresponding lines on the time axis. The resulting curve is C.

7.8. Selection of motion. Some of the factors that must be considered in selecting a motion are functional requirements, speed, mass of moving parts, external loads, elasticity of parts, and cost of manufacture. When operating speeds are low, selection of the motion is usually not critical. All types of motion cannot be used at high speeds. The finite instantaneous changes in acceleration may lead to vibration and noise. Harmonic motion has a higher peak acceleration for a given lift in a given time than a motion of uniform acceleration and deceleration. It can be used for higher speeds if the outward and return motions each equal 180° of cam rotation. When this is not true the acceleration graph is discontinuous, as shown in Fig. 7.6. Cycloidal motion has a higher peak acceleration than harmonic motion but there are no discontinuities in the acceleration graph.

In the above examples deformation of the parts was not considered. Deformations are always present and sometimes they may be large. *Actually in a large radial aircraft engine at take-off speed, the sum of the forces due to inertia, valve-spring force, and gas pressure may be a ton or more, resulting in deflections of the order of* $\frac{1}{8}$ *in. at the valve.* A method has been developed for determining a motion that compensates for deflections and produces smooth action at high speeds.*

7.9. Cam profile determinations. After the displacement diagram and type of follower are chosen to fulfill the requirements of the machine, the cam profile is determined. To simplify the work inversion is used. Instead of a fixed frame and a rotating cam the cam is fixed and the frame is rotated in such a manner that the relative motions of the parts are unchanged. When this concept is grasped cam layout becomes very simple. Several examples will be considered. The technique used by the author in some of the examples is not necessarily the only way of determining the cam profiles. The reader can probably develop variations.

7.10. Disk cam with reciprocating knife-edge follower. This type of cam and follower is shown in Fig. 7.8. The displacement graph

* W. M. Dudley, "New Methods in Valve Cam Design," *SAE Quart. Trans.*, January, 1948, Vol. 2, No. 1, p. 19.

for one revolution of the cam is shown. The diagram is divided into 12 equal time intervals and the cam is divided into 12 corresponding equal angles. The displacements for the 12 positions are projected on the centerline of the follower as 0′, 1′, 2′, 3′, etc. This is called the displacement scale. The distance from the point of the follower in its lowest position to the center of the cam is the radius of the base circle. When the cam is rotated clockwise the follower is to move according to the displacement scale. When the cam turns clockwise 2 spaces, the edge

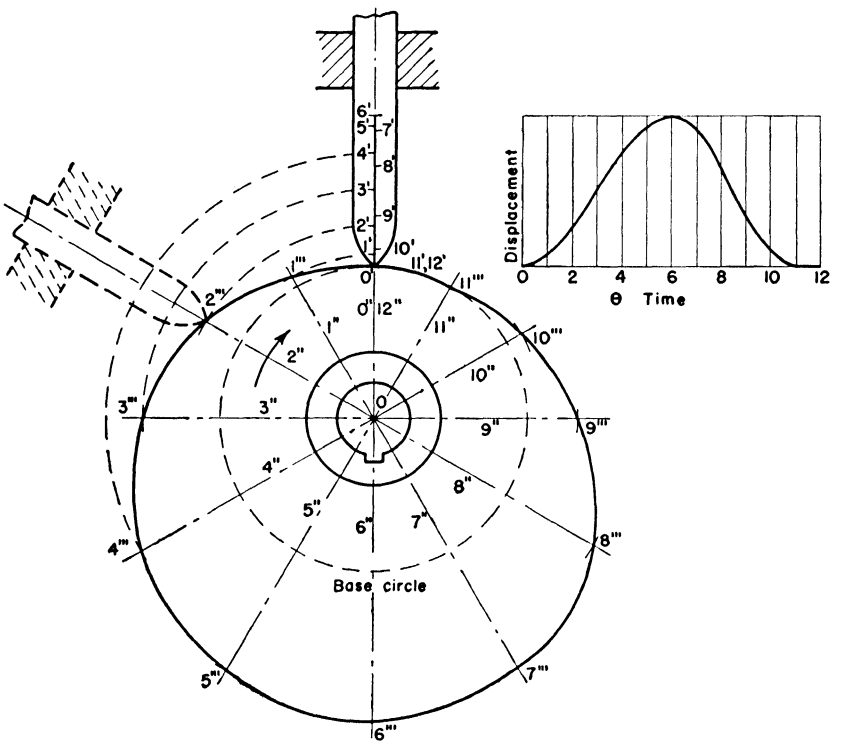

Fig. 7.8

of the follower is to be pushed to position 2′. To produce the same relative motion with the cam fixed the frame is rotated CCW 2 spaces and the edge of the follower is moved radially out a distance 0′2′. This locates point 2‴ a point on the cam profile. Points 1‴, 3‴, 4‴, etc. are determined in the same manner. A smooth curve through these points is the cam profile. For greater accuracy more points should be located for drawing the profile.

Knife-edge followers are subject to excessive wear and are not practical in most applications.

7.11. Disk cam with reciprocating roller follower. This type of cam and follower is shown in Fig. 7.9(a). The follower is to move radially

according to the scale indicated on the centerline. The lowest point on the scale, 0′, is at the center of the roller, and 0′0 is the radius of the base circle. The centers of the roller for the other positions, 1‴, 2‴, 3‴, etc. are determined as in the previous example. A smooth curve through these points is the pitch profile of the cam. Arcs with radii equal to the roller radius are struck from these points. The envelope of these arcs is the cam profile. It is necessary to determine first the pitch profile, because contact between cam and follower is not on the radial line through

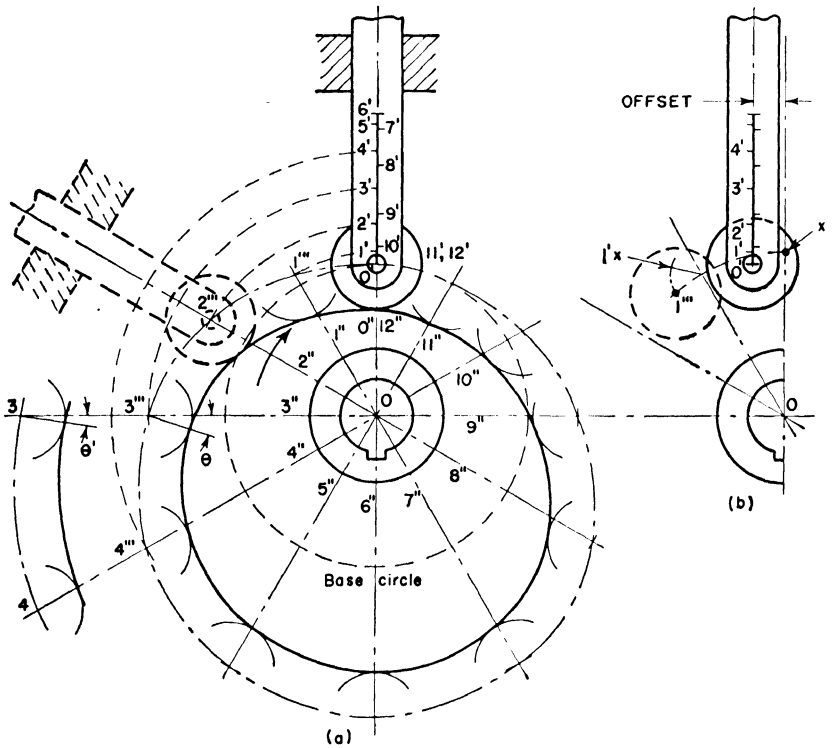

Fig. 7.9

the center of the roller except during periods of dwell. When the follower is moving, contact is shifted to one side or the other. This results in a pressure angle shown as θ for position 3‴. The resultant force between cam and roller, neglecting friction, will lie along the common normal. This produces an undesirable side force on the follower that tends to cause it to bind in its guide. The pressure angle can be reduced by increasing the radius of the base circle. This is shown at the left of the figure. Then θ is reduced to θ'. This is because the follower movement is produced by a greater length of cam profile; 3–4 is greater than 3‴–4‴.

In Fig. 7.9(b) the follower is shown in an offset position. The cam profile is determined as before, with one additional construction for each roller center. This is shown for position 1. An arc with 0 as the center and radius of 01′ is drawn locating point x. The offset $1'x$ is used to locate $1'''$ as shown.

7.12. Disk cam with reciprocating flat-face follower. This is shown in Fig. 7.10. The cam is to turn clockwise and move the follower

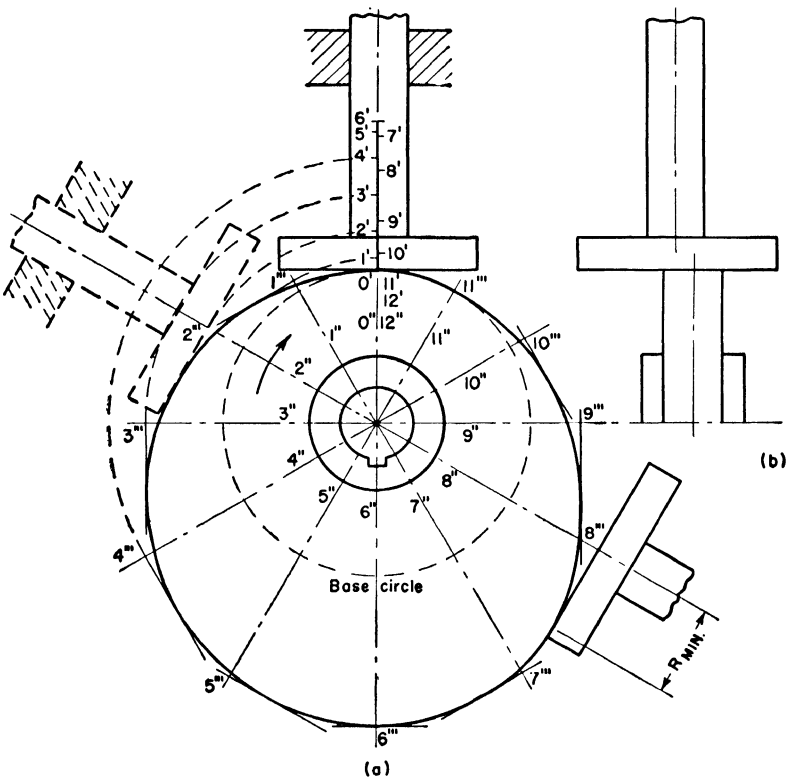

Fig. 7.10

according to the scale on its centerline. Points $1'''$, $2'''$, $3'''$, etc. are determined as in the previous examples. At each of these points a line normal to the radial line is drawn. The envelope of these lines is the desired cam contour.

The diameter of the flat face must be of sufficient size to reach the point of contact in all phases. This is determined by inspection. In phase 8 the point of contact is farthest from the radial line. This is indicated R minimum. The flat face should be made a little larger.

A portion of the side view of the cam and follower is shown at (b). A small offset as shown is often used to produce rotation of the follower. This results in more uniform wear.

7.13. Disk cam with oscillating flat-face follower. This mechanism is shown in Fig. 7.11. The cam is to turn clockwise and the follower is to oscillate according to the scale indicated. An angular scale can be used but it is usually more convenient to work with arc lengths that represent the corresponding angular values. The flat face extended is tangent to a circle of radius r with center at 0‴. The construction for phase 3 (90° CW rotation of the cam) is shown. Point 3‴ is located by

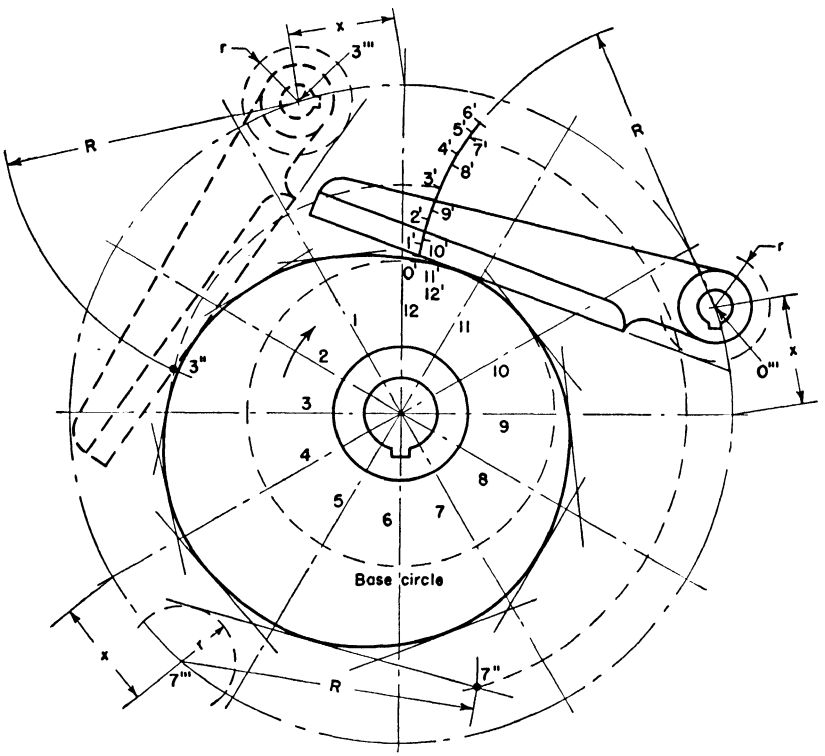

Fig. 7.11

any convenient means 90° CCW from 0‴. Point 3″ is the intersection of arc of radius 03′ with 0 as the center and the arc of radius R with 3‴ as the center. A line through 3″ tangent to the circle of radius r with center at 3‴ is the correct position for the follower face. The construction for position 7 is also shown.

7.14. Disk cam with two followers. The base circle of a cam with primary and secondary followers is shown in Fig. 7.12. The offset is too large to use a single follower as was done in Fig. 7.9. The scale for the required motion of the secondary follower is shown on the centerline as 0′, 1′, 2′, etc. This scale is transferred to the primary follower on any convenient arc with O as the center. The construction for phases 0, 5,

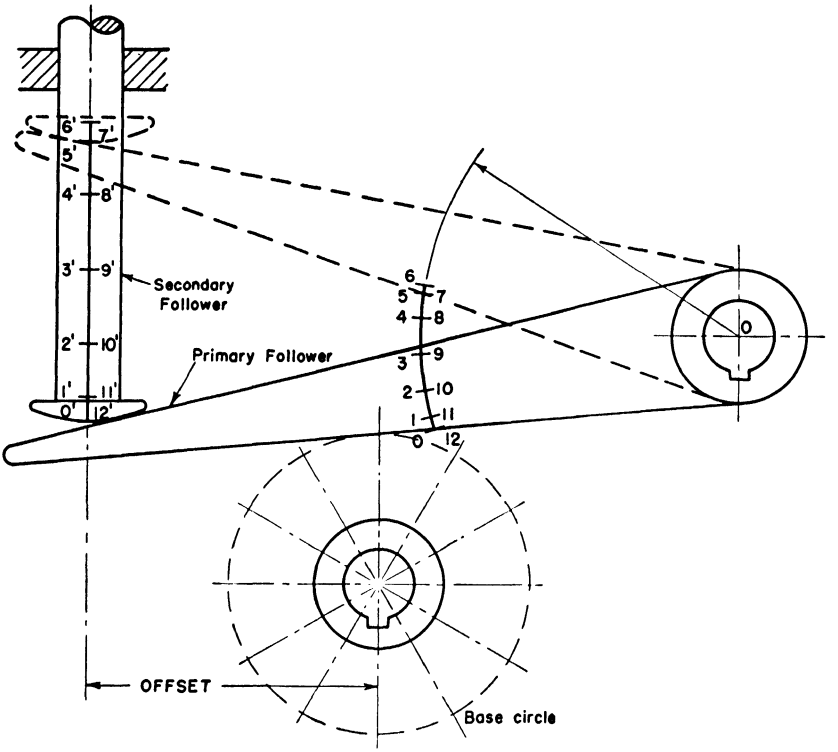

Fig. 7.12

and 7 are shown. The cam profile is then determined from the primary follower as in the previous example.

7.15. Design limitations. The usual procedure in cam design is to assume the displacement scale, the type of follower, and the base circle. These assumptions are not always compatible. When this is the case, modification of one or more of the assumptions will usually lead to a practical solution.

In Fig. 7.13(a) the assumptions produced the pitch profile with a point at B. It can be seen that the working profile will not force the roller along the pitch contour to the point B. The center of the roller will follow the dotted path shown. The desired motion can be approached by making the base circle larger or by making the diameter of the roller smaller.

In (b) the reciprocating flat-face follower is to move according to the scale indicated. The radius of the base circle is R_1. The follower face is drawn in the different positions $1''$, $2''$, $3''$, etc. It can be seen that a smooth curve cannot be drawn tangent to all these, since $3''$ lies beyond the intersection of $2''$ and $4''$. When the radius of the base circle is increased to R_2 the new positions $2'''$, $3'''$, $4'''$ are satisfactory.

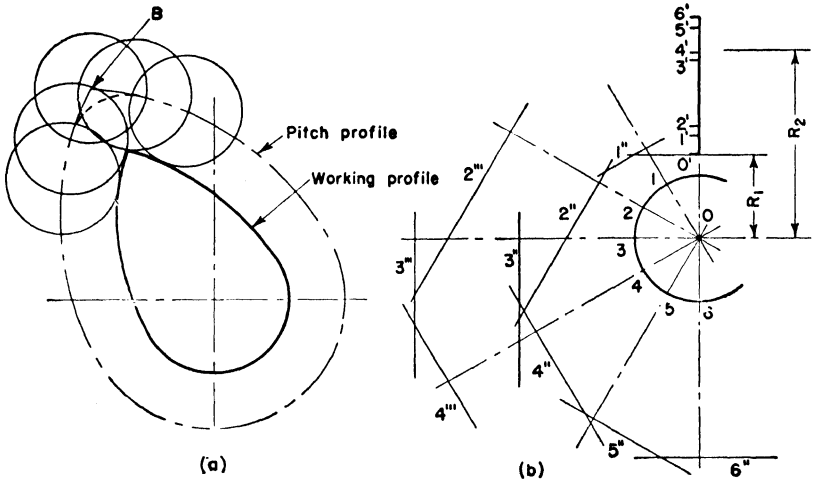

Fig. 7.13

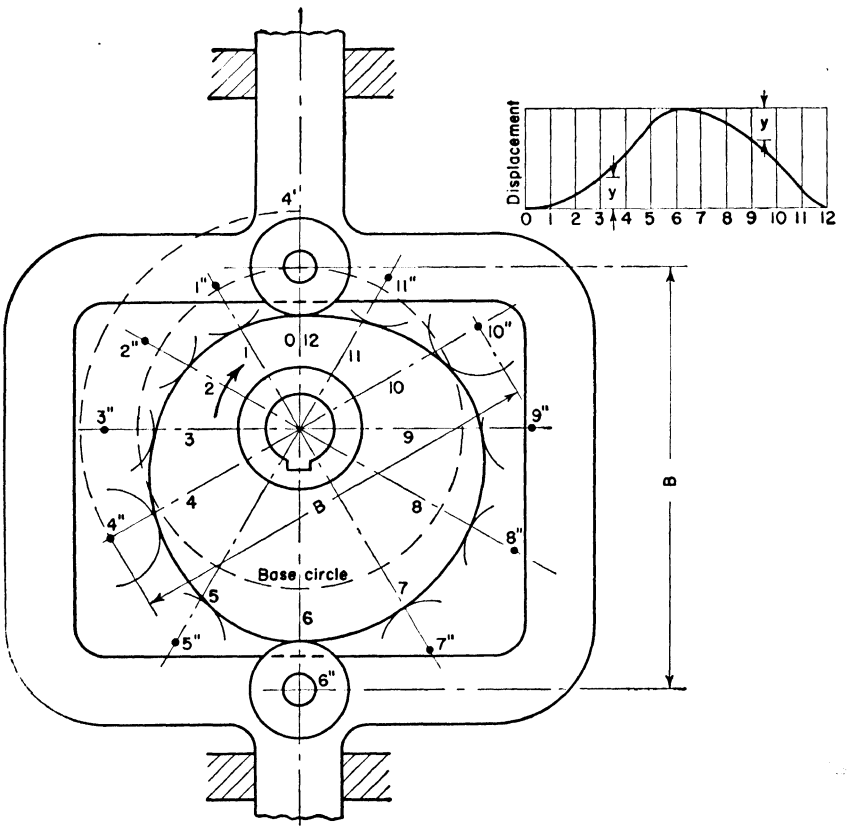

Fig. 7.14

7.16. Positive return cams. In the previous examples the return motion of the follower was not positive. An external force such as a spring force is required to maintain contact between cam and follower during portions of the cycle. Abnormal conditions such as lack of lubrication or spring failure may occur and the follower may not return. In some applications this would do no damage. In applications where damage would result, mechanical restraint should be introduced for the entire cycle.

A constant diameter cam is shown in Fig. 7.14. The two rollers produce constraint over the entire cycle. This type of cam requires that the outward and return motions be the same. The outward motion is according to the given displacement graph, points 0 to 6. The cam profile for this motion is determined in the usual manner. Distance B

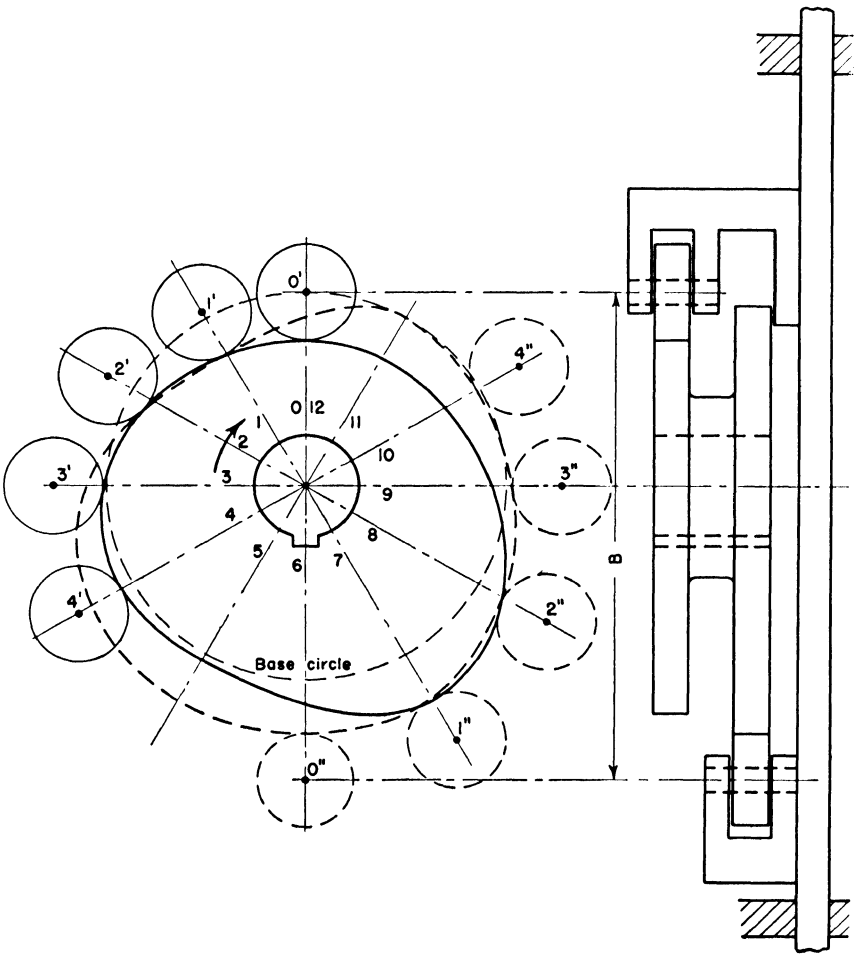

Fig. 7.15

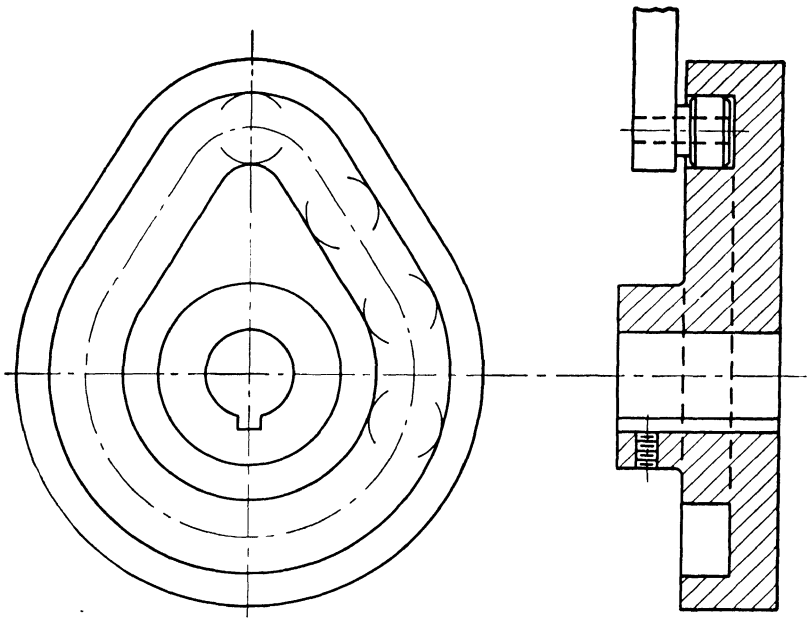

Fig. 7.16

is equal to the sum of the base circle diameter and the total displacement. Centers 7″, 8″, 9″, etc. are located by making 1″7″ = 2″8″ = 3″9″, etc. = B. This construction produces a return motion that is the same as the outward motion.

If the outward and return motions are to be different, two cams must be used as shown in Fig. 7.15. The entire profile of the cam shown solid is determined in the usual manner. The second cam, shown by a broken line, is determined by letting 0′0″ = 1′1″ = 2′2″, etc. = B, a constant.

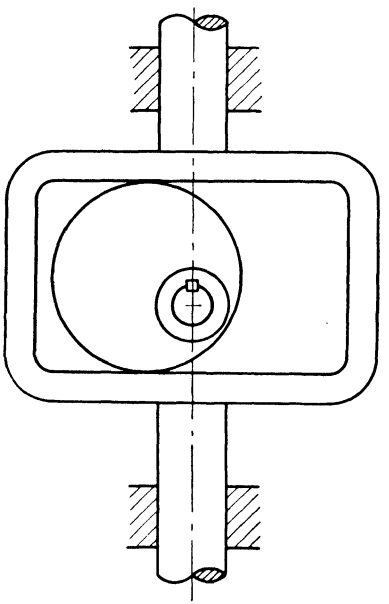

Fig. 7.17

Another type of positive return cam is shown in Fig. 7.16. The roller follower is constrained to move in the groove. This mechanism has an undesirable feature in that each time the roller changes contact from one side of the groove to the other its direction of rotation is reversed.

The eccentric cam shown in Fig. 7.17 produces constrained simple harmonic motion.

7.17. Auxiliary linkages. The maximum angular displacement of an oscillating follower is usually about 45°. A larger angular motion can be obtained with an auxiliary linkage. One type is shown in Fig. 7.18(a). The assumed ϕ scale is transferred to the primary follower 3.

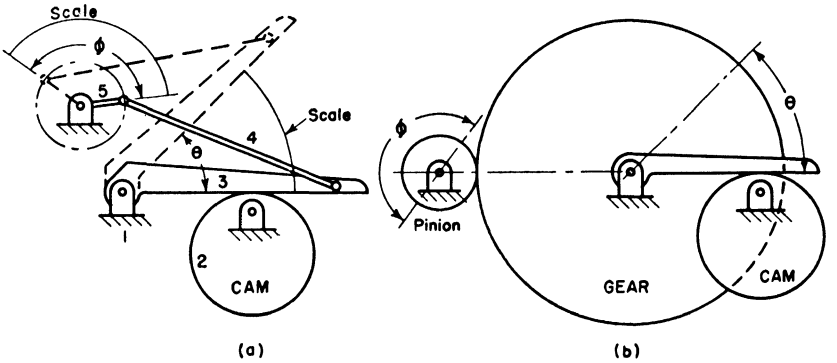

Fig. 7.18

The cam profile is determined from this. A greater displacement ratio can be obtained with gears as shown at (b).

7.18. Automotive cams. A typical automotive valve cam for use with a flat-face follower is shown in Fig. 7.19. It is symmetrical about the vertical centerline. Portions *BC*, *CD*, and *EF* are circular arcs of

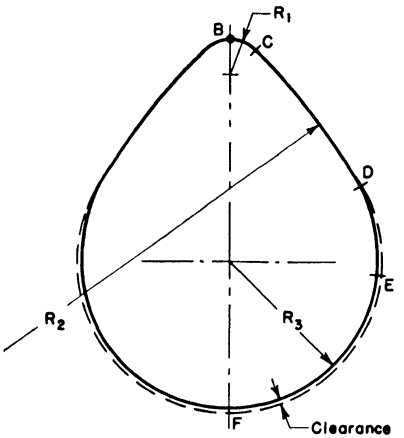

Fig. 7.19

radii R_1, R_2, and R_3, respectively. The portion of the profile from *D* to *E* is called the ramp. The radial distance of this curve from the center of the cam increases at a uniform rate from *E* to *D*. For the average cam this increase is about 0.0006 in. per degree. This produces a slow lift and closes the gap between the follower and the valve stem. When

hydraulic valve lifters are used the clearance and ramp are unnecessary. When hydraulic lifters are not used the clearance is necessary to allow for inaccuracies in adjustment and unequal expansion of the engine parts. A hydraulic valve lifter automatically adjusts itself for these conditions.

Under ideal conditions the valve lift begins at D. The follower motion consists of portions of harmonic motion cycles. The acceleration graph is discontinuous. This type of valve cam is not always satisfactory at high speeds.

7.19. Cylindrical cams. Cylindrical cams are made by machining grooves in a cylinder, Fig. 7.20, or by fastening guide strips on the outside

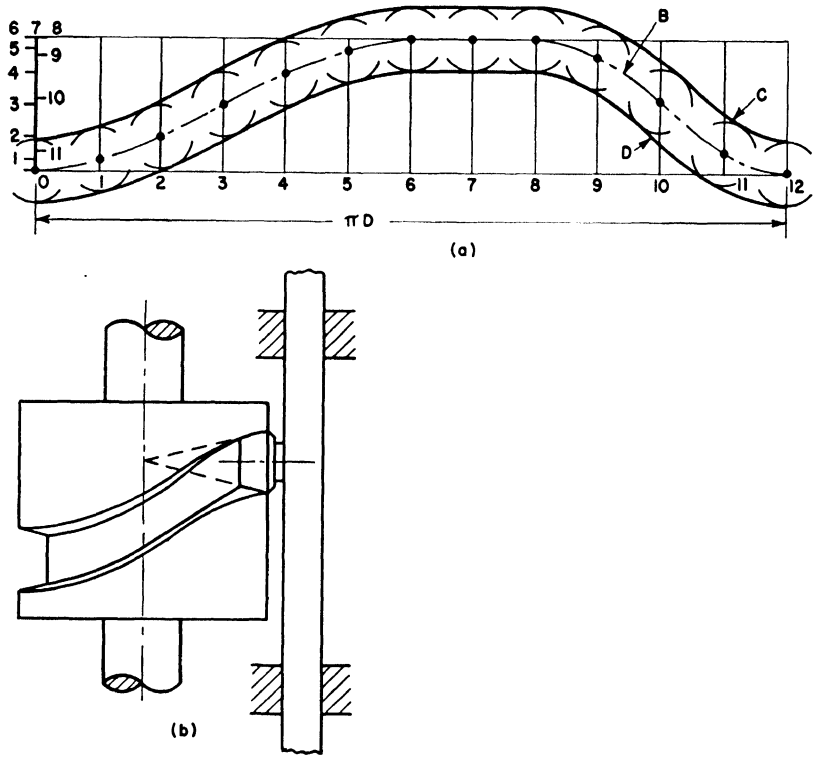

Fig. 7.20

of a cylinder, Fig. 7.22. The cam in Fig. 7.20 drives a reciprocating roller follower. If the roller is a cylinder it will not have rolling contact with the side of the groove. If the roller is a frustum of a cone with the apex on the axis of the cam, it will have rolling contact with the side of the groove during periods of dwell, e.g., when the groove is circular, and approximate rolling when the groove is a helix. (Rolling cones will be considered in the next chapter.)

When the cam in Fig. 7.20 turns one revolution it is to move the follower according to the displacement graph B. The displacement scale

is drawn full size and the length of the time axis is equal to the circumference of the cam cylinder. Curves C and D are obtained by drawing arcs equal in radius to that of the roller. If this diagram is wrapped around the cylinder it can be used as a template for scribing lines to

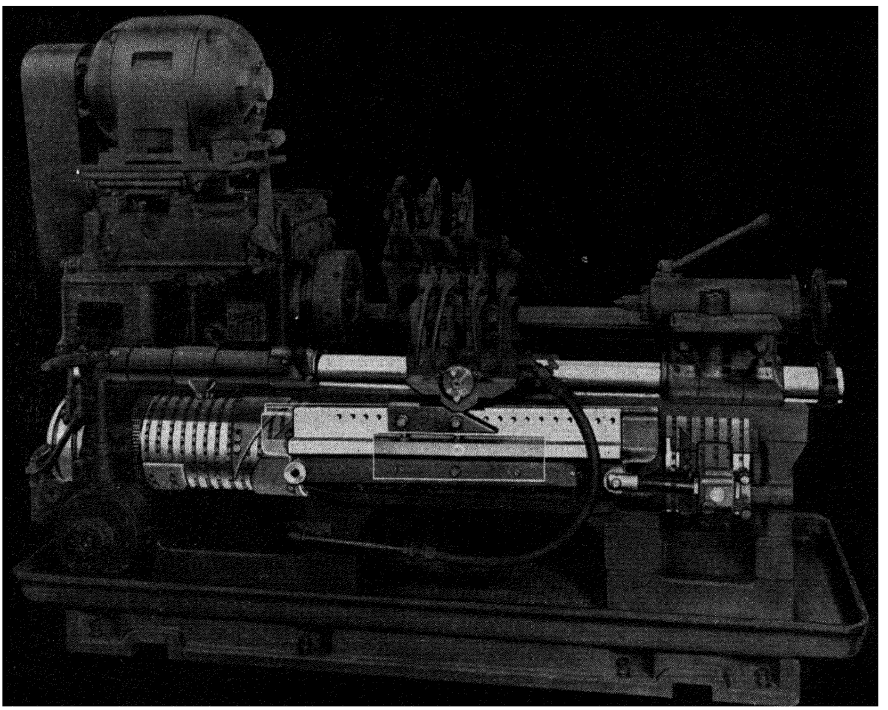

Fig. 7.21. Fay automatic lathe. (Courtesy of Jones & Lamson Machine Co.)

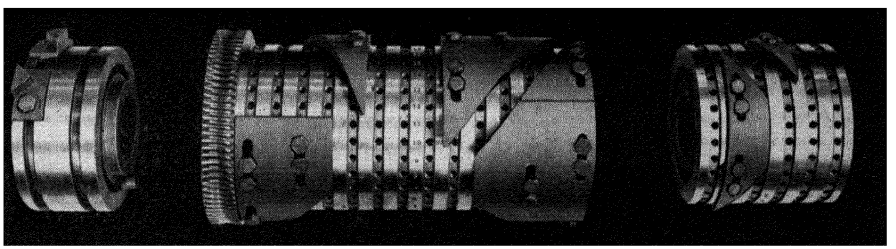

Fig. 7.22. (Courtesy of Jones & Lamson Machine Co.)

outline the groove that is to be cut. Cams are usually made in a different manner as shown in Fig. 7.23. In this illustration the groove is being cut with a conical milling cutter. Rotation of the disk cam or former shown at the lower left produces a vertical motion of the head that carries the cutter. Rotation of the former and the cam blank are coordinated

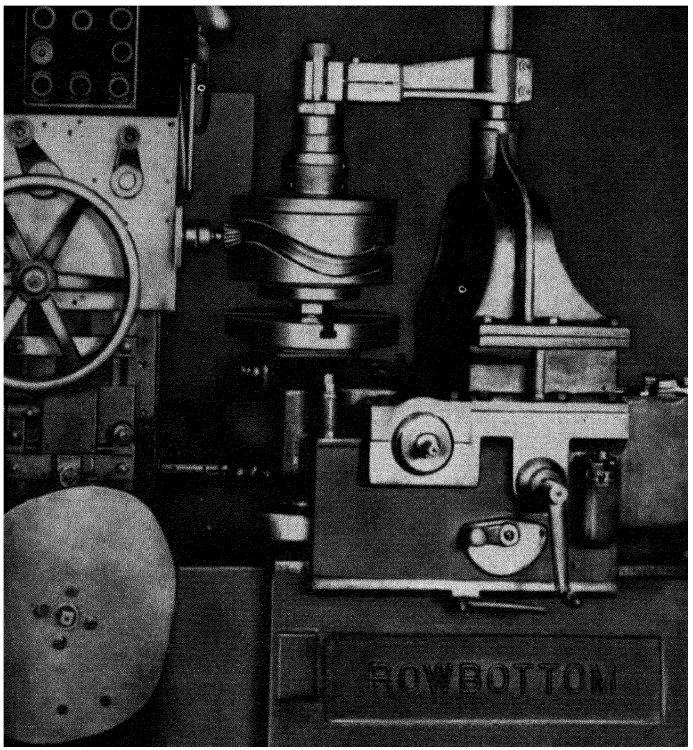

Fig. 7.23. Cam milling machine. (Courtesy of Rowbottom Machine Co.)

through a gear train. The profile of the former is designated to produce the required groove for the particular cam being cut.

7.20. Coordinated cams. Each of the cams in Fig. 7.1 is designed to produce specific movements in the Linotype machine. The coordination of these movements was considered in the determination of each displacement diagram. The cams are assembled with the correct angular relationship to produce the correct sequence of motions throughout the machine.

This is also true of the cylindrical cams on the Fay automatic lathe, Fig. 7.21. This lathe is completely automatic. The operator places the work in the machine and pulls the starting lever. All necessary operations are performed automatically, including stopping the lathe when the part is finished. A set of cams must be designed for each product that is to be machined. The cams are easily attached to the drums by means of capscrews.

If a point on a follower is to move according to arbitrarily chosen vertical and horizontal scales two cams must be used. An example is shown in Fig. 7.24. Two cams are to move the pen so that it writes the word "Jets." Points 0, 1, 2, 3, etc. are selected to outline the word.

The two cams can then be laid out simultaneously by using the methods of the previous examples. Another method is to construct the mechanism except for the cams. Circular disks of cardboard, wood, or sheet metal are placed on the cam axis. When the pen is placed on a numbered point the disks are turned to the corresponding displacement and points

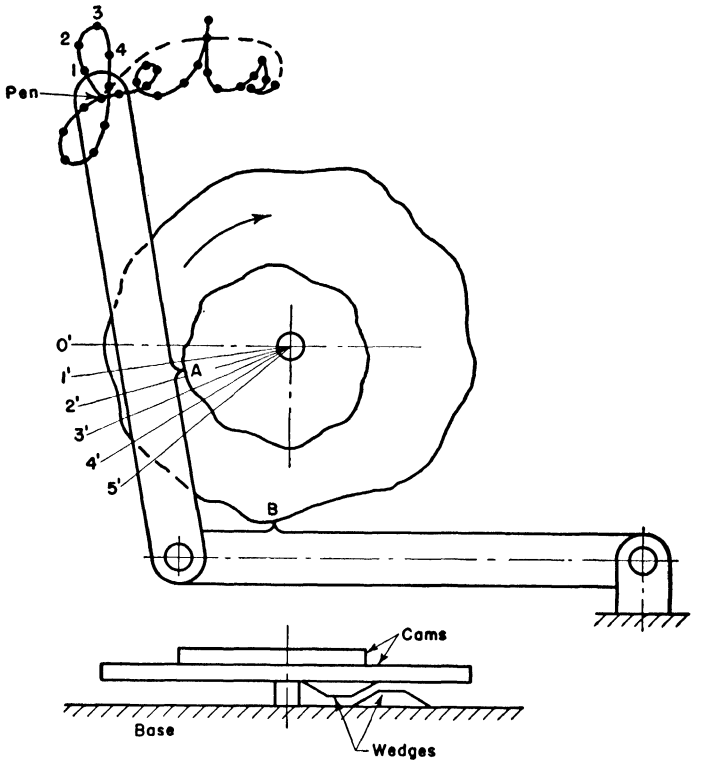

Fig. 7.24

A and B marked. The arm carrying the pen can be lifted from the paper for those portions of the word shown dotted by fastening wedges on the under surface of the cam and the base.

PROBLEMS

7.1. In this problem various types of displacement time graphs are to be constructed. The displacements are to be $1\frac{1}{4}$ in. and 30° intervals are to be used. In some cases it will be necessary to divide some of the 30° intervals into smaller units. The motions are arbitrarily chosen to give practice in plotting these types of graphs.

(a) Outward, constant acceleration 75° and constant deceleration 75°, dwell 60°, return, constant acceleration 60° and constant deceleration 60°, dwell 30°.

(b) Outward, constant acceleration 30°, constant velocity 90°, constant deceleration 60°, return, constant acceleration 120°, and constant deceleration 60°.

(c) Outward, constant acceleration 60°, constant velocity 60°, constant deceleration 30°, dwell 30°, return, constant acceleration 60°, and constant deceleration 120°.

(d) Outward, constant acceleration 60°, constant velocity 30°, constant deceleration 90°, dwell 30°, return SHM 150°.

(e) Outward, SHM 120°, dwell 30°, return, SHM 180°, dwell 30°.

(f) Outward motion $\frac{3}{4}$ in. SHM 60°, dwell in this position 30°, remainder of outward motion SHM 90°, return SHM 150°, dwell 30°.

(g) Outward, cycloidal 180°, dwell 30°, return cycloidal 120°, dwell 30°.

(h) Outward, cycloidal 210°, return, cycloidal 150°.

7.2. Determine the maximum velocity and acceleration of the follower in feet and seconds during the outward and during the return motion for:

(a) Prob. 7.1(a). Speed of cam 350 rpm.
(b) Prob. 7.1(b). Speed of cam 600 rpm.
(c) Prob. 7.1(c). Speed of cam 400 rpm.
(d) Prob. 7.1(d). Speed of cam 700 rpm.
(e) Prob. 7.1(e). Speed of cam 650 rpm.
(f) Prob. 7.1(f). Speed of cam 850 rpm.

7.3. (a) Differentiate Eq. (7.2) and obtain equations for velocity and accelerations of the follower.

(b) Same as Prob. 7.2 but applied to Prob. 7.1(g). Speed of cam is 600 rpm.
(c) Same as Prob. 7.2 but applied to Prob. 7.1(h). Speed of cam is 400 rpm.

7.4. In this problem cam contours are to be laid out graphically, using methods described in the book. The type of follower is indicated by specifying Figs. P 7.1, P 7.2, P 7.3, P 7.4, or P 7.5. The follower motion is indicated by specifying Prob. 7.1(a), (b), (c), (e), or (f). The direction of the cam is indicated as CW (clockwise) or CCW (counterclockwise). Oscillating follower displacement scales are to be laid off on an arc of $3\frac{1}{2}$-in. radius unless otherwise specified.

(a) Fig. P 7.1, Prob. 7.1(a), CW.
(b) Fig. P 7.1, Prob. 7.1(b), CCW.
(c) Fig. P 7.1, Prob. 7.1(a), CW, follower offset $\frac{1}{2}$ in. to the left.
(d) Fig. P 7.2, Prob. 7.1(a), CW. Determine the maximum pressure angle.
(e) Fig. P 7.2, Prob. 7.1(a), CW, follower offset $\frac{1}{2}$ in. to the right. Determine the maximum pressure angle.
(f) Fig. P 7.2, Prob. 7.1(b), CCW.
(g) Fig. P 7.2, Prob. 7.1(c), CW.
(h) Fig. P 7.3, Prob. 7.1(a), CW.
(i) Fig. P 7.3, Prob. 7.1(a), CCW.
(j) Fig. P 7.3, Prob. 7.1(b) CW.
(k) Fig. P 7.3, Prob. 7.1(e), CCW.
(l) Fig. P 7.4, Prob. 7.1(a), CW.
(m) Fig. P 7.4, Prob. 7.1(a), CCW, the follower to oscillate through an angle of 15°.

(n) Fig. P 7.4, Prob. 7.1(b), CW.
(o) Fig. P 7.4, Prob. 7.1(f), CCW.
(p) Fig. P 7.5, Prob. 7.1(a), CW.
(q) Fig. P 7.5, Prob. 7.1(a), CCW, the follower to oscillate through an angle of 20°.
(r) Fig. P 7.5, Prob. 7.1(e), CW.
(s) Fig. P 7.5, Prob. 7.1(f), CW.
(t) Fig. P 7.5, Prob. 7.1(b), CCW, the follower to oscillate through an angle of 20°.

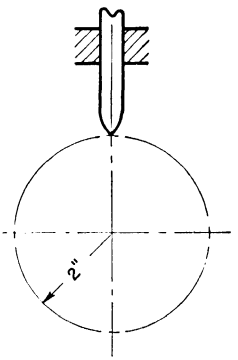

Fig. P 7.1

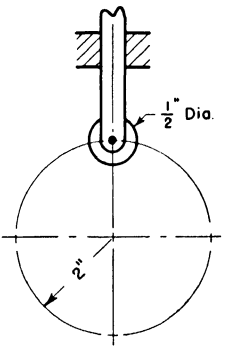

Fig. P 7.2

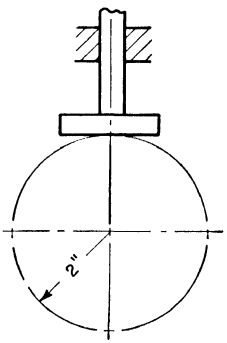

Fig. P 7.3

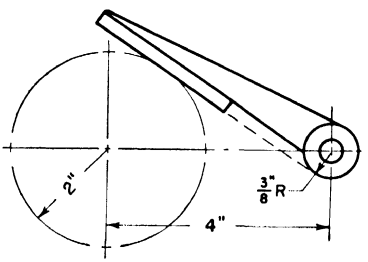

Fig. P 7.4

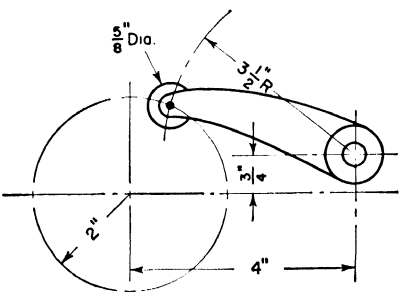

Fig. P 7.5

7.5. Lay out the contour of a positive return cam that is similar to Fig. 7.14. Here B is 4 in. and the roller diameters are $\frac{3}{4}$ in. The displacement is 1 in., and the outward motion is constant acceleration 60°, constant deceleration 90°, dwell 30°. The cam rotates CCW.

7.6. Lay out the contour of a positive return cam that is similar to Fig. 7.15. Here B is $4\frac{1}{2}$ in. and the roller diameters are $\frac{3}{4}$ in. The displacement scale is that of Prob. 7.1(a). The cam rotates CCW.

CHAPTER 8

Rolling Contact

8.1. Introductory. A study of bodies having rolling contact is of value for several reasons. Rolling bodies are used to transmit power and produce desired motions; they are used in machine elements such as ball and roller bearings; an understanding of rolling bodies is necessary for the development of the theory of gearing.

8.2. Conditions of pure rolling. In Art. 2.16 it was shown that rolling contact exists when the point of contact lies on the line of centers of the two bodies. When the centers of rotation of the two bodies are fixed it is obvious that the sum of the contact radii is constant. When pure rolling exists there is no slipping, the lengths of arcs making contact in any interval of time must therefore be equal. It was shown in Art. 3.8 that the point of contact is the instant center of the two bodies.

8.3. Rolling cylinders. A cylinder or ball rolling on a plane is the simplest type of rolling contact (Fig. 8.1). The plane can be considered

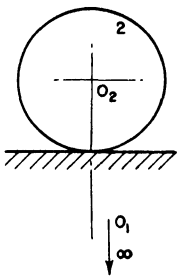

Fig. 8.1

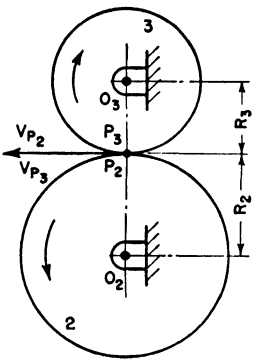

Fig. 8.2

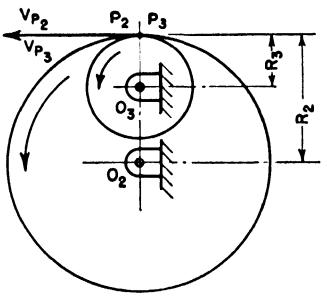

Fig. 8.3

a cylinder with its center at infinity. When cylinder 2 is rotated once, it moves over the plane a distance equal to its circumference. Rolling external cylinders are shown in Fig. 8.2 and an external and internal cylinder in Fig. 8.3.

In Fig. 2.24 rolling contact exists for the phase shown. When 2 is turning CCW there is a component of motion along the common normal

in the direction of the follower. In Figs. 8.2 and 8.3 the common normal lies along the line of centers. The direction of motion of the point of contact in the driver is along the common tangent. Positive driving does not exist; force is transmitted by means of friction. In some applications this is undesirable and in others desirable. Friction wheels could not be used to drive the camshaft of an automobile engine. In some cases where overloading of a machine is possible, friction wheels or other friction drives can be used as safety devices. The friction drive is designed to slip before any of the machine parts are damaged.

Large forces can be transmitted by means of rolling friction drives. The force that is required to move a freight train is transmitted through rolling friction of steel on steel. In general, rolling friction drives are not used to transmit large forces because of high bearing loads that are present in this type of drive.

In Art. 2.16 it was shown that for bodies having rolling contact the angular velocity ratio of driver and follower is inversely as the contact radii.

$$\frac{\omega_2}{\omega_3} = \frac{R_3}{R_2} \tag{8.1}$$

If the center distance and angular velocity ratio are known, the radii of the cylinders can be found as follows. If the cylinders are to rotate in opposite directions, external cylinders must be used (Fig. 8.2) then

$$R_2 + R_3 = O_2O_3$$
$$R_3 = O_2O_3 - R_2$$

Substituting this in Eq. (8.1) gives

$$\frac{\omega_2}{\omega_3} = \frac{O_2O_3 - R_2}{R_2} = \frac{O_2O_3}{R_2} - 1$$

$$R_2 = \frac{O_2O_3}{1 + \omega_2/\omega_3} \tag{8.2}$$

If the cylinders are to rotate in the same direction an internal and an external cylinder must be used (Fig. 8.3). Following the procedure for external cylinder gives

$$R_2 = \frac{O_2O_3}{1 - \omega_2/\omega_3} \tag{8.3}$$

8.4. Rolling cones. Cones can be used to transmit motion between shafts with intersecting axes. In Fig. 8.4 the frusta of two cones are shown connecting shafts that intersect at an angle ϕ. The cones have a common apex at D. If there is pure rolling contact at P the angular velocity ratio will be

$$\frac{\omega_2}{\omega_3} = \frac{PC}{PB}$$

Rolling will occur at all other points of contact P' on the line of contact since, from similar triangles,

$$\frac{P'C'}{\overline{P'B'}} = \frac{PC}{\overline{PB}}$$

If the cones do not have a common apex the above relationship does not hold. A common apex is therefore a necessary requirement for rolling.

Cylinders can be considered cones with a common apex at infinity.

The most common problem is to design a pair of cones to transmit motion between shafts that intersect at a specified angle at a specified angular velocity ratio. For the case of external cones, Fig. 8.4, the directions of rotation of the shafts have an opposite sense.

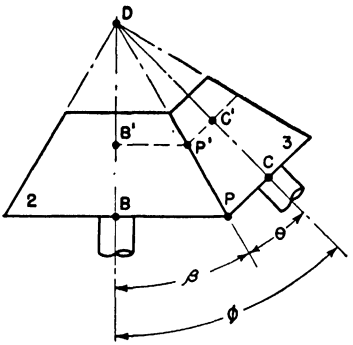

Fig. 8.4

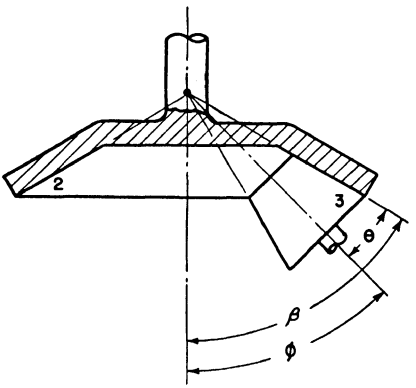

Fig. 8.5

The cone angles β and θ can be expressed as

$$\sin \beta = \frac{BP}{PD} \quad \text{and} \quad \sin \theta = \frac{PC}{PD}$$

Then

$$\frac{\sin \beta}{\sin \theta} = \frac{BP}{PC} = \frac{\omega_3}{\omega_2} = \frac{\sin (\phi - \theta)}{\sin \theta}$$

This can be written in the form

$$\frac{\sin \phi \cos \theta - \cos \phi \sin \theta}{\sin \theta} = \frac{\omega_3}{\omega_2}$$

Dividing numerator and denominator by $\cos \theta$ and solving for $\tan \theta$ gives

$$\tan \theta = \frac{\sin \phi}{\omega_3/\omega_2 + \cos \phi} \tag{8.4}$$

If the directions of rotation of the shafts are to have the same sense an internal and an external cone must be used (Fig. 8.5). For this case the relationship is

$$\tan \theta = \frac{\sin \phi}{\omega_3/\omega_2 - \cos \phi} \tag{8.5}$$

The cone angles can also be determined graphically. In Fig. 8.6 external cones are to be made such that

$$\frac{\omega_3}{\omega_2} = \frac{3}{2}$$

Distances DF of three units and DE of two units are laid off on the respective cone axes, and P is located at the intersection of lines through E

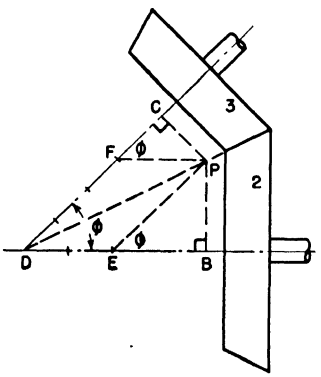

Fig. 8.6

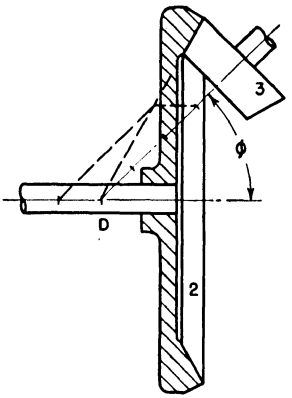

Fig. 8.7

and F parallel to the axes. The construction can be proved as follows. Triangles EPB and FCP are similar. Then

$$\frac{\omega_3}{\omega_2} = \frac{PB}{PC} = \frac{EP}{FP} = \frac{DF}{DE}$$

The contact radii PB and PC are therefore correctly proportioned.

The construction for an internal and external cone of ratio of $\frac{\omega_3}{\omega_2} = \frac{3}{1}$ is shown in Fig. 8.7.

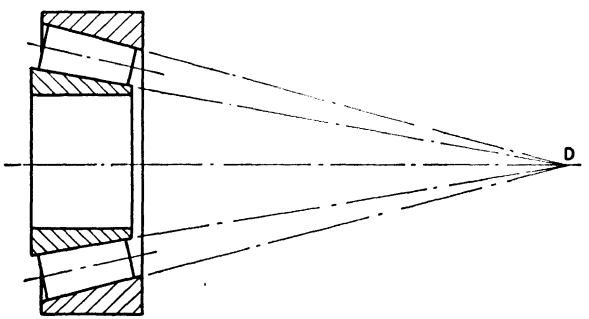

Fig. 8.8

Tapered roller bearings, Fig. 8.8, turn with rolling contact. Each point in a set of rolling cones remains a constant distance from the

common apex. Each point therefore moves on the surface of a sphere.

As is the case of circular cylinders, cones of circular cross section do not have positive driving. Motion is transmitted by means of friction. A differential mechanism that is used in radar computing machines is shown in Fig. 8.9. Cones A and B are driven by means of selsyns.

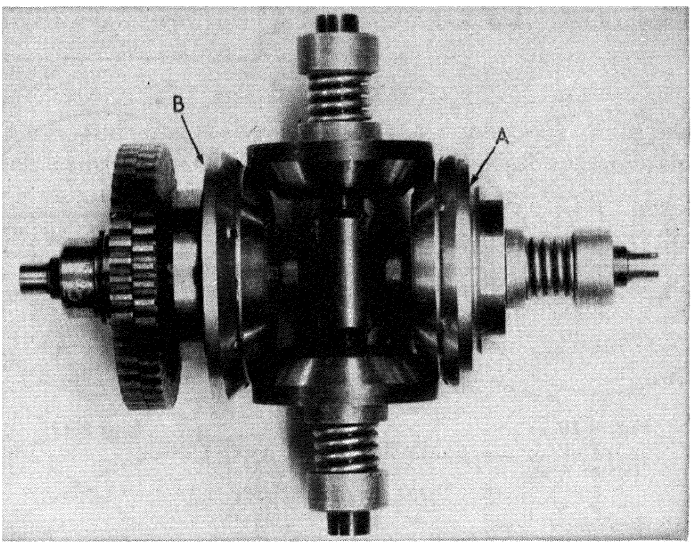

Fig. 8.9

The input motions must be transmitted with a high degree of accuracy. Since the torques are small, slipping is negligible and the mechanism is satisfactory.

8.5. Disk and roller. A disk and roller mechanism is shown in Fig. 8.10. There is pure rolling at only one point on the line of contact. This point is approximately at the center of the roller. The angular velocity ratio will be

$$\frac{\omega_2}{\omega_3} = \frac{R_3}{R_2}$$

The angular velocity ratio can be changed by shifting the roller along its axis. When the roller is shifted to the opposite side of the centerline of the disk, shown dotted, the directional relationship is reversed.

In Fig. 8.11 an intermediate ball is placed between the roller and the disk. This produces point contact and pure rolling exists. The desired angular velocity ratio is obtained by shifting the ball along its axis, parallel to the roller axis, by means of a guide. A mechanism of this type (Fig. 8.12) is used in radar computing machines. The rolling elements are pressed together by means of the spring at the top.

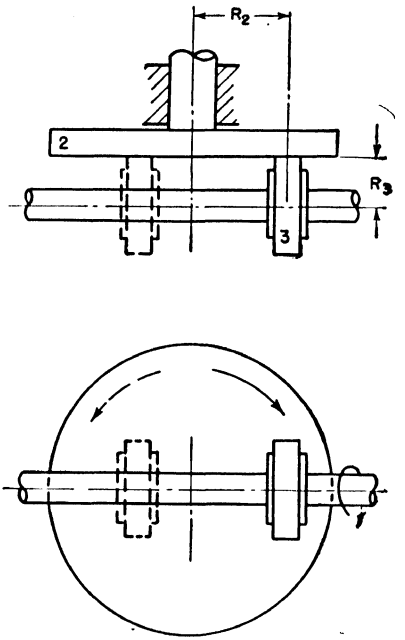

Fig. 8.10

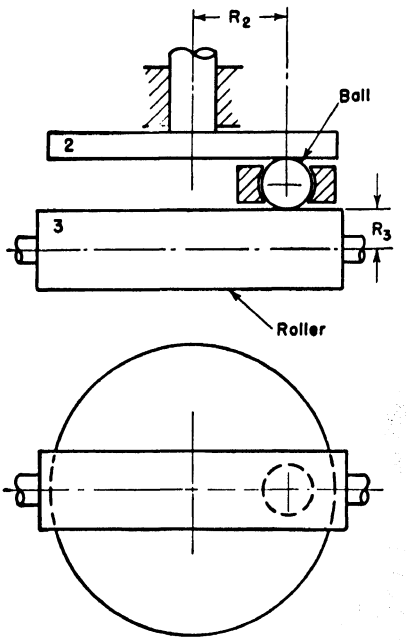

Fig. 8.11

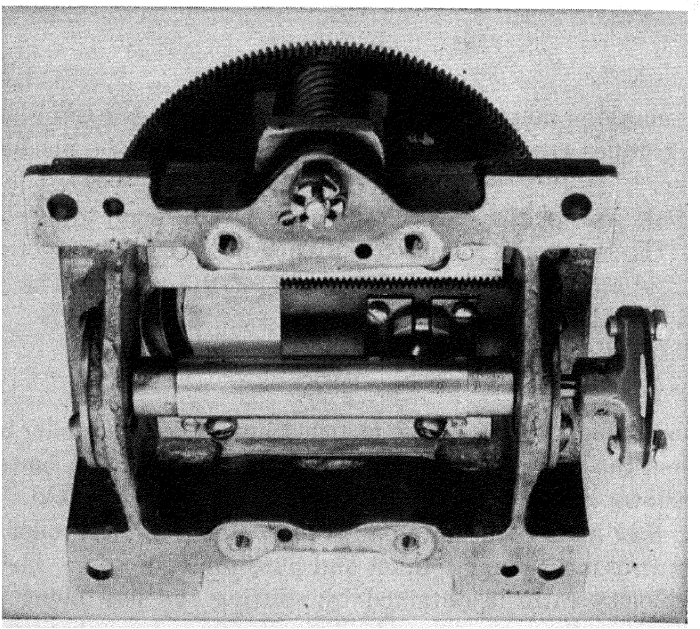

Fig. 8.12

8.6. Hyperboloids. Two hyperboloids are shown in Fig. 8.13. Hyperboloid 2 is generated by rotating line A-A about axis B-B. The distance R_2 and angle ϕ are held constant during rotation. Hyperboloid 3 is generated by rotating line A-A about axis C-C; R_3 and θ are held constant. The minimum circles of radii R_2 and R_3 are called gorge circles. It can be shown that if the hyperboloids are to fit together with contact along A-A as shown in Fig. 8.13, these radii must be proportional to the tangents of the angles made by line A-A with the axes, i.e.,

$$\frac{R_2}{R_3} = \frac{\tan \phi}{\tan \theta} \tag{8.6}$$

The pitch surfaces of hypoid gears are portions of hyperboloids. Pairs of rolling hyperboloids are used in steel mills for straightening rods and tubing.

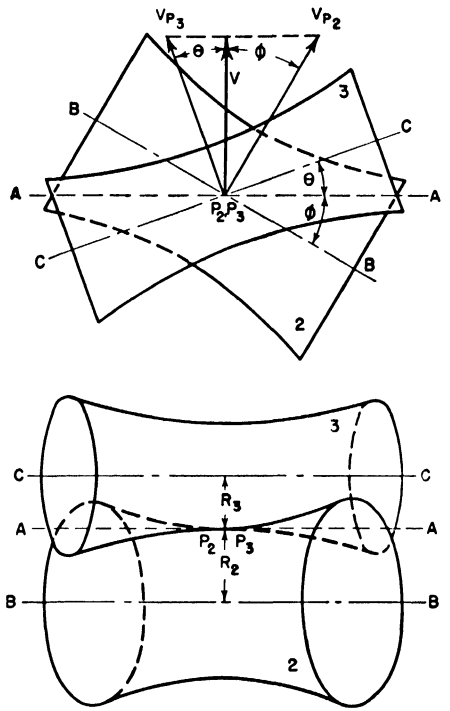

Fig. 8.13

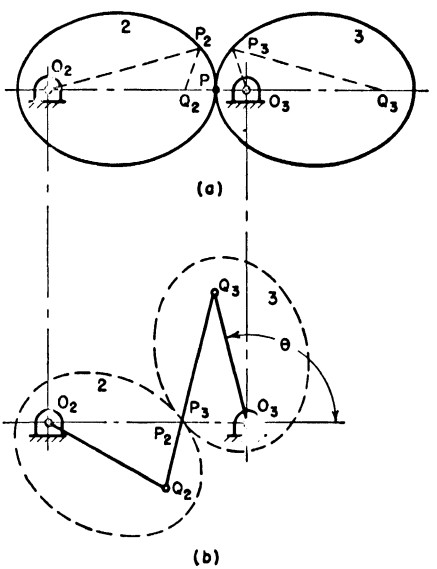

Fig. 8.14

8.7. Rolling ellipses. Two equal ellipses if initially placed together as shown in Fig. 8.14(a) will roll together; O_2, Q_2, O_3, and Q_3 are foci. The center distance O_2O_3 is equal to the major axis of each ellipse. One of the properties of an ellipse is that the sum of the distances from any point on the circumference to the foci is equal to the major axis. Since the two ellipses are equal, $O_2P_2 + P_2Q_2 = O_3P_3 + P_3Q_3 =$ major axis $= O_2O_3$.

If the points P_2 and P_3 are chosen such that the elliptical arcs PP_2 and PP_3 are equal, then from the symmetry of the figure

$$O_2P_2 = P_3Q_3 \qquad \text{and} \qquad P_2Q_2 = P_3O_3$$

Hence

$$O_2P_2 + P_3O_3 = O_2O_3$$

The conditions for pure rolling are therefore satisfied.

At (b) the ellipses are shown with 3 displaced through angle θ. If the ellipses are replaced with the linkage $O_3Q_3Q_2O_2$, links O_3Q_3 and O_2Q_2 will have the same relative motion as the ellipses. This is true since $Q_2P_2 + P_3Q_3$ is a constant and link Q_2Q_3 always intersects the line of centers at the point where the ellipses are in contact.

8.8. General case of rolling curves. The general case can be considered in three ways depending on the requirements:

1. The angular displacement relationship is chosen for one cycle.
2. The angular velocity relationship is chosen for one cycle.
3. For a finite number of points in the cycle both the displacement and velocity relationships are chosen.

These cases will be considered separately.

1. Angular Displacement Relationship. An example will be used to illustrate this method for determining the contours of rolling bodies. An assumed displacement curve is shown in Fig. 8.15, and the rolling curves are shown in Fig. 8.16. The θ axis represents the displacement of member 3 and the ϕ axis represents the displacement of member 2. Both axes are 360° in length so that rotations can be continuous. Points 0 to 7 were chosen for plotting. The corresponding displacements θ_1, θ_2, θ_3, . . . , ϕ_1, ϕ_2, ϕ_3, . . . were measured and laid off in Fig. 8.16. The lengths of the radii are determined from the slopes and the relationships

$$r_0 + R_0 = r_1 + R_1 = r_2 + R_2 = \ldots = O_2O_3$$

and r_0/R_0 = slope at point 0, r_1/R_1 = slope at point 1, etc. The driver usually rotates with constant angular velocity. Even when this is not true one of the axes can be considered a time axis, since an angular velocity ratio is desired. It is necessary that the two displacement scales be equal. The slope at point 0 is 72°. In the original drawing $O_2O_3 = 4$ in.

$$\tan 72° = 3.08 = \frac{r_0}{R_0}, \qquad R_0 + r_0 = 4 \text{ in.}$$

$$r_0 = 3.02 \text{ in.}, \qquad R_0 = 0.98 \text{ in.}$$

The curve in Fig. 8.15 is made up of two circular arcs and a straight line. The slopes at 0 and 7 are equal. The straight-line portion represents uniform velocity. The corresponding rolling curves are therefore circles. The second derivative at points 0, 3, and 4 are discontinuous. This produces discontinuities in the slopes of the rolling curves at the corresponding points. For smooth operations the second derivatives should be continuous.

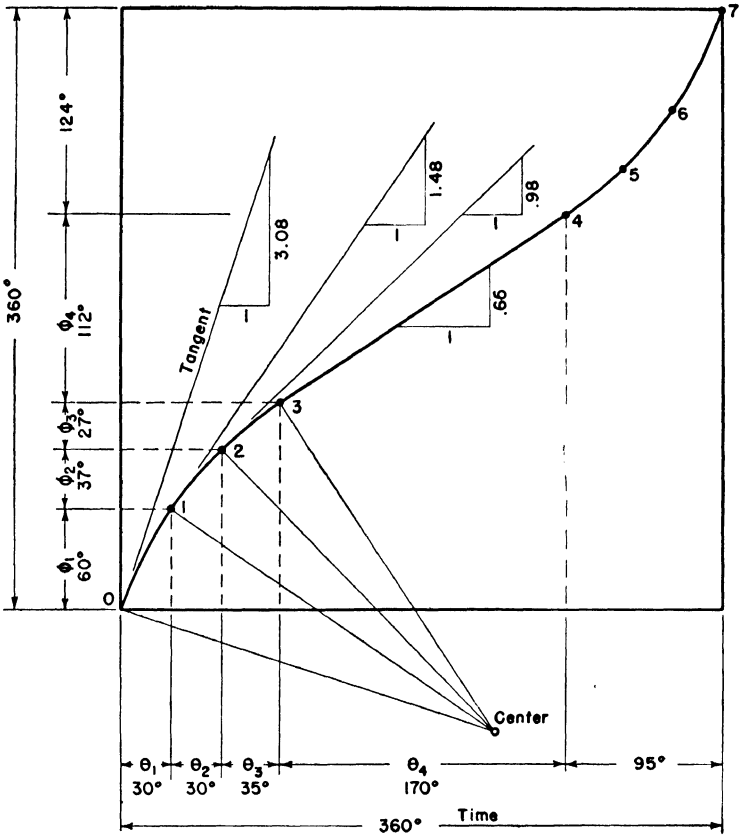

Fig. 8.15

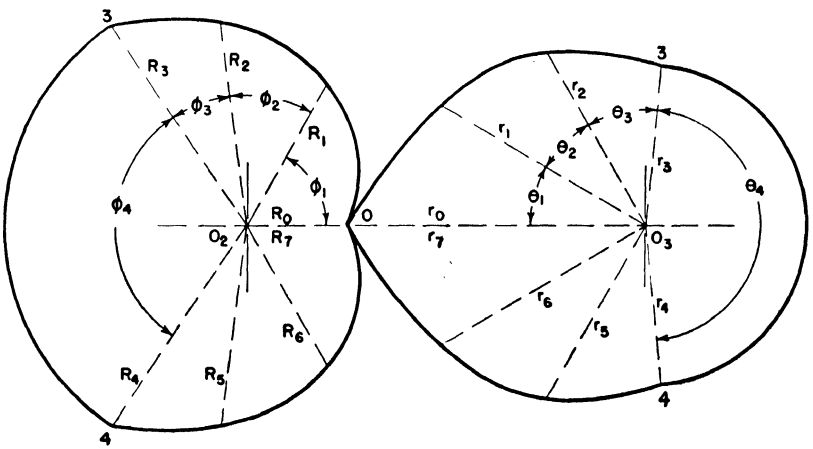

Fig. 8.16

The example above was done graphically. For most purposes many more points must be taken and the work done analytically. The method is theoretically correct and errors of calculation are not cumulative.

2. Angular Velocity Relationship. When this method is used, the curve for the velocity relationship is chosen and the displacements are determined from this. The space that would be required to describe this method is more than is justified in a book of this type. The method is described elsewhere.* The pitch surfaces for the gears shown in Fig. 9.59 were determined by this method.

3. Displacement and Velocity for a Finite Number of Points. This method is similar to that of type one. In Fig. 8.17, points 0, 1, 2, and 3

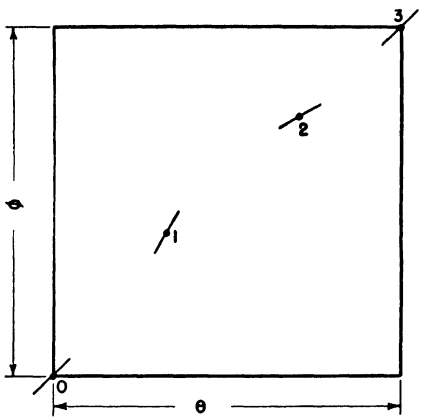

Fig. 8.17

and the indicated slopes represent the displacement and velocity requirements. It is necessary to pass a curve through the points with the required slopes or to fit separate curves between the points. The method of type one is then applied to determine the rolling curves.

Methods for determining arc length and for machining the rolling bodies are described in the references given below.*†

PROBLEMS

8.1. Power is to be transmitted from one shaft to a parallel shaft. The shafts are 14 in. apart and they are to turn in opposite directions with an angular velocity ratio of 1.5. Determine the diameters of the cylinders.

8.2. Same as Prob. 8.1 except shafts are to turn in the same direction.

8.3. Same as Prob. 8.1 except the center distance is 7 in. and the angular velocity ratio is 1.25.

* Golber, H. E., "Rollcurve Gears," *Trans. ASME*, 1938.

† Lockenvitz, Oliphint, Wilde, and Young, "Noncircular Cams and Gears," *Machine Design*, May, 1952.

8.4. Same as Prob. 8.3 except shafts are to turn in the same direction.

8.5. The axes of two shafts intersect at 60°. Power is to be transmitted from one shaft to the other by means of rolling cones. The angular velocity ratio is 3 and the directional sense is to be opposite. The maximum diameter of the larger cone is to be 10 in. Determine the cone angles β and θ and the maximum diameter of smaller cone. Use graphical methods.

8.6. Same as Prob. 8.5 but the rotational sense is the same.

8.7. Same as Prob. 8.5 except analytical methods are to be used.

8.8. Same as Prob. 8.6 except analytical methods are to be used.

8.9. The axes of two shafts intersect at 45°. Power is to be transmitted from one shaft to the other by means of rolling cones. The angular velocity ratio is 2.5 and the directional sense is to be opposite. The maximum diameter of the larger cone is to be 7 in. Determine the cone angles β and θ and the maximum diameter of the smaller cone. Use graphical methods.

8.10. Same as Prob. 8.9 except the rotational sense is to be the same.

8.11. Same as Prob. 8.9 except the analytical methods are to be used.

8.12. Same as Prob. 8.10 except analytical methods are to be used.

8.13. A displacement graph for two rolling bodies is shown in Fig. P 8.13. It consists of two equal circular arcs. The axes of the rolling bodies are to be 3 in. apart.

(a) Construct the rolling curves graphically for 30° intervals of θ.

(b) Using analytical methods calculate ϕ, R, and r for the position $\theta = 60°$.

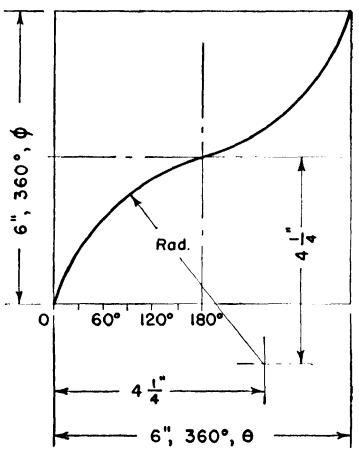

Fig. P 8.13

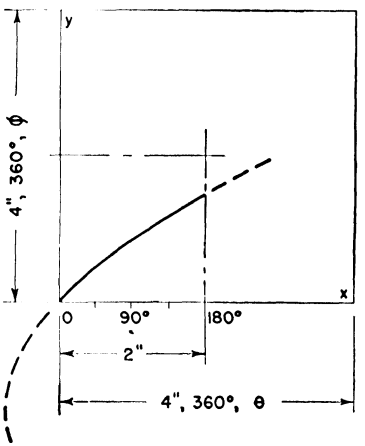

Fig. P 8.14

8.14. A portion of a displacement graph for two rolling bodies is shown in Fig. 8.14. Its equation is a parabola, $y^2 + 4y - 4x = 0$. The axes of the rolling bodies are to be 3 in. apart. Using analytical methods calculate ϕ, R, and r for positions corresponding to $\theta = 0, 45, 90, 135, 180°$. Plot the rolling curves.

CHAPTER 9

Gearing

9.1. History. It is believed that toothed gears were used as early as 350 B.C. Ctesibius in 150 B.C. used spur and bevel gears in his water-clocks. The Trojan Column, erected in Rome in 114 A.D., contains sculptured gears. Drawings of Leonardo da Vinci include spur, bevel, and worm gears. All these gears were of the "cog wheel" variety. Even if they could have been made accurately according to the designer's ideas they would not have run smoothly.

A Danish astronomer, Olaf Roemer, in 1674, first offered a theory of correct tooth shapes. He proposed the use of cycloidal teeth. A Frenchman, Philippe de Lahaire, in 1695, proposed the use of involute profiles.

Figure 9.1 is from *Mechanic-Powers.** This illustrates the method of determining a tooth profile to operate with a pin gear. Circle *POB*

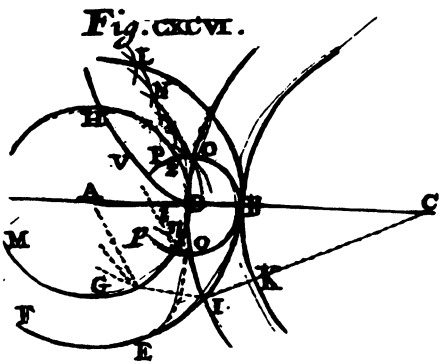

Fig. 9.1

is a pin on the wheel with center at *A*, and *HVD* is an epicycloid obtained by rolling circle *HDGM* on the circle with radius *CI*. The tooth profile on the gear with center at *C* is obtained by drawing arcs of radius equal to the pin radius, using the epicycloid as the locus of the centers. The

* Mandy and Moxon, *Mechanic-Powers*, London, 1696.

envelope of these arcs *ONL* is the tooth profile. This is theoretically correct. Note that inversion was used to obtain the tooth profile.

The authors also suggest that the pin be made in the form of a roller on a smaller pin so that the contacting teeth have rolling instead of sliding friction. This is described by the authors.

Behold here a particular conſtruction for the Teeth of Wheels of a great Engin, where the faces which rencounter themſelves or meet, are made ſo that they touch one another without rubing or wearing, and what remains is only made on the Axis,or Pivot.

The conſtruction of theſe Teeth is the ſame as thoſe of the firſt Example of the 6th. Propoſition, but the Application is different: In the 6th. Propoſition the circular Tooth propoſed is ſtayed firmly by the Wheel; but in thoſe here that is a little wheel which is movable abour its centre D, on an axle-tree, or pin, placed at the end of the Radius A D; there will be then no other fretting, or wearing, in this Engin, than that of the little wheel ꝥ Z P on its axis; for the circumference will apply it ſelf every way, without fretting, or wearing, on the Curve of the other Tooth O N L.

Theory was of little use until accurate methods were developed for machining the gears. In 1864 Joseph R. Brown invented the formed milling cutter that could be sharpened by grinding without changing the shape of the cutting faces. In 1884 Hugo Bilgram invented the generating method for cutting teeth. This is the principal method used today.

9.2. Introductory. Power transmission by means of rolling bodies was discussed in Chapter 8. It was shown that rolling bodies of circular cross section do not have positive transmission. Motion transmitted by gears is equivalent to that of rolling bodies but is positive. Comparing pairs of members of the same size, gears will transmit much larger torques than rolling members. *Gears* are machine elements that transmit motion by means of successively engaging teeth.* Spur gears and their equivalent cylindrical friction surfaces are shown in Fig. 9.2. Bevel gears and their equivalent conical friction surfaces are shown in Fig. 9.3. Other types of gears are shown in the pages that follow. Most gears are circular, and the angular velocity ratio of driver and follower is constant. The discussion of noncircular gears will be confined to the last article in this chapter.

* Extracted from *American Standard Gear Nomenclature* (ASA B6.10-1950), with the permission of the publishers, The American Society of Mechanical Engineers, 29 West 39th Street, New York 18, New York. All definitions in italics are taken from this source.

Gearing is a large subject. The design of many gear drives requires the work of experts. The author's aim is to present the fundamental concepts of the theory of gears and to indicate some of the practical aspects that must always be considered when a machine element is to

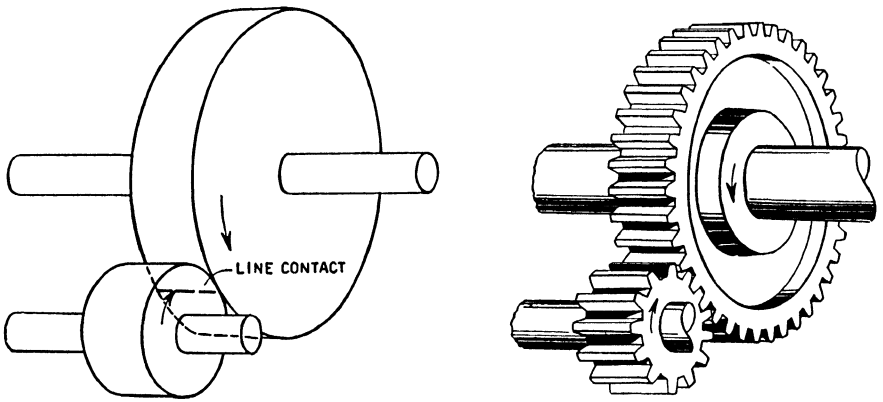

Fig. 9.2. (Courtesy of Socony-Vacuum Oil Co.)

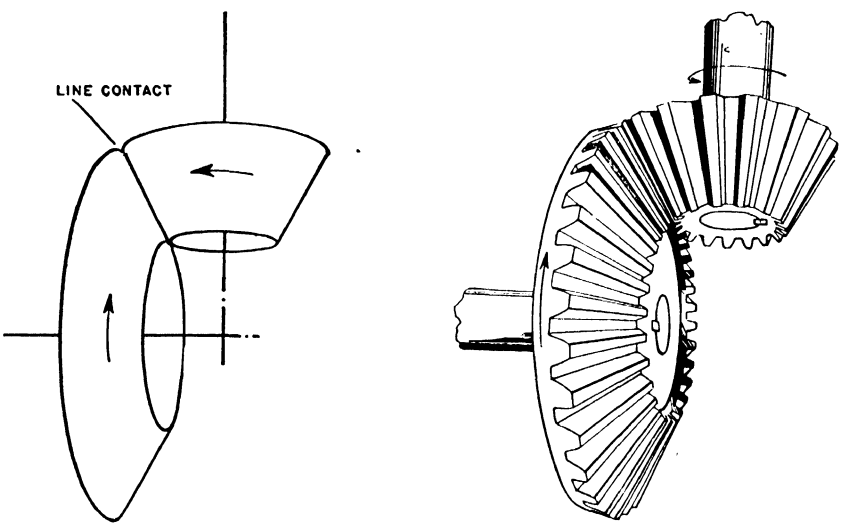

Fig. 9.3. (Courtesy of Socony-Vacuum Oil Co.)

be produced in physical form. An understanding of this chapter should be an adequate background for further study in the works of Buckingham* and the writings of others.

9.3. Classification. Gears can be classified according to the relationship of their axes. Any two lines in space must fall into one of the

* Buckingham, Earl, *Analytical Mechanics of Gears* and *Spur Gears*, New York: McGraw-Hill Book Co., Inc.

three relationships listed below. The gears that are used with each one are listed.

Parallel axes:

Straight spur, stepped, parallel helical

Intersecting axes:

Straight bevel, spiral bevel, face

Nonparallel nonintersecting axes:

Crossed helical, worm, face, hypoid

Each of these types will be discussed.

9.4. Fundamental law of gearing. Gear design may be considered a special case of cam design. In Art. 2.12 it was shown that the angular velocity ratio of driver and follower is inversely as the segments cut by the common normal on the line of centers. In Fig. 9.4 the common normal intersects the line of centers at P. If the angular velocity ratio of 2 and 3 is to be constant, the common normal must pass through P for all phases. The angular velocity ratio will then be equivalent to that of rolling circles of radii O_3P and O_2P. These imaginary circles are called pitch circles. The fundamental law of gearing for circular gears is: *the common normal at the point of contact of the teeth must pass through a fixed point on the line of centers.* This is point P, the pitch point.

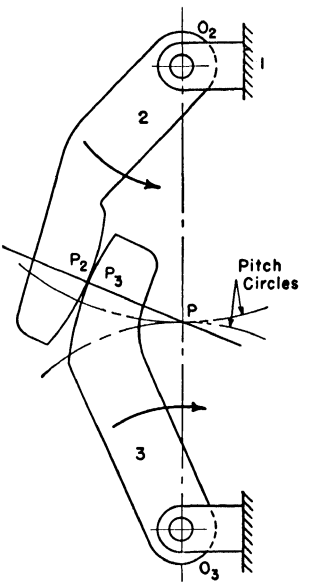

Fig. 9.4

Within reasonable limits one tooth profile can be arbitrarily chosen and the mating profile determined to fulfill the fundamental law. Any pair of teeth that fulfill the law are called conjugate teeth. For practical reasons to be discussed later, involute profiles are usually used.

9.5. Nomenclature. *Spur gears are cylindrical in form and operate on parallel axes. Their teeth are straight and parallel to the axes.* Spur gears are the simplest type of gears and will be discussed first. Much of the theory pertaining to them is basic to all gears. Some of the nomenclature given below is indicated in Fig. 9.5.

The circular pitch p is the distance along the pitch circle or pitch line between corresponding profiles of adjacent teeth.

The addendum a is the height by which a tooth projects beyond the pitch circle or pitch line; also the radial distance between the pitch circle and the addendum circle.

The dedendum b is the depth of a tooth space below the pitch circle or pitch line; also the radial distance between the pitch circle and the root circle.

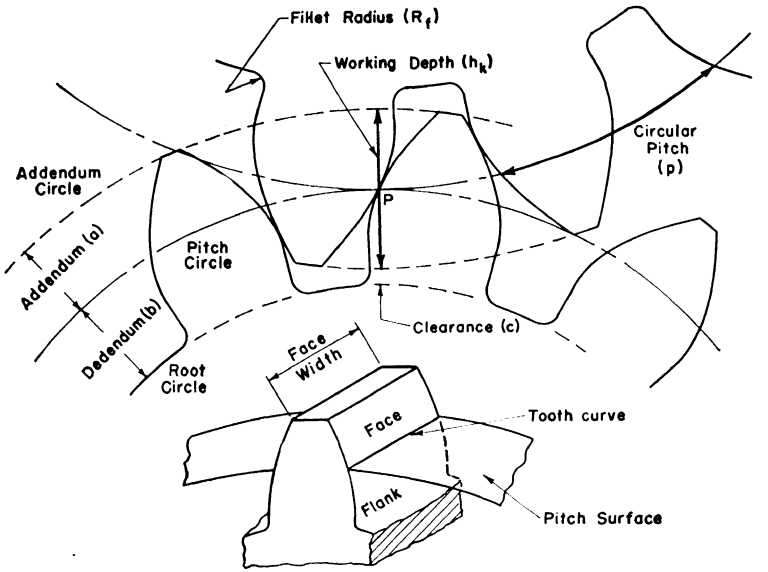

Fig. 9.5

The clearance c is the amount by which the dedendum in a given gear exceeds the addendum of its mating gear.

The working depth h_k is the depth of engagement of two gears, that is, the sum of their addendums.

The whole depth h_t is the total depth of a tooth space, equal to addendum plus dedendum, also equal to working depth plus clearance.

The backlash B is the amount by which the width of a tooth space exceeds the thickness of the engaging tooth on the pitch circles.

The diametral pitch P_d is the ratio of the number of teeth to the number of inches in the pitch diameter. There is a fixed relation between diametral pitch P_d and circular pitch p, namely, $p = \pi/P_d$. Let N be the number of teeth and D the diameter of the pitch circle; then

$$p = \frac{\pi D}{N} \quad \text{and} \quad P_d = \frac{N}{D} \quad \text{giving} \quad p = \frac{\pi}{P_d} \tag{9.1}$$

Some of the standard diametral pitches are shown in Fig. 9.6.

The module m (inch) is the ratio of the pitch diameter in inches to the number of teeth. It is the reciprocal of the diametral pitch.

The fillet curve is the concave portion of the tooth profile where it joins the bottom of the tooth space.

The fillet radius r_f is the radius of the fillet curve at the base of the gear tooth. In generated teeth, this radius is an approximate radius of curvature.

The gear ratio m_G is the ratio of the larger to the smaller number of teeth in a pair of gears.

A pinion is a gear with a small number of teeth. Of two gears that run together, the one with the smaller number of teeth is called the pinion.

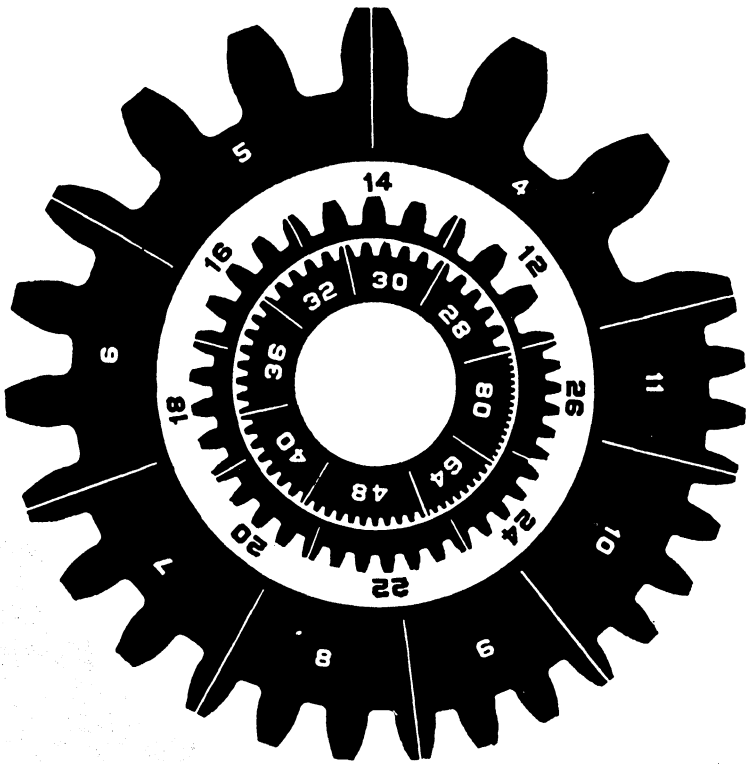

Fig. 9.6. (Courtesy of Barber-Colman Co.)

A tooth curve is a general term for the curve of intersection of a tooth surface and its pitch surface. The tooth curve of a straight tooth is a straight line.

9.6. Involute gear teeth. The involute of a circle is the curve described by the end of a thread as it is unwound from a stationary cylinder. This is illustrated in Fig. 9.7. The end of the thread D traces an involute. The direction of the motion of the end D at any instant is perpendicular to the thread, hence the normal at any point of an involute is tangent to the circle from which it was derived.

In Fig. 9.8 a plate R is attached to the cylinder, and the cylinder is allowed to rotate. If the end of the thread is moved in the direction indicated, any point D on the thread will trace an involute on the plate. This is merely an inversion of Fig. 9.7.

Two cylinders and a connecting thread $BCDEF$ are shown in Fig. 9.9. If cylinder 3 is rotated counterclockwise, the thread will act as a belt and cause clockwise rotation of cylinder 2. The thread will always

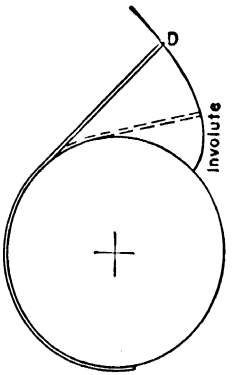

Fig. 9.7

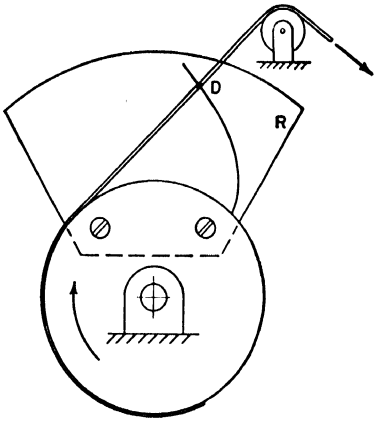

Fig. 9.8

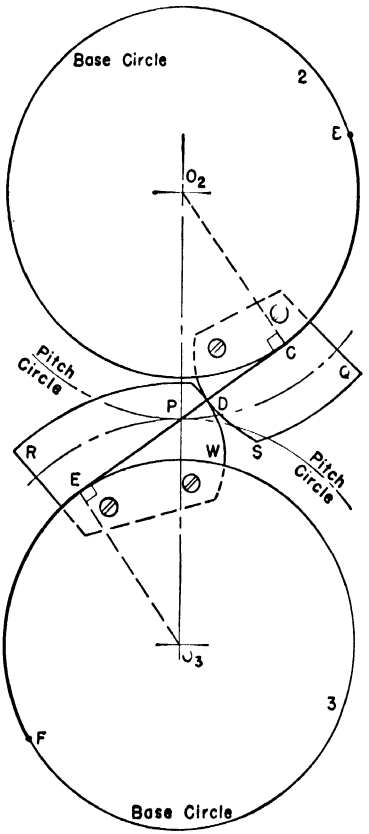

Fig. 9.9

pass through the fixed point P on the centerline. Plates Q and R are fastened to the cylinders. As movement takes place any point D will simultaneously trace involutes W and S on plates R and Q. If the plates are cut along the involutes they can serve as teeth. If cylinder 2 is rotated CW, profile S will push on profile W, causing cylinder 3 to rotate. The point of contact D and the common normal will always lie on the line CE. The fundamental law is fulfilled.

The base circle is the circle from which the involute tooth profiles are derived. Triangles O_3EP and O_2CP are similar; hence

$$\frac{O_3E}{O_2C} = \frac{O_3P}{O_2P}$$

The angular velocity ratio is also inversely as the base circle radii.

9.7. Construction of the involute. A method of constructing an involute is shown in Fig. 9.10(a). Assume that the involute is to originate from point B. Equal arc lengths B-1, 1-2, 2-3, 3-4 are stepped off. Perpendiculars are erected to the radii at 1, 2, 3, and 4. Lengths 1a, 2b, 3c, 4d are made equal to the corresponding arc lengths. Then *Babcd* is the desired involute.

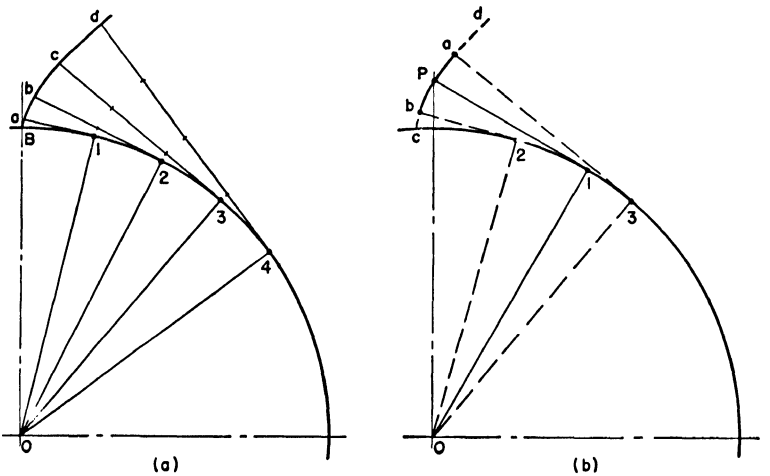

Fig. 9.10

An approximate construction is shown at (b). Assume that the involute is to pass through point P. A line is drawn through P tangent to the circle. With 1 as a center, an arc aPb is drawn. A line through b is tangent to the circle at 2. With 2 as a center, arc bc is drawn. Arc ad is drawn with 3 as a center. The more centers that are used the more accurate is the involute.

9.8. Involute gear tooth action. Portions of a pair of involute gears are shown in Fig. 9.11. The gear with center at O_2 is driving in a CW direction. The terminology and relationships that are necessary

for an understanding of gear tooth action are listed below. Line EC is the line of transmission or line of action. From triangle O_2CP the radius of the base circle in terms of the pitch circle is

$$R_b = R_p \cos \phi \tag{9.2}$$

It was shown that the point of contact of involute gear teeth lies on the line of action EC. In this case the first point of contact is K. It is the point on the line of action nearest C that can be reached by a tooth on 3. It is the intersection of the addendum circle of gear 3 and the line CE. Similarly L is the last point of contact, and KL is called the path of contact.

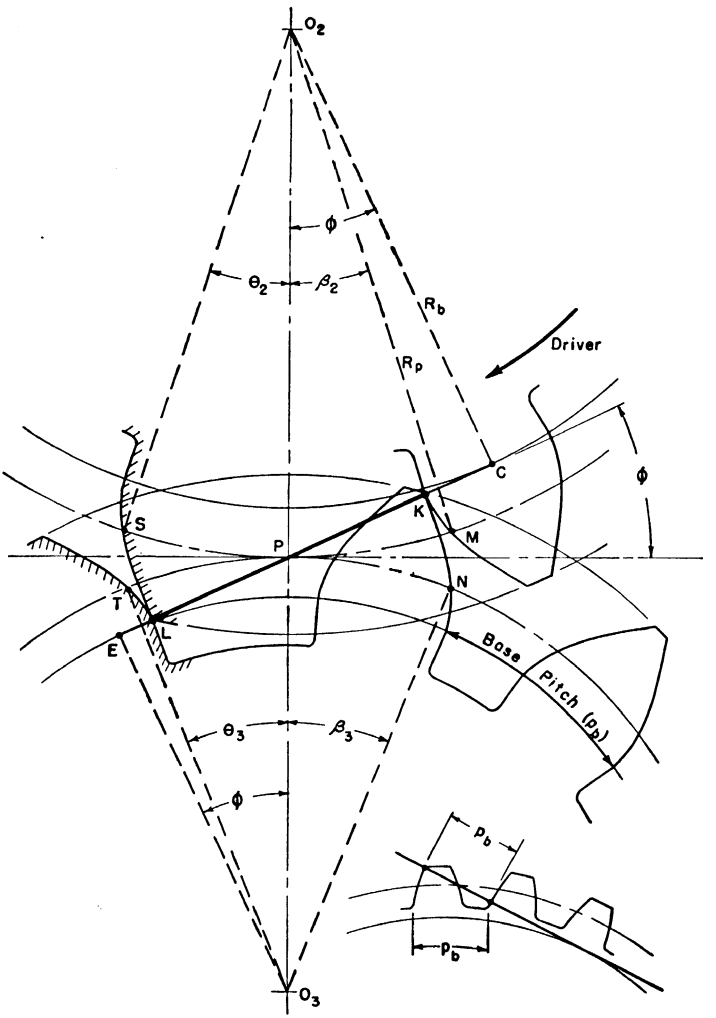

Fig. 9.11

The arc of action is the arc of the pitch circle through which a tooth profile moves from the beginning to the end of contact with a mating profile. This is shown as MS for gear 2 and NT for gear 3. The arc of action can be divided into MP, the arc of approach, and PS, the arc of recess. The corresponding angles β_2 and θ_2 are, respectively, the angles of approach and recess. Arc MP is equal to NP, and PS is equal to PT because of rolling of the pitch circles. Angle β_2 is not equal to β_3, and θ_2 is not equal to θ_3 except for the case of equal gears. It has been found from practice that gear tooth action is smoother in recess than in approach.

The base pitch p_b in an involute gear is the pitch on the base circle or along the line of action. Corresponding sides of involute gear teeth are parallel curves, and the base pitch is the constant and fundamental distance between them along a common normal in the plane of rotation. This is shown at the lower right of Fig. 9.11. The base pitch can be determined by dividing the circumference of the base circle by the number of teeth. The relationship between the circular and base pitch using Eq. (9.2) is

$$p_b = p \cos \phi \tag{9.3}$$

The contact ratio (m_c) is the ratio of the arc of action to the circular pitch, and sometimes is thought of as an average number of teeth in contact. For involute gears, the contact ratio is obtained most directly as the ratio of the length of action to the base pitch. The length of action is the path of contact KL. The contact ratio is KL/p_b. In order that action be continuous it is necessary that the ratio be at least unity. For smooth action it should be at least 1.4. This means that during 40 per cent of the time two pairs of teeth are in contact.

When the teeth are in contact at P, pure rolling exists. At all other points there is both rolling and sliding. The sliding component can be determined by the method of Art. 2.11 or of Prob. 3.25.

9.9. Involute rack and pinion. Portions of rack and pinion are shown in Fig. 9.12. A rack can be thought of as a portion of a gear of infinite radius. The infinite pitch circle of the rack is called the pitch line. The line of action is tangent to the base circle at infinity; hence the radius of curvature of a tooth profile is infinite.

9.10. Involute interference. In Fig. 9.12 the addendum a of the rack was chosen so that the first point of contact would coincide with C, the point of tangency of the line of action with the base circle of the pinion. The involute profile of the pinion tooth begins on the base circle. The portion of the profile inside the base circle is shown as a radial line. An involute tooth profile can not exist inside the base circle. Then PC is the maximum length of contact in approach. The maximum rack addendum that should be used in this case is a. In order to see the effect of a longer addendum it is shown as a'. When the teeth are in contact at C the additional portion of the rack face will lie along the

radial flank of the pinion. When the pitch circle of the pinion and the pitch line of the rack are rolled to the right there will be interference, as shown by the broken line profiles. In order that the fundamental law be fulfilled and that the teeth mesh it is necessary to remove part of the pinion teeth as shown at the right. This undercutting weakens the teeth

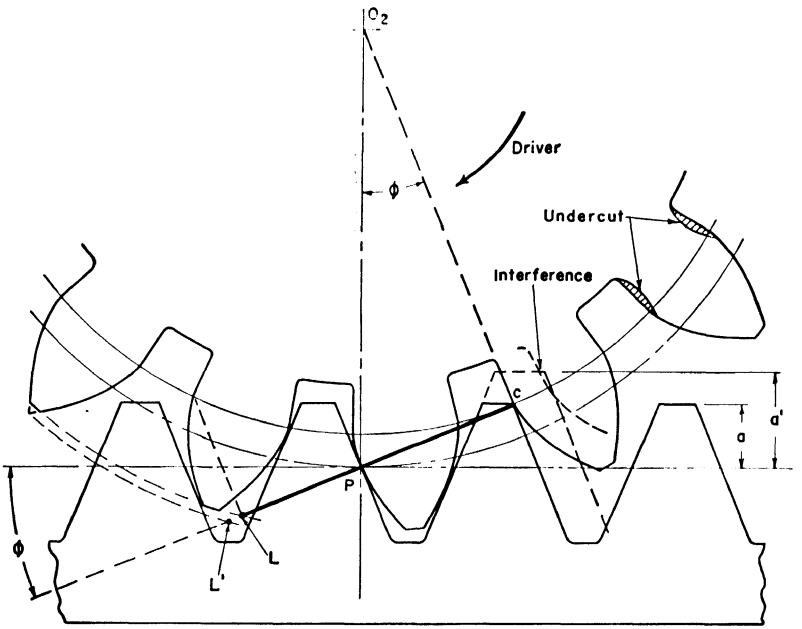

Fig. 9.12

and removes part of the involute profile, which shortens the path of contact.

There can be no interference due to a large addendum on the pinion, the point of tangency is at infinity. The maximum length of path in recess is PL', which is obtained with a pointed pinion tooth.

If a rack will mesh with a pinion without interference, any external gear having the same addendum as the rack will also mesh with the pinion without interference. This can be seen from Fig. 9.12. The addendum circle of any finite gear will intersect PC to the left of C.

9.11. Determination of contact ratio. The contact ratio can be determined semigraphically for any pair of involute gears (Fig. 9.13). The pitch circles, addendum circles, and pressure angle are known. This is sufficient for determining the length of the path of contact KL. This divided by the base pitch gives the contact ratio. The lengths of LP and PK can be calculated, using the trigonometric relationships included in the next article.

9.12. Checking for interference. Any pair of involute gears can be checked for interference by the method of Fig. 9.13. If either K or L falls beyond the limits C and E, there is interference.

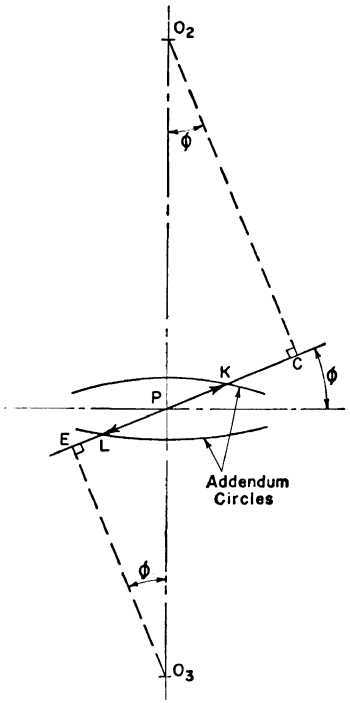

Fig. 9.13

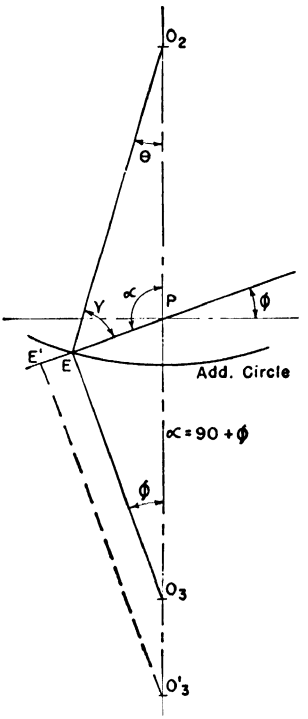

Fig. 9.14

Sometimes it is required to find the smallest pinion that will mesh with a given gear without interference. In Fig. 9.14, O_2P is the pitch radius, O_2E the addendum circle radius, and ϕ the pressure angle of the given gear. Line EO_3 drawn perpendicular to EP at point E is the radius of the base circle of the smallest pinion that will mesh without interference. Any larger pinion of base radius $E'O'_3$ will not have interference. The pitch radius PO_3 can be calculated using the following relationships for the solution of oblique triangles.

$$\gamma = \sin^{-1} \frac{PO_2 \sin \alpha}{O_2E} \tag{9.4}$$

$$\theta = 180 - (\alpha + \gamma) \tag{9.5}$$

$$EP = \frac{O_2E \sin \theta}{\sin \alpha} \tag{9.6}$$

$$PO_3 = \frac{EP}{\sin \phi} \tag{9.7}$$

9.13. Internal gears. External involute gears have convex profiles. As the number of teeth increases, the profiles approach an infinite radius of curvature and reach this condition for the rack. The profiles of internal gears are concave. As the number of teeth is increased the profiles approach a straight line. The rack is the limiting case for both external and internal gears. The basic theory is the same for both types of gears.

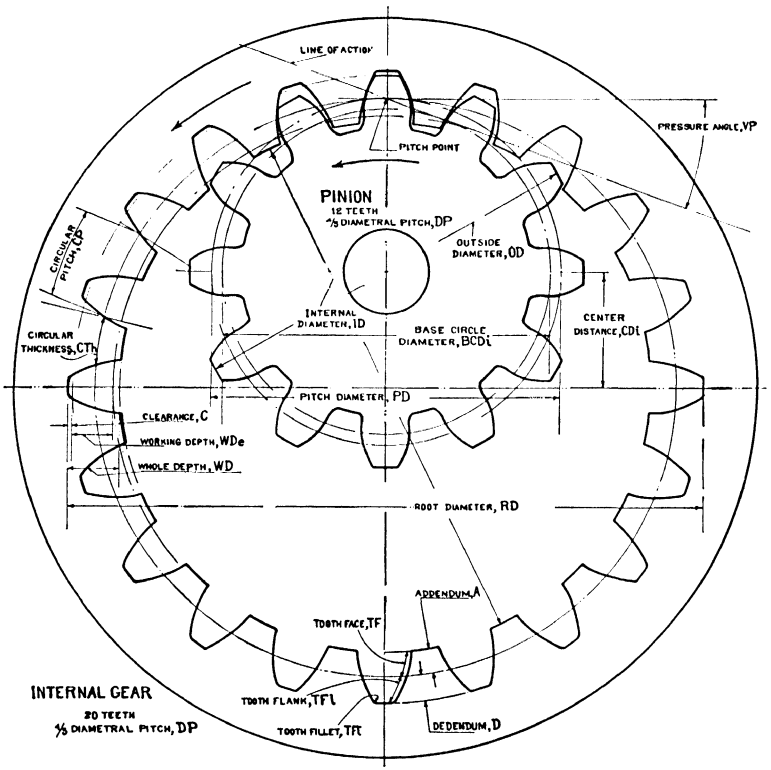

Fig. 9.15. (Courtesy of The Fellows Gear Shaper Co.)

An internal gear and pinion is shown in Fig. 9.15. This drive is more compact than an external gear drive. The concave-convex contact facilitates lubrication and reduces the contact stress.

The location of the interference point is shown in Fig. 9.16. The line of action is tangent to the gear base circle at L and to the pinion base circle at K. An involute profile for the gear can begin at L. The pinion involute cannot begin until K is reached. This is then the first possible point of contact, and the maximum addendum of the gear is as indicated. The length of path PM' in recess is limited only by the pinion tooth coming to a point.

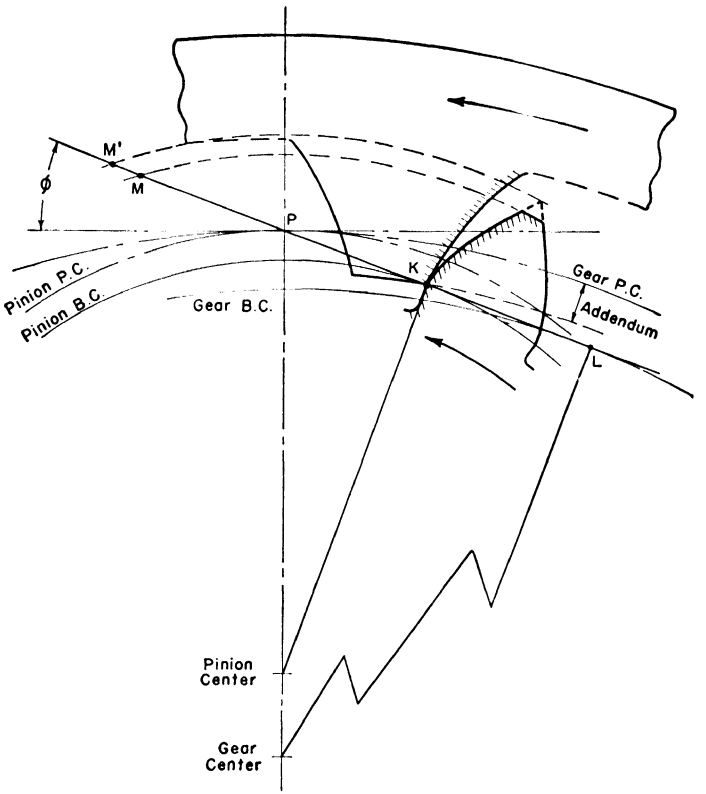

Fig. 9.16

9.14. Interchangeable gear-tooth forms. A set of gears is said to be interchangeable when any two of the set will mesh and fulfill the fundamental law. Obviously a watch gear will not mesh with an automobile transmission gear. The gears must have the same pitch. Two gears will not mesh if the addendum of one is greater than the dedendum of the other. There is one basic requirement pertaining to tooth profiles for interchangeable gears. *Gears of a set that are conjugate to a basic rack will be interchangeable if the path of contact of the system is symmetrical in relation to the pitch point. When this condition is met it follows that the basic rack profile will be symmetrical in relation to the pitch point.*

This requirement can be proved as follows: In Fig. 9.17(a) a pinion is shown in mesh with a rack having a symmetrical path of contact and profile. The point of contact is K. At (b) the same basic rack is meshed with another pinion. The point of contact K was chosen the same distance x from the centerline. From symmetry, y in (b) is equal to y in (a). Parts (a) and (b) are superimposed at (c). The racks and paths of contact coincide and the two pinion teeth are in contact at K. This will be true for any distance x that is chosen. Hence the pinions

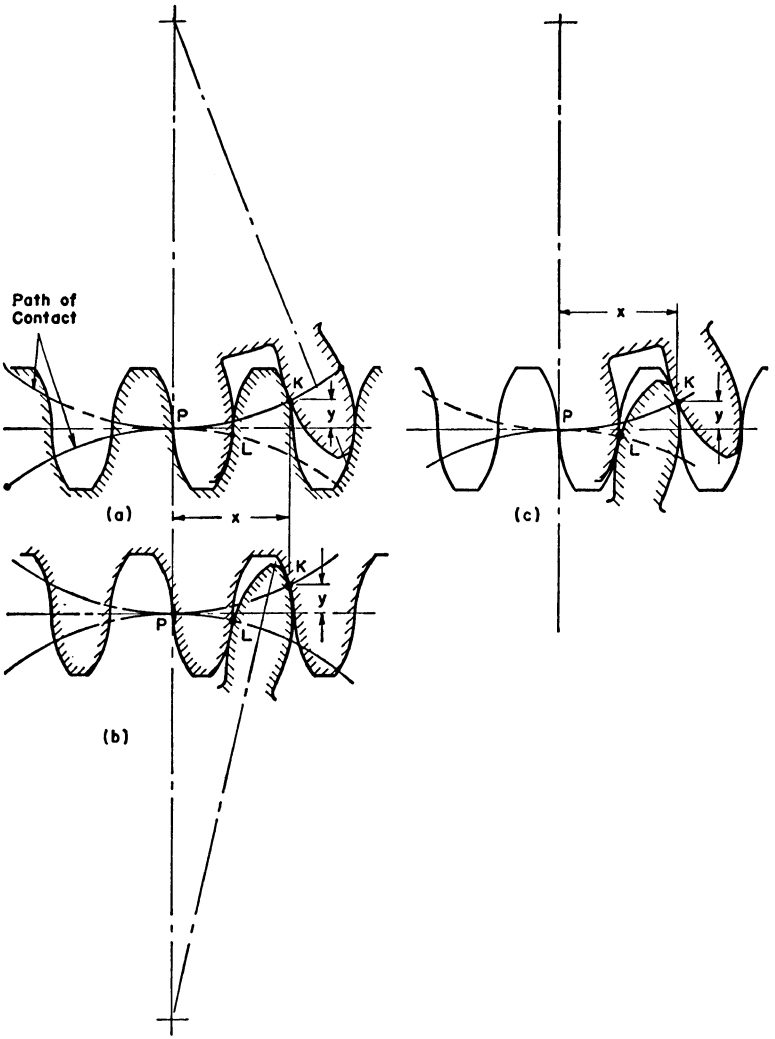

Fig. 9.17

are conjugate. If there is no backlash there will also be contact at L. If the tooth thickness of the rack is equal to the tooth space, measured on the pitch line (except an allowance for backlash), and the dedendum is greater than the addendum, all secondary requirements for interchangeability are met.

9.15. Cycloidal gears have been used in the past but are seldom used today. In order to obtain a more thorough understanding of gear tooth action it is desirable to consider at least one form in addition to the involute. This justifies a brief study of cycloidal gears. The cycloid was discussed briefly in Art. 2.17 and the epicycloid was mentioned in

Art. 9.1. A hypocycloid is the curve traced by a point on a circle as it rolls on the inside of a larger circle.

A cycloidal rack tooth profile is shown in Fig. 9.18(a). Generating circle 2 is tangent to the pitch line at the pitch point P. When this circle is rolled to the right the point that was originally in contact with the pitch point generates a cycloid. In a similar manner generating circle 3 generates the remainder of the tooth profile when it is rolled to the left.

A cycloidal tooth profile is shown in Fig. 9.18(b). It is generated by rolling circle 2 to the right on the outside of the pitch circle and circle 3 to the left on the inside of the pitch circle.

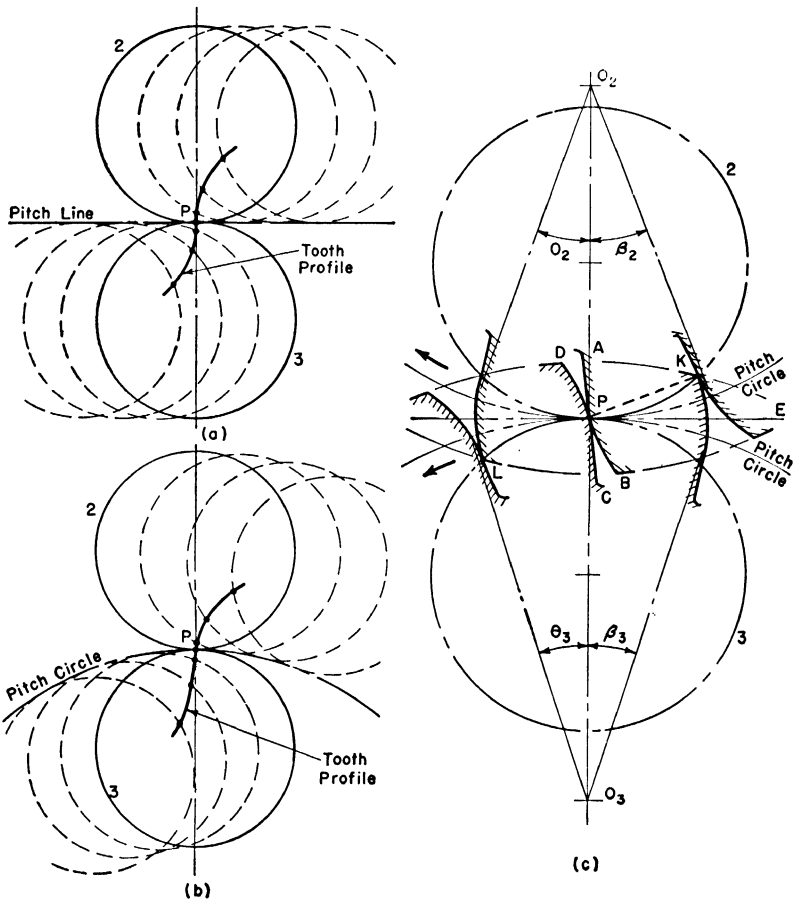

Fig. 9.18

In Fig. 9.18(c) the generating circles 2 and 3 are rolled on the pitch circles of the two gears. Points on these generating circles will generate or trace cycloidal tooth profiles on the two gears. When circle 2 is rolled to the left on the inside of the pitch circle of gear 2, point P on circle 2 will trace the profile PA. When circle 3 is rolled to the right on the

outside of the pitch circle of gear 2, point P on circle 3 will trace the profile PB. Profiles PD and PC are traced in a similar manner by rolling circle 2 and 3 on the pitch circle of gear 3.

A pair of teeth are shown in mesh at K, the first point of contact. It can be shown that cycloidal teeth fulfill the fundamental law of gear tooth action as follows. Point K on circle 2 may be considered a generating point. Circle 2 and the pitch circles of the two gears are tangent at P. If these three circles are rolled together point P will be their instant center. The direction of motion of point K as a point in 2, tracing simultaneously the two tooth profiles, will be perpendicular to KP. Therefore KP is the common normal of the two profiles. This will be true for any position. The reverse curve KPL, composed of portions of the two generating circles, is the path of contact.

The angle KPE is the pressure angle for the first point of contact. This angle changes with the position of the meshing teeth and is zero when contact is at the pitch point.

It follows from the previous article that the generating circles must be of the same size if the path of contact is to be symmetrical and the gears are to be interchangeable.

9.16. Advantages of involute teeth. The extensive use of involute spur gear teeth is the result of distinct advantages of this type compared with all other types. It was shown in Art. 9.9 that tooth profiles of an involute rack are straight. Cutting tools and grinding wheels having straight sides are used in the production of gears and cutters. This makes the production of accurate involute gears more economical than the production of other types.

The radius of curvature of a cycloidal tooth profile is zero at the pitch circle. For this reason it is difficult to machine accurately the portion of the profile near the pitch circle. The radius of curvature of an involute is zero at the base circle. By controlling the length of path of contact this portion can be eliminated from the active portion of the profile.

One of the principal advantages of involute gears is that they fulfill the fundamental law of gearing regardless of the center distance between the axes. In Fig. 9.19 a pair of teeth are shown in contact at h. The angular velocity ratio is $O_3P \div O_2P$. When center O_3 is moved to O_3' the tooth contact is at h'. The common normal to the teeth at h' is tangent to the base circles and intersects the line of centers at P'. Triangles O_2PC and O_3EP are similar. Triangles $O_2P'C'$ and $O_3'E'P'$ are similar; hence

$$\frac{E'O_3'}{C'O_2} = \frac{O_3'P'}{O_2P'} \quad \text{and} \quad \frac{EO_3}{CO_2} = \frac{O_3P}{O_2P}$$

But $O_2C = O_2C'$ and $O_3E = O_3'E'$

Hence $$\frac{O_3P}{O_2P} = \frac{O_3'P'}{O_2P'}$$

The angular velocity ratio is not changed. An increase in the center distance increases the backlash and pressure angle and decreases the length of path of contact but the fundamental law is fulfilled.

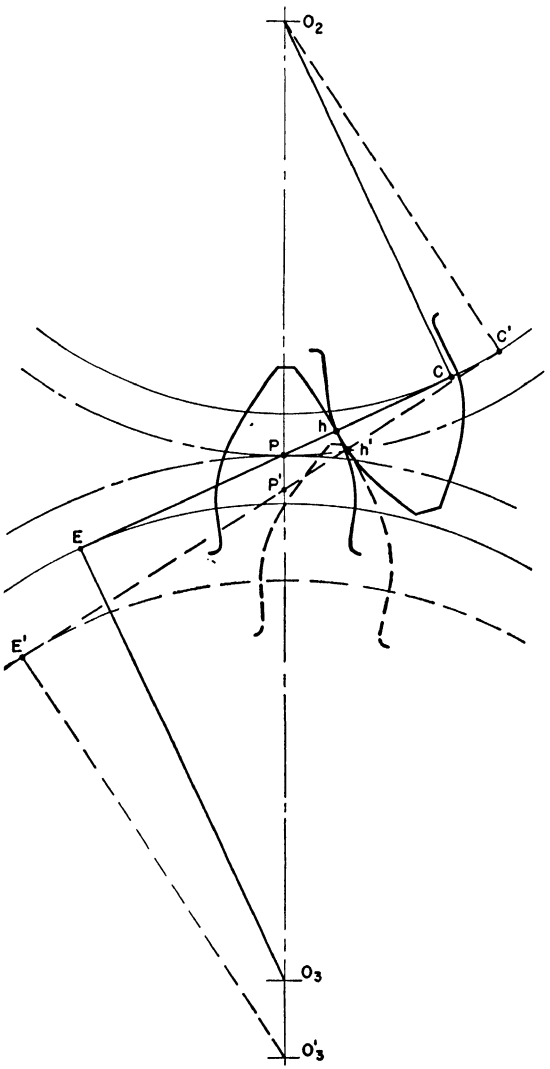

Fig. 9.19

The base circle is built into an involute gear. It is one of the necessary specifications. An involute gear has no pitch circle until it is meshed with another gear. When a pitch circle is used in specifying a gear it must be associated with a definite pressure angle. This in effect specifies the base circle.

Where the gears are to be cut with formed milling cutters, the number of cutters required to cover the range from the smallest pinion to a rack is less than for cycloidal profiles. This results from a smaller change in curvature over the range.

9.17. Summary of involute-curve properties. The previous discussion of involute teeth should be sufficient for an understanding of each of the following properties.*

1. The shape of the involute curve is dependent only upon the size of the base circle.

2. If one involute, rotating at a uniform rate of motion, acts against another involute, it will transmit a uniform angular motion to the second regardless of the distance between the centers of the two base circles.

3. The rate of motion transmitted from one involute to another depends only on the relative sizes of the base circles of the two involutes. This rate of motion is in inverse proportion to the sizes of the two base circles.

4. The common tangent to the two base circles is both the path of contact and the line of action. In other words, the two involutes will make contact with each other only along this common tangent to the two base circles.

5. The path of contact of an involute is a straight line. Any point on this line may therefore be taken as a pitch point, and the path of contact will remain symmetrical in relation to this pitch point.

6. The intersection of the common tangent to the two base circles with their common center line establishes the radii of the pitch circles of the mating involutes. No involute has a pitch circle until it is brought into contact with another involute, or with a straight line constrained to move in a fixed direction.

7. The pitch diameters of two involutes acting together are directly proportional to the diameters of their base circles.

8. The pressure angle of two involutes acting together is the angle between the common tangent to the two base circles and a line perpendicular to their common center line. No involute has a pressure angle until it is brought into contact with another involute, or with a straight line constrained to move in a fixed direction.

9. The form of the basic rack of the involute is a straight line. The pressure angle of an involute acting against such a rack is the angle between the line of action and a line representing the direction in which this rack moves.

10. The pitch radius of an involute acting against a straight-line rack form is the length of the radial line, perpendicular to the direction of motion of the rack, measured from the center of the base circle to its point of intersection with the line of action.

* Buckingham, Earl, *Analytical Mechanics of Gears*, McGraw-Hill Book Co., Inc., 1949.

9.18. Standard interchangeable tooth forms. For reasons of economy standard tooth forms have been adopted to meet various requirements. All gear designs are compromises. The tooth form chosen is the one that is most satisfactory when all conditions, functional and economic, are considered. The standard forms are described below.

The 14½° Composite System. This tooth form came into use when both cycloidal and involute gears were in use. The basic rack is shown in Fig. 9.20. The central portion of the tooth is involute and the remainder

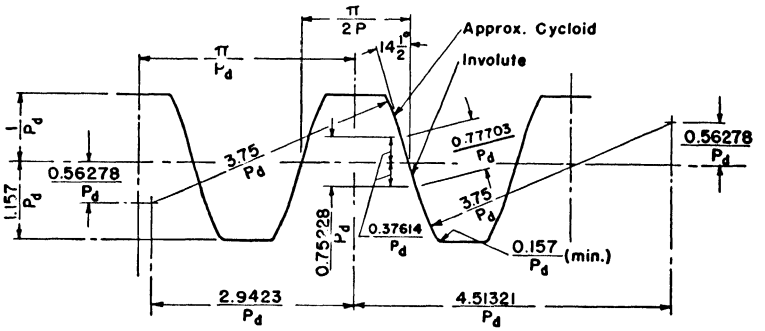

Fig. 9.20

is segmental. It is sometimes said that these portions are cycloidal because of the close approximation. The segmental form (circular arc) can be produced accurately with less difficulty than the cycloidal form. The rack tooth is symmetrical with respect to the pitch point, and gears conjugate to this rack will be interchangeable.

These gears must operate on fixed center distances. A change in center distance would cause a segmental curve on one tooth to be in contact with an involute curve on the other tooth and would produce incorrect tooth action. Only involute curves have the property of operating correctly with any center distance. Interference and undercutting of small pinions is avoided in this system.

The 14½° Full Depth System. The basic rack tooth for this system is shown in Fig. 9.21. Two 23-tooth pinions are the smallest pair of equal

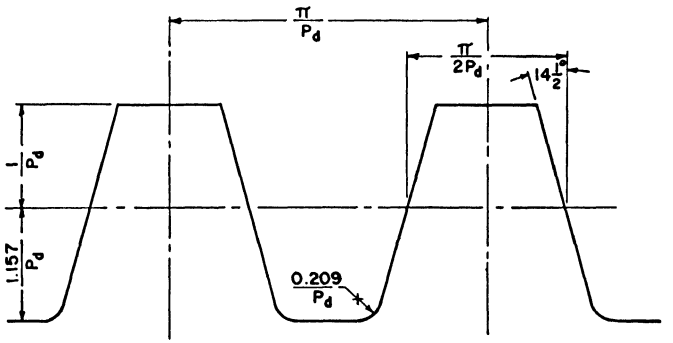

Fig. 9.21

gears that will have the desired minimum contact ratio of 1.4. The smallest pinion that will mesh with a rack without interference has 32 teeth. This system is usually used for gears having a large number of teeth, 40 to 50 and larger.

The 20° Full Depth System. The basic rack is shown in Fig. 9.22. This system is suitable for gears having smaller numbers of teeth than

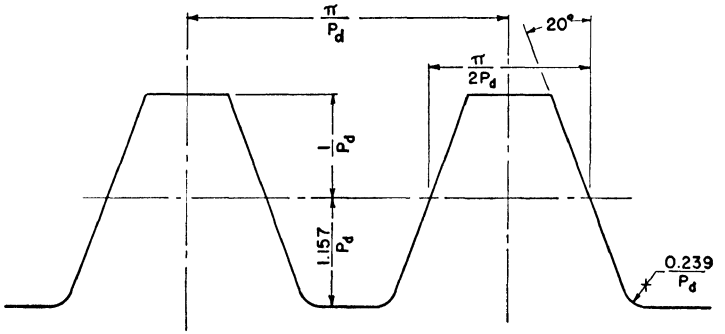

Fig. 9.22

are permitted with the $14\frac{1}{2}°$ systems. Two 14-tooth pinions will have a contact ratio of 1.415. The smallest pinion that will mesh with a rack without interference has 18 teeth. In general this is the best system for gears having small numbers of teeth.

The 20° Stub System. The basic rack for this system is shown in Fig. 9.23. This tooth form was introduced to meet the needs of gears having small tooth numbers and requiring high beam strength. A load

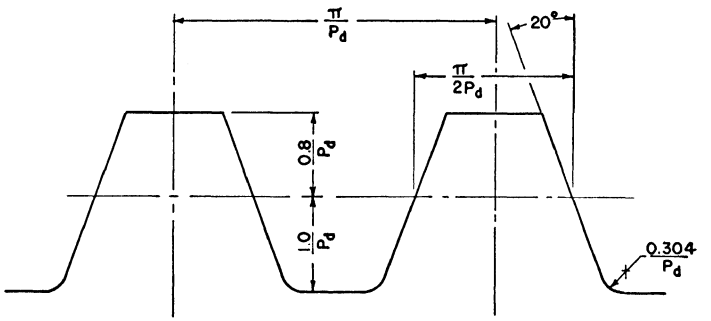

Fig. 9.23

on the end of a stub tooth does not produce as high a stress at the fillet as the same load on a longer tooth. Some of this advantage is lost since fewer pairs of teeth are in contact. Two 12-tooth pinions have a contact ratio of 1.185. A pinion and gear having 27 and 30 teeth have a contact ratio of 1.351. Gears of this system with small numbers of teeth do not have the desired minimum ratio of 1.4. For equal smoothness of oper-

ation these gears must be more accurately machined than gears having a greater contact ratio.

The 20° Fellows Stub Tooth Systems are similar to the 20° stub system described above but the tooth proportions are not the same for all sizes of teeth. The pitch designations are: 3/4, 4/5, 5/7, 6/8, 7/9, 8/10, 9/11, and 12/14. The numerator is the diametral pitch, the addendum is unity divided by the denominator, and the clearance is 0.25 divided by the denominator. For a gear of diametral pitch 5 the addendum is $\frac{1}{7}$ in. and the clearance is 0.25/7 in.

9.19. Parallel helical involute gears. A stepped gear, Fig. 9.24, consists of two or more gears fastened together as shown. Each is advanced relative to the adjacent one by an amount equal to the circular pitch divided by the number of gears. When accurately made, these gears are more quiet and smooth in action than conventional spur gears. Theoretically most gears run perfectly. Actually there are always inaccuracies in the teeth and deflections due to loads. This results in impact loading and noise. If the masses of the parts that meet with impact are reduced, the noise is less. In stepped gears the masses are reduced. There is also a greater variety of contact.

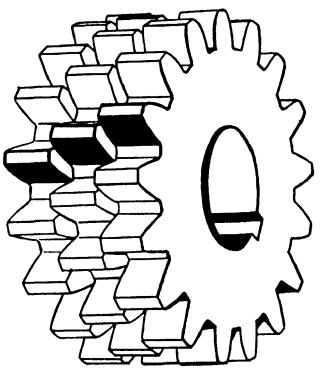

Fig. 9.24. (Courtesy of Socony Vacuum Oil Co.)

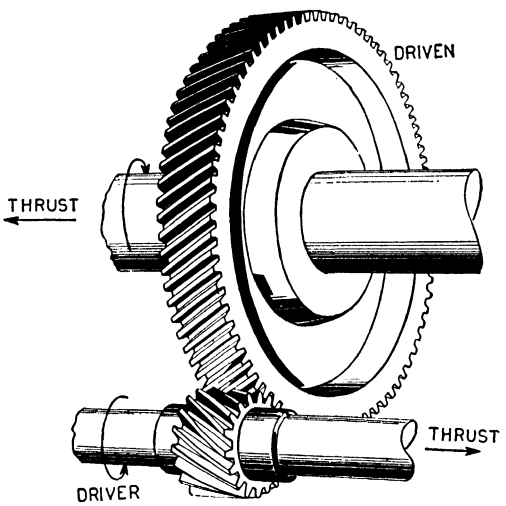

Fig. 9.25. (Courtesy of Socony-Vacuum Oil Co.)

Parallel helical gears, Fig. 9.25, are much more widely used than stepped gears. These gears can be thought of as stepped gears with infinite numbers of parts. A more basic way of considering these gears is shown in Fig. 9.26. A thin flat tape lying in the plane of action is used to connect the base cylinders of the gears. When the base cylinders are rotated, the diagonal lines on the tape generate the teeth of both

gears simultaneously. The line of contact of a pair of mating teeth lies along one of these lines as it moves in the plane of action. When the tape wraps around a base cylinder the diagonal generating lines become helices.

The helix angle ψ is the angle between any helix and an element of its cylinder. In helical gears and worms, it is the pitch diameter unless otherwise specified.

The lead angle λ is the complement of the helix angle.

The lead *l is the axial advance of a helix for one complete turn, as in the threads of cylindrical worms and teeth of helical gears.* If the base cylinder

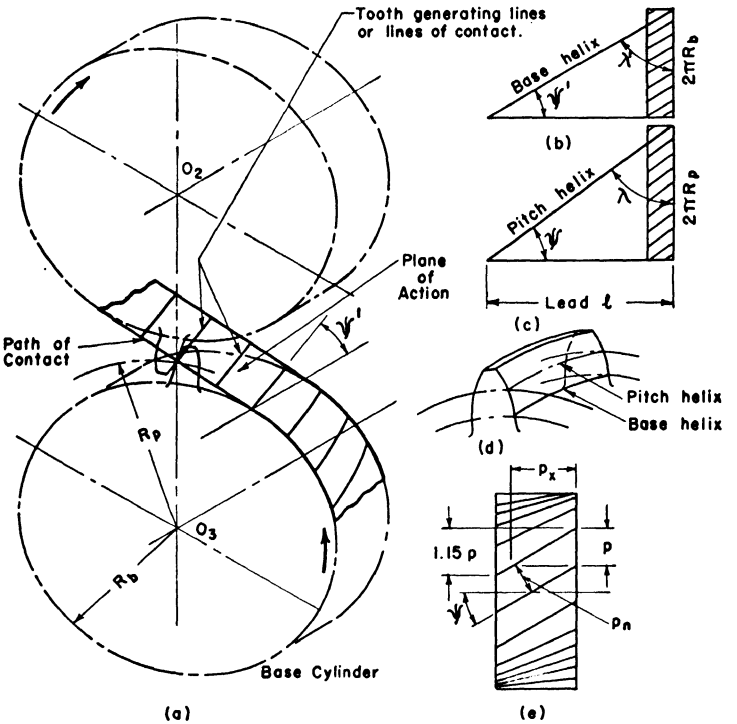

Fig. 9.26

is opened up and laid flat, the helix will appear as in Fig. 9.26(b). The helix on the pitch cylinder will appear as in (c). The relationship between the helix angles on the base and pitch cylinders is obtained from the equations

$$\tan \psi' = \frac{2\pi R_b}{l}$$

$$\tan \psi = \frac{2\pi R_p}{l}$$

and Eq. (9.2) $\qquad R_b = R_p \cos \phi$

giving $\qquad \tan \psi' = \tan \psi \cos \phi \qquad (9.8)$

Parallel helical gear tooth contact is progressive. Instead of the teeth coming into contact along the entire face width, contact starts at a point on the edge and progresses across the tooth, resulting in diagonal straight-line contact. These gears have less impact loading and can be run at higher speeds than gears having straight teeth.

To gain the full advantage of helical teeth it is recommended that the tooth advance corresponding to the face width be at least 15 per cent greater than the circular pitch. This is shown at (e). Under this condition at least one pair of teeth will always be in contact at the pitch point, and the contact ratio will always be sufficiently large.

The normal circular pitch p_n is the circular pitch in the normal plane, and also the length of arc along the normal helix between helical teeth or threads.

The axial pitch p_x is the circular pitch in the axial plane and in the pitch surface between corresponding sides of adjacent teeth, in helical gears and worms.

A disadvantage of helical gears is that they produce axial thrust as shown in Fig. 9.25. This is usually not serious. If ball or tapered roller bearings are used to carry the radial load, they will usually carry the thrust also.

The designation of the hand of a helical gear is the same as that used for screws. A screw has a right-hand thread if, when held in front of an observer and turned clockwise, it moves away from the observer. In Fig 9.25 the pinion is right-hand and the gear left-hand.

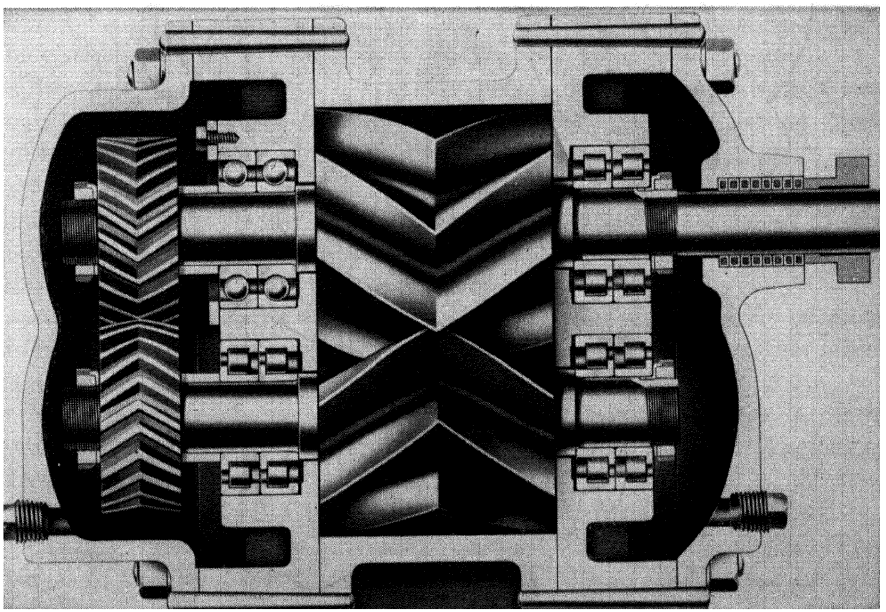

Fig. 9.27. (Courtesy of Warren Steam Pump Co.)

Thrust is eliminated in herringbone gears. They are equivalent to two helical gears of opposite hand placed side by side. The gears at the left of the pump in Fig. 9.27 are herringbone gears. The pump impellers are also herringbone gears. Pumps that are made to move fluids having lubricating qualities do not require the separate gear drive shown on the left.

9.20. Crossed helical involute gears. Crossed helical gears are used to transmit power between nonparallel, nonintersecting axes (Fig. 9.28). A pair of parallel helical gears are of opposite hand and equal helix angles. They have line contact and there is no sliding along the

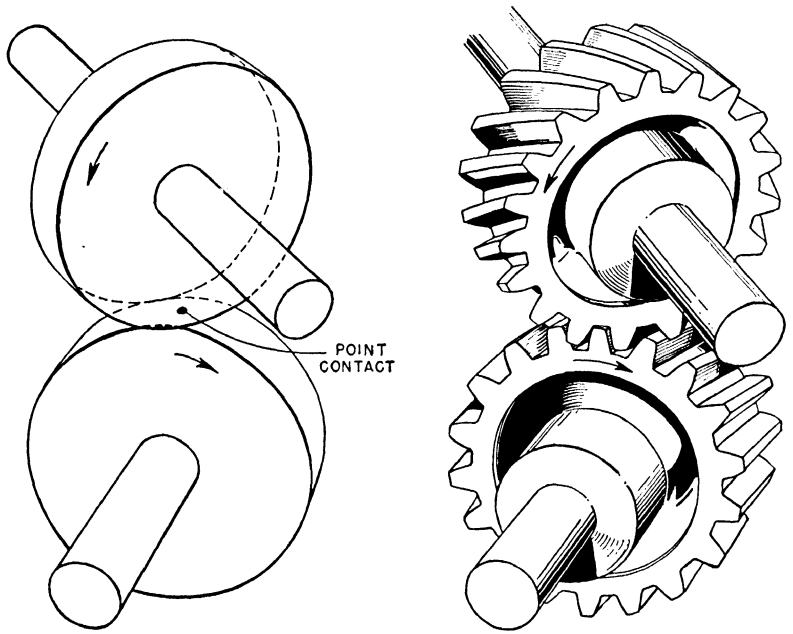

Fig. 9.28. (Courtesy of Socony-Vacuum Oil Co.)

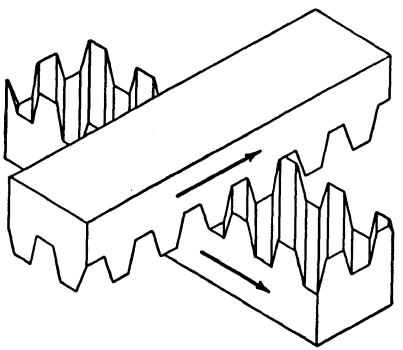

Fig. 9.29

elements of the teeth. The individual gears of a crossed helical pair are the same as parallel helical gears. When helical gears are meshed on nonparallel, nonintersecting axes, the tooth action is different. There is point contact and sliding along the elements of the teeth. Crossed helical gears are usually of the same hand and the helix angles need not be the same. A study of the action of the basic racks, Fig. 9.29, will aid in visualizing the tooth action of crossed helical gears.

In Fig. 9.30 gears 2 and 3 connect axes 2-2 and 3-3. Angles ψ_2 and ψ_3 are the helix angles of gears 2 and 3. The teeth are in contact at

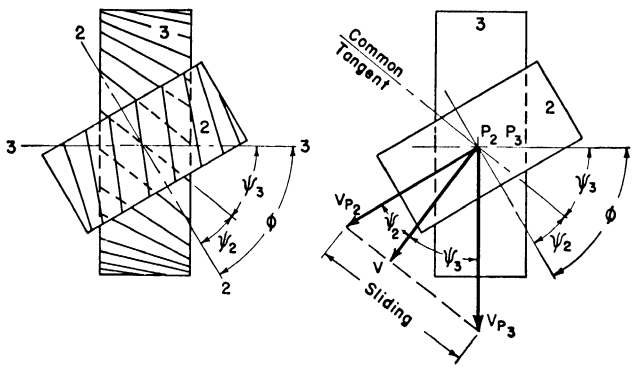

Fig. 9.30

P_2P_3. Velocity V_{p_3} is the velocity of P_3, and V_{p_2} is the velocity of P_2. These two velocities must have a common component V along the common normal. The normal pitches of the two gears must be equal; the circular pitches will be unequal if the helix angles are unequal.

Because of point contact, the power that can be transmitted is less than for other types of the same size having line contact. These gears are not sensitive to center distance changes. As a result of point contact the angular relationship of the axes can be changed without loss of theoretically correct conjugate tooth action. When these gears are not loaded above their capacity they are generally quieter and more satisfactory than any other type of gear drive.

As with all gears, the angular velocity ratio is inversely as the number of teeth. The angular velocity ratio will be inversely as the pitch diameters only when the helix angles are equal.

Each gear of a helical pair has two distinct pitch surfaces: a pitch cylinder and a pitch plane. This is discussed in Buckingham's *Analytical Mechanics of Gears.*

9.21. Production of straight and helical spur gears.

Milling. The method of milling gears is shown in Fig. 9.31. The profiles of the milling cutter faces are that of the tooth space to be cut. A tooth space is machined by passing the gear blank across the rotating

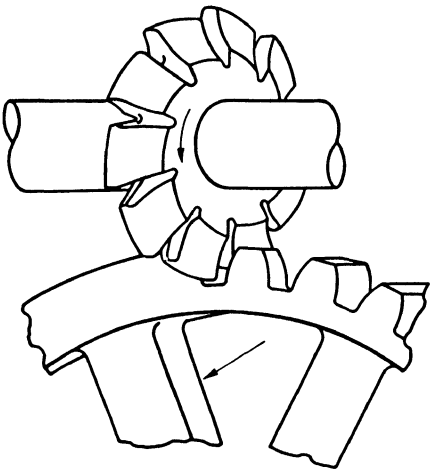

Fig. 9.31. (Courtesy of Barber-Colman Co.)

cutter. The gear is then indexed and another tooth space is cut. Milling cutters can be sharpened by grinding the faces without changing the cutting profiles. The shapes of gear teeth vary with the number of teeth. Theoretically a different cutter should be used for each number of teeth. In practice it has been found that for a single pitch a set of 15 cutters is sufficient for cutting all gears having numbers of teeth from 12 to a rack.

Fellows Gear Shaper. The generating process is used in cutting gears on a Fellows gear shaper. The principle is illustrated in Fig. 9.32.

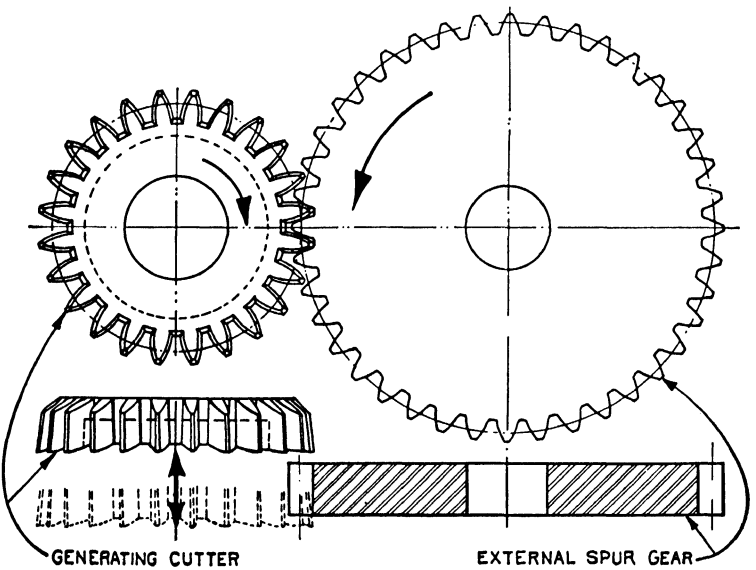

Fig. 9.32. (Courtesy of The Fellows Gear Shaper Co.)

The cutting edges of the cutter are in the form of a spur gear with addendums long enough to produce the required clearance. The cutting of a gear is started by feeding the gear blank into the reciprocating cutter until the desired depth is reached. While the cutter continues to reciprocate, the gear blank and cutter are both rotated a small amount after each cutting stroke with a motion that is equivalent to the rolling of the pitch circles. The manner in which a cutter tooth generates conjugate profiles is shown in Fig. 9.33.

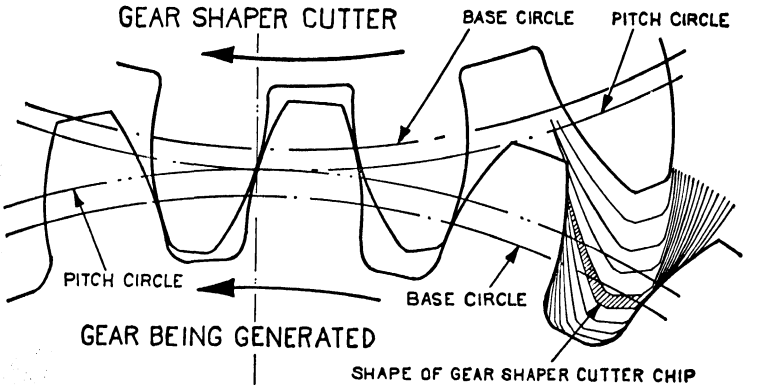

Fig. 9.33. (Courtesy of The Fellows Gear Shaper Co.)

Helical gears can be generated with a helical cutter (Fig. 9.34). In addition to the motions for cutting straight spur gears there is super-

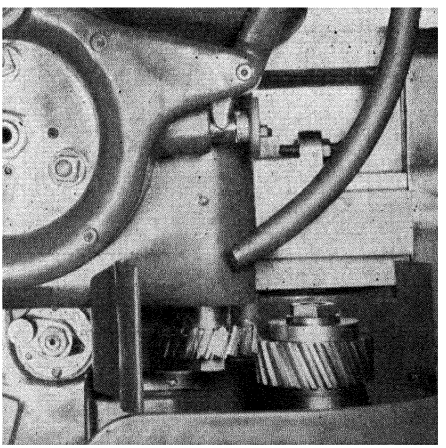

Fig. 9.34. (Courtesy of The Fellows Gear Shaper Co.)

imposed an oscillatory rolling of the cutter and gear blank pitch circles to produce the necessary helical path of the cutter relative to the gear blank.

Hobbing is the most rapid method of producing gears. The hobbing process is shown in Figs. 9.35 and 9.36. In Fig. 9.35 the third gear

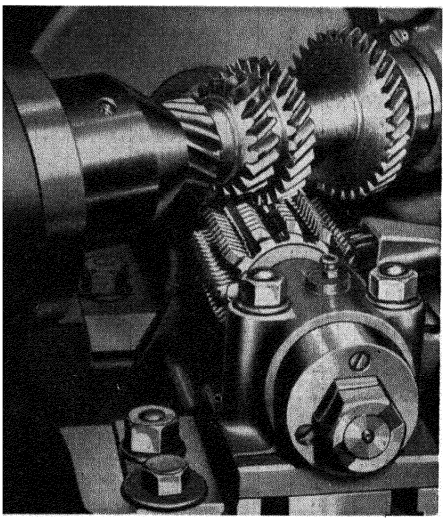

Fig. 9.35. (Courtesy of Barber-Colman Co.)

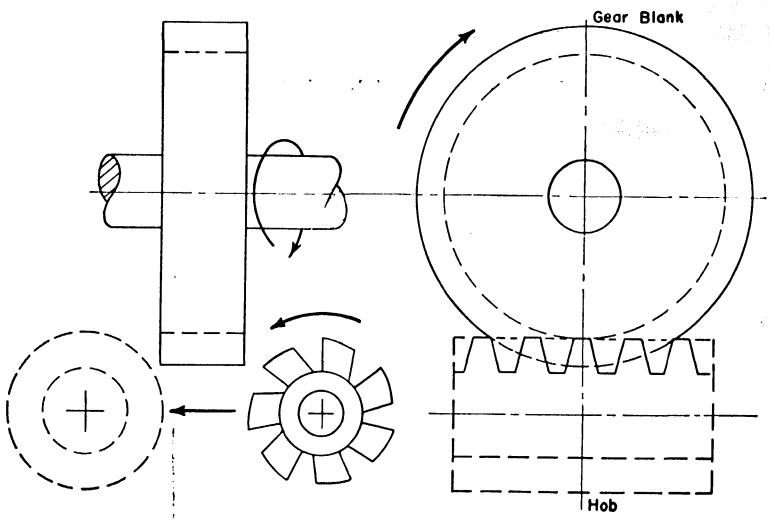

Fig. 9.36

from the left in the cluster is being generated. The hob is similar to a helical gear having a small number of teeth or threads, in some cases one. Axial gashes are made to produce cutting edges. The motions involved in hobbing a gear are shown in Fig. 9.36. The axes of the hob and the gear blank are set to produce the desired helix angle. The hob and the gear blank are rotated with an angular velocity ratio that is inversely

as the numbers of teeth on the hob and gear. The hob is then fed across the face of the gear.

Shaving. Gears can be made to a high degree of accuracy by finishing them with the shaving process (Fig. 9.37). A gear shaver is similar to

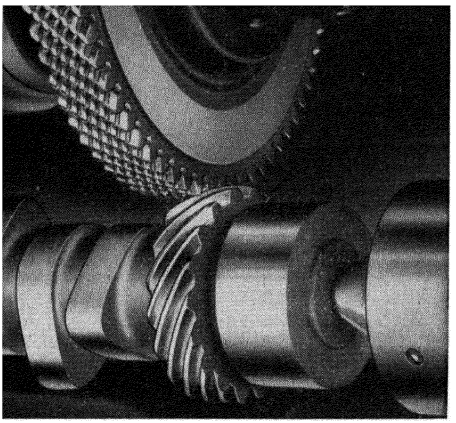

Fig. 9.37. (Courtesy of National Broach & Machine Co.)

either a straight or helical spur gear with circumferential gashes in it to produce cutting edges. The gear and shaver are forced together while rotating, and the gear is reciprocated along its axis. Surface smoothness is improved, and errors of index, helix angle, tooth profile, and eccentricity are reduced by the small amount of metal that is removed in the form of needle-like chips.

Grinding is an accurate method for finishing gears. Gears that are heat treated after rough machining can be finished by this process. The process is shown in Fig. 9.38. The flat side of a grinding wheel is used

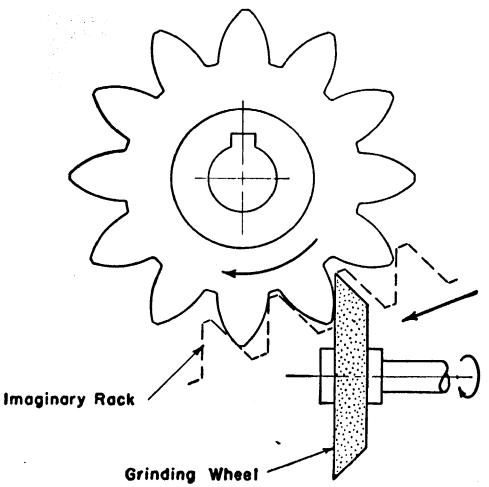

Fig. 9.38

to simulate a rack tooth profile. The gear and grinding wheel are moved in a manner that is equivalent to rolling of the gear pitch circle on the rack pitch line.

9.22. Unequal-addendum gears. The undercutting that results from the use of a small pinion and a large gear can often be eliminated by using unequal-addendum gears. This can be understood most easily by considering a rack and pinion. A 12-tooth pinion and rack of the full-depth 20° system is shown in Fig. 9.39(a). If the pinion is generated

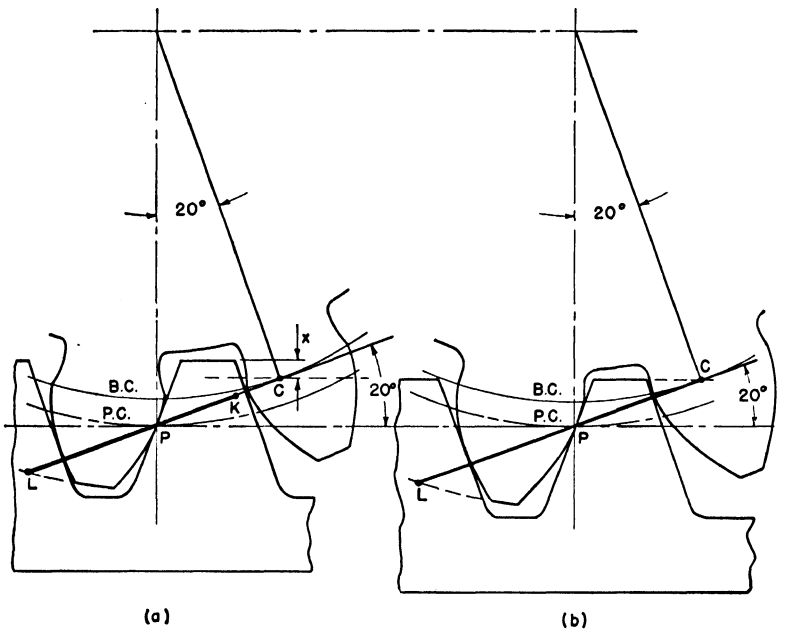

Fig. 9.39

with a rack cutter, it will be undercut as shown. The pinion teeth are weakened. The path of contact LK corresponds to a contact ratio of 1.049. It can be seen that the rack tooth is too long by an amount x. In (b) the rack has been withdrawn an amount x and the pinion addendum increased by the same amount. The resulting conjugate pinion tooth is shown. It is stronger, and the contact ratio has been increased to approximately 1.44. The base circle, pitch circle, and pressure angle remain the same.

The method of cutting unequal-addendum gears with standard generating cutters is to decrease the radius of the gear blank so that interference is eliminated. The gear teeth are cut to the standard whole depth. The radius of the pinion blank is increased by the amount that the gear was decreased, and the teeth are cut to the standard whole depth.

9.23. Worm gears are similar to crossed helical gears. The drive shown in Fig. 9.40 is of crossed helical gears. The pinion, or worm, shown at the right has one tooth. Because the appearance of a worm is

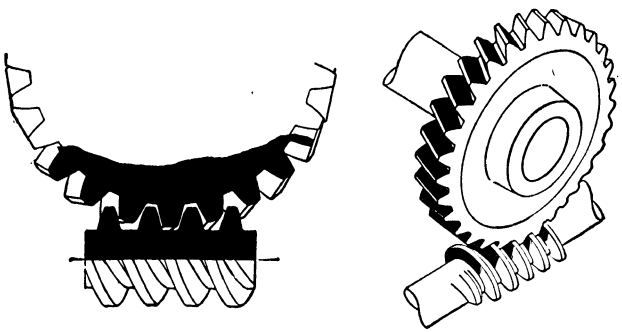

Fig. 9.40. (Courtesy of Socony-Vacuum Oil Co.)

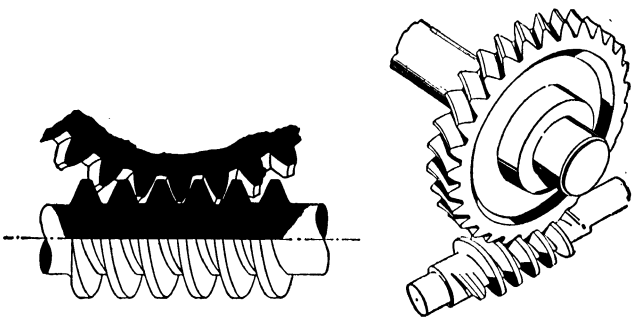

Fig. 9.41. (Courtesy of Socony-Vacuum Oil Co.)

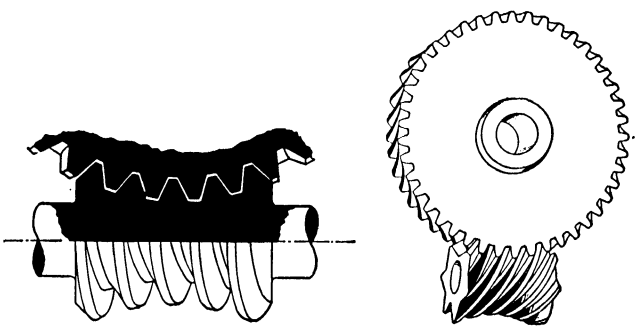

Fig. 9.42. (Courtesy of Socony-Vacuum Oil Co.)

similar to that of a screw, the teeth are usually called threads. Three worms are shown in Fig. 9.43; (a) has one thread and is called a single worm, (b) has two threads and is called a double worm, (c) is a triple worm. The capacity of a worm drive can be increased by introducing line contact instead of point contact that is present in crossed helical

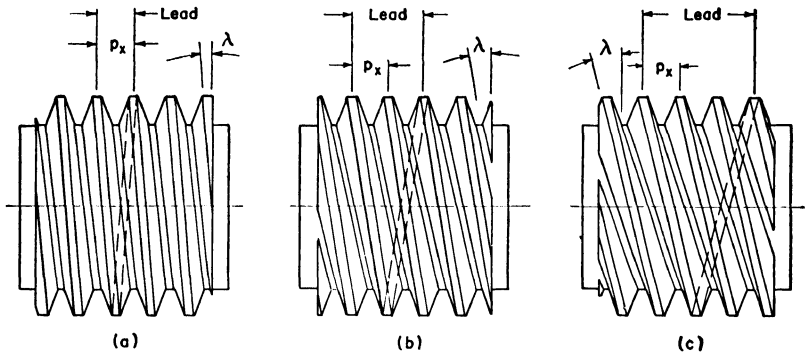

Fig. 9.43

gears. This is done by making the gear, or worm wheel, envelop the worm (Fig. 9.41). The method by which this is accomplished can be understood if the cutting process is considered (Fig. 9.44). Instead of

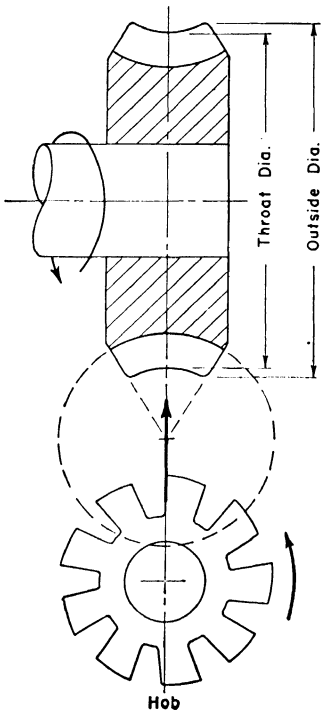

Fig. 9.44

passing the hob across the face of the gear as is done in cutting helical gears, it is fed into the face along the central plane of the gear. When a worm that is substantially the same size as the hob is meshed with the worm wheel, conjugate tooth action with line contact results.

In Fig. 9.42 both the worm and worm wheel are throated, each envelops the other. This is called a Hindley worm. The Hindley worm has the advantage that more teeth are in contact, but has the disadvantage that the axial location of the worm relative to the worm wheel must be accurately maintained or binding will result. The type shown in Figs. 9.41 and 9.45 is most widely used.

As with all gear drives the angular velocity ratio is inversely as the numbers of teeth. The lead (Fig. 9.43) is always equal to or a multiple

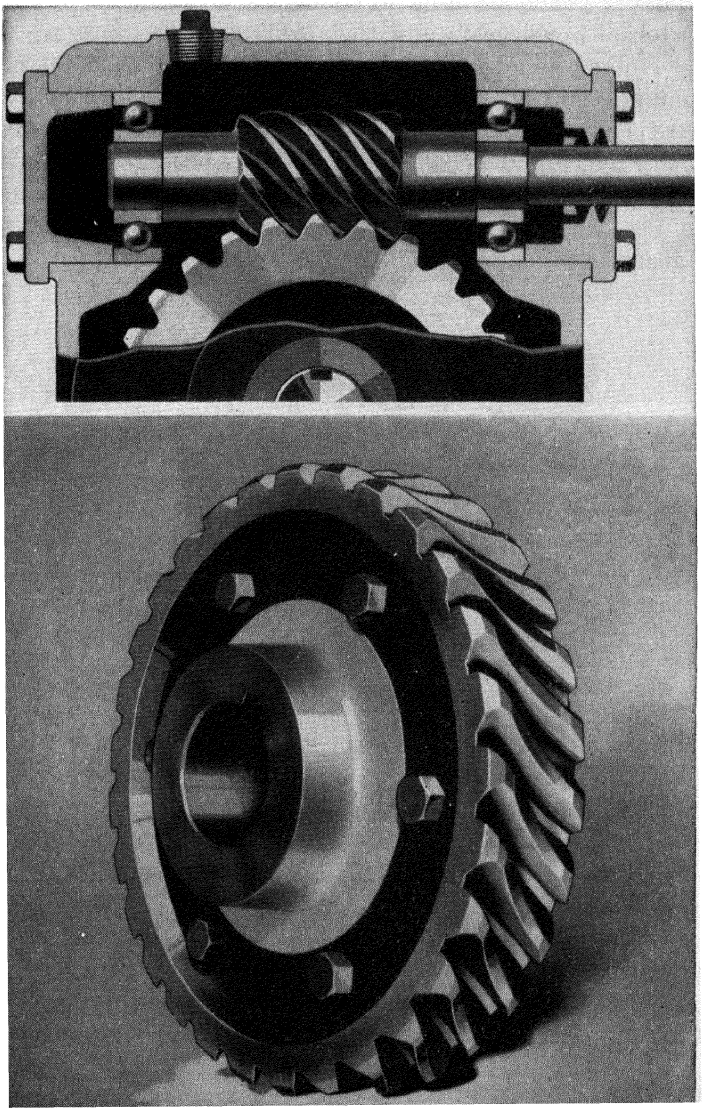

Fig. 9.45. (Courtesy of The Cleveland Worm & Gear Co.)

of the pitch. The axes of most worm drives are at right angles. When this is the case the axial pitch of the worm is equal to the circular pitch of the worm wheel. The relationships of Fig. 9.26(b) and (c) apply to the worms of Fig. 9.43.

Worm drives form compact units, especially for large gear ratios. They are quiet and highly efficient when the lead angle of the worm is between 30° and 60°. Excessive sliding reduces the efficiency when the lead angle is small.

9.24. Bevel gears are used to connect shafts that have intersecting axes. External bevel gears and their rolling pitch cones are shown in Fig. 9.3. Rolling cones have spherical motion. Each point in a bevel gear remains a constant distance from the common apex of the cones; hence there is no sliding along the tooth elements. A pinion and a crown gear are shown in Fig. 9.46. The pitch surface of a crown gear is a plane and corresponds to a rack in spur gearing. An internal bevel gear is shown in Fig. 9.47. Due to limitations in the machining of this type of bevel gear the pitch angle cannot greatly exceed 90°.

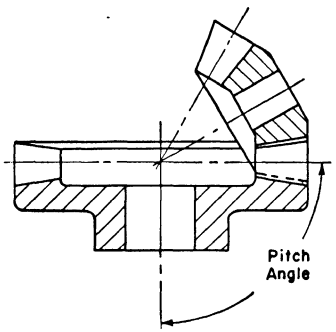

Fig. 9.46

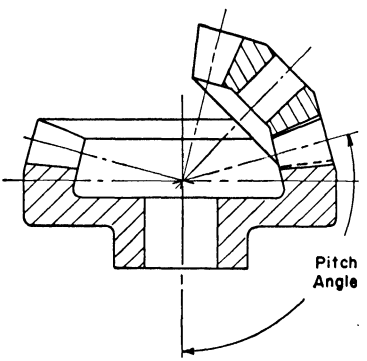

Fig. 9.47

Bevel gear terminology is shown in Fig. 9.48. All tooth elements converge at the apex of the cone. The teeth, if extended to this point, would be difficult to cut, the small portions would not carry a large load, a more accurate alignment of the axes would be required, and the shaft could not extend through the gear. For these reasons the face width is usually limited to one-third of the cone distance.

A pair of bevel gears with equal numbers of teeth and with axes at right angles are called *miter gears.*

Involute Bevel Gears. It was shown that one of the principal advantages of involute spur gears was that an involute rack tooth has a straight profile. This does not hold for bevel gearing. An involute crown gear tooth is shown in Fig. 9.49. The base cone angle must be less than the 90° pitch angle. When the generating plane is rolled on the base cone

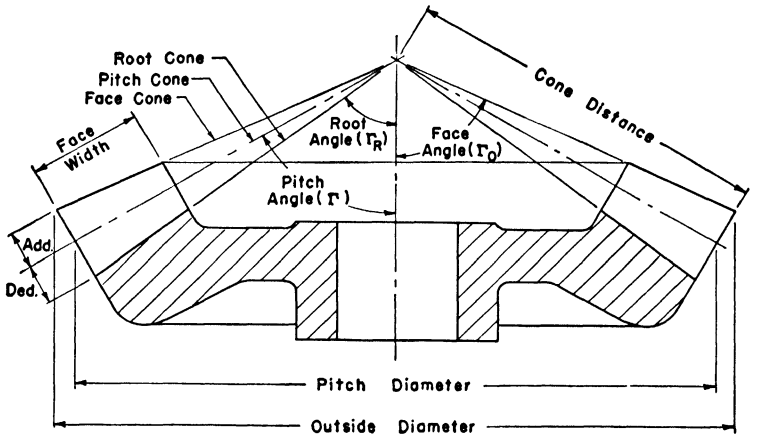

Fig. 9.48

the generating line WV sweeps out the spherical involute tooth shown. These teeth are difficult to cut and are not used.

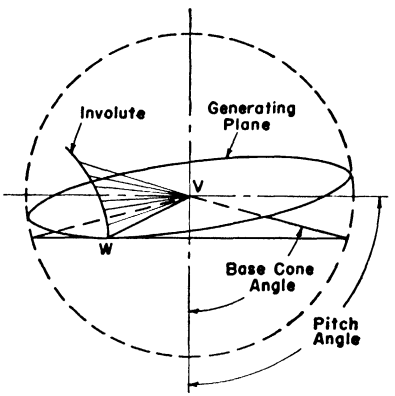

Fig 9.49

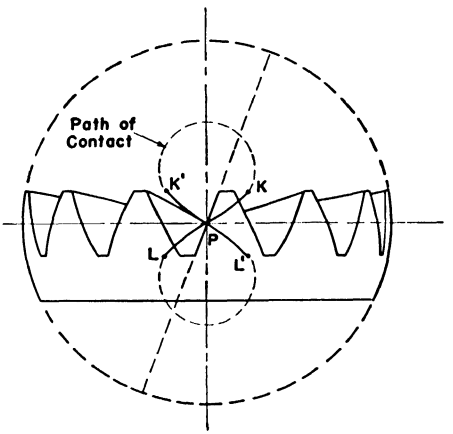

Fig. 9.50

Octoid Bevel Gears are gears that are conjugate to a crown gear having teeth made with straight sides. An octoid crown gear is shown in Fig. 9.50. The sides of the teeth lie in planes that pass through the center of the sphere. When meshed with a conjugate gear the complete path of contact on the surface of a sphere is in the form of a figure 8; hence the name octoid. Only a portion of the path is used, KLP or $K'PL'$. These portions are nearly straight. Because of the symmetry of the tooth the path of contact will also be symmetrical and gears conjugate to this basic crown gear will be conjugate to each other.

Bevel Gear Tooth Action should be considered on the basis of spherical motion. Because of the difficulty of working with a spherical surface

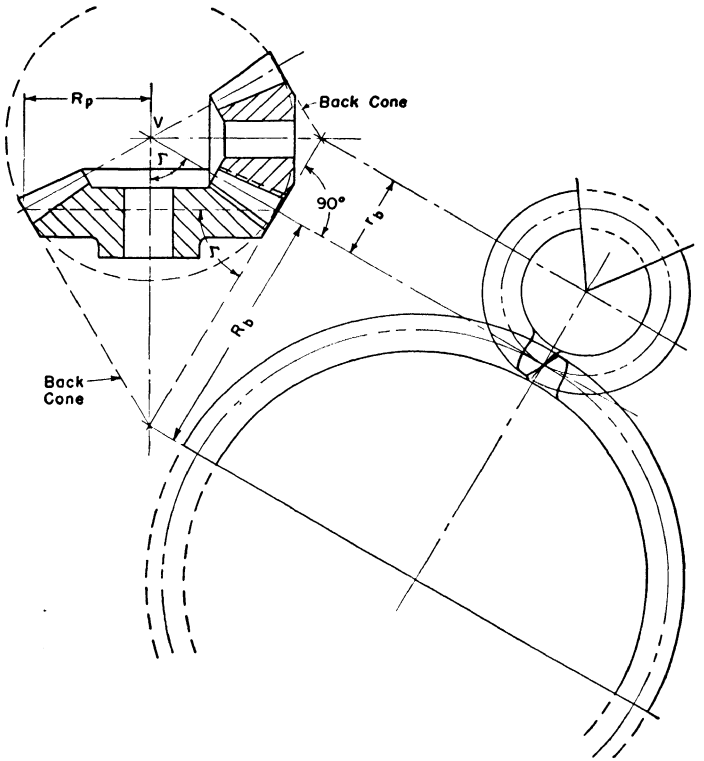

Fig. 9.51

an approximation in a plane is used. The back of the gear is usually made conical instead of spherical, Fig. 9.51. The back cones very nearly approximate the sphere in the region of tooth contact. The slight variation in distances from the center V to points on the outer ends of the meshing teeth means that they are not quite flush. This does not affect the theoretical tooth action in the least. In order to study the bevel gear tooth action the back cones are laid out flat. Each cone forms a portion of a spur gear. The pitch radii are equal to the back cone distances R_b and r_b. The flat surface is a close approximation of the spherical surface in the region of tooth contact. This is called Tredgold's approximation. The tooth action of the bevel gears is the same as the tooth action for the larger spur gears. The number of teeth N_b on the spur gear in terms of N_G, the number on the bevel gear, is

$$N_b = N_G \frac{R_b}{R_p} = \frac{N_G}{\cos \Gamma} \tag{9.9}$$

Spiral Bevel Gears. The tooth action of spiral bevel gears, Fig. 9.52, compared with that of straight bevel gears is similar to a comparison of tooth action of helical and straight spur gears. Tooth contact begins

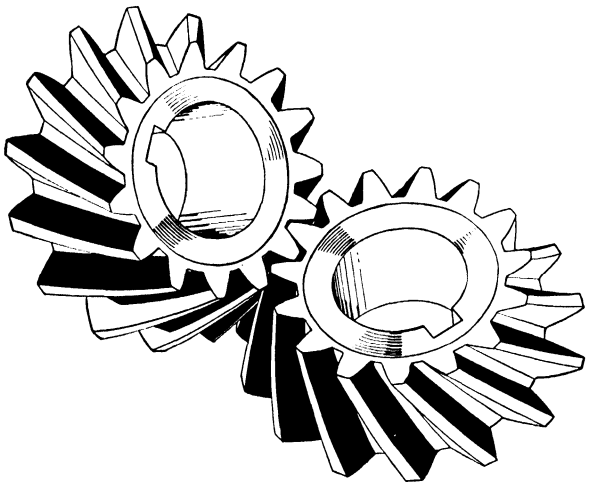

Fig. 9.52. (Courtesy of Socony-Vacuum Oil Co.)

A diagram for obtaining the face contact ratio is shown in Fig. 9.53(b). To gain the full advantage of the spiral tooth, the face advance should be at least 1.25 times the circular pitch. The tooth curve is not a true spiral but a circular arc.

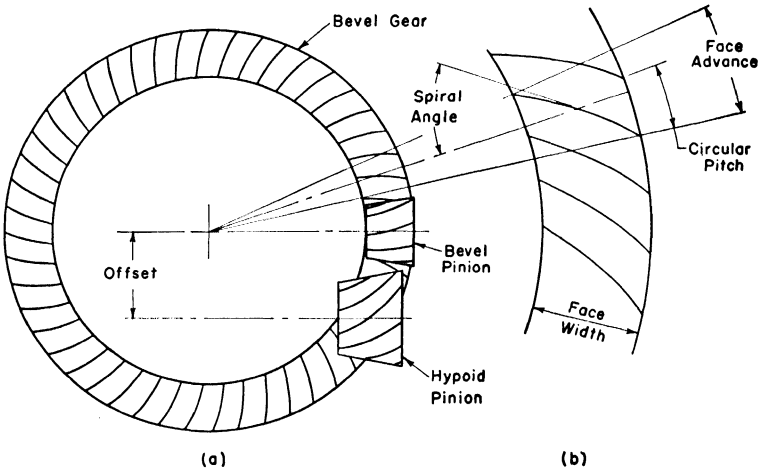

Fig. 9.53

Crown Gear Generation. The principle of generating a straight bevel gear that is conjugate to a crown gear is illustrated in Fig. 9.54(a). A reciprocating tool simulates one side of a crown gear tooth. When the pitch cone of the pinion blank is rolled on the pitch surface of the crown gear, the reciprocating tool generates one side of a pinion tooth. The motion required to roll the pitch surfaces is produced by the machine.

Spiral gear generation is shown in Fig. 9.54(b). In this case the cutter simulates one side of a curved tooth.

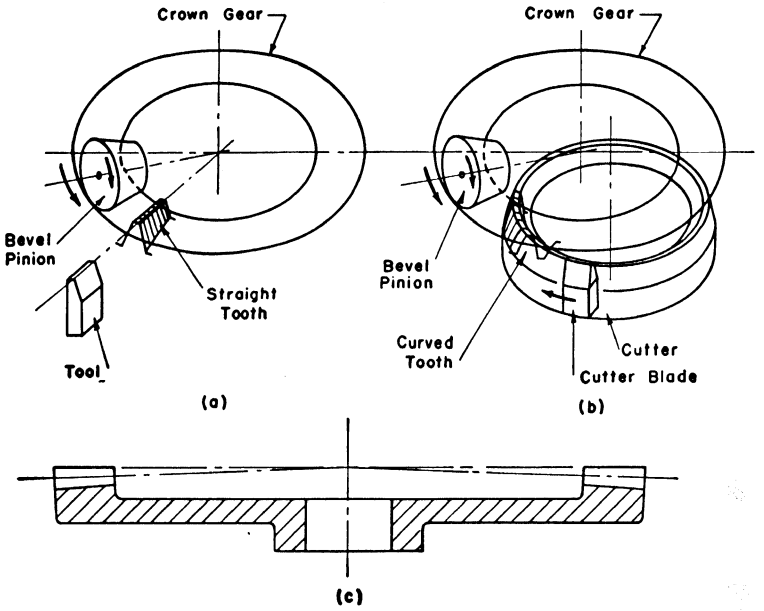

Fig. 9.54

In practice the cutters do not simulate a true crown gear tooth but an approximate crown tooth [Fig. 9.54(c)]. The tips of the cutters move in a plane. The pitch angle is slightly less than 90°. The error in tooth form that results from this approximation is negligible.

Fellows "On Center" Face Gear. Another type of bevel gear drive (Fig. 9.55) consists of an involute spur pinion and a conjugate face gear.

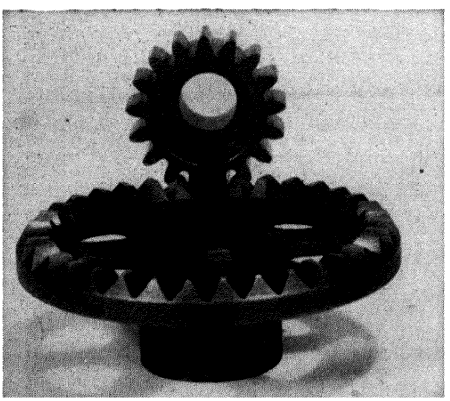

Fig. 9.55. (Courtesy of The Fellows Gear Shaper Co.)

The method of generation is shown in Fig. 9.56. This is similar to spur gear generation; the cutter reciprocates, and the rotations of cutter and face gear are inversely as their numbers of teeth. When a pinion of

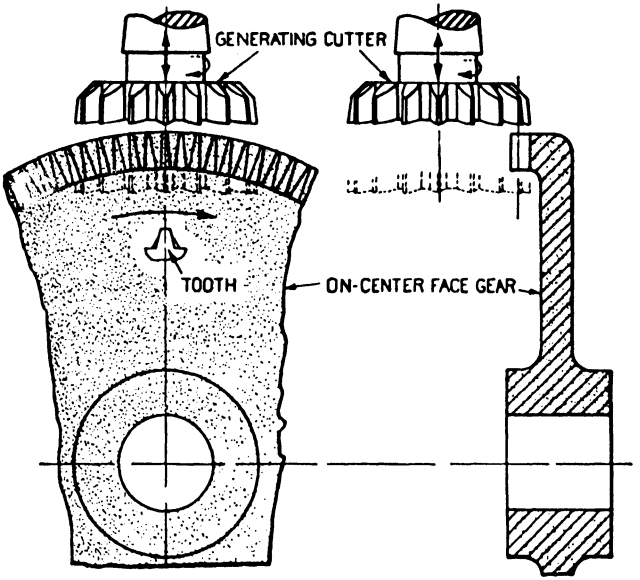

Fig. 9.56. (Courtesy of The Fellows Gear Shaper Co.)

substantially the same size as the cutter is meshed with the face gear, conjugate tooth action results.

The pitch surfaces are rolling cones, Fig. 9.57. The portion of the line of contact of the pitch cones between P and P' is the locus of the pitch points. The common normal at any point of contact of meshing teeth passes through this line of contact. This results from a variable pressure angle across the face of the gear. It is a maximum at r_0, as is shown at (b). The common normal is tangent to the pinion base circle of radius r_b and passes through pitch point P. The pressure angle is a minimum at r_i as shown at (c). The common normal is tangent to the pinion base circle and passes through pitch point P'.

It was shown in Art. 9.16 that an involute spur gear does not have a pitch circle until it is meshed with another gear. The following general statement is also true: *no single gear has a pitch surface. The pitch surfaces do not exist until two gears are meshed together.*

If, in Fig. 9.56, a helical cutter is used, a helical pinion of substantially the same size as the cutter will mesh with the face gear and conjugate tooth action will result. The pitch surfaces will be cones as before.

The Fellows face gear drive can be made for axes that intersect at any angle.

9.25. Hypoid gears. Hypoid gears are used to connect nonparallel, nonintersecting axes. The pitch surfaces are hyperboloids of revolution as described in Art. 8.6. The line of contact of the two hyperboloidal pitch surfaces is the locus of the pitch points. There is sliding along the

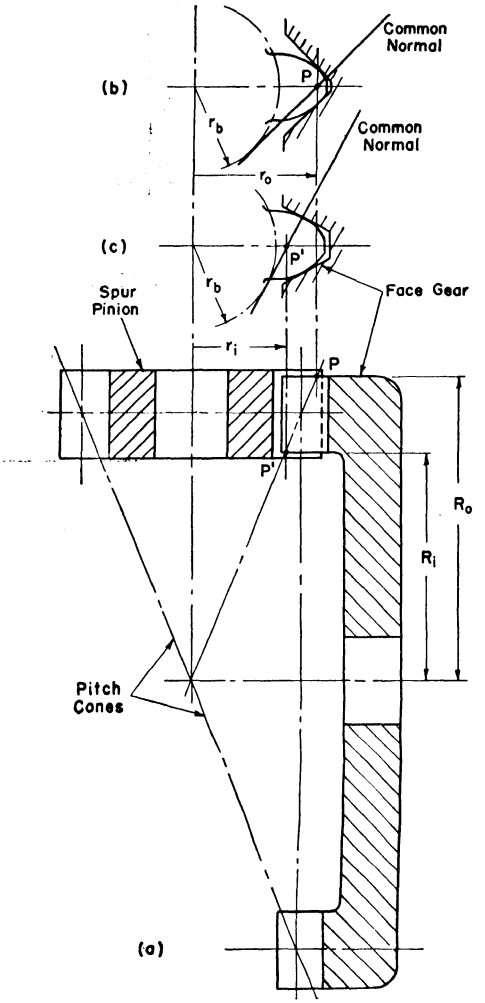

Fig. 9.57

line of contact of rolling hyperboloids; hence there is sliding along the tooth elements of hypoid gears.

Theoretically it is possible to develop an interchangeable tooth system for hypoid gears. In practice only those gears that can be conveniently cut are produced. At the present time all hypoid gear sets consist of a pair, one of which, within reasonable limits, is arbitrarily chosen and the other is made conjugate to the chosen one.

The Fellows "Off Center" Face Gear, Fig. 9.58, is one of the simplest hypoid gear sets to produce. The axis of the cutter is offset as shown; with the exception of this offset, the generation is the same as in Fig. 9.56. When a pinion of substantially the same size as the cutter is meshed

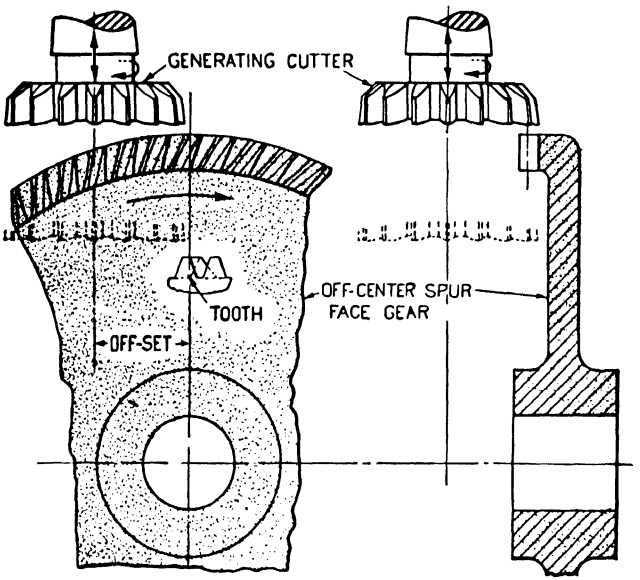

Fig. 9.58. (Courtesy of The Fellows Gear Shaper Co.)

with the off-center face gear, a hypoid pair having hyperboloidal pitch surfaces is formed.

Bevel Type Hypoid Gears Are the Most Widely Used. A pair consists of a bevel gear and a conjugate pinion. When these two are meshed, hyperboloidal pitch surfaces are formed. The generation of a hypoid pinion is similar to the generation of a bevel pinion. Some additional adjustments are required on the gear-cutting machine.

A bevel gear and conjugate bevel pinion are shown in Fig. 9.53(a). A conjugate hypoid pinion having the same number of teeth as the bevel pinion, when offset in the direction that increases the spiral angle, has a larger diameter. A hypoid set of this type is shown in an automobile drive, Fig. 11.12.

9.26. Noncircular gears are used to produce a variable angular velocity ratio. Noncircular rolling curves were discussed in Chapter 8. If rolling curves are used for pitch curves, toothed gears can be made to produce motion that is equivalent to that of the rolling curves. The fundamental law for noncircular gears is: *the common normal of teeth in contact must pass through the point on the line of centers where the pitch curves are tangent.* The law for circular gearing is a special case of this general law, for circular gears the point is fixed. Noncircular gears would be more widely used if they could be produced more economically.

The gears in Fig. 9.59 were generated with a Fellows cutter. A cam was used to produce rolling of the pitch circle of the cutter on the pitch

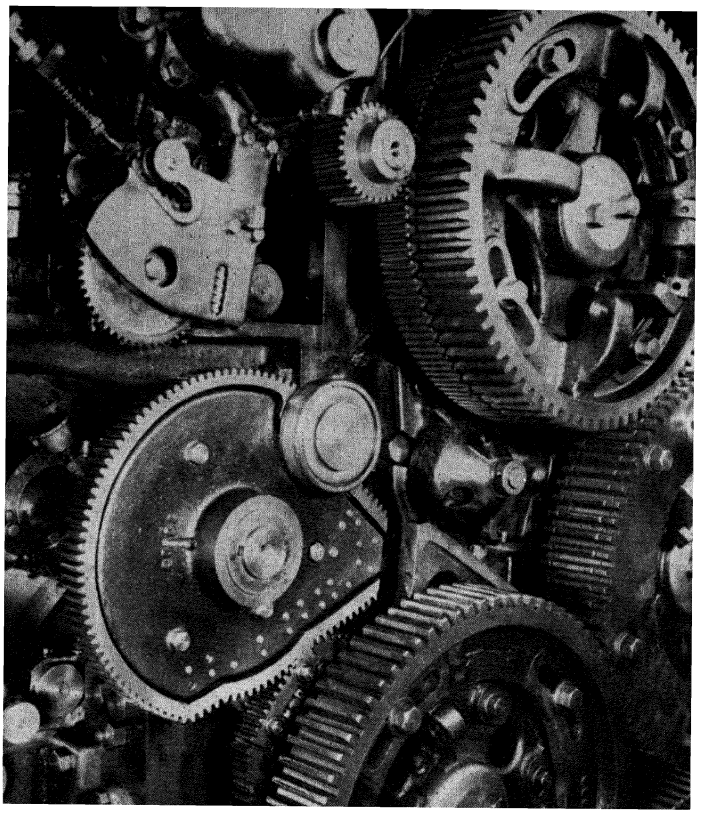

Fig. 9.59. (Courtesy of Miehle Printing Press & Mfg. Co.)

curve of the noncircular gear. The design and production of this type of gear has been described in a paper by Golber.*

PROBLEMS

9.1. A pair of meshing spur gears have 17 and 32 teeth, respectively. The diametral pitch is 8 and the pinion speed is 1160 rpm. Determine the following: (a) pitch diameters, (b) center distance, (c) circular pitch, (d) pitch line velocity in fps, (e) rpm of gear.

9.2. Same as Prob. 9.1 except 15 and 40 teeth, 10 diametral pitch, pinion speed 1800 rpm.

9.3. A pair of spur gears have a diametral pitch of 10, a velocity ratio of 2.5, and a center distance of 3.5 in. Determine the number of teeth on each gear.

9.4. A pair of spur gears have 16 and 22 teeth, 2 diametral pitch, $\frac{1}{2}$ in. addendum, $\frac{9}{16}$ in. dedendum, and 20° pressure angle. The pinion drives in a CCW direc-

* Golber, H. E., "Rollcurve Gears," *Trans. ASME*, 1939, 61:223.

tion. Determine the following: (a) pitch circle radii, (b) base circle radii, (c) circular pitch, (d) base pitch, (e) length of path of contact, (f) contact ratio, (g) angles of approach and recess for driver and follower. Indicate the pitch point and the first and last points of contact.

9.5. Same as Prob. 9.4, except 13 and 17 teeth, $1\frac{1}{2}$ diametral pitch, $\frac{9}{16}$ in. addendum, $\frac{5}{8}$ in. dedendum, and $22\frac{1}{2}°$ pressure angle. The pinion is the driver in a CW direction.

9.6. Same as Prob. 9.4, except the pinion is replaced with a rack. The gear drives in a CCW direction.

9.7. Same as Prob. 9.5, except the pinion is replaced with a rack. The gear drives in a CW direction.

9.8. The diametral pitch of a rack is 2 and the addendum is $\frac{1}{2}$ in. Determine the smallest pinion that will mesh with a rack without interference when the pressure angle is (a) $14\frac{1}{2}°$, (b) 20°, (c) $22\frac{1}{2}°$.

9.9. A pair of gears have 14 and 16 teeth, the diametral pitch is 2, the addendum is $\frac{1}{2}$ in., and the pressure angle is $14\frac{1}{2}°$. Show that the gears have interference. Determine graphically the amounts of the addendums of the gears that must be removed if interference is to be eliminated. Determine the contact ratio for this new condition.

9.10. Same as Prob. 9.9, except that the gears have 12 and 18 teeth.

9.11. A gear has 30 teeth, 3 diametral pitch, $\frac{3}{8}$ in. addendum, and 20° pressure angle. Determine (a) the smallest pinion that will mesh with the gear without interference, (b) the contact ratio.

9.12. A gear has 26 teeth, 2 diametral pitch, $\frac{7}{16}$ in. addendum, and $22\frac{1}{2}°$ pressure angle. Determine (a) the smallest pinion that will mesh with the gear without interference, (b) the contact ratio.

9.13. A pair of gears have 24 and 36 teeth, 6 diametral pitch, and 20° pressure angle. Determine the center distance of the axes. The center distance is increased 0.12 in. Determine the pressure angle that corresponds to the new center distance.

9.14. Same as Prob. 9.13 except 30 and 40 teeth, 8 diametral pitch, and $14\frac{1}{2}°$ pressure angle.

9.15. For a gear having a 6 diametral pitch, determine the addendum, dedendum, and clearance for the following systems: $14\frac{1}{2}°$ composite, $14\frac{1}{2}°$ full depth, 20° full depth, 20° stub, Fellows stub.

9.16. Same as Prob. 9.15, except the diametral pitch is 4.

9.17. A 24-tooth helical spur gear has a diametral pitch in the plane of rotation of 8, and a face width of 1.25 in. The tooth advance is 1.15 times the circular pitch. Determine: (a) pitch helix angle, (b) lead, (c) axial pitch, (d) normal pitch, (e) pitch diameter.

9.18. An 18-tooth helical spur gear has a diametral pitch in the plane of rotation of 6, a face width of 1.5 in. and a helix angle of 23°. Determine the (a) tooth advance in terms of the circular pitch, (b) axial pitch, (c) normal pitch, (d) lead, (e) pitch diameter.

9.19. A pair of helical gears have 20 and 30 teeth. The pinion speed is 900 rpm and the normal diametral pitch is 8. The pinion is left-hand and the helix angle is 30°. The gear is left-hand and the helix is 40°. Determine: (a) angular relationship of the axes, (b) circular pitches in the planes of rotation, (c) pitch diameters, (d) velocity of sliding in the tangent plane when the gears are in contact at the pitch point. (*Note:* The relationship between the diametral pitch and the normal pitch is the same as for the diametral pitch and circular pitch in the plane of rotation, i.e., the product of the normal pitch and normal diametral pitch is π.)

9.20. A pair of gears are to have 9 and 36 teeth. They are to be cut with a 20° full depth cutter of 3 diametral pitch.

(a) Determine the amount that the addendum of the gear must be decreased in order to eliminate interference.

(b) The addendum of the pinion is to be increased the same amount. Determine the contact ratio.

9.21. A double-thread worm drives a gear having 58 teeth. The axes are at 90°. The axial pitch of the worm is $1\frac{1}{4}$ in. and the pitch diameter is 3 in. Determine the helix angle of the worm, the lead, and the center distance of the gears.

9.22. The relationship of the axes of a worm and gear are shown in Fig. P 9.22. The right-hand triple worm has an axial pitch of $\frac{1}{2}$ in. and a pitch diameter of 3 in. The gear has 40 teeth. Determine the circular pitch, helix angle, and pitch diameter of the gear.

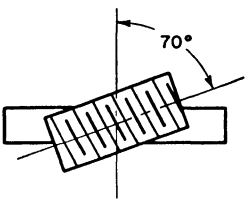

Fig. P 9.22

9.23. A pair of bevel gears have 20 and 40 teeth. The diametral pitch is 5 and the axes are 90°. The addendum and dedendum are the same as for 20° involute stub teeth. Determine the following for the gear: (a) pitch angle, (b) face angle, (c) root angle, (d) pitch diameter, (e) outside diameter, (f) cone distance, (g) formative radius, (h) formative number of teeth.

9.24. Same as Prob. 9.23, except gears have 20 and 60 teeth and the diametral pitch is 4.

CHAPTER 10

Flexible Connectors

10.1. Introductory. Belts, chains, and ropes are common members of this class of links. Some of these can be used in three-dimensional drives. They are usually used in tension, although there is one notable exception, the use of flexible cables in torsion.

There are two types of flexible connectors:

1. Connectors that obtain their flexibility from distortion of the material; for example, belts, ropes, and thin steel bands. Motion is usually transmitted by means of friction.

2. Connectors made from small rigid parts that are joined in such a manner as to permit relative motion of the parts; for example, chains. Motion is usually transmitted by positive means.

They can also be classified according to use in three major groups:

1. Hoisting
2. Conveyors
3. Power transmission

10.2. Flat belts. The replacement of central power sources in shops with individual motor drives has reduced the use of flat belts. These belts still have a place in power transmission, especially for large center distances.

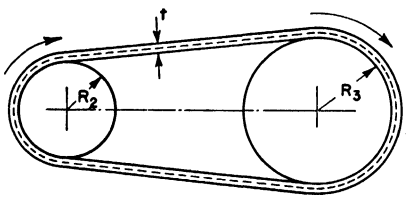

Fig. 10.1

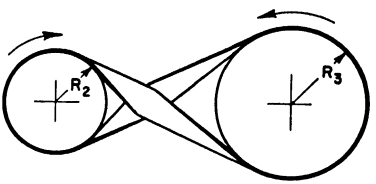

Fig. 10.2

Belt drives can be either of the open or crossed type, Figs. 10.1 and 10.2. The pulleys of an open belt drive rotate in the same direction, and pulleys of the crossed belt drive rotate in opposite directions. When a belt is bent around a pulley the outer fibers are in tension and the inner

fibers in compression. The neutral axis is approximately at the center. The angular velocity ratio of the pulleys is (Art. 2.12)

$$\frac{\omega_2}{\omega_3} = \frac{R_3 + t/2}{R_2 + t/2} \cong \frac{R_3}{R_2} \tag{10.1}$$

Since the belt thickness is small in comparison with the pulley radius it is usually neglected.

In order to design and specify a belt drive it is necessary to determine the angles of contact and the belt length. These can be found as follows:

Open belt (Fig. 10.3)

$$\phi = \frac{1}{57.2} \sin^{-1} \frac{R_3 - R_2}{C}, \quad K = C \cos \phi, \quad \begin{matrix} \theta_2 = \pi - 2\phi \\ \theta_3 = \pi + 2\phi \end{matrix}$$

where ϕ and θ are in radians.

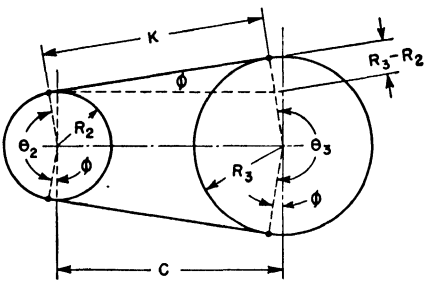

Fig. 10.3

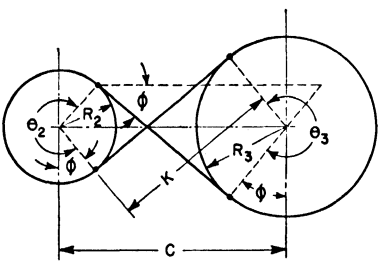

Fig. 10.4

The length of the belt is the sum of the two arcs of contact and $2K$.

$$\text{length} = \theta_2 R_2 + \theta_3 R_3 + 2C \cos \phi \tag{10.2}$$

Crossed belt (Fig. 10.4)

$$\phi = \frac{1}{57.2} \sin^{-1} \frac{R_3 + R_2}{C}, \quad K = C \cos \phi, \quad \theta_2 = \theta_3 = \pi + 2\phi$$

$$\text{length} = \theta_2(R_2 + R_3) + 2C \cos \phi \tag{10.3}$$

Like all friction drives the transmission of motion is not positive. In addition to slipping as it is usually thought of there is another type called creep. The belt on the tight side stretches more than on the loose side. An element of belt becomes shorter as it passes around the driver from the tight to the loose side and becomes longer when it passes around the follower from the loose to the tight side. This is always present and causes the follower to turn at a lower speed. In an average drive the combined slip and creep is 2 to 4 per cent of the ideal speed.

A flat belt will work off a pulley during operation unless means are taken to keep it centered. The most common method is to crown one or both pulleys. The surface of a crowned pulley (Fig. 10.5) consists of the frustra of two cones with their common base at the center. A belt when placed on one side of a crowned pulley and subjected to tension will take the form shown. When the pulley is rotated one-quarter turn the

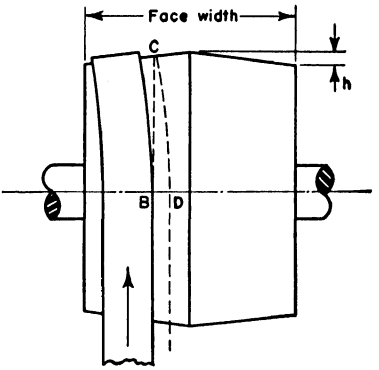

Fig. 10.5

friction between the belt and pulley will move point B on the belt to C. The edge of the belt will lie along line CD. Further rotation will carry the belt to the center of the pulley. If the belt on a moving pulley is forced to one side and then released, it will very quickly climb to the center. The crowning, indicated as h, is usually $\frac{1}{8}$ to $\frac{1}{4}$ in. per foot of width of the pulley face.

10.3. Flat belts connecting nonparallel shafts. The law of belting requires that the center line of the belt on the side approaching the pulley must lie in the plane of the pulley. A quarter-turn belt is shown in Fig. 10.6. For the directions of rotation shown, the law of belting is fulfilled. If the directions are reversed, the belt will not stay on the pulleys. If a quarter turn belt is to operate in either direction

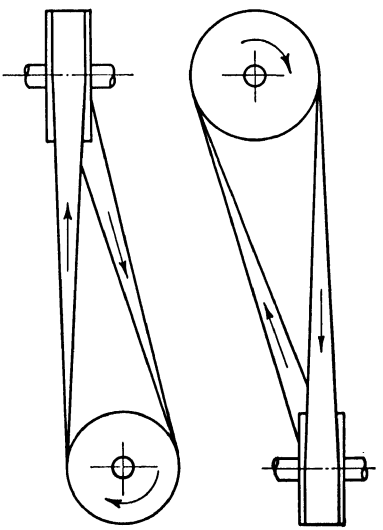

Fig. 10.6

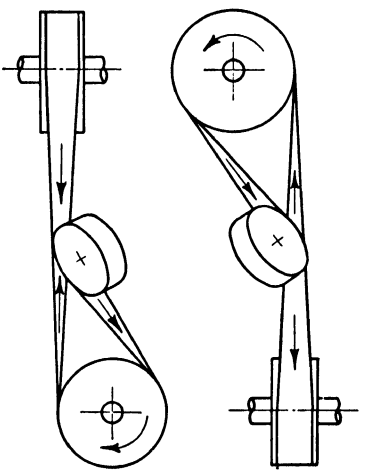

Fig. 10.7

(Fig. 10.7), a guide pulley must be used. This pulley must be properly placed so that the law will be fulfilled for either direction of rotation.

Any two pulleys in space can be connected with a flat belt if a sufficient number of properly spaced guide pulleys are used.

10.4. V-Belts. The cross section of a V-belt is trapezoidal. A typical section is shown in Fig. 10.8(a). In order to utilize the advantages of a V-belt the groove should be deep enough so that the belt does not bottom in the groove. This produces a wedging action and the belt will transmit power with very little initial tension. This permits the use of short center distances, and frequent adjustments are not required.

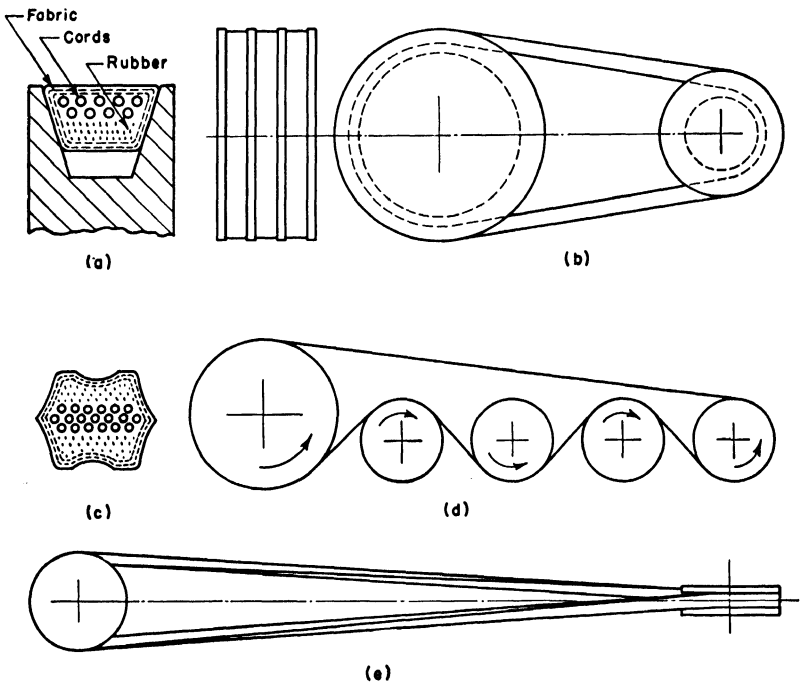

Fig. 10.8

V-belts are usually made endless, the several components being vulcanized in a mold. If one belt will not transmit the power, two or more can be used in parallel. When it is necessary to replace one belt the entire set should be replaced. A new belt when used with worn belts will carry more than its share of the load.

If both sides of a belt are to be used for driving, the type shown at (c) should be used.

A V-belt can be used on a quarter-turn drive [Fig. 10.8(e)] if the speed ratio is not greater than 2.4:1 and the center distance is 6 to $6\frac{1}{2}$ times the diameter of the larger pulley.

10.5. Roller chains are used principally for power transmission. A section of chain is shown in Fig. 10.9. The pin is fastened to the outer set of links so that it does not rotate relative to them. The bushing is fastened to the inner links. This insures that the only sliding in the joint will be that due to the pin turning in the bushing. The area of contact is large and the wear is slight. The hardened steel roller is free to turn on the bushing.

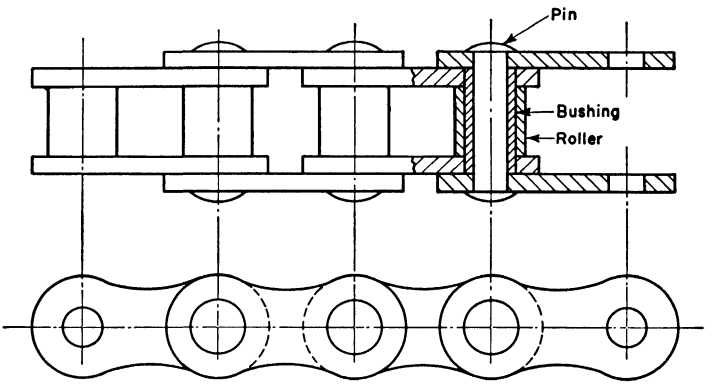

Fig. 10.9

If a single-strand chain does not have the required capacity, a multiple-strand chain can be used. These are equivalent to two or more single strands placed side by side, with long pins passing through the entire width of the chain.

The seating of a roller chain on a sprocket is shown in Fig. 10.10. When the chain is new the rollers seat at the bottom of the tooth spaces. As the chain wears the pitch becomes longer. The tooth profiles are made so that the force of the sprocket on the roller has a component

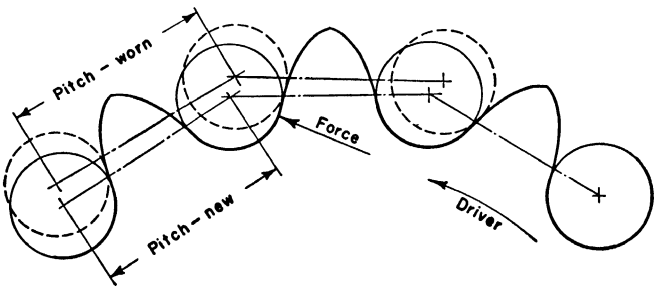

Fig. 10.10

radially outward. This force causes a worn chain to take a position on the sprocket teeth that corresponds to the worn pitch. This distributes the load among all the teeth that are in contact with the chain.

Roller chains can be used for drives similar to that in Fig. 10.8(d).

10.6. Impact loading. It was shown in the chapter on gearing that theoretically correct gear teeth come into contact without impact. Because of inaccuracies in machining and deflections there is always some impact. This can be reduced by using gears made with a high degree of accuracy. In roller chains, impact loading is inherent in the design. The impact velocity between a chain roller and a sprocket can be determined using Fig. 10.11. When the sprocket turns with uniform angular velocity through angle θ, link BC rotates relative to the sprocket through angle θ with velocity ω and strikes the sprocket. This can be seen if inversion is considered. The sprocket is fixed and the chain is wrapped around it with angular velocity ω. The impact velocity is the velocity of B along the arc BD. It is

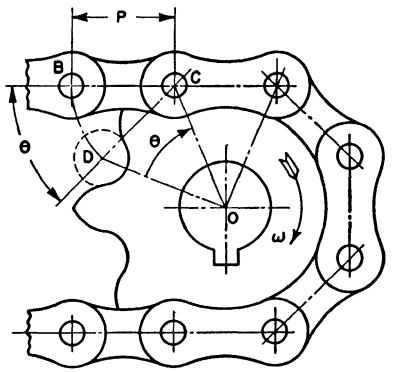

Fig. 10.11

$$V = R\omega = \frac{P}{12}\omega = \frac{\pi PN}{6} \text{ fps}$$

where P is the pitch in inches and N is the speed of the sprocket in revolutions per second. The presence of impact loading is one reason why chains with large pitches cannot be operated at high speeds.

10.7. Chordal action. In general the sprockets of a chain drive do not have a constant angular velocity ratio, and the linear velocity of the chain is not constant. This is because the chain does not wrap around the sprocket in the form of a pitch circle, but in the form of a pitch polygon. It was shown in the previous article that this also produced impact loading.

Two 6-tooth sprockets and a chain are shown in Fig. 10.12. For a constant ω the linear velocity of the chain for the phase shown with solid lines is $V = R\omega$ and for the phase shown with broken lines is $V = R\omega \cos 30°$. The centerline of the chain on the driving side remains

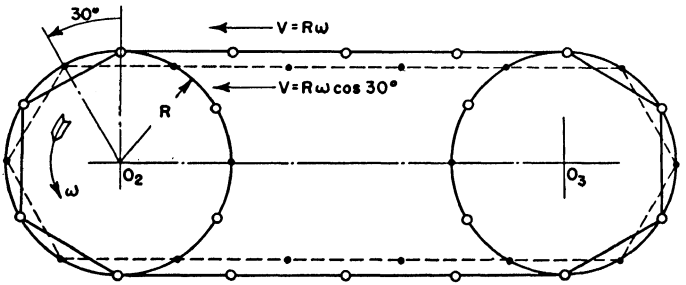

Fig. 10.12

parallel to the line of the centers for all phases, and the angular velocity ratio of the two sprockets is constant.

Chordal action is more pronounced with sprockets having a small number of teeth. The per cent variation in chain velocity, $C \div R$, for sprockets having different numbers of teeth is shown in Fig. 10.13.

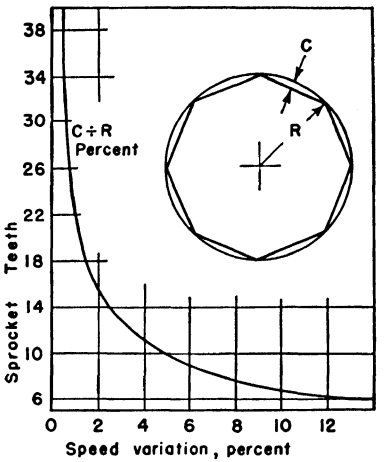

Fig. 10.13

When it is necessary to use small sprockets those with an odd number of teeth are usually selected. When the chain velocity is increasing on one side it is decreasing on the other. The inertia forces on the two sides tend to balance each other.

Unequal sprockets are shown in Fig. 10.14. In addition to a variable chain velocity the angular velocity ratio of the sprockets is not constant.

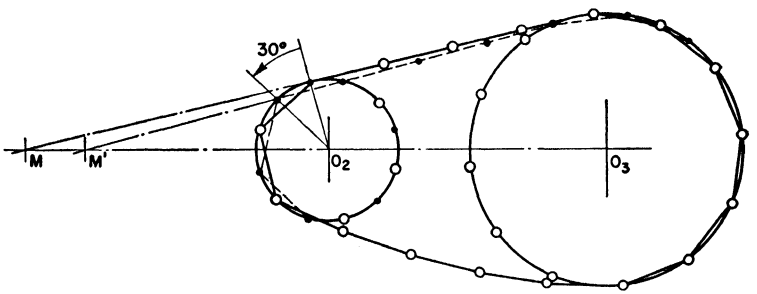

Fig. 10.14

The line of transmission cuts the line of center at different points. Two locations, M and M', are shown.

10.8. Silent or inverted tooth chains are used for power transmission. A Morse Hy-Vo silent chain drive is shown in Fig. 10.15 and

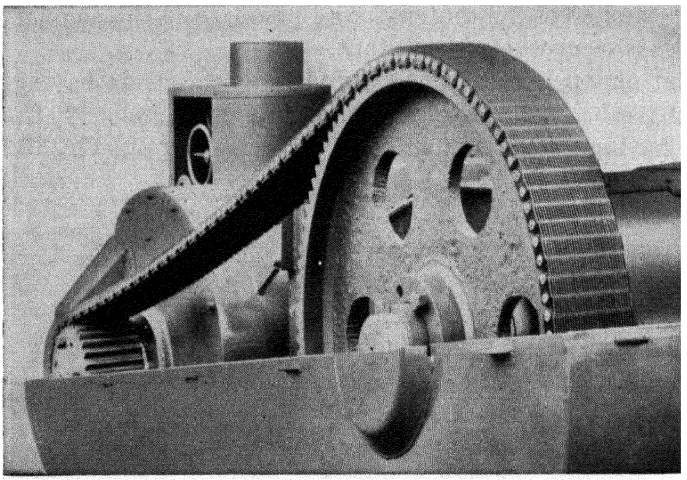

Fig. 10.15. (Courtesy of Morse Chain Co.)

a conventional Morse silent chain and sprocket is shown in Fig. 10.16. A rocker joint consisting of two parts A and B is used. Each part is

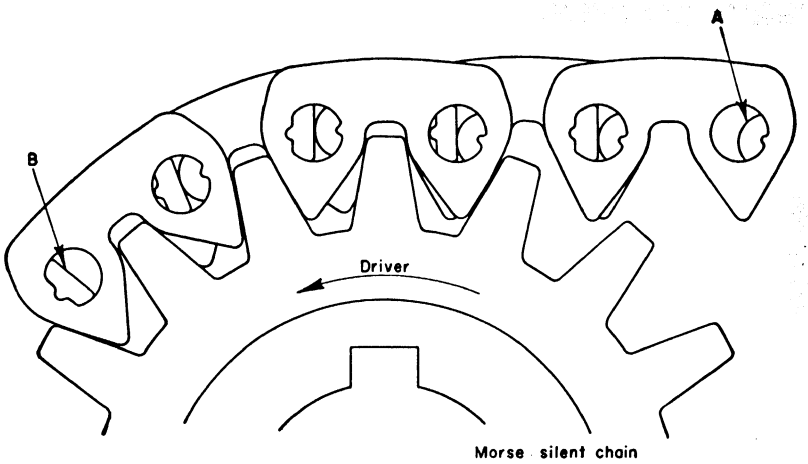

Fig. 10.16

fixed relative to one set of links. When a joint is flexed there is approximate rolling of A on B. The joint of a Link Belt chain is shown in Fig. 10.17. Two partial bushings and a cylindrical pin are used. One bushing is fixed relative to one set of links and the other bushing is fixed relative to the other set of links. When a joint is flexed the only sliding that occurs is between the bushings and the pin. Compared with a pin only, this arrangement nearly doubles the area of contact and provides a single area that facilitates lubrication.

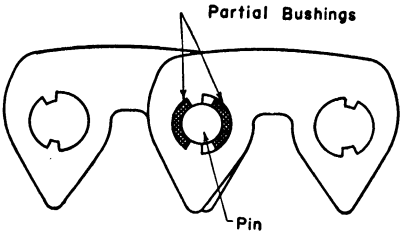

Fig. 10.17

In many silent chain drives chordal action is present. In some designs it has been practically eliminated. One such chain is made by the Link Belt Company, Fig. 10.18. The chain profiles are curved to produce

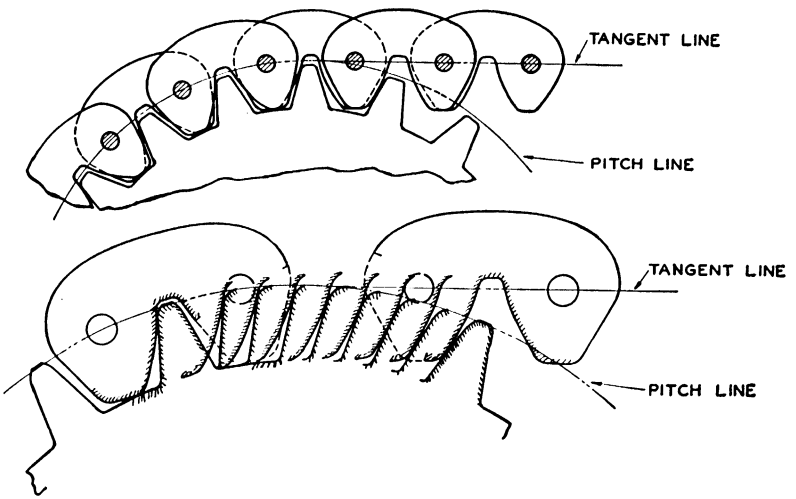

Fig. 10.18. (Courtesy of Link-Belt Co.)

gradual seating and to hold the tangent line in a fixed position. A series of positions are shown to illustrate the seating of a link. The determination of these contours is somewhat analogous to designing a conjugate rack and pinion. Another type that has very little chordal action is the Morse Hy-Vo. In this drive the chain profiles are straight and the sprocket teeth are involute. A comparison of a roller chain (top) and a Hy-Vo chain (bottom) is shown in Fig. 10.19. Both chains are 2 in. pitch and are operating at a speed of 3600 fpm.

10.9. Bead chains. A three-dimensional bead chain drive is shown in Fig. 10.20. The beads in these chains range in size from $\frac{3}{32}$ to $\frac{3}{8}$ in. in diameter. The range of tensile strength is from 18 to 185 pounds. They are used in applications where a positive drive is desired and the load is small, as for example, in business machines. These drives are inexpensive.

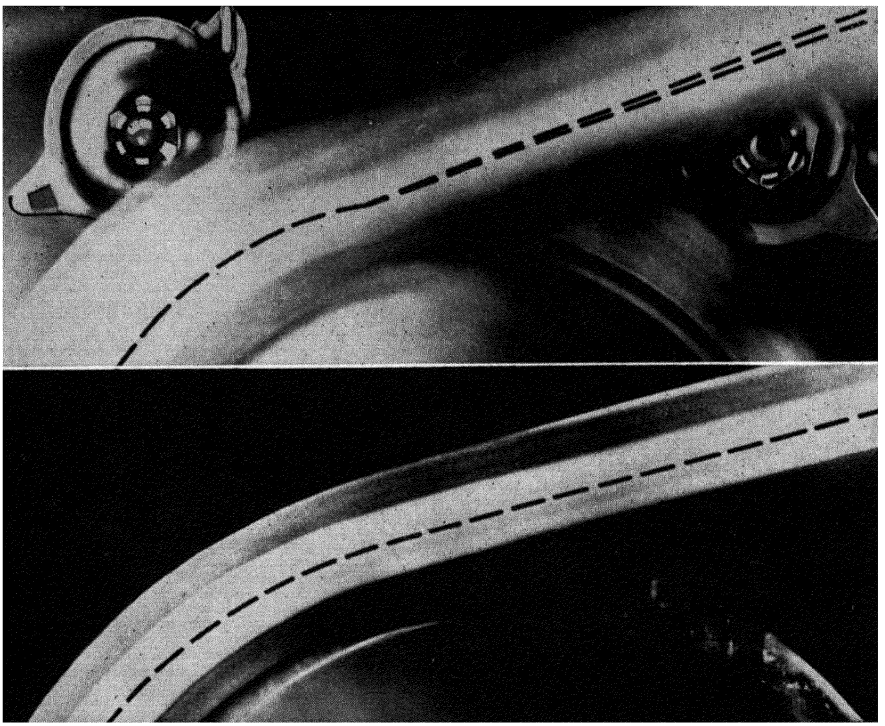

Fig. 10.19. (Courtesy of Morse Chain Co.)

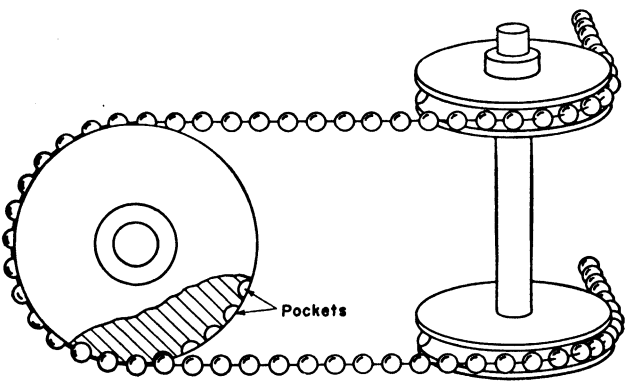

Fig. 10.20

10.10. Conveyor chains. There are many types of conveyor chains, two of which are shown in Fig. 10.21. The Ewart detachable link chain is shown at (b); one link is shown in a partially assembled position. These links are malleable castings. The Ewart link at (a) is made from strip steel. It is one of the many types of attachment links. A pintle chain is shown at (c).

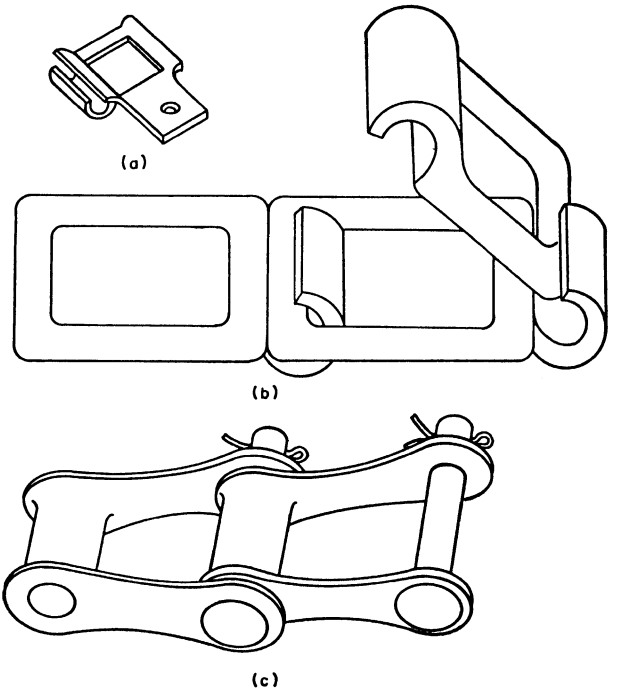

Fig. 10.21

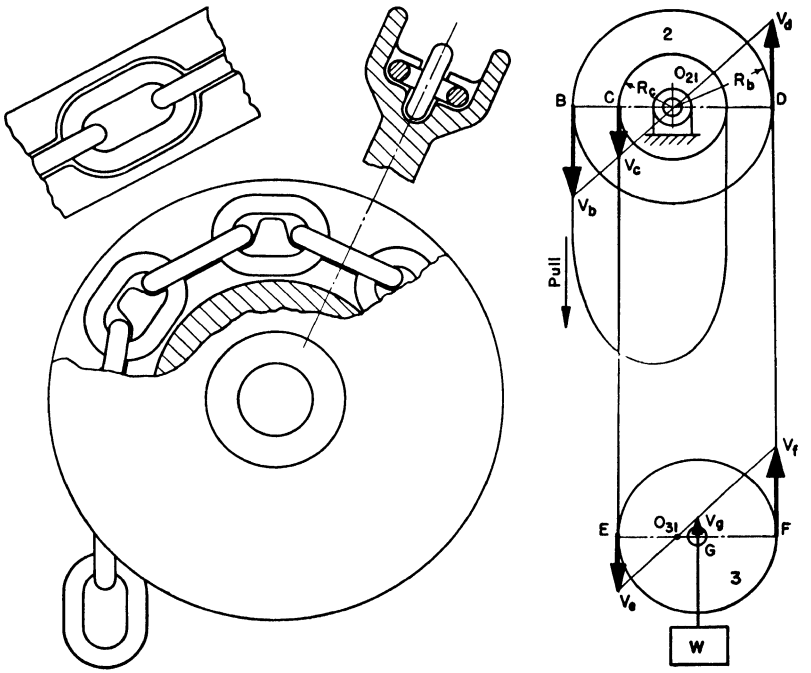

Fig. 10.22

10.11. Differential chain hoist. A differential hoist using coil chain is shown in Fig. 10.22. The manner in which the links engage the sprocket is shown at the left. A load W is raised by pulling on the chain indicated. The two sprockets at the top are fastened together and form a compound sprocket. The circumference of the pitch polygon of the larger sprocket is N_BP, where N_B is the number of the pitches and P is the pitch. The circumference of the smaller sprocket is N_CP. When the compound sprocket is turned once, the chain that supports the lower pulley is shortened the amount $(N_B - N_C)P$. The movable pulley is supported by two chains; hence the lift is $\frac{1}{2}(N_B - N_C)P$. The mechanical advantage is

$$\text{M. A.} = \frac{N_BP}{\frac{1}{2}(N_B - N_C)P} = \frac{2}{(1 - N_C/N_B)}$$

The mechanical advantage can also be determined by the use of velocity vectors (Art. 4.4), where V_b is the assumed input velocity. Velocities V_c and V_d are determined and then transferred to E and F. Velocity V_g is the upward velocity of the weight. The mechanical advantage is V_b/V_g.

10.12. Variable-speed drives. One of the simplest types of variable speed drives is shown in Fig. 10.23. The sides of each pulley can be moved axially relative to each other. This produces variable-pitch

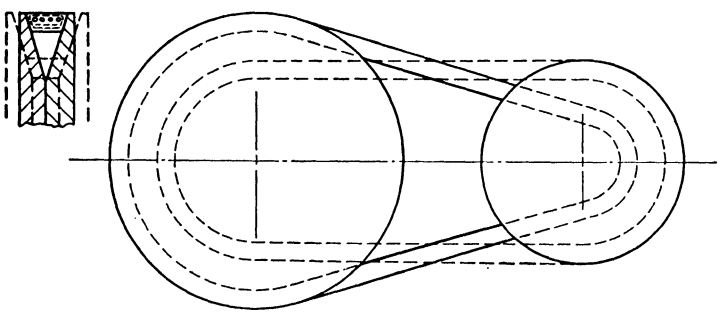

Fig. 10.23

pulleys. Two positions for the belt are shown. V-belts that are standard except for their extra width are made for use in this type of drive. The extra width makes a wider speed range possible.

The Link Belt Company's P.I.V. (Positive Infinitely Variable) drive is shown in Fig. 10.24. The conical surfaces of the sprockets are fluted, the ridges on one side being opposite grooves on the other. Each link in the chain contains a stack of thin flat steel strips that are free to move perpendicularly to the length of the chain. As the chain engages the sprockets, the ridges on one side push strips into the grooves on the opposite side, making a positive drive. The hand wheel at the left

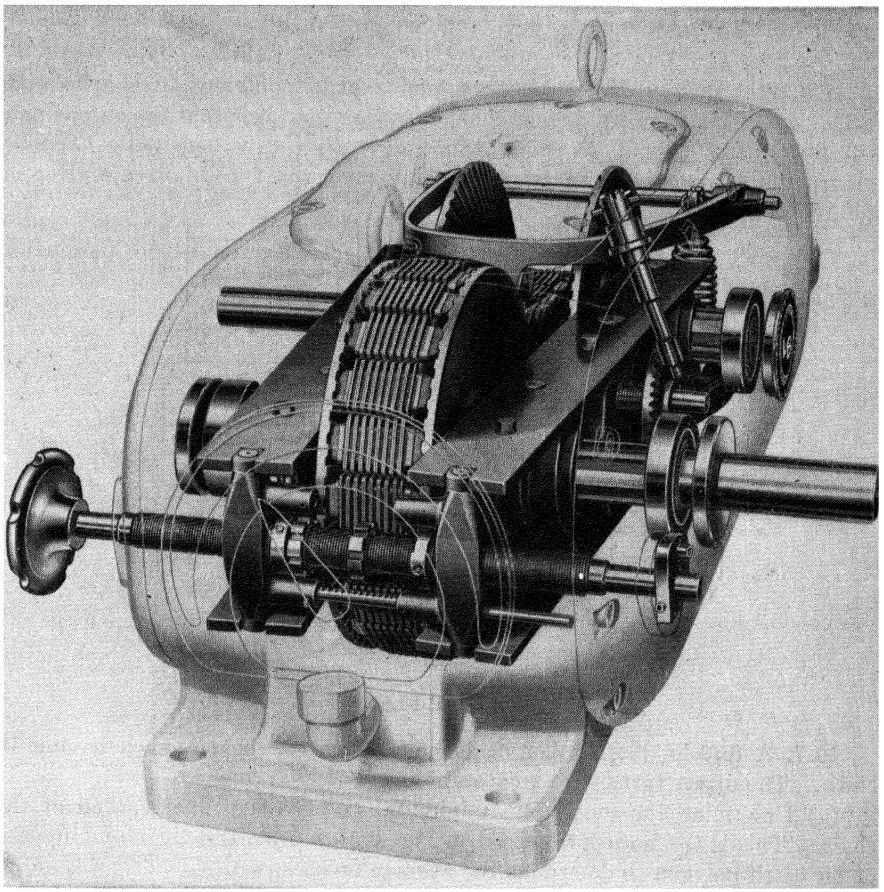

Fig. 10.24. (Courtesy of Link-Belt Co.)

controls the speed ratio. The sprocket halves are mounted in such a way that when one pair is moved closer together the other pair moves farther apart.

PROBLEMS

10.1. The diameter of the small pulley of an open belt drive is 10 in., the rpm is 900, and that of the large pulley is 300. The center distance is 8 ft. Neglect slip and creep. Determine: (a) diameter of the large pulley, (b) belt speed, (c) angles of belt contact on the two pulleys, (d) length of belt.

10.2. Same as Prob. 10.1, except rpm of large pulley is 250 and center distance is 6.5 ft.

10.3. Same as Prob. 10.1, except belt is crossed.

10.4. Same as Prob. 10.2, except belt is crossed.

10.5. Same as Prob. 10.1, except the combined slip and creep is assumed to be 3%.

10.6. Step pulleys, Fig. P 10.6, are used to obtain different angular velocity ratios by shifting the belt. Show that a single crossed belt that fits on one pair will fit on any pair if $D_1 + d_1 = D_2 + d_2 = D_3 + d_3 = \text{constant}$. (This is not true for an open belt. A graphical solution for this type of drive is given in the Marks *Handbook*.)

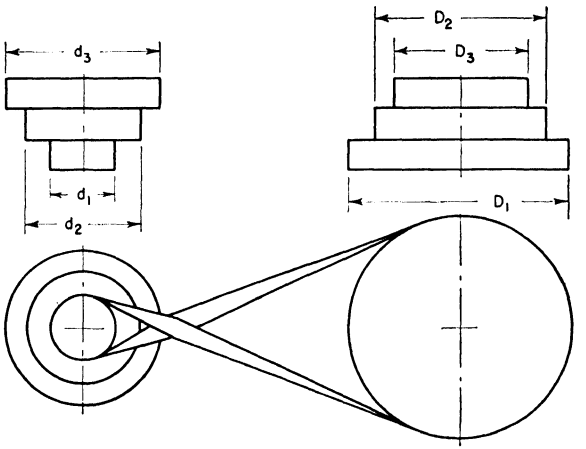

Fig. P 10.6

10.7. A 0.75-in. pitch roller chain engages two sprockets, each having 10 teeth. The driver turns with a constant speed of 1200 rpm.

(a) Determine the maximum, minimum, and average linear speed of the chain. This is the horizontal speed in Fig. P 10.7 (a). Use the circumference of the pitch polygon to determine the average linear speed.

(b) Determine the impact velocity between sprocket and chain.

(c) Show that the linear velocity-time curve consists of portions of sine curves as shown at (b). Determine the maximum horizontal acceleration of the chain. Determine a time interval t_1. Note that the chain also has vertical velocity and acceleration. Values can be determined in the same manner as above. If whip of the chain is neglected, the analysis can be made using the equivalent 4-bar linkage shown at (c).

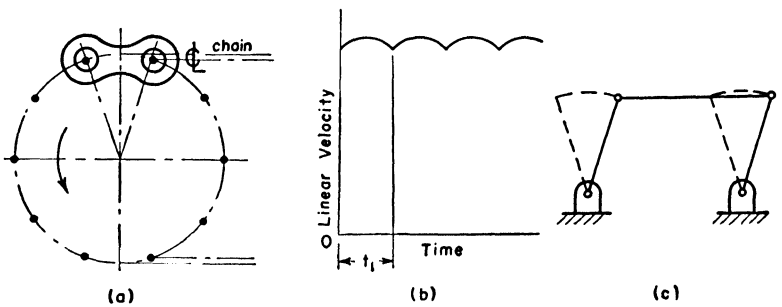

Fig. P 10.7

10.8. Same as Prob. 10.7, except pitch is 0.625 in., number of sprocket teeth is 9, rpm is 1400.

10.9. The compound sprocket of a differential chain hoist has 20 and 22 teeth. Assuming a pull on the hand chain of 150 lb and 100% efficiency, determine the weight that can be lifted.

10.10. The compound sprocket of a differential chain hoist has 15 and 16 teeth. The load to be lifted is 1800 lb and the efficiency is 100%. Determine the required pull on the hand chain.

CHAPTER 11

Gear Trains, Translation Screws

11.1. Definitions. Two or more gears form a gear train when they are used to transmit motion from one shaft to another. Belts, chains, and screws are often used in conjunction with gear trains and are considered a part of the train. There are two types of gear trains, ordinary and epicyclic. The axes of all gears of an ordinary gear train are fixed relative to the frame. In the epicyclic train the axis of at least one gear moves in the path of a circle.

The angular velocity ratio of any pair of meshing gears is always inversely as the numbers of teeth. In general, when there is sliding along the tooth elements as in worm, helical, and hypoid gears, the angular velocities are not inversely as the diameters. If gears having parallel axes rotate in the same direction, the ratio is positive, if in opposite directions, it is negative.

11.2. Ordinary gear trains are of two types, simple and compound. In a simple train, Fig. 11.1, there is only one gear on each axis. Gear A

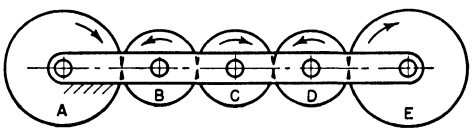

Fig. 11.1

drives B, B drives C, C drives D, and D drives E. The pitch line velocities of all gears are the same. The angular velocity ratio of A to E is inversely as the numbers of teeth on A and E. Gears B, C, and D are called idler gears. They are used for two purposes: to control the directional relationship of A and E and to make possible a large center distance without the use of large gears. A train similar to Fig. 11.1 has been used in opposed-piston Diesels for connecting the two crankshafts. The easiest way to keep track of directions is to draw directional arrows on the gears.

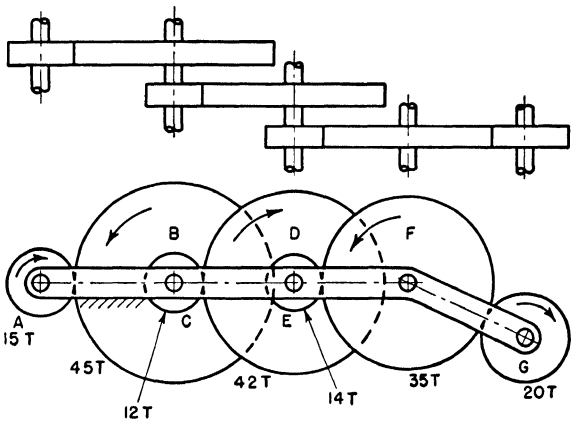

Fig. 11.2

A compound train has one or more shafts with two gears (Fig. 11.2). If the speed of A is 1200 rpm CW, the speeds of the other shafts will be

$$\omega_B = 1200 \times \tfrac{15}{45} = 400 \text{ rpm CCW}$$
$$\omega_D = 400 \times \tfrac{12}{42} = 114 \text{ rpm CW}$$
$$\omega_F = 114 \times \tfrac{14}{35} = 45.6 \text{ rpm CCW}$$
$$\omega_G = 45.6 \times \tfrac{35}{20} = 80 \text{ rpm CW}$$

The train value is the ratio of the speeds of the first and last shafts. In this case it is

$$e = \frac{-1200}{-80} = +15$$

The train value can be found from the products of the ratios of all pairs of gears. It is

$$e = \frac{\text{product of numbers of teeth on driven gears}}{\text{product of numbers of teeth on driving gears}}$$
$$= (\tfrac{45}{15})(\tfrac{42}{12})(\tfrac{35}{14})(\tfrac{20}{35}) = +15$$

The idler F serves as both a driver and driven gear. Its only effect on the train value is on the sign.

11.3. Automobile transmission. A typical three-speed transmission is shown in Fig. 11.3. When the input and output shafts are coaxial, as is the case here, the train is called a reverted train. Gear A turns with the engine shaft. Gears B, C, E, and G are made in one unit or are rigidly fastened to the countershaft. Gear H is an idler that meshes with G. These gears are always in motion when the shaft to engine is in motion. Gears D and F can slide axially on the spline shaft to rear wheels. The transmission is shown in neutral, so that there is no connection between the shaft to engine and shaft to rear wheels.

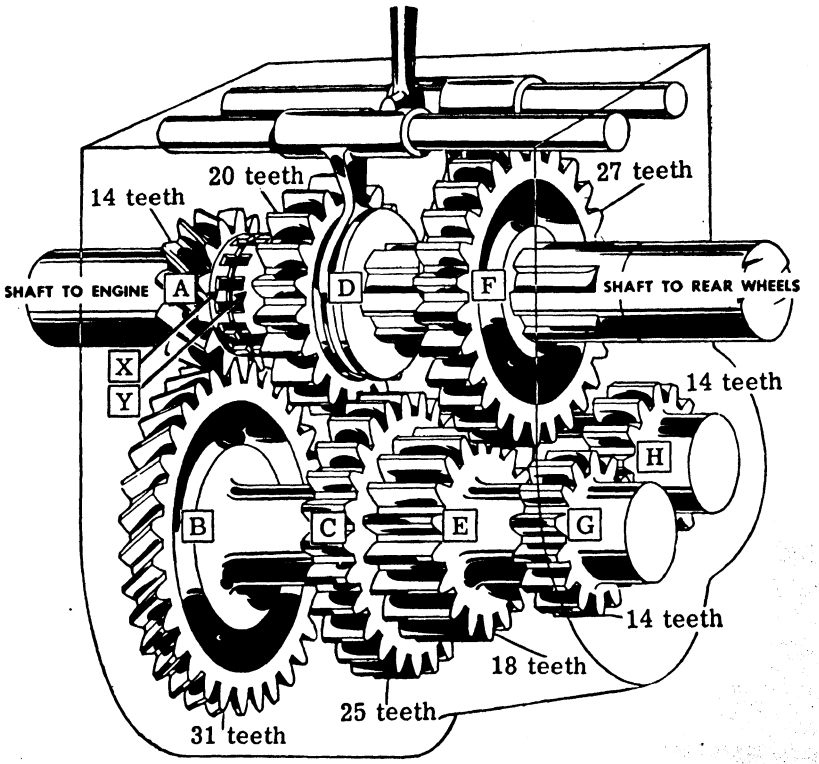

Fig. 11.3. (Courtesy of General Motors Corp.)

For low or first speed, F is shifted to the left and meshes with E. The train value of $ABEF$ is

$$e = \tfrac{31}{14} \times \tfrac{27}{18} = 3.32$$

For second or intermediate speed, D is shifted to the right and meshes with C. The train value of $ABCD$ is

$$e = \tfrac{31}{14} \times \tfrac{20}{25} = 1.77$$

Gear A is made with a jaw clutch face X and D with clutch face Y. For high or third speed D is shifted to the left, engaging X and Y. This gives a direct drive with velocity ratio of 1.

For reverse F is shifted to the right and engages with idler H. The ratio of the drive through $ABGHF$ is

$$\tfrac{31}{14} \times \tfrac{14}{14} \times \tfrac{27}{14} = -4.27$$

11.4. Epicyclic gear trains are also called planetary gear trains. The gear at the center is called the sun, and the gears that have moving axes are called planets. A few words about the movement of the earth will help in understanding epicyclic gear trains. The earth turns on its axis $366\frac{1}{4}$ times in one year. A sidereal day has 23 hours, 56 minutes,

4.09 seconds of mean solar time. An astronomer when tracking a star in space must set his telescope to rotate at the rate of one revolution per sidereal day. When tracking the sun he sets it to rotate at one revolution in a solar day or 24 hours.

If the earth had no rotation about its own axis relative to the universe but still moved around the sun in the manner of a ferris wheel car, there would be one day in a year. This is shown in Fig. 11.4. Here O is an

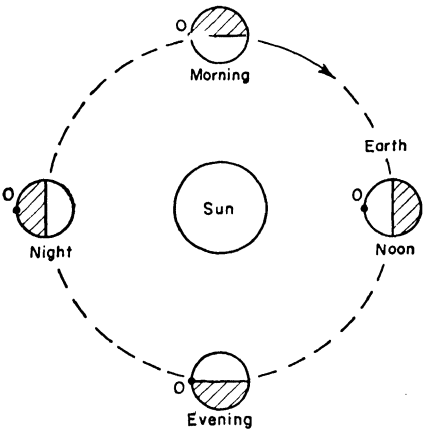

Fig. 11.4

observer on the earth. If the earth turned on its axis in the opposite direction or went around the sun in the opposite direction there would be $367\frac{1}{4}$ days in a year instead of $365\frac{1}{4}$. The absolute rotation would still be $366\frac{1}{4}$ turns a year. The principle of relative motion that is involved here appears in the calculations of every epicyclic gear train.

In Fig. 11.5(a) gear C is attached to an arm. If the gear does not turn relative to the arm and the arm is turned one revolution, the gear will also turn once in the same direction, *i.e.*, the gear makes one absolute

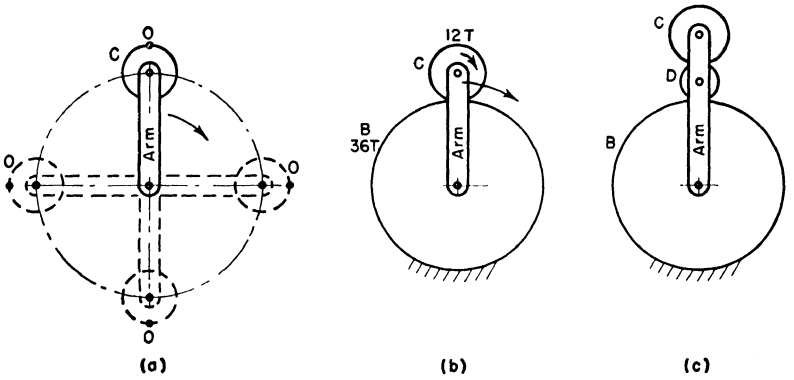

Fig. 11.5

turn. At (b) gear C of 12 teeth meshes with the fixed gear B of 36 teeth. Gear C is free to turn relative to the arm. If the arm is rotated once in a negative (CW) direction, C will roll on the outside of B and make $\frac{36}{12} = 3$ turns relative to the arm in a CW direction. But the arm has also made one CW turn. Hence the absolute turns of C is $-3 - 1 = -4$. At (c) an idler gear D is placed between B and C. When the arm is rotated once CW, gear C makes 3 CCW turns relative to the arm. The absolute turns of C is then

$$+3 - 1 = +2$$

It is possible to solve epicyclic gear train problems step by step using this type of reasoning. Most problems become so involved that it is almost impossible to prevent errors. It is desirable to develop a simple general method that can be applied in all cases. Equation (11.1) expresses a relationship that is easy to apply.

$$e = \frac{n_f - a}{n_l - a} \tag{11.1}$$

where n_f = number of absolute turns of the first gear in the train
n_l = number of absolute turns of the last gear in the train
a = number of absolute turns of the arm
e = train value relative to the arm

It was shown in Art. 2.7 that the motion of one body relative to a second body is the vector difference of their absolute motions. In this case the turns of the first gear in the train relative to the arm is the absolute turns of the gear minus the absolute turns of the arm, $n_f - a$. Likewise the turns of the last gear in the train relative to the arm is $n_l - a$. The ratio of the turns of the first and last gears in the train relative to the arm is the train value e relative to the arm. The motions of all parts of the train are correctly related in this equation. Any one of the terms can be the unknown. The use of this equation will be illustrated with several examples.

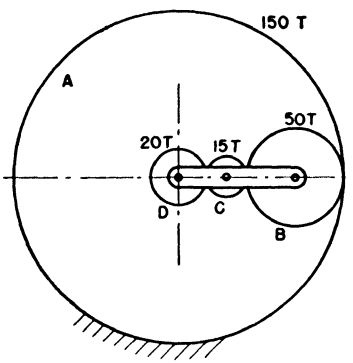

Fig. 11.6

Example 1. The arm of the train shown in Fig. 11.6 turns once in a positive direction. It is desired to find the number of turns made by gear D. Using Eq. (11.1),

$$e = \left(\frac{N_l \cdot \cdot \cdot \cdot \cdot \cdot \cdot \cdot}{\cdot \cdot \cdot \cdot \cdot \cdot \cdot \cdot N_f}\right) = \frac{n_f - a}{n_l - a}$$

the train value is determined from the numbers of teeth on the gears, N_l, N_f, ... The gear on either end can be considered the first. In this example let D be the first and the fixed internal gear A the last; then

$$e = \frac{150}{50} \times \frac{50}{15} \times \frac{15}{20} = +7\tfrac{1}{2} = \frac{n_f - (+1)}{0 - (+1)}$$

$$n_f = -6\tfrac{1}{2}$$

The arm and gear D turn in opposite directions.

Example 2. A reverted train is shown in Fig. 11.7. It is desired to find the number of turns that the arm makes when A turns once. Let the fixed gear D be the first, and A be the last gear. Then from Eq. (11.1),

$$\frac{101}{100} \times \frac{101}{100} = +1.021 = \frac{0 - a}{1 - a}$$

$$a = +50.7$$

The arm and gear A turn in the same direction.

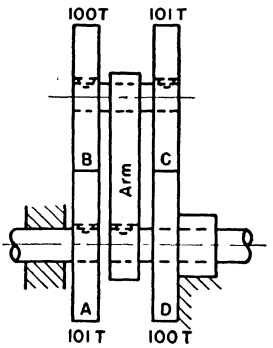

Fig. 11.7

11.5. Tabular method. Another method of solving epicyclic gear trains is to break the motions of all elements into a sequence of two absolute motions. In Example 1 (Fig. 11.6) the arm was rotated once in a positive direction. This produced definite angular displacements of B, C, and D. These same displacements can be made as follows. Lock the train so that the parts can have no relative motion and rotate it one positive turn. The arm has now been displaced its proper amount but the gears have not. Gear A should have remained fixed. This is taken care of by holding the arm fixed and rotating A one negative turn. This brings it back to its original fixed position. The rotation of A rotates B, C, and D so that they arrive at their proper displacements.

Example 3. Example 1 will be worked by this method. It is convenient to use a table similar to the one shown below.

Member	Arm	*A*	*B*	*C*	*D*
Train locked and given one positive turn	+1	+1	+1	+1	+1
Arm fixed, *A* given one negative turn	0	−1	$-\frac{150}{50}$	$+\frac{150}{50} \times \frac{50}{15}$	$-\frac{150}{50} \times \frac{50}{15} \times \frac{15}{20}$
Resultant turns	+1	0	−2	+11	$-6\frac{1}{2}$

Example 4. Example 2, Fig. 11.7, will be worked by this method.

Member	Arm	*A*	*B*	*C*	*D*
Train locked and given one positive turn	+1	+1	+1	+1	+1
Arm fixed, *D* given one negative turn	0	$-\frac{100}{101} \times \frac{100}{101}$	$+\frac{100}{101}$	$+\frac{100}{101}$	−1
Resultant turns	+1	+0.0197	1.99	1.99	0

The ratio of the turns of the arm to gear *A* is

$$\frac{1}{0.0197} = 50.7$$

11.6. Epicyclic trains having no fixed gear

Example 5. An example of this type of train is shown in Fig. 11.8. The speed of the shaft carrying *A* and *B* is +300 rpm. The speed of gear *J* is wanted.

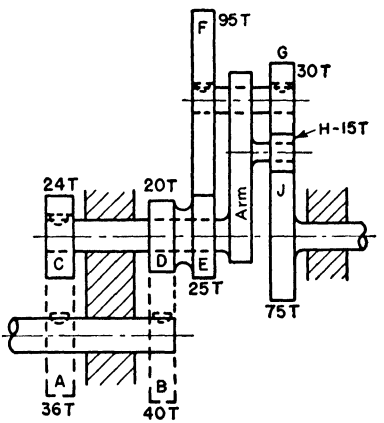

Fig. 11.8

The speed of gear *C* and the arm is

$$+300 \times (-\tfrac{36}{24}) = -450 \quad \text{rpm}$$

The speed of gears *D* and *E* is

$$+300 \times (-\tfrac{40}{20}) = -600 \quad \text{rpm}$$

Gears A and B are drawn with broken lines since they are not part of the epicyclic train. The basic train consists of $EFGHJ$ and the arm. Let E be the first gear and J the last. Then

$$\frac{75}{15} \times \frac{15}{30} \times \frac{95}{25} = -9.5 = \frac{-600 - (-450)}{n_J - (-450)}$$

$$n_J = -434.3 \text{ rpm}$$

11.7. Epicyclic drive for controllable-pitch propeller. This is shown in Figs. 11.9 and 11.10. Two trains are used, $ABCDE$ and

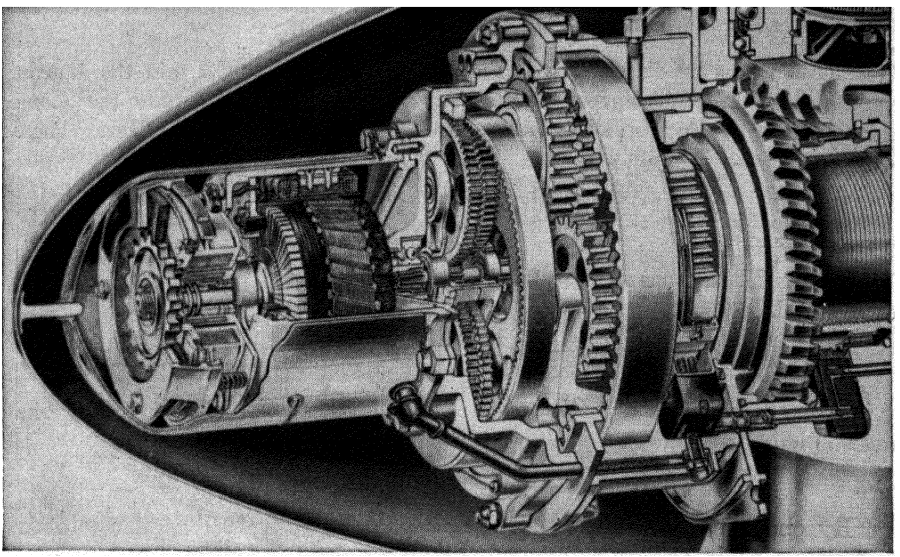

Fig. 11.9. (Courtesy of Curtiss Wright Corp.)

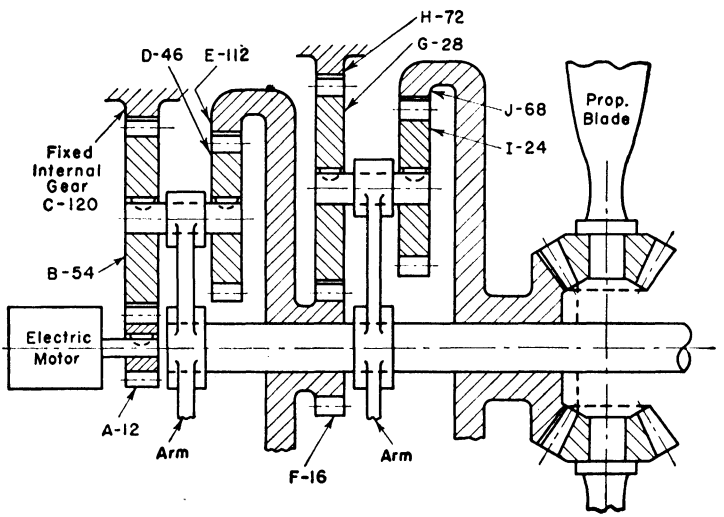

Fig. 11.10

FGHIJ. The total reduction ratio is the product of the reduction ratios of the individual trains. This will be worked as an example.

Example 6. Train *ABCDE* will be considered first. Neither the relationship between *A* and the arm nor between *E* and the arm is known. There are too many unknowns to work this in one step. Here *ABC* and the arm will be considered first to obtain a relationship between *A* and the arm. Let *A* be the first gear, *C* the last, and let the arm have one positive turn. Then

$$\frac{120}{54} \times \frac{54}{12} = -10 = \frac{n_a - 1}{0 - 1}$$

$$n_a = 11$$

Gear *C* can now be disregarded if this relationship between *A* and the arm is maintained. This is the type of problem treated in the previous example. Consider the train *ABDE* and the arm. Let *A* be the first and *E* the last. Then

$$\frac{112}{46} \times \frac{54}{12} = -10.956 = \frac{11 - 1}{n_e - 1}$$

$$n_e = 0.08725$$

When *A* turns 11 times *E* turns 0.08725 times in the same direction. The ratio of *A* to *E* is

$$\frac{11}{0.08725} = 126$$

In like manner the reduction ratio of train *FGHIJ* is found to be 59.5. The over-all reduction is then

$$\text{over-all reduction} = 126 \times 59.5 = 7497$$

By changing the numbers of teeth it is possible to design a similar reducer to fit in the same housing having a ratio of 188,400:1. This is equivalent to the reduction of a single pair of gears, the pinion being 1 in. in diameter and the gear diameter approximately 3 miles.

11.8. Epicyclic bevel-gear trains. A compound train is shown in Fig. 11.11. This train can be analyzed in the manner of the previous example. Here *A* turns +1200 rpm. The speed of *E* is desired. The

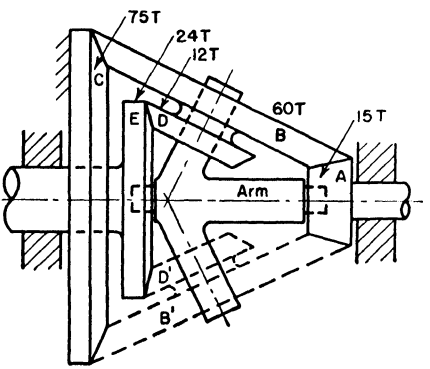

Fig. 11.11

train ABC and the arm are considered first to obtain a relationship between A and the arm. Let A be the first gear and C the last. Then

$$\frac{75}{60} \times \frac{60}{15} = -5 = \frac{1200 - a}{0 - a}$$

$$a = +200 \quad \text{rpm}$$

Next consider the train $ABDE$ and the arm. Let A be the first gear and E the last. Then

$$\frac{24}{12} \times \frac{60}{15} = -8 = \frac{1200 - 200}{n_E - 200}$$

$$n_E = +75 \quad \text{rpm}$$

Gears B' and D' are shown with broken lines. Kinematically they are not necessary but are usually included to maintain balance. Their use also distributes the tooth load among more gears, and the gears can be made smaller.

11.9. The automobile differential or epicyclic equalizing gear (Figs. 11.12 and 11.13) is used to prevent slipping of the wheels when

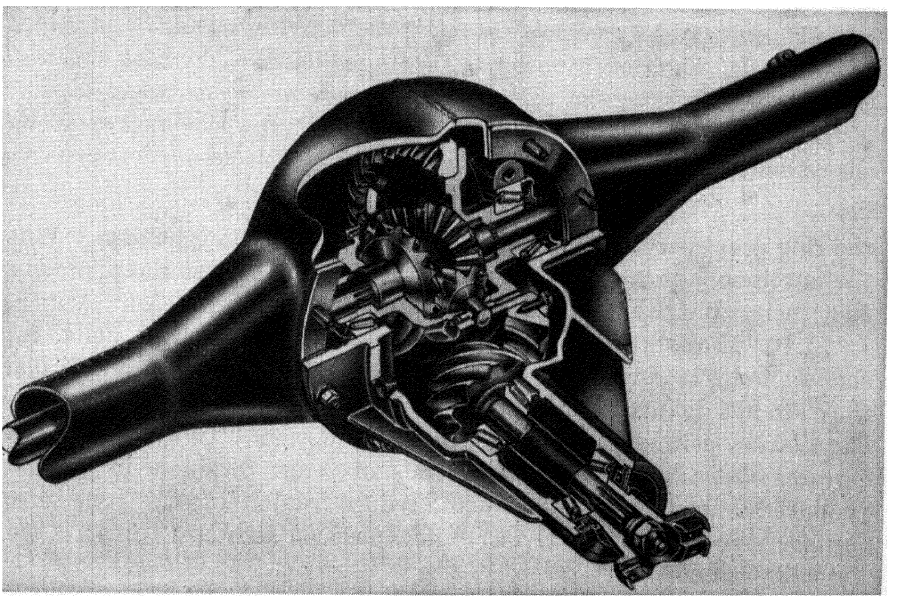

Fig. 11.12. (Courtesy of Ford Motor Co.)

the automobile moves in a curved path. It is necessary to permit the outside wheel to rotate faster than the inside wheel. In Fig. 11.13 the arm is attached to the ring gear. Gears A and C are the same size. Let the angular velocity of the ring gear and arm be k. Let A be the first gear, C the last, and N the number of teeth. Then

$$e = \frac{N_c}{N_b} \times \frac{N_b}{N_a} = -1 = \frac{n_A - k}{n_C - k}$$

giving $n_A + n_C = 2k$. When the automobile is traveling in a straight path, $n_A = n_C = k$. Here A, B, and C have no rotation relative to each other. If the left wheel is on dry pavement and the right wheel is on ice with insufficient friction to cause motion of the automobile, the left wheel will remain stationary and the right wheel will rotate at twice

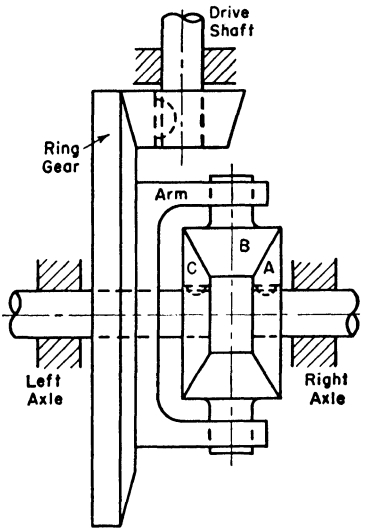

Fig. 11.13

the ring gear speed. This is a disadvantage of this mechanism. When the automobile moves in a curved path, A and C adjust their speeds so that there is no sliding. Their sum is always $2k$.

11.10. Translation screws. Screw fastenings such as bolts, capscrews, and setscrews are used for holding. When they are put in place they are not disturbed unless it is necessary to disassemble the machine. Translation screws are used to produce motion. The shapes of the threads often differ from the threads of screw fasteners in order to produce better wearing qualities and reduce friction losses. Four thread forms are shown in Fig. 11.14. The American standard thread is used for screw fasteners.

The lead and pitch of a screw have the same meaning as for worms (Fig. 9.43). Unless otherwise stated it is assumed that a screw is right-hand and single. A jack having a single right-hand thread with $\frac{1}{4}$ in. pitch is shown in Fig. 11.15. One clockwise turn of the handle when viewed from below will raise the load $\frac{1}{4}$ in. If the thread is triple, one turn of the handle will raise the load $\frac{3}{4}$ in. The base of the jack serves as a stationary nut.

A compound screw consists of two screws in series arranged so that the resultant motion produced is the sum of the individual motions.

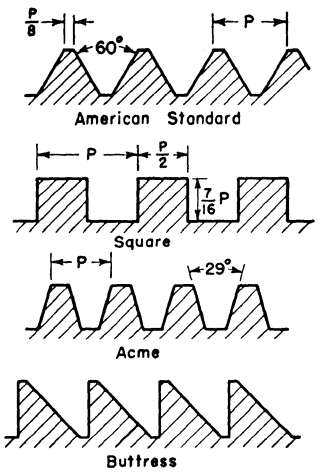

Fig. 11.14

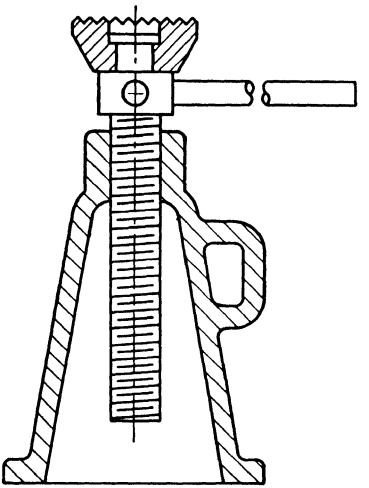

Fig. 11.15

In Fig. 11.16 the large screw has 6 threads per inch and the small screw 7 threads per inch. If the handle is turned once clockwise when viewed from the right, the screw moves $\frac{1}{6}$ inch to the left relative to the frame and block 3 moves $\frac{1}{7}$ inch to the left relative to the screw. The total movement of the block relative to the frame is $\frac{1}{7} + \frac{1}{6} = 0.31$ inch to the left.

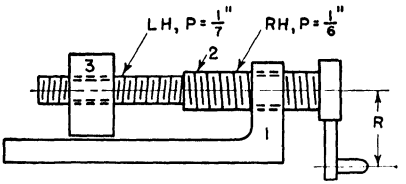

Fig. 11.16

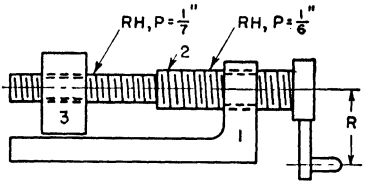

Fig. 11.17

A differential screw consists of two screws in series arranged so that the resultant motion produced is the difference of the individual motions. In Fig. 11.17 the handle is turned once clockwise when viewed from the right. The screw moves $\frac{1}{6}$ inch to the left relative to the frame. The block moves $\frac{1}{7}$ inch to the right relative to the screw. The resultant motion of the block relative to the frame is $\frac{1}{6} - \frac{1}{7} = 0.0238$ inch to the left.

PROBLEMS

11.1. Determine the speed and direction of rotation of gear G in the gear train shown in Fig. P 11.1.

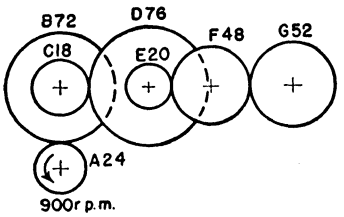

Fig. P 11.1

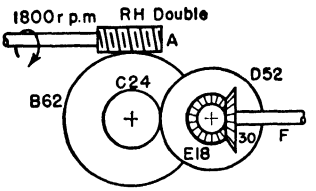

Fig. P 11.2

11.2. Determine the speed and direction of rotation of shaft F in the gear train shown in Fig. P 11.2.

11.3. Gear H in the train shown in Fig. P 11.3 is to rotate at approximately 14.3 rpm. Determine the number of teeth on gear H. Do H and A rotate in the same or opposite directions?

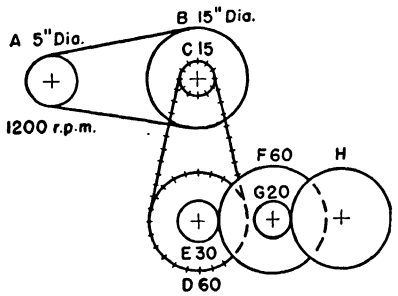

Fig. P 11.3

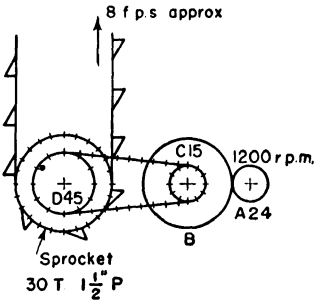

Fig. P 11.4

11.4. A conveyor belt, Fig. P 11.4, is to move with the velocity shown. Determine the number of teeth on gear B and the direction of rotation of gear A.

11.5. The train value of the reverted train shown in Fig. P 11.5 is to be 12. The diametral pitches of gears A and B is 8, and of gears C and D is 10. Determine suitable numbers of teeth for the gears. No gear is to have less than 24 teeth.

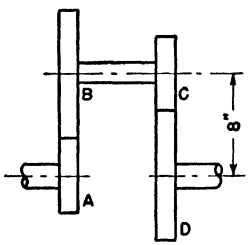

Fig. P 11.5

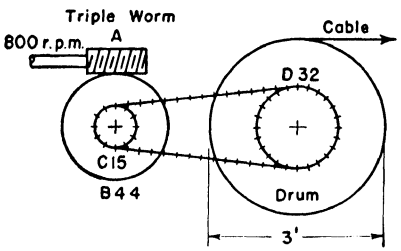

Fig. P 11.6

11.6. Determine the speed of the cable shown in Fig. P 11.6.

11.7. Determine the mechanical advantage of the cable-winding mechanism shown in Fig. P 11.7.

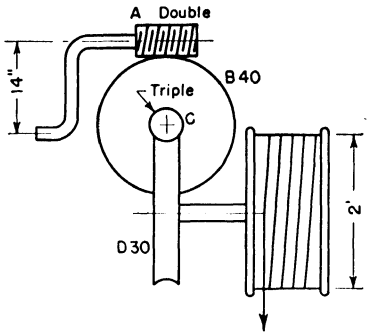

Fig. P 11.7

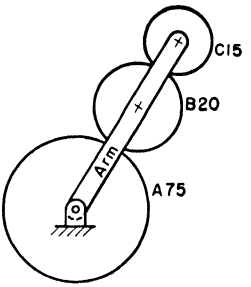

Fig. P 11.8

11.8. In Fig. P 11.8, gear A is fixed and the arm is turned 3 revolutions in a clockwise direction. Determine the number and direction of absolute turns of gear C.

11.9. In Fig. P 11.8, gear A turns 2 revolutions in a counterclockwise direction while the arm turns 4 revolutions in a clockwise direction. Determine the directions and absolute turns of gears B and C.

11.10. In Fig. P 11.10, gear A is fixed. The arm is turned once in a clockwise direction. Determine the number of absolute turns and directions of gears B, C, D, and E.

11.11. In Fig. P 11.10, gear B is fixed. The arm is turned once in a clockwise direction. Determine the number of absolute turns and directions of gears A, C, D, and E.

11.12. Determine the speed and direction of rotation of gear F in Fig. P 11.12.

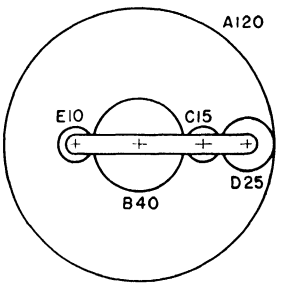

Fig. P 11.10

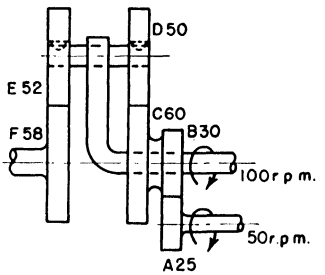

Fig. P 11.12

11.13. A ball bearing is shown in Fig. P 11.13. The inner race rotates with the shaft at 1000 rpm. Assume pure rolling between the rollers and races. Determine the speed of the roller cage.

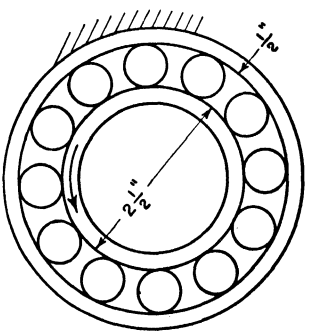

Fig. P 11.13

11.14. In Fig. P 11.14, the diameter of the hand-chain sprocket A is 14 in. and the diameter of the hoisting chain sprocket E is 5 in. Determine the mechanical advantage of the hoist.

11.15. Determine the speed and direction of rotation of gear E in Fig. P 11.15.

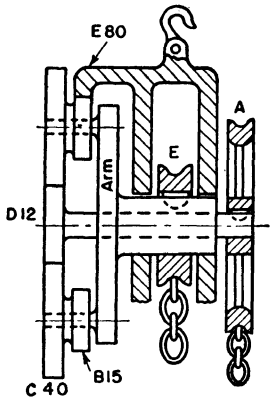

Fig. P 11.14

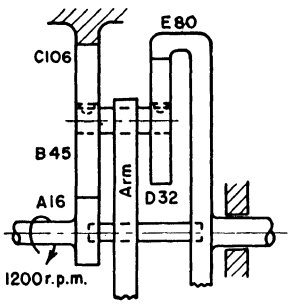

Fig. P 11.15

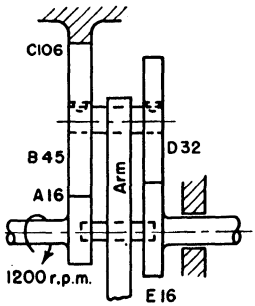

Fig. P 11.16

11.16. Determine the speed and direction of rotation of gear E in Fig. P 11.16.

11.17. Determine the speed and direction of rotation of gear A in Fig. P 11.17. Gears B, C, and E are one rigid unit.

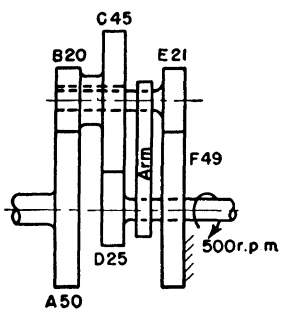

Fig. P 11.17

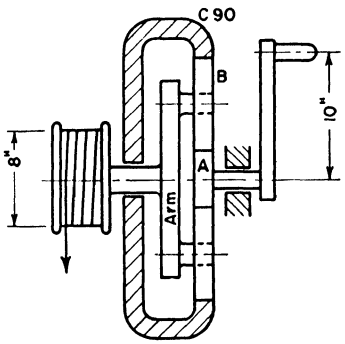

Fig. P 11.18

11.18. The mechanical advantage of the hoist shown in Fig. P 11.18 is to be approximately 25. Determine the numbers of teeth on gears A and B.

11.19. The mechanism shown in Fig. P 11.19 is similar to that of Fig. 8.9. Cone B turns 10 times and cone D turns 4 times. Determine the number and directions of the turns of E.

11.20. In Fig. P 11.20, gears A and C turn once. Determine the number and directions of the turns of gear L.

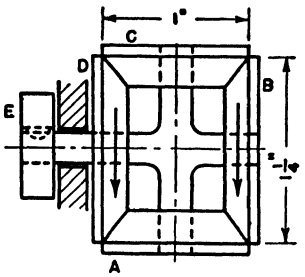

Fig. P 11.19

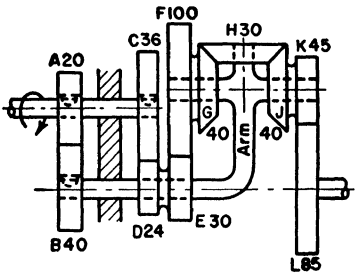

Fig. P 11.20

11.21. In Fig. P 11.21, gears A and H turn once. Determine the number and direction of the turns of the arm.

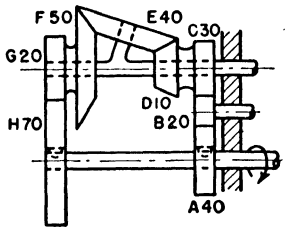

Fig. P 11.21

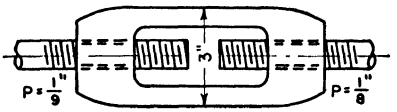

Fig. P 11.23

11.22. The pitch of the screwjack thread (Fig. 11.15) is $\frac{3}{8}$ in. and the radius of the handle is 12 in. Determine the mechanical advantage.

11.23. The turnbuckle (Fig. P 11.23) is to be turned without the use of a lever or wrench. Determine the mechanical advantage when: (a) the threads are the same hand, (b) the threads are of opposite hand.

11.24. A differential screw press is shown in Fig. P 11.24. How many times must the handwheel be turned to lower the plate $\frac{1}{16}$ in.

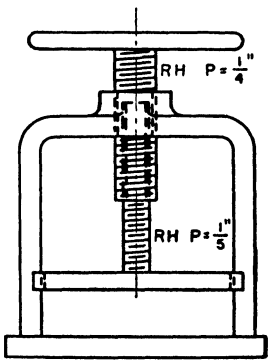

Fig. P 11.24

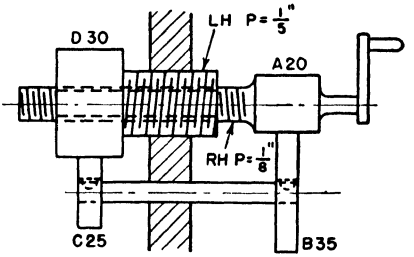

Fig. P 11.25

11.25. The crank in Fig. P 11.25 is turned once in a clockwise direction when viewed from the right. Determine the direction and distance that the small screw moves relative to the frame.

CHAPTER 12

Miscellaneous Mechanisms

12.1. Four-bar linkages* are of such importance that it is sometimes desirable to build an adjustable mechanism to make rapid investigations of their motions. One such mechanism is shown in Figs. 12.1 and 12.2. The lengths of the four links AB, BC, CD, and DA can be controlled by adjustments at joints 2, 3, and 4. Here E is a point in coupler link BC. Its position relative to points B and C is controlled

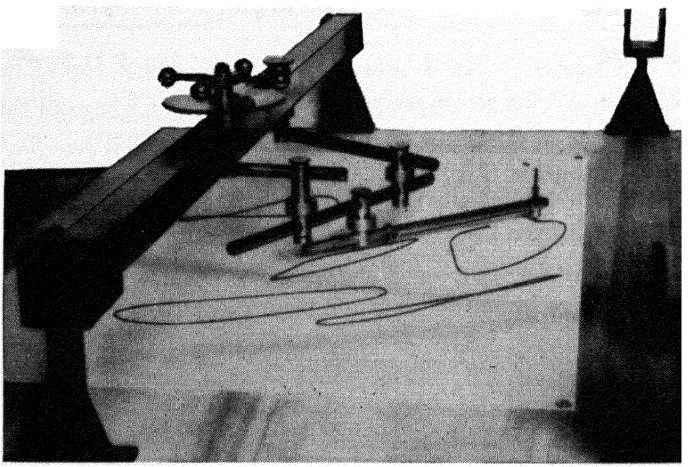

Fig. 12.1. (Courtesy of *Machine Design.*)

by the adjustment at F. A pencil is placed at E. When the handwheel is turned the pencil traces the coupler curve. Some typical curves are shown in Fig. 12.3(a). The proportions of the mechanism are changed each time until a satisfactory curve is obtained. An example is shown in Fig. 12.3(b). This mechanism is used to produce intermittent film motion. Other examples can be found in automatic machines such as those for wrapping, packaging, printing, weaving, vending, etc.

* This article is taken from "Four-bar Linkages" by Josef Boehm, *Machine Design*, August 1952.

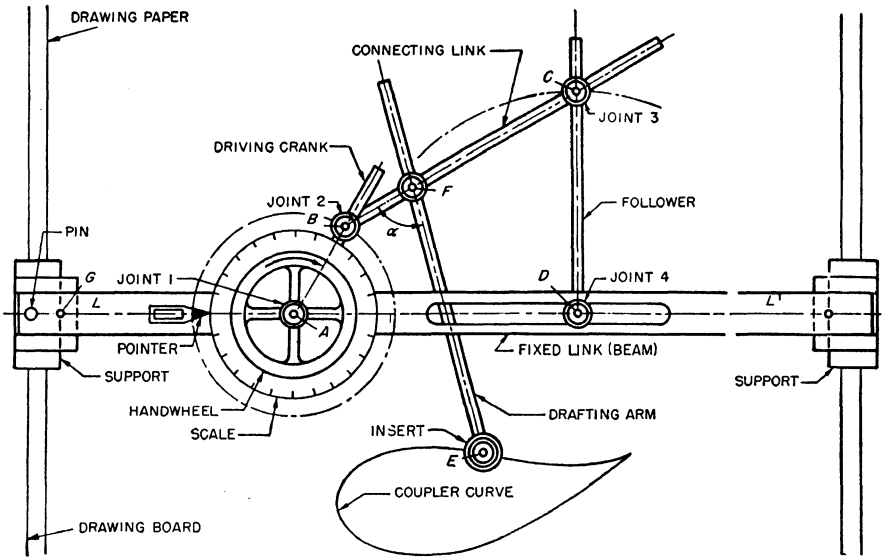

Fig. 12.2. (Courtesy of *Machine Design.*)

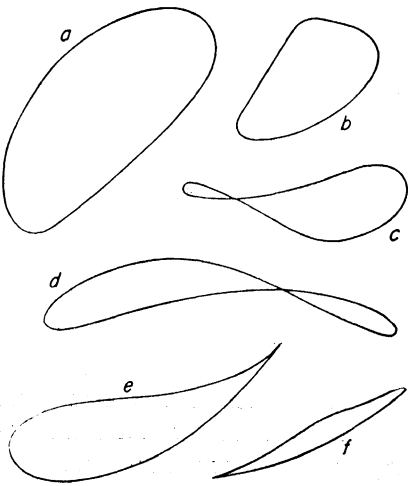

Fig. 12.3a. (Courtesy of *Machine Design.*)

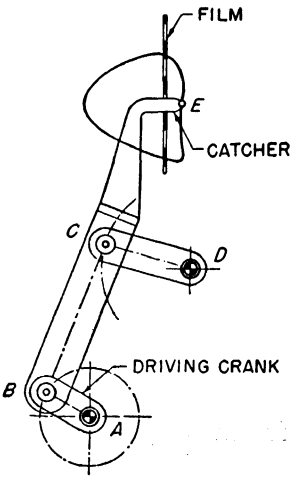

Fig. 12.3b. (Courtesy of *Machine Design.*)

The approximate velocity of point E can be obtained by using a sharp point instead of a pencil at E. The coupler curve is plotted as a series of points pricked in the paper and corresponding to a series of equal angular settings of the handwheel. The distances between the points can be used to estimate the velocity. After a satisfactory curve is obtained an accurate velocity and acceleration analysis can be made by the methods previously considered.

12.2. Universal joints are used to connect intersecting shafts. One of the simplest types, Fig. 12.4, is used in toys. It is included here because of its simplicity and its basic theory. Shafts 2 and 3 are of very small diameter and are equally bent, $\phi_2 = \phi_3$. For the phase shown with solid lines the point of contact of 2 and 3, point B, lies in the plane of the paper. It also lies in the homokinetic plane. This is the plane that is normal to the plane containing the shafts and bisects the angle between them. The velocity of B as a point in 3 coincides with that of B as a point in 2. The perpendiculars to the axes, BC and BD, are equal. These same conditions hold for the phase shown with broken lines. Because of symmetry the point of contact B will lie in the homokinetic

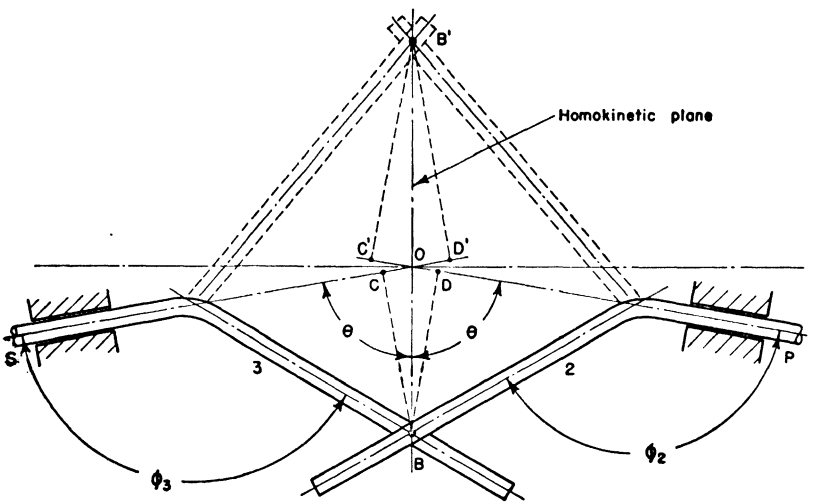

Fig. 12.4

plane for all other phases. Velocities V_{B_2} and V_{B_3} do not coincide for the phases that are not in the plane of the paper. Because of symmetry they will make equal angles with the homokinetic plane. The driving and driven components of these two vectors in the homokinetic plane must be equal. Then V_{B_2} and V_{B_3} are equal in magnitude. The perpendiculars to the axes are also equal. The angular velocity ratio of driver and follower is therefore unity for all phases.

The requirement of a universal joint to transmit motion with a constant velocity ratio is fulfilled if the power-transmitting elements (in the above example there is only one, the point of contact B) lie in the homokinetic plane for all phases.

The Bendix-Weiss joint is shown in Figs. 12.5 and 12.6. Power is transmitted from one fork to the other through balls. The small ball in Fig. 12.5 is used at the center for a spacer. The principle of the joint is shown in Fig. 12.6. Each ball fits in two grooves or races, one being

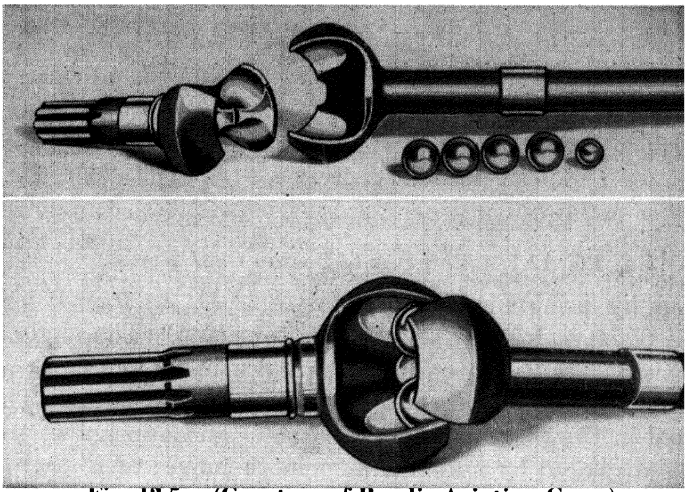

Fig. 12.5. (Courtesy of Bendix Aviation Corp.)

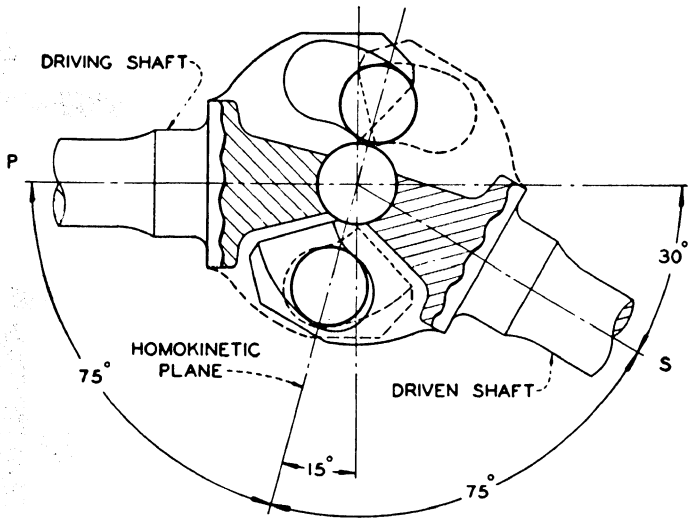

Fig. 12.6. (Courtesy of Bendix Aviation Corp.)

in each fork. The grooves are designed so that they always intersect in the homokinetic plane. The balls can lie only at the intersection of the grooves. This joint therefore transmits motion with a constant angular velocity ratio.

The Hooke or Cardan* joint is shown in Fig. 12.7. A schematic diagram is shown in Fig. 12.8(a). The nature of the motion can be

* An Italian, Cardan (1501–1576), was the first to describe this joint. An Englishman, Robert Hooke (1635–1703), first applied it for the transmission of rotary motion. Hooke was a physicist, mathematician, and inventor. He is most widely known for Hooke's law, which is stated in all strength of materials books.

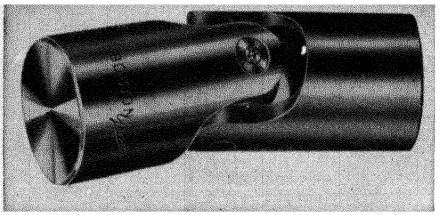

Fig. 12.7. (Courtesy of Boston Gear Works.)

determined by using Fig. 12.8(b) and (c). At (b) fork P lies in the horizontal plane and fork S in the vertical plane. The angle between the shafts is β. As P rotates, points B and C move in a circle as shown in (c). Points D and E move in a circle of the same size. This circle is projected in the plane of the paper in (c) and appears as an ellipse. When P is displaced by an angle ϕ, point B moves to B' and D to D'. Angle DOD' is equal to ϕ. (A little consideration will show that this is correct. At (d) right angle BOD lies in the plane of the paper. Point D

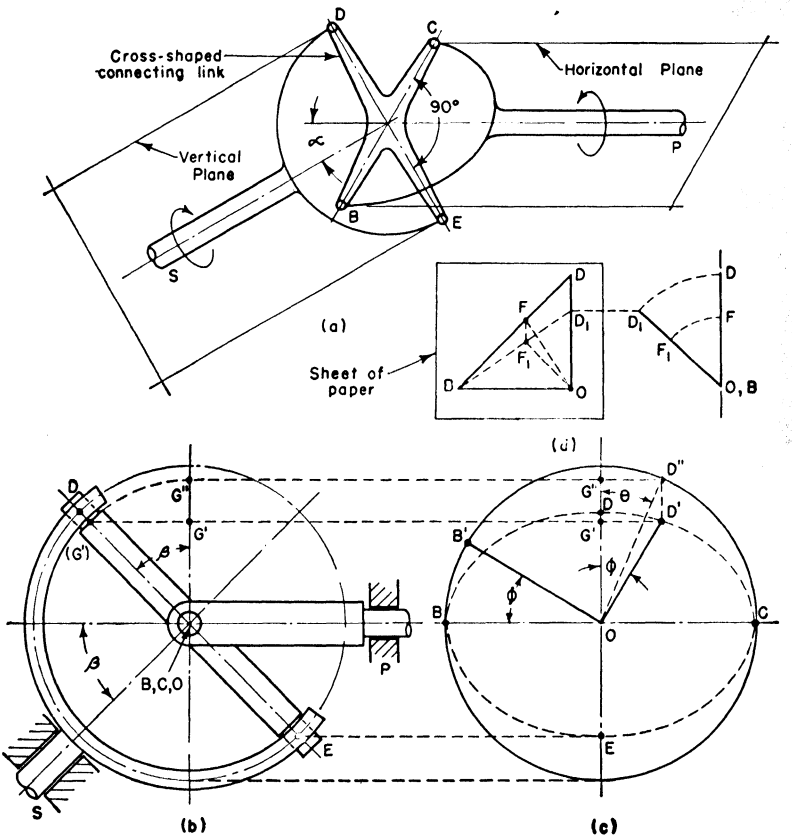

Fig. 12.8

is swung out of the plane of the paper to position D_1. Angle BOD_1 when projected back to the paper is equal to BOD. Angle FOD when swung out and projected back is F_1OD_1 and is not equal to FOD.) It appears that S has moved through the same angle as P. This is not correct, since the true angle must be measured in a circle that represents the path of D. This can be done most conveniently by using the circle in (c). Point D' is projected vertically to D''. The true angle turned through by S is θ.

This joint does not transmit motion with a constant angular velocity ratio. The power transmission elements B, C, D, and E lie in a plane that passes through O, but the plane wobbles as motion takes place. From (b) it can be seen that when fork P turns 180°, fork S will also turn 180°. When fork P is turned to the vertical position, fork S is horizontal. Both have turned 90°. For four phases in each cycle the displacements are equal. For all other phases they are not. Part of the time the follower is ahead and part of the time it is behind the driver.

The relationship between θ and ϕ can be determined as follows, noting that $G'D' = G''D''$ and $OG'' = O(G')$.

$$\frac{\tan\theta}{\tan\phi} = \frac{G''D''/G''O}{G^1D^1/G'O} = \frac{G'O}{G''O} = \frac{G''O\cos\beta}{G''O} = \cos\beta$$

or

$$\tan\phi = \frac{\tan\theta}{\cos\beta} \tag{12.1}$$

Angle β is usually a constant in a given application. It is assumed constant in this development.

The angular velocity ratio is obtained by differentiating Eq. (12.1) with respect to time.

$$\sec^2\phi\frac{d\phi}{dt} = \frac{\sec^2\theta}{\cos\beta}\frac{d\theta}{dt}$$

Letting

$$\frac{d\phi}{dt} = \omega_p \qquad \text{and} \qquad \frac{d\theta}{dt} = \omega_s$$

gives

$$\frac{\omega_s}{\omega_p} = \frac{\sec^2\phi\cos\beta}{\sec^2\theta} = \frac{\sec^2\phi\cos\beta}{1+\tan^2\theta}$$

Angle θ is eliminated, using Eq. (12.1), giving

$$\frac{\omega_s}{\omega_p} = \frac{\sec\phi\cos\beta}{1+\sec^2\beta\tan^2\phi} = \frac{\cos\beta/\cos^2\phi}{(\cos^2\phi+\cos^2\beta\sin^2\phi)/\cos^2\phi}$$

Letting $\cos^2\beta = 1 - \sin^2\beta$ gives

$$\frac{\omega_s}{\omega_p} = \frac{\cos\beta}{1-\sin^2\beta\sin^2\phi} \tag{12.2}$$

For a constant angular velocity of P the angular acceleration of S is

$$\alpha_s = \frac{d\omega_s}{dt} = \frac{d}{dt}\left(\omega_p \frac{\cos\beta}{1 - \sin^2\alpha \sin^2\phi}\right)$$

$$= \omega_p \left[\frac{\cos\beta \sin^2\beta\, 2 \sin\phi \cos\phi (d\phi/dt)}{(1 - \sin^2\beta \sin^2\phi)^2}\right]$$

$$= \omega_p^2 \frac{\cos\beta \sin^2\beta \sin 2\phi}{(1 - \sin^2\beta \sin^2\phi)^2} \tag{12.3}$$

If an intermediate shaft R (Fig. 12.9) and two Hooke's joints are used to connect shafts P and S, one joint can be made to compensate

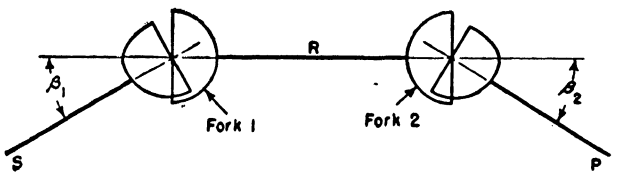

Fig. 12.9

for the other. Shafts P and S do not have to intersect. The angular velocity ratio of P and S will be unity for all phases if R is placed so that the angle between R and S is equal to that between R and P, and fork 1 is made to lie in the plane of R and S when fork 2 lies in the plane of R and P.

12.3. Oldham coupling [Fig. 12.10(a)] is used to connect parallel shafts. Member 1 has two tongues at right angles that fit into grooves

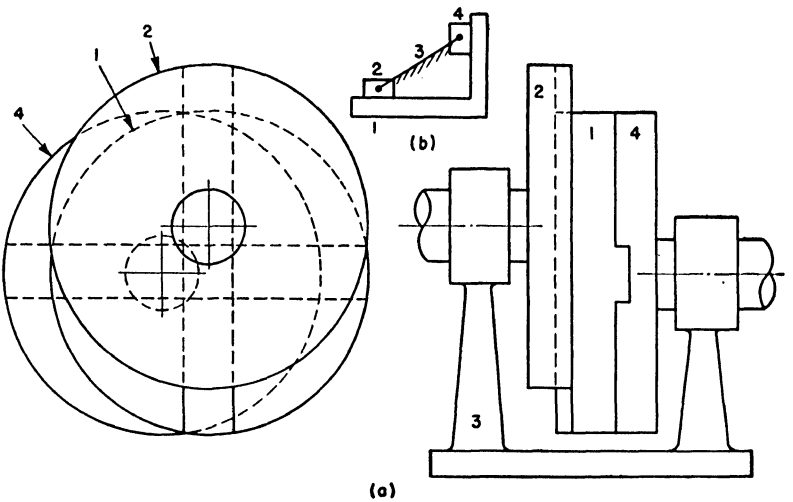

Fig. 12.10

in members 2 and 4. The only relative motion between 2 and 1 is translation. The same is true of 1 and 4. Therefore any angular motion of member 4 will be imparted exactly to member 2. The angular velocity ratio of this coupling is unity.

This mechanism is an inversion of the double slider mechanism shown at (b). If member 3 is fixed, 2 and 4 will rotate equally with 1.

12.4. The elliptic trammel (Fig. 12.11) is another application of the double-slider mechanism. It can be used for drawing ellipses. From Fig. 12.11,

$$x = a \cos \phi$$
$$y = b \sin \phi$$

Then
$$\frac{x^2}{a^2} + \frac{y^2}{b^2} = \cos^2 \phi + \sin^2 \phi = 1 \qquad (12.4)$$

This is the equation of the ellipse with center at the origin, where a is the semimajor axis and b is the semiminor axis. Axes a and b are equal

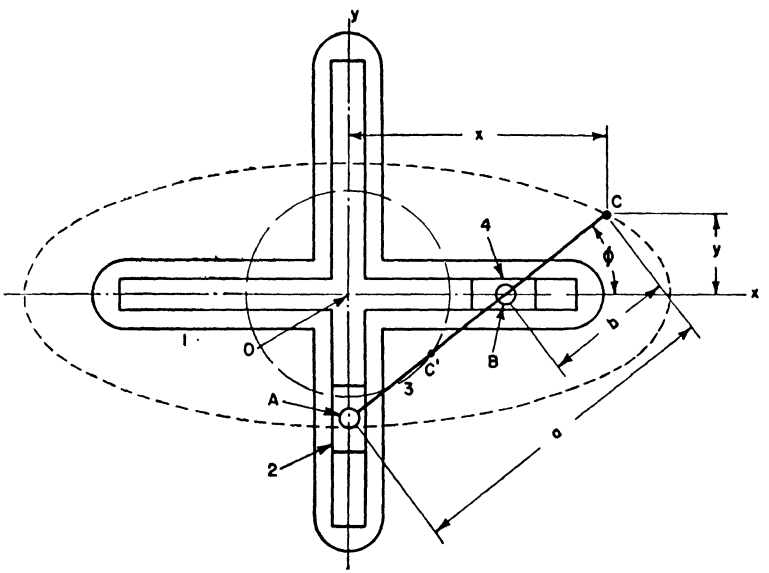

Fig. 12.11

when C is chosen at C' midway between A and B. The path of C' is a circle of radius a. Equation (12.4) becomes

$$x^2 + y^2 = a^2$$

This mechanism, when made for drawing, carries a pen or pencil at C, and the lengths AB and BC are adjustable.

12.5. Generation of second-degree curves.* The general equation of the second degree is

$$Ax^2 + Bxy + Cy^2 + Dx + Ey + F = 0 \tag{12.5}$$

By translation and rotation of the axes a second-degree equation can always be reduced to one of the conic equations.

Ellipse	$\frac{x^2}{a^2} + \frac{y^2}{b^2} = 1$
Hyperbola	$\frac{x^2}{a^2} - \frac{y^2}{b^2} = 1$
Parabola	$y^2 = 2px$

A machine based on theorems from projective geometry can be made to generate these curves.

Theorem 1. If a right angle moves in its plane in such a way that its vertex describes a fixed circle, while one of the arms passes always through a fixed point, the envelope of the other arm will be a conic section concentric with the given circle, and having one focus at the fixed point. The conic is an ellipse or a hyperbola according as the given point lies within or without the given circle.

Theorem 2. If a right angle moves in its plane so that its vertex describes a fixed straight line, while one of the arms passes always through a fixed point, the other arm will envelop a parabola having the fixed point for the focus and the fixed straight line for the tangent at the vertex. The fixed point or focus must not lie on the chosen fixed straight line.

Kinematical schemes for generating the ellipse, hyperbola, and parabola in accordance with the foregoing theorems are illustrated in Fig. 12.12(a), (b), and (c), respectively. Here F is a focus and FJK is a right angle. A curve that looks like a conic but actually is a conic less a constant dimension measured normal to the curve will be generated if the plane of the cutter is advanced, say to a position L-L as shown in (a). This property of parallel curves can be applied in allowing for roller radius in the generation of a conic-section cam to operate with a roller follower. Templates with an allowance for thickness of sheet metal might be made in this manner. Solids of revolution can be made by rotating the work during the machining operation.

A curve that is larger than a conic by a constant dimension measured normal to the curve would be generated by withdrawing the cutting surface to some position M-M. Thus a conic can be roughed out just slightly oversize before finish grinding exactly to size.

* This article is taken from "Generation of the Conic Sections with Machine Tools" by Rolland T. Hinkle, *Product Eng.*, August, 1947.

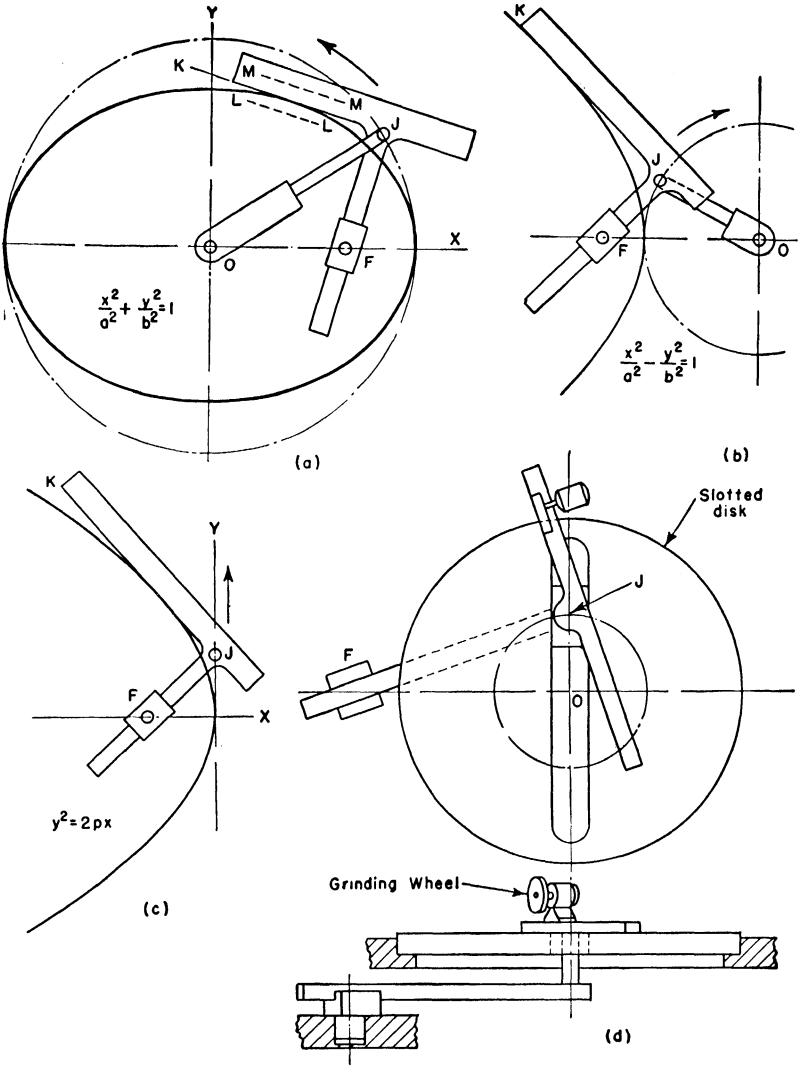

Fig. 12.12

A machine for generating any conic is shown at (d). When the slotted wheel is fixed in the position shown and slider J is moved in the slot, the grinding wheel sweeps out a parabola. When the slider is fixed in the slot and the disk is rotated the grinding wheel sweeps out an ellipse or hyperbola depending on the location of F.

12.6. The pantograph is used to enlarge or reduce movements. In Fig. 12.13(a) link ABC is parallel to OD, and OA is parallel to BD. A line through C and O intersects BD at P. If C is moved to trace a given path, point P will trace a path that is similar but of a different size.

In order that the movement of P be similar to that of C it is necessary that triangles OPD and PBC be similar for all positions. Here OD and BC are always parallel, as are PD and BP. For any position the line OC

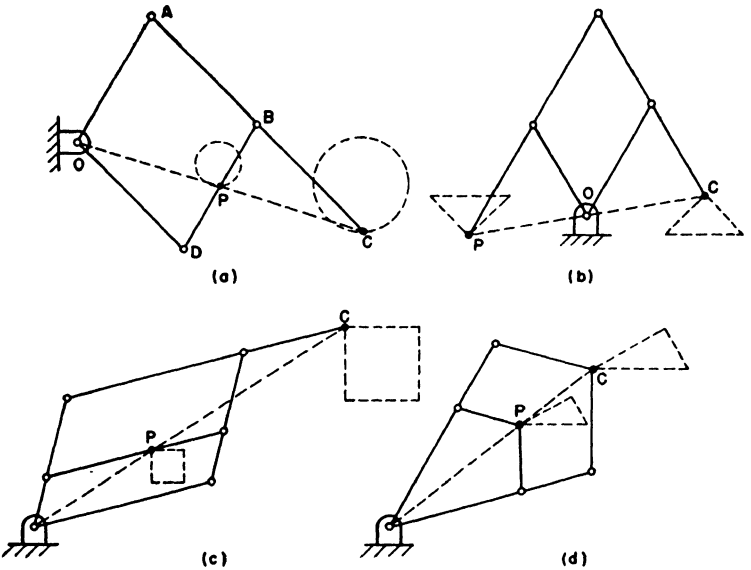

Fig. 12.13

will produce parallel sides OP and PC. Since OD and BC are fixed lengths, PD and BP will also be fixed. The ratio of the sizes of the motions will be

$$\frac{\text{motion of } C}{\text{motion of } P} = \frac{OC}{OP} = \frac{AC}{AB}$$

Other arrangements are shown at (b), (c), and (d).

Pantographs are used for reproducing drawings to a different scale. Maps are a common example. They are also used to guide cutting tools. Printing type is first drawn by hand several inches high. A pantograph is used to reduce the type and cut the moulds.

12.7. Straight-line motions. Most of the mechanisms that produce straight-line motions without the use of sliders were developed before plane surfaces could be machined accurately. At the present time the need for these mechanisms is not so great as in the past but they still have useful applications. The mechanisms can be classed in two groups, exact and approximate.

Peaucellier's Mechanism (Fig. 12.14) was developed in 1864 by a Frenchman, Peaucellier. Links of equal length are $AB = BC = CD = DA$, $OA = OC$, and $OE = ED$. From symmetry a line through OB will pass through D and AC will bisect DB at F. It will be shown that point B moves in a straight line.

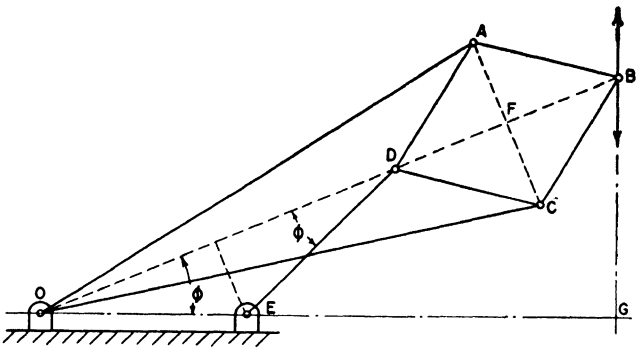

Fig. 12.14

From right triangles OFA and DFA,

$$\overline{OF}^2 = \overline{OA}^2 - \overline{AF}^2 \quad \text{and} \quad \overline{DF}^2 = \overline{DA}^2 - \overline{AF}^2$$

Eliminating $\overline{AF}^2$ from the equations gives

$$\overline{OF}^2 - \overline{DF}^2 = \overline{OA}^2 - \overline{DA}^2$$

or

$$(OF + DF)(OF - DF) = \overline{OA}^2 - \overline{DA}^2$$

But $OF + DF = OB = \dfrac{OG}{\cos \phi}$ and $OF - DF = OD = 2(OE)\cos \phi$

Then

$$\frac{OG}{\cos \phi} 2(OE)\cos \phi = \overline{OA}^2 - \overline{DA}^2$$

or

$$OG = \frac{\overline{OA}^2 - \overline{DA}^2}{2(OE)} = \text{a constant}$$

The projection of B on a line through OE is a fixed point G. Therefore B moves in a straight line perpendicular to OE.

Kempe's Mechanism (Fig. 12.15) produces rectilinear translation of a member with the use of pin-connected links. The proportions of the links are, $AB = AD = 2CD = 4FE = 4ED$. Links BCF' and FCB' are rigid members. Here $CB'A'E'F'D'$ is a duplication of the left half of the mechanism. If link AED is fixed, the only motion that link $D'E'A'$ can have is horizontal.

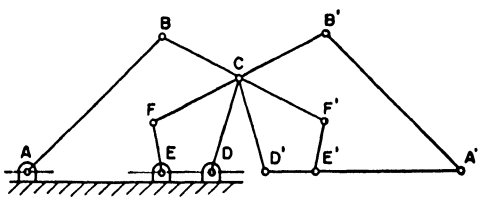

Fig. 12.15

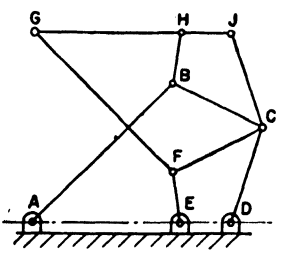

Fig. 12.16

Another arrangement is shown in Fig. 12.16. The only motion that link *GHJ* can have is rectilinear translation in a vertical direction.

Sarrut's Mechanism (Fig. 12.17) is one of the simplest and perhaps the earliest mechanism to produce straight-line motion. When 1 is

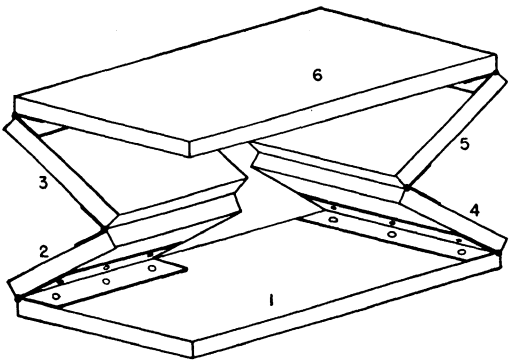

Fig. 12.17

fixed, the only motion that 6 can have is rectilinear translation in a vertical direction.

Robert's Mechanism (Fig. 12.18) produces approximate straight-line motion. Here E moves very nearly along the line AD. The proportions of the links are $AB = BE = EC = CD$, and $AD = 2BC$. The accuracy of the motion is increased as the height of the mechanism is made greater in relation to its width.

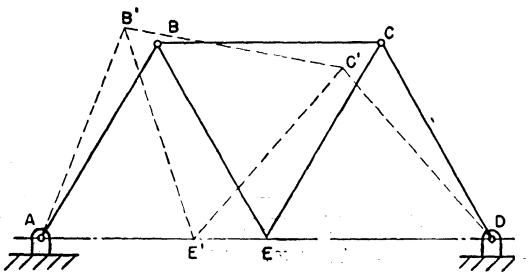

Fig. 12.18

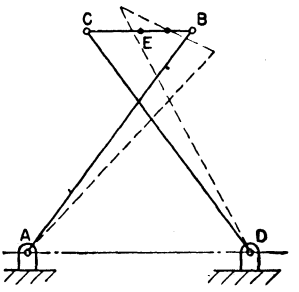

Fig. 12.19

Tchebicheff's Mechanism (Fig. 12.19) produces approximate straight-line motion. The mid-point E of CB moves very nearly along the line CB. The proportions of the links are $AB = CD = 1.25\ AD$, and $AD = 2CB$.

The Scott-Russell and Watt straight-line mechanisms are shown in Figs. P 2.3 and P 2.4.

An Engine Pressure Indicator is shown in Fig. 12.20. Piston B moves against a spring and is displaced in proportion to the pressure in the cylinder. This motion is transmitted through the linkage and produces a

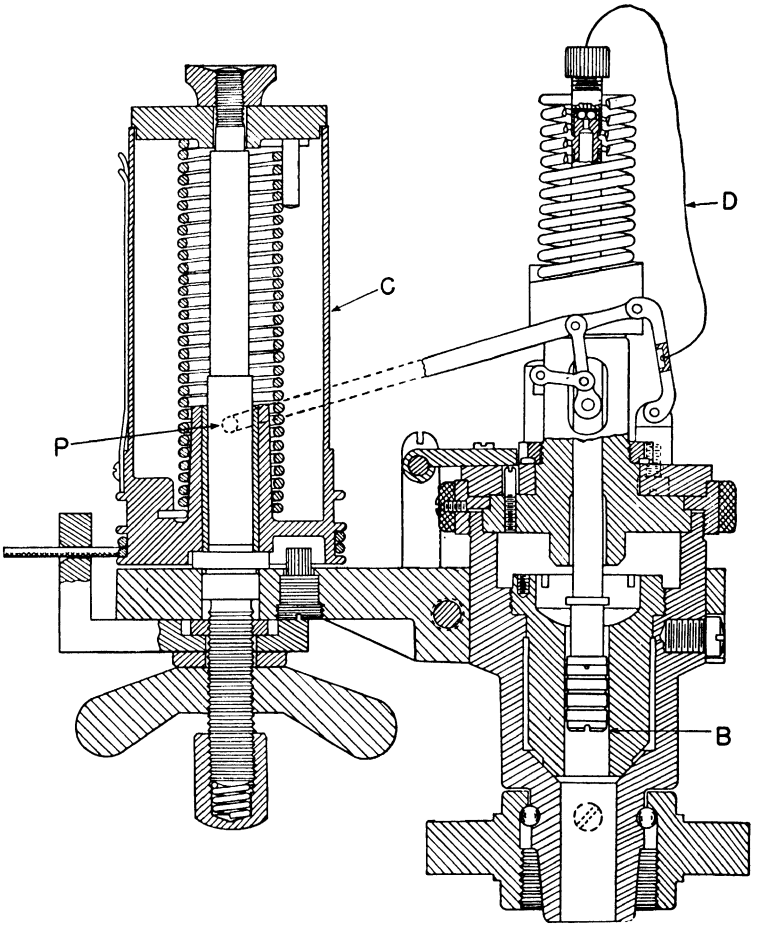

Fig. 12.20. (Courtesy of Bacharach Industrial Instrument Co.)

larger vertical motion of the pencil P. A pressure displacement diagram is traced on a paper that is wrapped around cylinder C. The cylinder is rotated in accordance with the piston displacement. It is necessary not only that P move in an approximate straight line, but that its motion be proportional to that of B. The wire D is used with spark ignition engines. Ignition is recorded on the diagram by a hole burned through the paper at P.

12.8. A multiplying linkage that is used in computors is shown in Fig. 12.21. In the drawing the ratio of a to b is 2. This setting is used to multiply any number by 2. When member 2 is moved 6 units to the right, member 4 moves $6 \times 2 = 12$ units to the left. Any two numbers can be multiplied by moving B so that the ratio of a to b is equal to one of the numbers. The linkage can also be used for dividing.

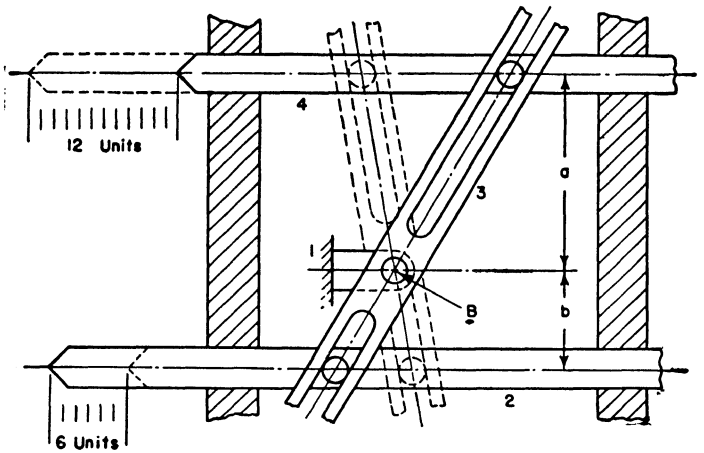

Fig. 12.21

12.9. Escapements are used to prevent a wheel from rotating in an uncontrolled manner and to cause it to rotate with a definite intermittent motion. The Graham escapement that is used in clocks and watches is shown in Fig. 12.22. A clockwise torque is applied to the escape wheel by means of a spring or weight. The anchor oscillates on the axis E, which is called the verge. A balance wheel or pendulum is attached to the anchor. The ends of the anchor are called pallets. The pallets are close enough together so that there is no position of the anchor that allows the escape wheel to rotate continuously. If the pendulum is displaced and then released, it will oscillate and allow the

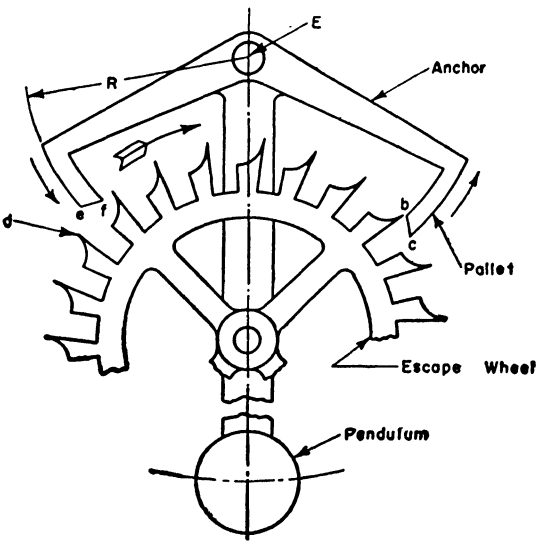

Fig. 12.22

escape wheel to rotate intermittently as the pallets alternately pull out of the tooth spaces. This motion will soon cease because of friction unless energy is supplied to the pendulum. The required energy is supplied by the spring or weight by means of the escape wheel and the inclined surfaces *bc* and *ef*. For the phase shown the pendulum is swinging to the right, and the end of a tooth is in contact with the right pallet at *b*. The torque on the escape wheel causes the end of the tooth to slide along the surface *bc*. This pushes the pallet to the right and adds energy to the pendulum. Before the end of the tooth reaches *c*, point *e* on the left pallet enters a tooth space and is in a position to catch the adjacent tooth and stop the motion. When the pendulum swings to the left, point *d* slides along surface *ef* and supplies energy to the pendulum. During one cycle the pendulum receives two energy impulses, and the escape wheel has rotation corresponding to one tooth. Surfaces of the pallets are circular arcs with *E* as center. When these surfaces are in contact with the escape wheel rotation of the anchor does not cause rotation of the escape wheel.

12.10. Ratchets are used to convert rotation or oscillation into intermittent rotation or translation. In Fig. 12.23 rotations of crank 6 in either direction cause intermittent counterclockwise rotation of the ratchet wheel 2. If the pawl 3 is changed to the dotted position, the ratchet wheel will rotate in a clockwise direction.

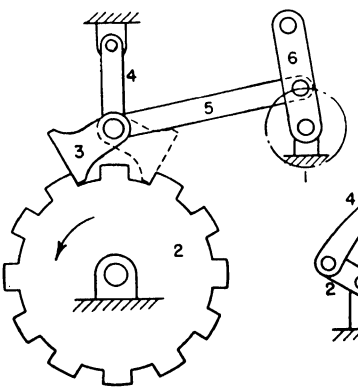

Fig. 12.23

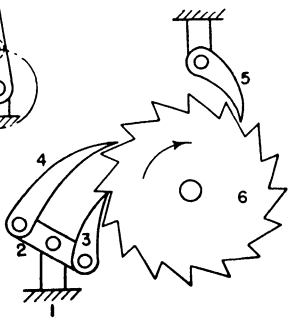

Fig. 12.24

In Fig. 12.24, oscillation of 2 causes intermittent clockwise rotation of 6. Two pawls 3 and 4, are used to produce rotation for both directions of motion of 2. Member 5 is a holding pawl. It is sometimes necessary to use springs on the pawls to hold them against the ratchet wheel.

A silent or friction ratchet is shown in Fig. 12.25. Oscillation of 3 causes intermittent counterclockwise rotation of 2. Here 5 is a holding pawl.

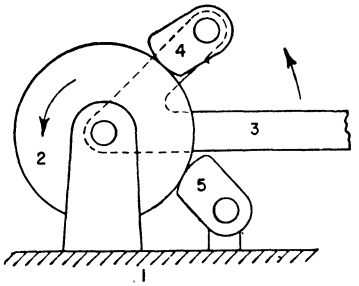

Fig. 12.25

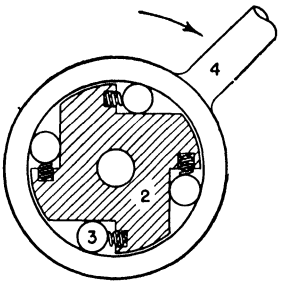

Fig. 12.26

Another type of silent ratchet is shown in Fig. 12.26. Light springs push balls 3 into the wedge-shaped spaces formed by 2 and 4. Here 2 can be the driver in a counterclockwise direction, or 4 can be the driver in a clockwise direction.

12.11. Zero back lash gears. A train of conventional gears with zero backlash would require that the gears and mountings be dimensionally perfect and that all parts change equally with a change in temperature. A practical way of eliminating backlash in a gear train is shown in Fig. 12.27. This is an end view of the mechanism shown in Fig. 8.9.

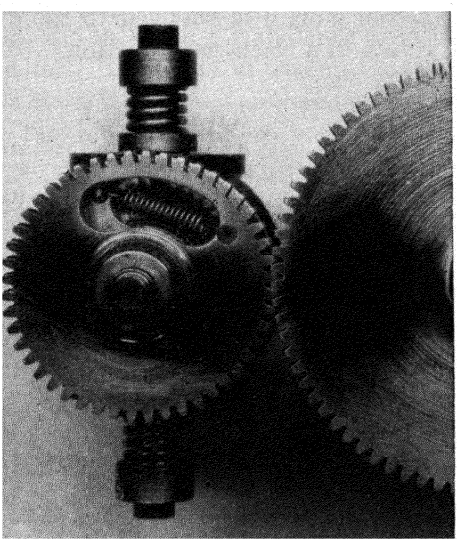

Fig. 12.27

The pinion is made in two parts and the parts connected with a spring. In assembly the parts are rotated so that the spring is in tension. If the torque produced by the spring is greater than the torque applied to the shaft, the pinion can transmit motion in either direction with zero backlash. In a train with several gears, alternate gears are made in this manner.

Index

A

Acceleration:
  angular, 13
  complete graphical determination, 70
  complex mechanisms, 78
  Coriolis, 73
  image, 67
  linear, 13
  normal, 14
  polygon, 66
  revolved, 92
  slider crank, 67, 92, 95
  tangential, 14
Addendum, 137
  circle, 138
Angle of action, 143
Angular velocity graph, 90
Angular velocity ratio theorem, 22
Arc of action, 143
Automobile:
  differential, 203
  transmission, 195

B

Back cone, 170
Backlash, 138
  zero, 226
Base pitch, 143
Belt drives, 179
  creep, 180
  flat, 179
  law, 181
  nonparallel shafts, 181
  V-, 182
Bevel gear, 168
  involute, 168
  octoid, 169
  on center face, 172
  production, 171
  spiral, 170
  terminology, 168
  Tredgold's approximation, 170
Bilgrim, Hugo, 135
Boehm, Joseph, 210
Brown, Joseph R., 135
Buckingham, Earl, 136

C

Cam:
  automotive, 115
  auxiliary linkage, 115
  constant acceleration, 100
  constant velocity, 102
  co-ordinated, 118
  cycloidal, 105
  cylindrical, 116
  design limitations, 111
  disk, 106
  displacement diagrams, 100
  follower offset, 108, 109
  knife-edge follower, 106
  machining, 117
  modified constant velocity, 102
  oscillating flat-face follower, 110
  positive return, 113
  profile determination, 106
  reciprocating flat-face follower, 109
  reciprocating roller follower, 107
  selection of motion, 106
  simple harmonic, 104
  translation, 100
  two followers, 110
Cardan, 213
Chain:
  bead, 187
  chordal action, 184
  coil, 190
  conveyor, 188
  differential hoist, 190
  Ewart, 188
  impact loading, 184
  Morse Hy-Vo, 185
  pintle, 188
  pitch, 183
  roller, 183
  silent, 184
  speed variation, 184
Circular pitch, 137
Clearance, 138
Complex mechanisms, 78
Composite teeth, 153
Conic sections, 218
Constant angular velocity ratio, 24

Constrained motion, 6
  criterion, 64
Contact ratio, 143
  determination, 144
Controllable-pitch propeller drive, 201
Coriolis' law, 73
Coupler curve, 210
Crossed helical gears, 158
Crown gear, 168
  generation, 171
Crowning, 180
Ctesibius, 134
Cycle, 8
Cycloid, 26, 148
Cycloidal:
  cam, 105
  gear, 148

D

da Vinci, Leonardo:
  frontispiece
  gears, 134
  relative motion, 19
Dead-center phase, 25
Dedendum, 138
de Lahaire, Philippe, 134
Diametral pitch, 138
Differential:
  automobile, 203
  chain hoist, 190
  screw, 205
Directional relationship, 24
Displacement, 11
Drag link mechanism, 27
Dudley, W. M., 106

E

Eccentric, 4
Ellipse:
  generation, 218
  rolling, 129
Elliptic trammel, 217
Engine pressure indicator, 222
Epicyclic gear train, 196
  bevel, 202
  equation, 198
  tabular method, 199
Equivalent linkage, 71
Escapement, Graham, 224
Ewart chain, 188

F

Face gear:
  off center, 174
  on center, 172
Face width, 138
Fellows:
  gear shaper, 160
  tooth system, 155
Fillet:
  curve, 138
  radius, 138
Flank, 138
Flat face cam follower, 109, 110
Fretting corrosion, 27
Friction drive, 124
Full depth teeth, 153, 154
Fundamental law of gearing, 137

G

Gauge line, 31
Gear:
  base circle, 141
  bevel, 168
  classification, 136
  contact ratio, 143, 144
  crossed helical, 158
  definition, 135
  fundamental law:
    circular, 137
    noncircular, 175
  grinding, 163
  helical, 155
  herringbone, 157
  history, 134
  hobbing, 162, 166
  hypoid:
    bevel, 175
    face, 174
  idler, 194
  interference, 143, 145
  milling, 159
  miter, 168
  nomenclature, 137
  noncircular, 175
  pin, 134
  ratio, 138
  shaping, 160
  shaving, 163
  spur, 137
  standard tooth forms, 153
  stepped, 155
  tooth curve, 139
  unequal addendum, 164
  variable center distance, 150
  worm, 165
  zero backlash, 226
Gear train:
  compound, 195
  epicyclic, 196
  ordinary, 194
Generating circle, 149
Generating method, 135, 160

Geneva stop, 91
Gnome aircraft engine, 21
Golber, H. E., 132
Graham escapement, 224
Graphical differentiation, 84
  relative error, 86

H

Hall, A. S., 74
Harmonic motion, (*see* Simple harmonic motion)
Helical gear, 155
Helical motion, 8
Helix angle, 156
Herringbone gear, 157
Hindley worm, 167
Hobbing, 162, 166
Hoist, differential chain, 190
Homokinetic plane, 212
Hooke, Robert, 213
Hooke's joint, 213
Hrones, J. A., 105
Huckert's theorem, 26
Hyperbola, 218
Hyperboloid, 129
Hypoid gear, 173

I

Idler gear, 194
Image:
  acceleration, 67
  velocity, 47
Instant center:
  definition, 30
  in direct contact mechanisms, 34
  location, 33
  number, 33
  obvious centers, 38
  tabulation, 39
Interchangeable gears, 147
Internal gear, 146
Inversion, 19
Inverted tooth chain, 185
Involute of circle, 139
  construction, 141
Involute teeth:
  advantages, 150
  center distance variation, 150
  interference, 143
  spherical, 168
  summary of properties, 152
  tooth action, 141

J

Jack, 204

K

Kempe's mechanism, 221
Kennedy's theorem, 33
Kinematic:
  chain, 6
  link, 6
  synthesis, 99
Kinematics, definition, 1
Knife-edge follower, 106

L

Lead, 156
  angle, 156
Linear acceleration, 13
  from polygons, 67
Line of action, 142
Line of transmission, 21
Link, kinematic, 6
Linotype, 1, 2, 3, 99
Localized vector, 9
Lockenvitz, A. E., 132

M

Machine, definition, 7
Mechanical advantage, 57
Mechanism, definition, 7
Milling, 159
Miter gears, 168
Module, 138
Morse Hy-Vo chain, 185
Motion:
  absolute, 17
  constrained, 6
  helical, 8
  plane, 7
  rectilinear, 7
  relative, 17
  selection of cam, 106
  simple harmonic, 15
  spherical, 8
Motion transfer:
  Huckert's theorem, 26
  methods, 21
Multiplying linkage, 223

N

Noncircular gears, 175
Normal acceleration, 14
  graphical determination, 70
Normal circular pitch, 157

O

Octoid bevel gears, 169
Offset follower, 108, 109
Oldham coupling, 216

P

Pair, 4, 5
Pantograph, 219
Parabola, 218
Parallel line construction, 36
Path of contact, 142
Peaucellier's mechanism, 220
Period, 8
Phase, 8
Pinion, 139
Pintle chain, 188
Piston:
  acceleration, 67, 92, 95
  velocity, 67, 88, 90, 95
Pitch circle, 137
Pitch point, 137
Plane motion, 7
Planetary gear train, 196
Polar-velocity graph, 90
Positive driving, 25
Positive motion cam, 113
Positive variable-speed transmission, 190
Power transmission chain, 183
Pressure angle:
  cam, 108
  gear, 150
Pulley, 179
  crown, 181

Q

Quarter turn belt, 181
Quick-return mechanism, 88, 94

R

Rack, 143
Ratchet, 225
Relative motion, definition, 17
Resolution, linear velocities by, 40
Revolved polygon, 87
Ritterhaus construction, 92, 94
Roemer, Olaf, 134
Roller bearing, tapered, 126
Roller chain, 183
Rolling:
  cones, 124
  contact, 25, 26, 123
  cylinders, 123
  disk and roller, 127
  ellipses, 129
  hyperboloids, 129
Rolling curves, general case, 130

S

Sarrut's mechanism, 222
Scotch yoke, 16
Scott-Russell mechanism, 27
Screw thread, 205
Second degree curves, 218
Segmental teeth, 153
Shaving, 163
Silent chain, 185
Simple harmonic motion, 15
  cam, 104
Slider crank, 4
  acceleration analysis, 67, 92, 95
  velocity, 67, 88, 90, 95
Sliding, 22
  gear teeth, 143
Spherical motion, 8
Spiral angle, 171
Spiral bevel gear, 170
Sprocket, 183, 186, 187
Spur gear, 137
Stepped gear, 155
Straight line mechanisms, 27, 28, 220
Structure, 6
Stub teeth, 154
Synthesis, kinematic, 99

T

Tchebicheff's mechanism, 222
Toggle pliers, 58
Train value, 195
Translation:
  cam, 100
  definition, 7
  screw, 204
Tredgold's approximation, 170
Trial solution:
  acceleration, 78
  velocity, 52

U

Undercutting, 144
Unequal addendum gears, 164
Universal joint, 212
  Bendix-Weiss, 212
  Hooke, 213

V

Variable speed drive, 190
Vector:
  addition and subtraction, 9
  composition and resolution, 9
  definition, 8
Velocity image, 47
Velocity, linear and angular, 12
Velocity polygon, 46
  angular velocity, 49
  mechanical advantage, 57
  revolved polygon, 87, 89
  trial solution, 52
Virtual displacement, 57

Virtual velocity, 57
Virtual work, 57

W

Walschaert valve gear:
acceleration, 80
velocity, 56
Watt straight line mechanism, 28
Whole depth, 138
Working depth, 138
Worm gear, 165

Z

Zero backlash gear, 226